THERMOMECHANICAL CONSTITUTIVE MODELING OF VISCOELASTIC MATERIALS UNDERGOING DEGRADATION

A Dissertation

by

SATISH KARRA

Submitted to the Office of Graduate Studies of
Texas A&M University
in partial fulfillment of the requirements for the degree of

DOCTOR OF PHILOSOPHY

May 2011

Major Subject: Mechanical Engineering

THERMOMECHANICAL CONSTITUTIVE MODELING OF VISCOELASTIC MATERIALS UNDERGOING DEGRADATION

A Dissertation

by

SATISH KARRA

Submitted to the Office of Graduate Studies of
Texas A&M University
in partial fulfillment of the requirements for the degree of

DOCTOR OF PHILOSOPHY

Approved by:

Chair of Committee,	Kumbakonam R. Rajagopal
Committee Members,	Jay R. Walton
	Anastasia Muliana
	Kalyana Babu Nakshatrala
Head of Department,	Dennis O'Neal

May 2011

Major Subject: Mechanical Engineering

ABSTRACT

Thermomechanical Constitutive Modeling of Viscoelastic Materials undergoing Degradation. (May 2011)

Satish Karra, B. Tech., Indian Institute of Technology, Madras;

M. S., Texas A&M University

Chair of Advisory Committee: Dr. Kumbakonam R. Rajagopal

Materials like asphalt, asphalt concrete and polyimides that are used in the transportation and aerospace industry show viscoelastic behavior. These materials in the working environment are subject to degradation due to temperature, diffusion of moisture and chemical reactions (for instance, oxidation) and there is need for a good understanding of the various degradation mechanisms. This work focuses on: 1) some topics related to development of viscoelastic fluid models that can be used to predict the response of materials like asphalt, asphalt concrete, and other geomaterials, and 2) developing a framework to model degradation due to the various mechanisms (such as temperature, diffusion of moisture and oxidation) on polyimides that show non-linear viscoelastic solid-like response. Such a framework can be extended to model similar degradation phenomena in the area of asphalt mechanics and biomechanics.

The thermodynamic framework that is used in this work is based on the notion that the 'natural configuration' of a body evolves as the body undergoes a process and the evolution is determined by maximizing the rate of entropy production.

The Burgers' fluid model is known to predict the non-linear viscoelastic fluid-like response of asphalt, asphalt concrete and other geomaterials. We first show that different choices for the manner in which the body stores energy and dissipates energy and satisfies the requirement of maximization of the rate of entropy production that

leads to many three dimensional models. All of these models, in one dimension, reduce to the model proposed by Burgers.

A thermodynamic framework to develop rate-type models for viscoelastic fluids which do not possess instantaneous elasticity (certain types of asphalt show such a behavior) is developed next. To illustrate the capabilities of such models we make a specific choice for the specific Helmholtz potential and the rate of dissipation and consider the creep and stress relaxation response associated with the model.

We then study the effect of degradation and healing due to the diffusion of a fluid on the response of a solid which prior to the diffusion can be described by the generalized neo-Hookean model. We show that a generalized neo-Hookean solid - which behaves like an elastic body (i.e., it does not produce entropy) within a purely mechanical context - creeps and stress relaxes when infused with a fluid and behaves like a body whose material properties are time dependent.

A framework is then developed to predict the viscoelastic response of polyimide resins under different temperature conditions. The developed framework is further extended to model the phenomena of swelling due to diffusion of a fluid through a viscoelastic solid using the theory of mixtures. Finally, degradation due to oxidation is incorporated into such a framework by introducing a variable that represents the extent of oxidation. The data from the resulting models are shown to be in good agreement with the experiments for polyimide resins.

To my wife Pranava

ACKNOWLEDGMENTS

I would like to express my deepest gratitude to my advisor, Professor K. R. Rajagopal, for the independence and intellectual freedom that he has given me in my Ph.D. research. He has encouraged me to implement and publish my ideas, which has been an incredible learning process. Our numerous discussions and his emphasis on precision and attention to detail have made me grow as a researcher. His tremendous energy and passion for mechanics will always be a great source of inspiration for me.

Professor A. R. Srinivasas course on Solid and Fluid Motion inspired me to pursue a Ph.D. in the field of mechanics. His guidance led me to work with Professor Rajagopal and his teaching will always serve as a benchmark for me.

Professor K. B. Nakshatrala, my Graduate Teaching Academy mentor, gave me invaluable advice on teaching, preparing class materials, and pursuing an academic career. He has helped me appreciate the challenging and interesting field of computational mechanics.

I would like to thank Professors J. R. Walton, A. Muliana, and K. B. Nakshatrala for serving on my research committee and providing their support and suggestions.

I would like to thank Air Force Office of Scientific Research and the Air Force Research Laboratory for their financial support. I have also truly enjoyed the unique opportunity to teach as a lecturer for five semesters in the Department of Mechanical Engineering at Texas A&M University. A portion of my Ph.D. research was completed during this time and I appreciate this support by the department.

My gratitude goes to Shriram Srinivasan and Saradhi Koneru for our discussions on Linux, LaTeX and life in general. A special thanks to Dr. Vít Průša, whose humble nature and excellent work ethic are an inspiration to me.

Words cannot express my gratitude for the love and support of my parents. I will

always be thankful to my parents for the sacrifices they made to further my education, and for the friendship and encouragement of my brother Siddesh, my uncle Prasad, and my aunt Sudha.

I am forever indebted to my wife and best friend, Pranava, for being the sole motivator during my Ph.D., and for always helping me edit and improve my writing. The discussions I have with her everyday on topics ranging from spirituality to tax or patent law have helped me think in a more logical and refined manner, making every day an exciting learning experience.

TABLE OF CONTENTS

CHAPTER Page

CHAPTER Page

LIST OF TABLES

LIST OF FIGURES

FIGURE Page

FIGURE Page

FIGURE Page

FIGURE Page

FIGURE Page

FIGURE Page

CHAPTER I

INTRODUCTION

Viscoelastic response is shown by a wide range of materials that are used in the areas of civil engineering (e.g., asphalt and asphalt mixtures), aerospace engineering (e.g., polyimides and their composites), biomechanics (e.g., tissues, tendons, cartilages, blood), and geomechanics (e.g., molten lava). Polymers and polymer composites that are extensively used in the automobile, appliance, and electronic industries also show such a behavior (see [1] for the extensive list of examples). Viscoelastic response can be viewed as a response that is in between elastic and viscous responses. Such a behavior shows simultaneous elastic and viscous characteristics. These viscoelastic materials that show time-dependent behavior are capable of storing as well as dissipating energy.

Initial linear one-dimensional models were proposed by Maxwell [2], Kelvin [3], Voigt [4], to describe the behavior of viscoelastic materials. Later on, one-dimensional models were developed by assuming that the microstructure of the viscoelastic material is mechanically equivalent to a network of linear viscous and elastic elements (see Chapter II in [5]). With the introduction of various frame-indifferent rates in the continuum mechanics literature (like Oldroyd derivatives (upper- and lower-convected), Jaumann derivative, Truesdell derivate etc.), these one-dimensional models were generalized to three dimensional rate-type models. This extension to three dimensions makes the models non-linear as these frame-indifferent derivatives are non-linear in nature [6].

Some of these rate-type models can be integrated to express in an integral form. Using the linearity in response and by approximating that the stress at a given time is

---

The journal model is *IEEE Transactions on Automatic Control.*

by a superposition of responses to step strain histories, the linear viscoelastic model is developed [7], [8], [9], [10], [11], [12], [13]. These ideas have been extended by Pipkin and Rogers [14] to develop a single intergral non-linear viscoelastic solid model. To model the non-linear viscoelastic response of biological materials, Fung [15] modified the linear viscoelastic model by choosing a non-linear strain measure. Such a model can be shown to be a special case of the Pipkin-Rogers model. Unfortunately, these integral models were not derived based on any thermodynamic basis. See the review articles by Drapaca et al. [16] and Wineman [17] for further discussion on the non-linear integral models. In the area of viscoelastic fluids, the K-BKZ integral model [18], [19] has been extensively used.

Recently, a thermodynamic framework has been developed by Rajagopal and co-workers [20], [21] that has been shown to model a variety of responses including viscoelasticity, classical plasticity, superplasticity, twinning, phase-phase transformation and so on. In the area of viscoelasticity, it has been shown that using such a framework various three-dimensional models like the Maxwell model, Oldroyd-B model, Kelvin-Voigt model etc., can be derived. Our work is this dissertation is based upon such a framework. Details of such a framework is given in the later chapters.

This dissertation addresses topics related to: a) development of viscoelastic fluid models that can be used to predict the behavior of materials like asphalt, asphalt mixtures, soil, and other geomaterials, and b) modeling the non-linear viscoelastic behavior of polyimides and their response under various degradation processes.

The following sub-problems relevant to thermomechanical modeling of viscoelastic fluids are addressed in the first part of the dissertation:

1. As discussed previously, a thermodynamic framework has been put to place to

model viscoelasticity and other phenomenon that uses the notion of maximizing the rate of entropy production (or rate of dissipation in case of isothermal processes). In Chapter I, by choosing four different combinations of specific Helmholtz potential and the rate of dissipation, and by imposing this stronger condition that the rate of dissipation is to be maximum (see Fig. (1)), we derive four different models. All of these models in one-dimension reduce to the model proposed by Burgers. Since, typically, three-dimensional models are corroborated by using one- and two-dimensional experimental data, it is not clear as to which of these three-dimensional models is the correct model. Thus, it is imperative to develop better experimental techniques, so that one can isolate the correct three-dimensional model. Burgers' fluid model is used to model asphalt mixtures [22] and other geomaterials [23], and hence our three-dimensional models in Chapter I can be applied to predict the behavior of such materials.

2. Although there have been several rate-type fluid models like the Maxwell model, Oldroyd-B model, Burgers' model, etc., that can be used to predict the response of viscoelastic fluids that show instantaneous elasticity under creep (see Fig. (2)), there is no framework to develop rate-type models that capture the response of those without instantaneous elasticity. In Chapter II, we develop a thermodynamic framework to address this issue. The models developed using such a framework can be used to predict the behavior of certain kinds of asphalt that do not show instantaneous elasticity as recorded by Cheung and Cebon [24].

Polyimides due to their excellent mechanical, thermal, electrical, adhesive properties are used in a plethora of applications including gas separation, electronic pack-

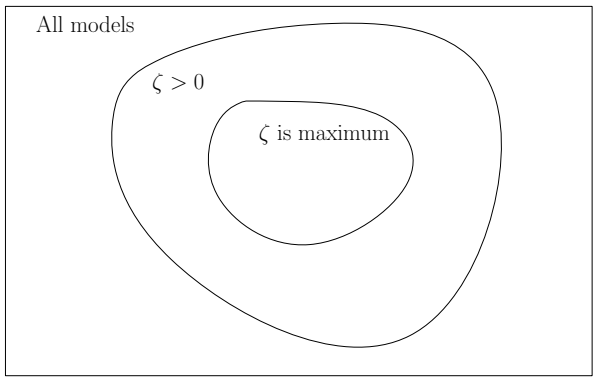

Fig. 1.: Venn diagram showing that the class of models considered in our framework are the ones obtained by using a much stricter condition of maximization of rate of entropy production.

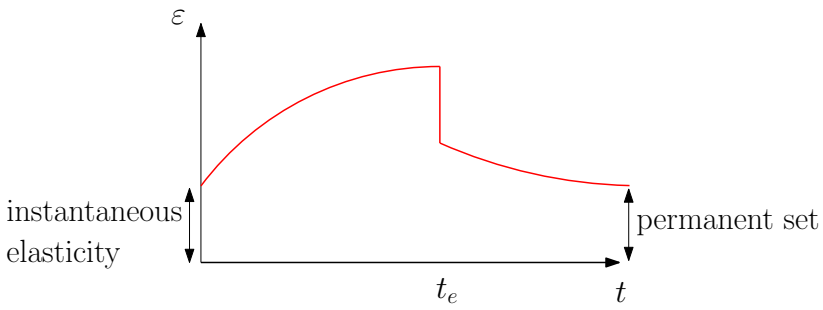

Fig. 2.: Illustration of a viscoelastic fluid that shows instantaneous elasticity in creep.

aging, semiconductor, and automobile industries. In the aerospace industry, due to their extreme stability under high temperatures ($> 300^o$C), they are used as resins for advanced composites in the propulsion and engine components as well as in some of the body parts of an aircraft [25], [26]. Due to exposure to high temperatures, moisture and oxygen during the service conditions of an aircraft, these polyimide composites undergo degradation [27]. The second part of the dissertation focuses on developing a systematic thermodynamic framework to model the various degradation mechanisms on polyimides (specifically degradation due to temperature, moisture diffusion and oxidation as shown in Fig. (3)). The following relevant sub-problems are dealt in this part:

1. We first consider degradation due to diffusion of fluid through a solid, in order to understand how its load bearing capacity is affected by such a phenomenon. The solid is considered to be a generalized neo-Hookean elastic body, and the concentration of the fluid is assumed to follow an advection-diffusion equation. We solve the problem of torsion of a cylindrical annulus coupled with advection-diffusion equation for the concentration of a fluid under different boundary conditions. We also consider the case when the body is healing due to diffusion of a fluid.

2. In order to model the various degradation mechanisms mentioned above on polyimides, our next aim is to develop a model that can predict the mechanical response of a polyimide. Since, experimental data for polyimides suggests that these materials show non-linear viscoelastic solid-like response, to this end, a viscoelastic solid model is developed in Chapter V. Degradation due to temperature is also included in such a model, and results from our model are compared with experimental data for PMR-15 and HFPE-II-52.

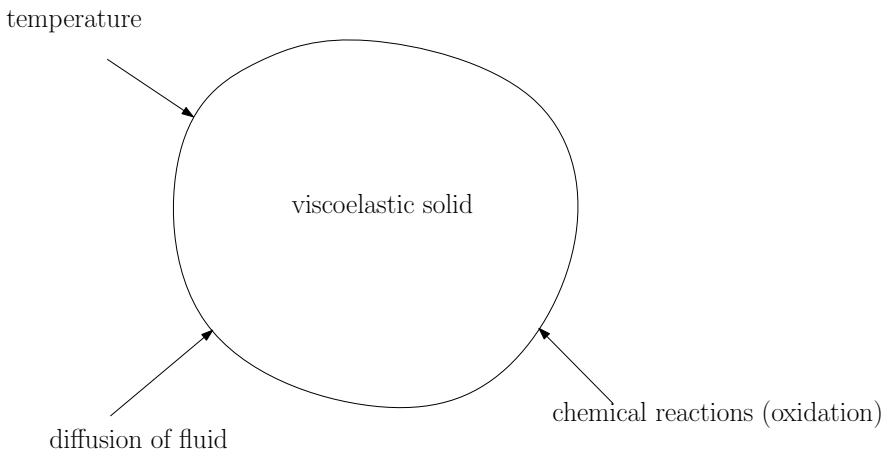

Fig. 3.: Illustration of the various degradation mechanisms on a polyimide (that shows viscoelastic solid-like behavior).

3. In Chapter VI, the framework built to develop the viscoelastic solid model in Chapter V is extended to include diffusion of a fluid, using ideas from mixture theory, in addition to the notion of maximization of rate of entropy production. The phenomena of free swelling of a viscoelastic solid and stress-assisted swelling are studied. Numerical results using our model are compared with experimental data for free swelling of PMDA-ODA and HFPE-II-52 due to diffusion of various solvents.

4. Finally in Chapter VII, degradation due to oxidation on polyimide is modeled by extending the framework in Chapter V by introducing a variable that represents the extent of oxidation. The forms for the Helmholtz potential and the rate of dissipation used in Chapter V are modified to include oxidative degradation. The model developed in this chapter is compared with the experimental data for creep of PMR-15 that is aged in air for various amounts of time.

Details of the literature, preliminaries, constitutive assumptions, solution method-

ology, results, and conclusions concerning to each of the sub-problem are given in the respective chapters. Summary of all the chapters, and a discussion on directions for future research is given in Chapter VIII.

CHAPTER II

DEVELOPMENT OF THREE DIMENSIONAL CONSTITUTIVE THEORIES BASED ON LOWER DIMENSIONAL EXPERIMENTAL DATA*

Most three dimensional constitutive relations that have been developed to describe the behavior of bodies are correlated against one dimensional and two dimensional experiments. What is usually lost sight of is the fact that infinity of such three dimensional models may be able to explain these experiments that are lower dimensional. Recently, the notion of maximization of the rate of entropy production has been used to obtain constitutive relations based on the choice of the stored energy and rate of entropy production, etc. In this chapter, we show different choices for the manner in which the body stores energy and dissipates energy and satisfies the requirement of maximization of the rate of entropy production that leads to many three dimensional models. All of these models, in one dimension, reduce to the model proposed by Burgers to describe the viscoelastic behavior of bodies.

A. Introduction

An observation of a phenomenon or a set of phenomena leads one to conjecture as to its cause and forms the basis for the crude first step in the development of a model. An experiment is then deliberately and carefully fashioned to test and refine the conjecture. Unfortunately, this procedure is rendered most daunting as one is not usually accorded the luxury of being able to perform sufficiently general three dimensional experiments while the models that one would like to develop are fully

*With kind permission from Springer Science + Business Media: Applications of Mathematics, Development of three dimensional constitutive theories based on lower dimensional experimental data, 54(2), 2009, 147–176, Satish Karra and K. R. Rajagopal.

three dimensional models. Most of the general three dimensional constitutive models that are being used in continuum mechanics have been developed on the basis of information gleaned from one or two dimensional special experiments. It does not take much mathematical acumen to recognize the dangers fraught in the process of such generalizations as infinity of three dimensional models could be capable of explaining the lower dimensional experimental data. Of course, one does not corroborate a three dimensional model by merely comparing against data from a single one dimensional experiment. One tests the model against several different experiments, but these experiments tend to be simple experiments in view of the extraordinary difficulties in developing an experimental program that can truly test the full three dimensionality of the model, especially when the response that is being described is complex. In order to obtain a meaningful three dimensional model on the basis of experimental data in lower dimensions, one needs to be guided by enormous physical insight and intuition. This is easier said than done and in fact most models that are currently in use are based on flimsy and tenuous rationale.

One might be tempted to think that the dictates of physics would greatly aid in the development of models from experimental data. For instance, the second law of thermodynamics could play a stringent role in the class of admissible models. Similarly, invariance requirements such as Galilean invariance could also provide restrictions on the class of allowable models. Unfortunately, the sieve provided by all such restrictions is far too coarse as it permits several models to go through that exhibit undesirable properties.

While modeling, one might start directly by assuming a constitutive relation between the stress and other relevant quantities. This relation could be an explicit expression (function) for the stress in terms of kinematical variables as in the case of Hooke's law or the Navier-Stokes model, or it could be an implicit relation as in

the case of many rate type non-Newtonian fluid models. Assuming such constitutive relations implies six scalar constitutive relations (in the case of the stress being symmetric). One could also assume forms for the manner in which energy is stored and entropy is produced by the body and determine the constitutive relation for the stress by appealing to a general thermodynamic framework that has been put in place (see the review articles by Rajagopal and Srinivasa [20], [21] for details of the framework). The framework casts the second law as an equation that defines the rate of entropy production (see Green and Naghdi [28], Rajagopal and Srinivasa [29]) and appeals to the maximization of the rate of entropy production (while Ziegler [30] had appealed to such a requirement, the context within which he made such an appeal is different from that required by Rajagopal and Srinivasa [20], [21]). The general thermodynamic framework has been used to describe a plethora of disparate material response: viscoelasticity, inelasticity, twinning, phase transition in solids, behavior of single crystals super alloys, mixtures, inhomogeneous fluid, etc. While the method seems exceedingly powerful, there are some interesting nuances concerning its application that the modeler should be aware of, and in this chapter by constructing explicit examples we illustrate these delicate issues. It is important to recognize that one can obtain the same constitutive relations for the stress by choosing different forms for the stored energy functions and the rate of entropy production (see Rao and Rajagopal [31] who develop the non-linear three dimensional Maxwell model by choosing two different sets of stored energy and rate of dissipation). In fact, it is possible that several sets of stored energy and rate of dissipation function can lead to the same model. We illustrate this by considering four different sets of stored energy and rate of dissipation to obtain the model developed by Burgers [32], and these four choices are different from a previous choice made by Murali Krishnan and Rajagopal [33]. It is interesting to note that by making the choice of two scalar functions, we can arrive

at a constitutive relation for the stress, a tensor with six scalar components. Many of the one-dimensional models that have been developed to describe the response of viscoelastic materials was by appealing to an analogy to mechanical systems of springs (means for storing energy), and dashpots (means for dissipating energy/ producing entropy), though in his seminal paper on viscoelasticity Maxwell [2] did not appeal to such an analogy. Within the context of these mechanical systems, it becomes clear how one can get the same form for the stress by choosing different stored energy and rate of entropy production functions as one can choose different networks of springs and dashpots to effect the same response.

In 1934 Burgers [32] developed the following one-dimensional model by appealing to a mechanical analog:

$$\sigma + p_1\dot{\sigma} + p_2\ddot{\sigma} = q_1\dot{\epsilon} + q_2\ddot{\epsilon}, \tag{2.1}$$

where p_1 and p_2 are relaxation times, q_1 and q_2 are viscosities, and σ and ϵ denote the stress and the linearized strain respectively. A three dimensional generalization of that was provided by Murali Krishnan and Rajagopal [33], within the context of a thermodynamic basis that requires that among an admissible class of constitutive relations that which is selected is the one that maximizes the rate of entropy production. The second law merely requires that the entropy production be non-negative and one would expect the requirement of maximization of the rate of entropy to cull the class of rate of entropy production functions. As we shall restrict our analysis to a purely mechanical context, instead of making a choice for the rate of entropy production we shall make a choice for the rate of dissipation (the rate at which working is converted to heat) which is the only way in which entropy is produced within the context of interest.

We shall assume that the class of bodies we are interested in modeling are vis-

coelastic fluids that are capable of instantaneous elastic response. A body that exists in a configuration κ_t under the action of external stimuli, on the removal of the external stimuli could attain a configuration $\kappa_{p(t)}$, which is referred to as a natural configuration corresponding to the configuration κ_t. However, more than one natural configuration could be associated with the configuration κ_t based on how the external stimuli is removed, whether instantaneously, slowly, etc. The natural configuration that is accessed depends on the process class allowed. In this study, we shall assume the natural configuration that is achieved is that due to an instantaneous unloading to which the body responds in an instantaneous elastic manner. A detailed discussion of the role of natural configurations can be found in Rajagopal [34] and the review article by Rajagopal and Srinivasa [20]. Even within the context of an instantaneous elastic unloading, it might be possible that the body could go to different natural configurations $\kappa_{p_i(t)}$, $i = 1, ..., n$.

When one provides a spring-dashpot mechanical analogy for a viscoelastic material one obtains a constitutive equation that holds at a point, i.e., the point is capable of storing energies like the various springs and dissipate energy as the dashpots, but it also has to take into account the arrangement of the springs and the dashpots. The central idea of Mixture Theory is that the various constituents of the mixture co-exist. That is, in a homogenized sense at a point, the model has to reflect the combined storage of energies in the springs and the dissipation of the dashpots based on the way in which they are arranged. Of course, a point is a mathematical creation that does not exist, and what is being modeled is a sufficiently small chunk in the body. This chunk can store and dissipate energy in different ways. The point of importance is various arrangements of springs and dashpots can lead to the same net storage of energy of the springs and the dissipation by the dashpots. Put differently, the chunk can respond in an identical manner for different ways in which the

springs and dashpots are put together. This is essentially the crux of the work in this chapter. We have five different three dimensional models, four that are developed in this chapter and one that was developed by Murali Krishnan and Rajagopal [33] and all five three dimensional models could claim equal status as generalizations of the one dimensional model developed by Burgers. Recently, Málek and Rajagopal [35] used the thermodynamic framework that we have discussed to obtain a model for two viscous liquids. In this chapter, we have a more complicated mixture in that we have two different elastic solids coexisting with two different dissipative fluids. We do not allow for relative motion between the constituents, we assume they coexist and move together.

The organization of the chapter is as follows. In section (B), we introduce the kinematics that is necessary to the study and the basic balance laws for mass, linear and angular momentum. We also introduce the second law of thermodynamics. This introduction is followed by a discussion of four different models which all reduce to Burgers' one dimensional model in sections (C)–(F). We make a few final remarks in the last section.

B. Preliminaries

Let $\kappa_R(\mathcal{B})$ and $\kappa_t(\mathcal{B})$ denote, respectively the reference configuration of the body, and the configuration of the body $\mathcal{B}$ at time t. Let $\mathbf{X}$ denote a typical point belonging to $\kappa_R(\mathcal{B})$ and $\mathbf{x}$ the same material point at time t, belonging to $\kappa_t(\mathcal{B})$. Let χ_{κ_R} denote a sufficiently smooth mapping that assigns to each $\mathbf{X} \in \kappa_R(\mathcal{B})$, a point $\mathbf{x} \in \kappa_t(\mathcal{B})$, i.e.,

$$\mathbf{x} := \chi_{\kappa_R}(\mathbf{X}, t)\,. \tag{2.2}$$

The velocity $\mathbf{v}$, the velocity gradient $\mathbf{L}$ and the deformation gradient $\mathbf{F}_{\kappa_R}$ are defined through

$$\mathbf{v} := \frac{\partial \chi_{\kappa_R}}{\partial t}, \quad \mathbf{L} := \frac{\partial \mathbf{v}}{\partial \mathbf{x}}, \quad \mathbf{F}_{\kappa_R} := \frac{\partial \chi_{\kappa_R}}{\partial \mathbf{X}}. \tag{2.3}$$

It immediately follows that

$$\mathbf{L} = \dot{\mathbf{F}}_{\kappa_R} \mathbf{F}_{\kappa_R}^{-1}. \tag{2.4}$$

We denote the symmetric part of the velocity gradient by $\mathbf{D}$, i.e.,

$$\mathbf{D} := \frac{1}{2}\left(\mathbf{L} + \mathbf{L}^T\right). \tag{2.5}$$

The left and right Cauchy-Green stretch tensors $\mathbf{B}_{\kappa_R}$ and $\mathbf{C}_{\kappa_R}$ are defined through

$$\mathbf{B}_{\kappa_R} := \mathbf{F}_{\kappa_R} \mathbf{F}_{\kappa_R}^T, \quad \mathbf{C}_{\kappa_R} := \mathbf{F}_{\kappa_R}^T \mathbf{F}_{\kappa_R}. \tag{2.6}$$

Let $\kappa_{p(t)}$ denote the preferred natural configuration associated with the configuration κ_t. We define $\mathbf{F}_{\kappa_{p(t)}}$ as the mapping from the tangent space at a material point in $\kappa_{p(t)}$ to the tangent space at the same material point at κ_t (see Fig. 4). We then define

$$\mathbf{B}_{\kappa_{p(t)}} := \mathbf{F}_{\kappa_{p(t)}} \mathbf{F}_{\kappa_{p(t)}}^T, \quad \mathbf{C}_{\kappa_{p(t)}} := \mathbf{F}_{\kappa_{p(t)}}^T \mathbf{F}_{\kappa_{p(t)}}. \tag{2.7}$$

The mapping $\mathbf{G}$ is defined through (see Fig. 4)

$$\mathbf{G} := \mathbf{F}_{\kappa_R \to \kappa_{p(t)}} := \mathbf{F}_{\kappa_{p(t)}}^{-1} \mathbf{F}_{\kappa_R}. \tag{2.8}$$

We can then define the tensor $\mathbf{C}_{\kappa_R \to \kappa_{p(t)}}$ in a manner analogous to $\mathbf{C}_{\kappa_R}$ through

$$\mathbf{C}_{\kappa_R \to \kappa_{p(t)}} := \mathbf{G}^T \mathbf{G}, \tag{2.9}$$

and it follows that

$$\mathbf{B}_{\kappa_{p(t)}} = \mathbf{F}_{\kappa_R} \mathbf{C}_{\kappa_R \to \kappa_{p(t)}}^{-1} \mathbf{F}_{\kappa_R}^T. \tag{2.10}$$

We shall also record balance of mass (assuming incompressibity), balance of linear

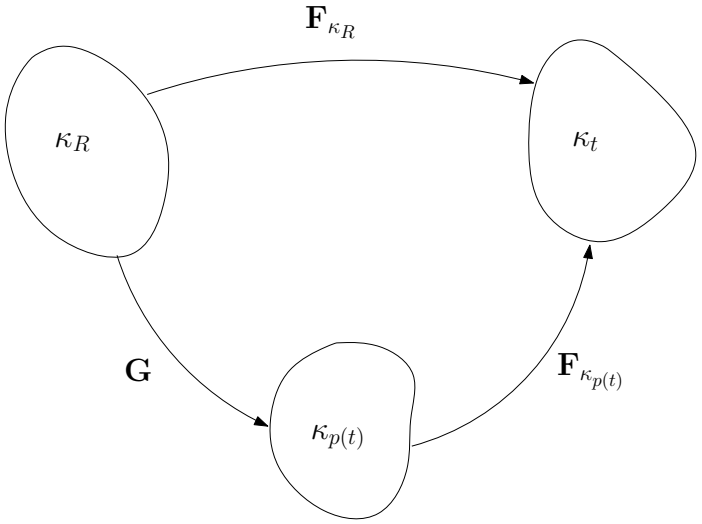

Fig. 4.: Schematic of the natural configuration $\kappa_{p(t)}$ corresponding to the current configuration κ_t and the relevant mappings from the tangent spaces of the same material point in κ_R, κ_t and $\kappa_{p(t)}$.

and angular momentum (in the absence of body couples):

$$div(\mathbf{v}) = 0, \quad \rho\dot{\mathbf{v}} = div(\mathbf{T}^T) + \rho\mathbf{b}, \quad \mathbf{T} = \mathbf{T}^T, \tag{2.11}$$

where ρ is the density, $\mathbf{v}$ is the velocity, $\mathbf{T}$ is the Cauchy stress tensor, $\mathbf{b}$ is the specific body force, $div(.)$ is the divergence operator with respect to the current configuration and $(.)^T$ denotes transpose. In addition, the local form of balance of energy is

$$\rho\dot{\epsilon} = \mathbf{T}.\mathbf{L} - div(\mathbf{q}) + \rho r, \tag{2.12}$$

where ϵ denotes the specific internal energy, $\mathbf{q}$ denotes the heat flux vector and r denotes the specific radiant heating. We shall invoke the second law of thermodynamics in the form of the *reduced energy dissipation equation*, for isothermal processes:

$$\mathbf{T}.\mathbf{D} - \rho\dot{\psi}|_{isothermal} := \xi \geq 0, \tag{2.13}$$

where ψ is the specific Helmholtz potential, ξ denotes the rate of dissipation (specifically rate of entropy production).

When one works with implicit constitutive models of the form

$$\mathbf{f}\left(\mathbf{T}, \mathbf{D}\right) = 0, \tag{2.14}$$

where $\mathbf{T}$ is the Cauchy stress, or more general models of the form

$$\mathbf{f}\left(\mathbf{T}, \overset{\triangledown}{\mathbf{T}}, \ldots, \overset{(n)}{\triangledown}\mathbf{T}, \mathbf{D}, \overset{\triangledown}{\mathbf{D}}, \ldots, \overset{(n)}{\triangledown}\mathbf{D}\right) = 0, \tag{2.15}$$

where the superscript $\overset{(n)}{\triangledown}$ stands for the n Oldroyd derivatives [36], and where $\mathbf{T}$ and $\mathbf{D}$ seem to have the same primacy in that the maximization could be with respect to $\mathbf{T}$ or $\mathbf{D}$. However, the superficial assumption that $\mathbf{T}$ and $\mathbf{D}$ have the same primacy is incorrect as $\mathbf{T}$ (or the applied traction which leads to the stresses) causes the deformation (the appropriate kinematic tensor). In order to get sensible constitutive equations one ought to keep $\mathbf{D}$ fixed and vary $\mathbf{T}$ to find how a body responds to the stress that is a consequence of the applied traction. This comes up naturally in the development of implicit constitutive theories (see Rajagopal and Srinivasa [37], Rajagopal and Srinivasa [38]). More recently, Rajagopal [39] has discussed at length the implicit nature of constitutive relations. When one thinks explicitly along classical terms of the stress being given explicitly in terms of the kinematical variables, it is natural to hold $\mathbf{T}$ fixed and maximize with respect to the kinematical variable, in our case $\mathbf{D}$. This is what is followed in this work.

C. Model 1

1. Preliminaries

Let κ_R denote the undeformed reference configuration of the body. We shall assume that the body has associated with it two natural configurations i.e., configurations to which it can be instantaneously elastically unloaded and corresponds to two mechanisms for storing energy (within one dimensional mechanical analog – two springs). Interestingly, one can get from the reference configuration to the two evolving natural configurations denoted by $\kappa_{p_i(t)}$, $i = 1, 2$ (see Fig. 5), via two dissipative responses. Let $\mathbf{F}_i$, $i = 1, 2, 3$, denote the gradients of the motion[1] from κ_R to $\kappa_{p_1(t)}$, $\kappa_{p_1(t)}$ to $\kappa_{p_2(t)}$, and $\kappa_{p_2(t)}$ to κ_t respectively. Also, we shall define the left Cauchy-Green stretch tensors,

$$\mathbf{B}_i := \mathbf{F}_i \mathbf{F}_i^T, \quad i = 1, 2, 3, \tag{2.16}$$

and the velocity gradients with their corresponding symmetric parts,

$$\mathbf{L}_i := \dot{\mathbf{F}}_i \mathbf{F}_i^{-1}, \quad \mathbf{D}_i := \frac{1}{2}\left(\mathbf{L}_i + \mathbf{L}_i^T\right), \quad i = 1, 2, 3. \tag{2.17}$$

Also, we note that[2]

$$\mathbf{F} = \mathbf{F}_3 \mathbf{F}_2 \mathbf{F}_1. \tag{2.18}$$

Let us denote the gradient of the motion from $\kappa_{p_1(t)}$ to κ_t by $\mathbf{F}_p$; then,

$$\mathbf{F}_p = \mathbf{F_3} \mathbf{F_2}, \tag{2.19}$$

and

$$\mathbf{F} = \mathbf{F}_p \mathbf{F}_1. \tag{2.20}$$

---

[1] In general, these are appropriate mappings of tangent spaces containing the same material point in different configurations.

[2] Henceforth, we shall denote $\mathbf{F}_{\kappa_R}$ by $\mathbf{F}$.

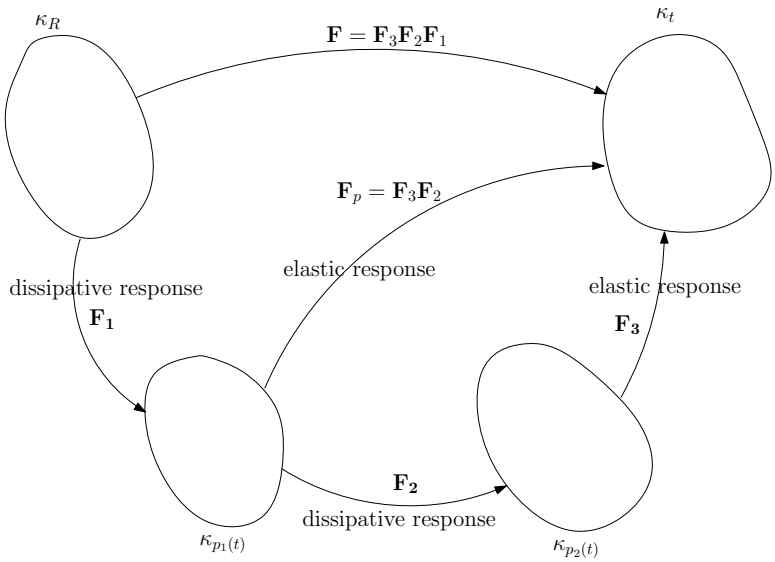

Fig. 5.: Schematic to illustrate the natural configurations for model 1. κ_R is the reference configuration, κ_t denotes the current configuration, and $\kappa_{p_1(t)}, \kappa_{p_2(t)}$ denote the two evolving natural configurations. The body dissipates energy like a viscous fluid as it moves from, κ_R to $\kappa_{p_1(t)}$, and $\kappa_{p_1(t)}$ to $\kappa_{p_2(t)}$. Also, as shown, the body stores energy during its motion from, $\kappa_{p_2(t)}$ to κ_t, and $\kappa_{p_1(t)}$ to κ_t.

The left Cauchy-Green stretch tensor, the velocity gradient with its symmetric part, corresponding to $\mathbf{F}_p$ are

$$\mathbf{B}_p := \mathbf{F}_p\mathbf{F}_p^T, \quad \mathbf{L}_p := \dot{\mathbf{F}}_p\mathbf{F}_p^{-1}, \quad \mathbf{D}_p := \frac{1}{2}\left(\mathbf{L}_p + \mathbf{L}_p^T\right), \tag{2.21}$$

respectively.

Now, taking the time derivative of Eq. (2.20) we get:

$$\begin{aligned} \dot{\mathbf{F}} &= \dot{\mathbf{F}}_p\mathbf{F}_1 + \mathbf{F}_p\dot{\mathbf{F}}_1 \\ \Rightarrow \quad \mathbf{LF} &= \mathbf{L}_p\mathbf{F}_p\mathbf{F}_1 + \mathbf{F}_p\mathbf{L}_1\mathbf{F}_1 \\ \Rightarrow \quad \mathbf{L} &= \mathbf{L}_p + \mathbf{F}_p\mathbf{L}_1\mathbf{F}_p^{-1}. \end{aligned} \tag{2.22}$$

Similarly, taking the time derivative of Eq. (2.19), we arrive at

$$\mathbf{L}_p = \mathbf{L}_3 + \mathbf{F}_3\mathbf{L}_2\mathbf{F}_3^{-1}. \tag{2.23}$$

Now,

$$\begin{aligned}\dot{\mathbf{B}}_p &= \mathbf{F}_p\dot{\mathbf{F}}_p^T + \dot{\mathbf{F}}_p\mathbf{F}_p^T \\ &= \mathbf{F}_p\mathbf{F}_p^T\mathbf{L}_p^T + \mathbf{L}_p\mathbf{F}_p\mathbf{F}_p^T \\ &= \mathbf{B}_p\mathbf{L}_p^T + \mathbf{L}_p\mathbf{B}_p.\end{aligned} \tag{2.24}$$

Post-multiplying Eq. (2.22) by $\mathbf{B}_p$, pre-multiplying the transpose of Eq. (2.22) by $\mathbf{B}_p$, and adding, we obtain

$$\overset{\nabla}{\mathbf{B}}_p = -2\mathbf{F}_p\mathbf{D}_1\mathbf{F}_p^T, \tag{2.25}$$

where $\overset{\nabla}{\mathbf{B}}_p := \dot{\mathbf{B}}_p - \mathbf{B}_p\mathbf{L}^T - \mathbf{L}\mathbf{B}_p$ is the Oldroyd derivative of $\mathbf{B}_p$. In a similar fashion, using Eq. (2.23) and the relation $\dot{\mathbf{B}}_3 = \mathbf{B}_3\mathbf{L}_3^T + \mathbf{L}_3\mathbf{B}_3$, we get

$$\overset{\nabla_p}{\mathbf{B}}_3 = -2\mathbf{F}_3\mathbf{D}_2\mathbf{F}_3^T, \tag{2.26}$$

where $\overset{\nabla_p}{\mathbf{B}}_3 := \dot{\mathbf{B}}_3 - \mathbf{B}_3\mathbf{L}_p^T - \mathbf{L}_p\mathbf{B}_3$. This is same as the Oldroyd derivative of $\mathbf{B}_3$, when the natural configuration $\kappa_{p_1(t)}$ is made the reference configuration.

We also note from Eq. (2.18) that

$$\begin{aligned}\dot{\mathbf{F}} &= \dot{\mathbf{F}}_3\mathbf{F}_2\mathbf{F}_1 + \mathbf{F}_3\dot{\mathbf{F}}_2\mathbf{F}_1 + \mathbf{F}_3\mathbf{F}_2\dot{\mathbf{F}}_1 \\ \Rightarrow \mathbf{L} &= \mathbf{L}_3 + \mathbf{F}_3\mathbf{L}_2\mathbf{F}_3^{-1} + \mathbf{F}_3\mathbf{F}_2\mathbf{L}_1\mathbf{F}_2^{-1}\mathbf{F}_3^{-1}.\end{aligned} \tag{2.27}$$

and hence

$$\begin{aligned}\mathbf{I}.\dot{\mathbf{B}}_3 &= \mathbf{I}.\left(\mathbf{L}_3\mathbf{B}_3 + \mathbf{B}_3\mathbf{L}_3^T\right)\\ &= \mathbf{I}.\left(\mathbf{L}\mathbf{B}_3 - \mathbf{F}_3\mathbf{L}_2\mathbf{F}_3^T - \mathbf{F}_3\mathbf{F}_2\mathbf{L}_1\mathbf{F}_2^{-1}\mathbf{F}_3^T + \mathbf{B}_3\mathbf{L}^T - \mathbf{F}_3\mathbf{L}_2^T\mathbf{F}_3^T - \mathbf{F}_3\mathbf{F}_2^{-T}\mathbf{L}_1^T\mathbf{F}_2^T\mathbf{F}_3^T\right)\\ &= 2\mathbf{B}_3.\mathbf{D} - 2\mathbf{C}_3.\mathbf{D}_2 - \mathbf{C}_3.\left(\mathbf{F}_2\mathbf{L}_1\mathbf{F}_2^{-1} + \mathbf{F}_2^{-T}\mathbf{L}_1^T\mathbf{F}_2^T\right).\end{aligned} \tag{2.28}$$

The relations derived, in this sub-section, are sufficient for the purpose of analyzing this model. In the following sub-section, we shall constitutively specify the forms for storage and rate of dissipation functions, and then we shall maximize the rate of dissipation subject to appropriate constraints (incompressibility and the energy dissipation equation), to determine the constitutive relation.

2. Constitutive assumptions

Let us assume the specific stored energy ψ and the rate of dissipation ξ of the form[3]

$$\psi \equiv \psi(\mathbf{B}_3, \mathbf{B}_p), \quad \xi \equiv \xi(\mathbf{D}_1, \mathbf{D}_2). \tag{2.29}$$

In particular, assuming that the instantaneous elastic responses from $\kappa_{p_1(t)}$ and $\kappa_{p_1(t)}$ are isotropic, and in virtue of incompressibility of the body, we choose

$$\psi(\mathbf{B}_3, \mathbf{B}_p) = \frac{\mu_3}{2\rho}(\mathbf{I}.\mathbf{B}_3 - 3) + \frac{\mu_p}{2\rho}(\mathbf{I}.\mathbf{B}_p - 3), \tag{2.30}$$

[3]One can also choose the rate of dissipation function to depend on the stretch i.e., of the form $\xi \equiv \xi(\mathbf{D}_1, \mathbf{D}_2, \mathbf{B}_3, \mathbf{B}_p)$. The resulting constitutive relations will be a variant of the relations obtained when ξ is of the form given in Eq. (2.29). The constitutive relations obtained by using $\xi(\mathbf{D}_1, \mathbf{D}_2, \mathbf{B}_3, \mathbf{B}_p)$ have relaxation times which depend on the stretch. Upon linearization, the two constitutive relations take the same form. Rajagopal and Srinivasa have discussed this issue for the Maxwell fluid in [6].

and

$$\xi(\mathbf{D}_1, \mathbf{D}_2) = \eta_1' \mathbf{D}_1.\mathbf{D}_1 + \eta_2' \mathbf{D}_2.\mathbf{D}_2. \tag{2.31}$$

The above assumption means that the body possesses instantaneous elastic response from the two evolving natural configurations $(\kappa_{p_1(t)}, \kappa_{p_2(t)})$ to the current configuration κ_t (Fig. 5); the body stores energy like a neo-Hookean solid during its motion, from $\kappa_{p_1(t)}$ to κ_t, and from $\kappa_{p_2(t)}$ to κ_t. In addition, the response is linear viscous fluid-like, as the body moves from κ_R to $\kappa_{p_1(t)}$, and from one natural configuration $(\kappa_{p_1(t)})$ to the other $(\kappa_{p_2(t)})$.

Also, since we have assumed that the material's instantaneous elastic response is isotropic, we shall choose the configurations $\kappa_{p_1(t)}, \kappa_{p_2(t)}$ such that

$$\mathbf{F}_3 = \mathbf{V}_3, \quad \mathbf{F}_p = \mathbf{V}_p, \tag{2.32}$$

where $\mathbf{V}_3, \mathbf{V}_p$ are the right stretch tensors in the polar decomposition i.e., the natural configurations are appropriately rotated.

Finally, using Eqs. (2.28) and (2.32), we get

$$\mathbf{I}.\dot{\mathbf{B}}_3 = 2\mathbf{B}_3.\left[\mathbf{D} - \mathbf{D}_2 - \frac{1}{2}\left(\mathbf{F}_2\mathbf{L}_1\mathbf{F}_2^{-1} + \mathbf{F}_2^{-T}\mathbf{L}_1^T\mathbf{F}_2^T\right)\right], \tag{2.33}$$

and similarly

$$\mathbf{I}.\dot{\mathbf{B}}_p = 2\mathbf{B}_p.(\mathbf{D} - \mathbf{D}_1). \tag{2.34}$$

Substituting Eqs. (2.30), (2.31) into (2.13) and using the relations in Eqs. (2.33), (2.34),

$$\mathbf{T}.\mathbf{D} - \mu_3\mathbf{B}_3.\left[\mathbf{D} - \mathbf{D}_2 - \frac{1}{2}\left(\mathbf{F}_2\mathbf{L}_1\mathbf{F}_2^{-1} + \mathbf{F}_2^{-T}\mathbf{L}_1^T\mathbf{F}_2^T\right)\right] - \mu_p\mathbf{B}_p.(\mathbf{D} - \mathbf{D}_1)$$
$$= \eta_1'\mathbf{D}_1.\mathbf{D}_1 + \eta_2'\mathbf{D}_2.\mathbf{D}_2, \tag{2.35}$$

which on further simplification leads to

$$\left(\mathbf{T}-\mu_3\mathbf{B}_3-\mu_p\mathbf{B}_p\right).\mathbf{D}+\mu_3\mathbf{B}_3.\mathbf{D}_2+\mu_p\mathbf{B}_p.\mathbf{D}_1+\frac{\mu_3}{2}\mathbf{B}_3.\left(\mathbf{F}_2\mathbf{L}_1\mathbf{F}_2^{-1}+\mathbf{F}_2^{-T}\mathbf{L}_1^T\mathbf{F}_2^T\right) = \eta_1'\mathbf{D}_1.\mathbf{D}_1+\eta_2'\mathbf{D}_2.\mathbf{D}_2. \tag{2.36}$$

We shall assume that the body can undergo only isochoric motions and so

$$tr(\mathbf{D})=0. \tag{2.37}$$

Also, since the body can actually attain the two natural configurations, the incompressibility constraint implies that

$$tr(\mathbf{D}_1)=0, \quad tr(\mathbf{D}_2)=0, \tag{2.38}$$

where $tr\,(.)$ is the trace of second order tensor.

Since the right hand side of Eq. (2.36) does not depend on $\mathbf{D}$, along with Eq. (2.37), we have

$$\mathbf{T}=-p\mathbf{I}+\mu_3\mathbf{B}_3+\mu_p\mathbf{B}_p, \tag{2.39}$$

where $-p\mathbf{I}$ is the reaction stress due to the constraint of incompressibility. Hence, Eq. (2.36) reduces to

$$\mu_3\mathbf{B}_3.\mathbf{D}_2+\mu_p\mathbf{B}_p.\mathbf{D}_1+\frac{\mu_3}{2}\mathbf{B}_3.\left(\mathbf{F}_2\mathbf{L}_1\mathbf{F}_2^{-1}+\mathbf{F}_2^{-T}\mathbf{L}_1^T\mathbf{F}_2^T\right)=\eta_1'\mathbf{D}_1.\mathbf{D}_1+\eta_2'\mathbf{D}_2.\mathbf{D}_2. \tag{2.40}$$

Following Rajagopal and Srinivasa [6], we maximize the rate of dissipation in Eq. (2.31) along with the constraints in Eq. (2.38), (2.40), by varying $\mathbf{D}_1, \mathbf{D}_2$ for

fixed $\mathbf{B}_2, \mathbf{B}_3$. We maximize the auxiliary function Φ defined by

$$\begin{aligned}\Phi := & \eta_1' \mathbf{D}_1.\mathbf{D}_1 + \eta_2' \mathbf{D}_2.\mathbf{D}_2 \\ & + \lambda_1 \left[\eta_1' \mathbf{D}_1.\mathbf{D}_1 + \eta_2' \mathbf{D}_2.\mathbf{D}_2 - \mu_3 \mathbf{B}_3.\mathbf{D}_2 - \mu_p \mathbf{B}_p.\mathbf{D}_1 - \frac{\mu_3}{2} \mathbf{B}_3.\left(\mathbf{F}_2 \mathbf{L}_1 \mathbf{F}_2^{-1} + \mathbf{F}_2^{-T} \mathbf{L}_1^T \mathbf{F}_2^T \right) \right] \\ & + \lambda_2 \mathbf{I}.\mathbf{D}_1 + \lambda_3 \mathbf{I}.\mathbf{D}_2 \end{aligned} \tag{2.41}$$

Now, setting $\partial\Phi/\partial\mathbf{D}_2 = 0, \partial\Phi/\partial\mathbf{D}_1 = 0$, and dividing the resulting equations by λ_1 and λ_2 respectively, for $\lambda_1, \lambda_2 \neq 0$, we get (also see appendix)

$$\begin{aligned} \mu_3 \mathbf{B}_3 &= \left(\frac{\lambda_1 + 1}{\lambda_1} \right) 2\eta_2' \mathbf{D}_2 + \frac{\lambda_3}{\lambda_1} \mathbf{I}, \\ \mu_p \mathbf{B}_p + \frac{\mu_3}{2} \left(\mathbf{F}_2^T \mathbf{B}_3 \mathbf{F}_2^{-T} + \mathbf{F}_2^{-1} \mathbf{B}_3 \mathbf{F}_2 \right) &= \left(\frac{\lambda_1 + 1}{\lambda_1} \right) 2\eta_1' \mathbf{D}_1 + \frac{\lambda_2}{\lambda_1} \mathbf{I}. \end{aligned} \tag{2.42}$$

Using Eq. (2.42) in Eq. (2.40), we get

$$\frac{\lambda_1 + 1}{\lambda_1} = \frac{1}{2} - \frac{\mu_3 \mathbf{B}_3.\mathbf{F}_2 \mathbf{W}_1 \mathbf{F}_2^{-1}}{2\eta_1' \mathbf{D}_1.\mathbf{D}_1 + 2\eta_2' \mathbf{D}_2.\mathbf{D}_2}, \tag{2.43}$$

where $\mathbf{W}_1 := \frac{1}{2}\left(\mathbf{L}_1 - \mathbf{L}_1^T \right)$. Hence,

$$\begin{aligned} \mathbf{T} &= -p\mathbf{I} + \mu_3 \mathbf{B}_3 + \mu_p \mathbf{B}_p, \\ \frac{\mu_3}{2} \left(\mathbf{F}_2^T \mathbf{B}_3 \mathbf{F}_2^{-T} + \mathbf{F}_2^{-1} \mathbf{B}_3 \mathbf{F}_2 \right) + \mu_p \mathbf{B}_p &= -p'\mathbf{I} + \eta_1 \mathbf{D}_1, \\ \mu_3 \mathbf{B}_3 &= -p''\mathbf{I} + \eta_2 \mathbf{D}_2, \end{aligned} \tag{2.44}$$

where $p',\ p''$ are the Lagrange multipliers with

$$\begin{aligned} -p' = \frac{1}{3}\left[\mu_3 tr(\mathbf{B}_3) + \mu_p tr(\mathbf{B}_p) \right], \quad -p'' = \frac{1}{3}\mu_3 tr(\mathbf{B}_3), \\ \eta_1 = 2\left(\frac{\lambda_1 + 1}{\lambda_1} \right) \eta_1', \quad \eta_2 = 2\left(\frac{\lambda_1 + 1}{\lambda_1} \right) \eta_2'. \end{aligned} \tag{2.45}$$

Now, Eqs. (2.25), (2.26) can be re-written as

$$\mathbf{D}_1 = -\frac{1}{2} \mathbf{V}_p^{-1} \overset{\nabla}{\mathbf{B}}_p \mathbf{V}_p^{-1}, \quad \mathbf{D}_2 = -\frac{1}{2} \mathbf{V}_3^{-1} \overset{\nabla_p}{\mathbf{B}}_3 \mathbf{V}_3^{-1}. \tag{2.46}$$

Using Eq. $(2.46)_b$ in Eq. $(2.44)_c$, and post-multiplying and pre-multiplying with $\mathbf{V}_3$, we have

$$\mu_3 \mathbf{B}_3^2 = \frac{1}{3}\mu_3 tr(\mathbf{B}_3)\mathbf{B}_3 - \frac{\eta_2}{2} \overset{\nabla_p}{\mathbf{B}_3} . \tag{2.47}$$

In addition, using Eq. $(2.46)_a$ in Eq. $(2.44)_b$, post-multiplying and pre-multiplying with $\mathbf{V}_p$, and using Eq. (2.19), we get

$$\frac{\mu_3}{2}\left(\mathbf{B}_p\mathbf{B}_3 + \mathbf{B}_3\mathbf{B}_p\right) + \mu_p \mathbf{B}_p^2 = \frac{1}{3}\left[\mu_3 tr(\mathbf{B}_3) + \mu_p tr(\mathbf{B}_p)\right]\mathbf{B}_p - \frac{\eta_1}{2} \overset{\nabla}{\mathbf{B}_p} . \tag{2.48}$$

Notice, from Eqs. (2.47), (2.48), that the evolution of the natural configurations $\kappa_{p_1(t)}$ and $\kappa_{p_2(t)}$ are coupled. These two equations are to be solved simultaneously to determine their evolution. We shall denote $\mu_3\mathbf{B}_3, \mu_p\mathbf{B}_p$ by $\mathbf{S}_1, \mathbf{S}_2$ respectively. Then, the final constitutive relations – Eqs. $(2.44)_a$, (2.47), (2.48) – reduce to

$$\begin{aligned} \mathbf{T} &= -p\mathbf{I} + \mathbf{S}_1 + \mathbf{S}_2, \\ \mathbf{S}_1^2 &= \frac{1}{3}tr(\mathbf{S}_1)\mathbf{S}_1 - \frac{\eta_2}{2} \overset{\nabla_p}{\mathbf{S}_1}, \\ \frac{1}{2}\left(\mathbf{S}_2\mathbf{S}_1 + \mathbf{S}_1\mathbf{S}_2\right) + \mathbf{S}_2^2 &= \frac{1}{3}\left[tr(\mathbf{S}_1) + tr(\mathbf{S}_2)\right]\mathbf{S}_2 - \frac{\eta_1}{2} \overset{\nabla}{\mathbf{S}_2} . \end{aligned} \tag{2.49}$$

In the next sub-section, we shall show that the above constitutive model reduces to Burgers' model in one dimension.

3. Reduction of the model to one dimensional Burgers' model

In this sub-section, we shall first linearize the constitutive model given by Eq. (2.44) (we shall use Eq. (2.44), here, instead of Eq. (2.49), for the sake of simplicity) by assuming the elastic response is small (we shall define what we mean by small, precisely, later). Then we shall show that, in one dimension, the equations reduce to the one dimensional linear model due to Burgers (see Eq. (2.1)).

Now, Eq. $(2.44)_c$ can be re-written as

$$\mu_3 \left(\mathbf{B}_3 - \mathbf{I}\right) = \mu_3 \left[\frac{1}{3} tr(\mathbf{B}_3) - 1\right] \mathbf{I} + \eta_2 \mathbf{D}_2. \tag{2.50}$$

If the displacement gradient with elastic response is small, i.e.,

$$\max_{\substack{\mathbf{X}\in\mathcal{B} \\ t\in\mathcal{R}}} \| \frac{\partial \mathbf{u}\left(\mathbf{X}, t\right)}{\partial \mathbf{X}} \| = \mathbf{O}(\gamma), \quad \gamma \ll 1, \tag{2.51}$$

then

$$\|\mathbf{B}_i - \mathbf{I}\| = \mathbf{O}(\gamma), \quad \gamma \ll 1, \quad i = 3, p, \tag{2.52}$$

and hence

$$tr(\mathbf{B}_i) = 3 + \mathbf{O}(\gamma^2), \quad i = 3, p, \tag{2.53}$$

and so the first term on the right hand side of Eq. (2.50) can be dropped for small strain and Eq. (2.50) reduces to

$$\mu_3 \left(\mathbf{B}_3 - \mathbf{I}\right) = \eta_2 \mathbf{D}_2. \tag{2.54}$$

If λ_i ($i = 1, 2, 3, p$ or no subscript) is the stretch, in one dimension, corresponding to the deformation gradient $\mathbf{F}_i$, then λ_i^2 and $\dot{\lambda}_i/\lambda_i$ are the equivalent values in one dimension, corresponding to $\mathbf{B}_i$ and $\mathbf{D}_i$. If ϵ_i is the true strain for the stretch λ_i, then $\epsilon_i = ln\lambda_i$ and so, $\dot{\epsilon}_i = \dot{\lambda}_i/\lambda_i$. Hence, Eq. (2.54) reduces to

$$\mu_3 \left(\lambda_3^2 - 1\right) = \eta_2 \frac{\dot{\lambda}_2}{\lambda_2} \tag{2.55}$$

or

$$\mu_3 \left(e^{2\epsilon_3} - 1\right) = \eta_2 \dot{\epsilon}_2, \tag{2.56}$$

which under the assumption of small strain (i.e., $\epsilon_3 \ll 1$), reduces to

$$2\mu_3 \epsilon_3 = \eta_2 \dot{\epsilon}_2. \tag{2.57}$$

Following a similar analysis, in one dimension, Eq. $(2.44)_b$ becomes

$$2\mu_3\epsilon_3 + 2\mu_p\epsilon_p = \eta_1\dot{\epsilon}_1, \tag{2.58}$$

and Eq. $(2.44)_a$ reduces to

$$\sigma = 2\mu_3\epsilon_3 + 2\mu_p\epsilon_p, \tag{2.59}$$

where σ is the one dimensional stress. In addition, Eq. (2.18), reduces to

$$\lambda = \lambda_1\lambda_2\lambda_3, \tag{2.60}$$

and so

$$\epsilon = \epsilon_1 + \epsilon_2 + \epsilon_3. \tag{2.61}$$

Similarly, Eqs. (2.19), (2.20) reduce to

$$\epsilon = \epsilon_p + \epsilon_1, \quad \epsilon_p = \epsilon_2 + \epsilon_3. \tag{2.62}$$

The Eqs. (2.57–2.59), (2.61), (2.62) are, in fact, the equations obtained if we have the spring-dashpot arrangement shown in Fig. 6(a).

We shall now show that these equations (i.e., Eqs. (2.57–2.59), (2.61), (2.62)) reduce to the form of Eq. (2.1). Now, differentiating Eq. $(2.62)_b$ with respect to time and using Eq. (2.57), we obtain

$$\dot{\epsilon}_p = \frac{2\mu_3}{\eta_2}\epsilon_3 + \dot{\epsilon}_3. \tag{2.63}$$

Also, differentiating Eq. (2.59) with respect to time and dividing by η_2, we find

$$\frac{\dot{\sigma}}{\eta_2} = \frac{2\mu_3}{\eta_2}\dot{\epsilon}_3 + \frac{2\mu_p}{\eta_2}\dot{\epsilon}_p, \tag{2.64}$$

and differentiating Eq. (2.59) twice with respect to time and dividing by $2\mu_3$ leads to

$$\frac{\ddot{\sigma}}{2\mu_3} = \ddot{\epsilon_3} + \frac{\mu_p}{\mu_3}\ddot{\epsilon}_p. \tag{2.65}$$

We add Eqs. (2.64), (2.65) and use Eq. (2.63), to get

$$\frac{\dot{\sigma}}{\eta_2} + \frac{\ddot{\sigma}}{2\mu_3} = \frac{2\mu_p}{\eta_2}\dot{\epsilon_p} + \left(1 + \frac{\mu_p}{\mu_3}\right)\ddot{\epsilon}_p. \tag{2.66}$$

From Eqs. (2.58), (2.59)

$$\sigma = \eta_1\dot{\epsilon_1} = \eta_1\left(\dot{\epsilon} - \dot{\epsilon_p}\right), \text{ or, } \quad \dot{\epsilon_p} = \dot{\epsilon} - \frac{\sigma}{\eta_1}. \tag{2.67}$$

Using Eq. (2.67) in Eq. (2.66) leads to

$$\frac{2\mu_p}{\eta_1\eta_2}\sigma + \left(\frac{1}{\eta_1} + \frac{\mu_p}{\mu_3\eta_1} + \frac{1}{\eta_2}\right)\dot{\sigma} + \frac{\ddot{\sigma}}{2\mu_3} = \frac{2\mu_p}{\eta_2}\dot{\epsilon} + \left(1 + \frac{\mu_p}{\mu_3}\right)\ddot{\epsilon}, \tag{2.68}$$

which can be re-written as

$$\sigma + \left(\frac{\eta_2}{2\mu_p} + \frac{\eta_2}{2\mu_3} + \frac{\eta_1}{2\mu_p}\right)\dot{\sigma} + \frac{\eta_1\eta_2}{4\mu_p\mu_3}\ddot{\sigma} = \eta_1\dot{\epsilon} + \frac{\eta_1\eta_2}{2\mu_p}\left(1 + \frac{\mu_p}{\mu_3}\right)\ddot{\epsilon}. \tag{2.69}$$

Eq. (2.69) is in the same form as Eq. (2.1), with

$$p_1 = \frac{\eta_2}{2\mu_p} + \frac{\eta_2}{2\mu_3} + \frac{\eta_1}{2\mu_p}, \quad p_2 = \frac{\eta_1\eta_2}{4\mu_p\mu_3}, \quad q_1 = \eta_1, \quad q_2 = \frac{\eta_1\eta_2}{2\mu_p}\left(1 + \frac{\mu_p}{\mu_3}\right). \tag{2.70}$$

D. Model 2

1. Preliminaries

Once again, let κ_R denote the reference configuration of the body. We shall assume that the body has two evolving natural configurations (denoted by $\kappa_{p_1(t)}, \kappa_{p_2(t)}$), but the manner in which they store the energy is different from that considered previously, with $\mathbf{F}_i, i = 1, 2, 3$, being the gradients of the motion as discussed in model 1. We

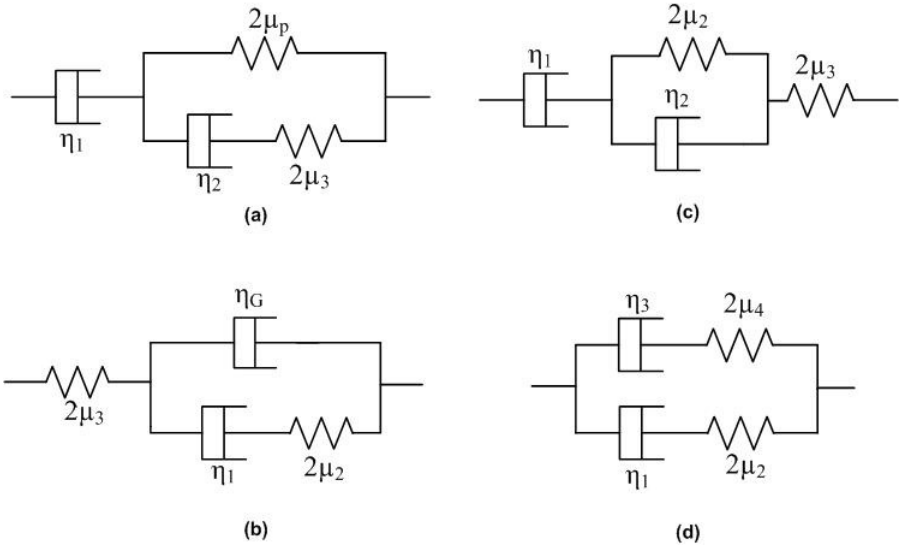

Fig. 6.: Various spring-dashpot arrangements which reduce to the one-dimensional Burgers' fluid model (Eq. (2.1)).

shall also use the definitions in Eqs. (2.16), (2.17). Thus, Eq. (2.18) applies here too. In addition, let us call the gradient of the motion from κ_R to $\kappa_{p_2(t)}$ by $\mathbf{F}_G$ (see Fig. 7). It immediately follows that

$$\mathbf{F}_G = \mathbf{F}_2\mathbf{F}_1. \tag{2.71}$$

We shall denote the velocity gradient and its symmetric part corresponding to $\mathbf{F}_G$ by

$$\mathbf{L}_G := \dot{\mathbf{F}}_G\mathbf{F}_G^{-1}, \quad \mathbf{D}_G := \frac{1}{2}\left(\mathbf{L}_G + \mathbf{L}_G^T\right). \tag{2.72}$$

Also, from Eqs. (2.18), (2.71),

$$\mathbf{F} = \mathbf{F}_3\mathbf{F}_G. \tag{2.73}$$

Following a procedure similar to the one followed previously for model 1, it can be shown that

$$\mathbf{D}_G = \mathbf{D}_2 + \frac{1}{2}(\mathbf{F}_2\mathbf{L}_1\mathbf{F}_2^{-1} + \mathbf{F}_2^{-T}\mathbf{L}_1^T\mathbf{F}_2^T), \quad \mathbf{D} = \mathbf{D}_3 + \frac{1}{2}(\mathbf{F}_3\mathbf{L}_G\mathbf{F}_3^{-1} + \mathbf{F}_3^{-T}\mathbf{L}_G^T\mathbf{F}_3^T), \tag{2.74}$$

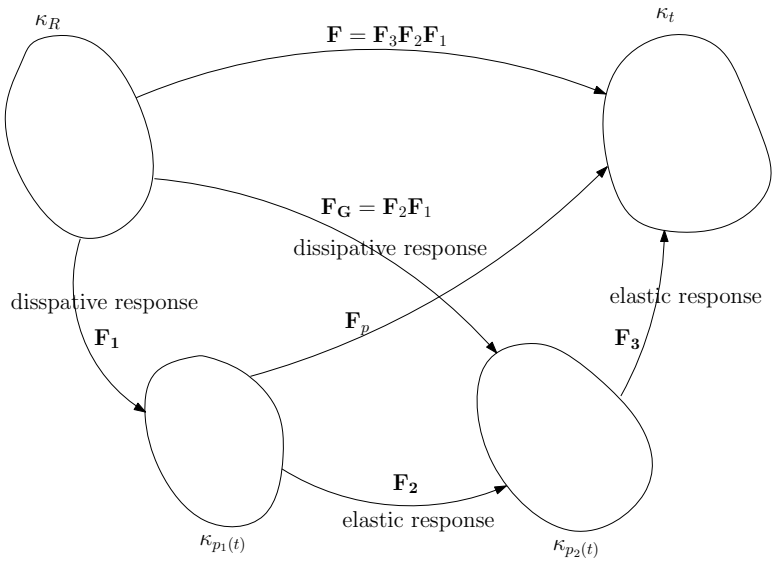

Fig. 7.: Schematic to illustrate the natural configurations for model 2. The body dissipates like a viscous fluid during its motion from, κ_R to $\kappa_{p_2(t)}$, and κ_R to $\kappa_{p_1(t)}$. The body stores energy like a neo-Hookean solid during its motion from $\kappa_{p_1(t)}$ to $\kappa_{p_2(t)}$ and $\kappa_{p_2(t)}$ to κ_t.

along with

$$\overset{\nabla}{\mathbf{B}}_3 = -2\mathbf{F}_3\mathbf{D}_G\mathbf{F}_3^T, \quad \overset{\nabla_G}{\mathbf{B}}_2 = -2\mathbf{F}_2\mathbf{D}_1\mathbf{F}_2^T, \tag{2.75}$$

where $\overset{\nabla_G}{\mathbf{A}} := \dot{\mathbf{A}} - \mathbf{A}\mathbf{L}_G^T - \mathbf{L}_G\mathbf{A}$ is the Oldroyd derivative when the natural configuration $\kappa_{p_2(t)}$ is the current configuration. In addition, from Eqs. (2.74) and (2.75), along with the assumption that $\mathbf{F}_2 = \mathbf{V}_2$, $\mathbf{F}_3 = \mathbf{V}_3$ in virtue of the body being isotropic, we get

$$\mathbf{I}.\dot{\mathbf{B}}_2 = 2\mathbf{B}_2.(\mathbf{D}_G - \mathbf{D}_1), \quad \mathbf{I}.\dot{\mathbf{B}}_3 = 2\mathbf{B}_3.(\mathbf{D} - \mathbf{D}_G). \tag{2.76}$$

These relations should suffice for our calculations for studying the response of model 2.

2. Constitutive assumptions

In this model, we shall assume ψ, and ξ, to be of the form

$$\psi \equiv \psi(\mathbf{B}_2, \mathbf{B}_3), \quad \xi \equiv \xi(\mathbf{D}_1, \mathbf{D}_G). \tag{2.77}$$

Now, assuming that the instantaneous elastic responses are isotropic and the body is incompressible, we choose

$$\psi(\mathbf{B}_2, \mathbf{B}_3) = \frac{\mu_2}{2\rho}(\mathbf{I}.\mathbf{B}_2 - 3) + \frac{\mu_3}{2\rho}(\mathbf{I}.\mathbf{B}_3 - 3), \tag{2.78}$$

and

$$\xi(\mathbf{D}_1, \mathbf{D}_G) = \eta_1 \mathbf{D}_1.\mathbf{D}_1 + \eta_G \mathbf{D}_G.\mathbf{D}_G. \tag{2.79}$$

The above assumption implies that the body possesses instantaneous elastic response from the current configuration κ_t to the natural configuration $\kappa_{p_2(t)}$ and from the natural configuration $\kappa_{p_1(t)}$ to the other natural configuration $\kappa_{p_2(t)}$. It stores energy like a neo-Hookean solid during these two motions. In addition, the responses from the two natural configurations $(\kappa_{p_1(t)}, \kappa_{p_1(t)})$ to the reference configuration κ_R are purely dissipative, similar to a linear viscous fluid. In fact, the response of the body as it moves from κ_R to $\kappa_{p_2(t)}$ is similar to that of a "variant" of an Oldroyd-B fluid (see Rajagopal and Srinivasa [6]) i.e., the natural configuration $\kappa_{p_2(t)}$ evolves like that of an Oldroyd-B fluid with respect to the reference configuration κ_R.

On substituting Eqs. (2.78), (2.79) in (2.13), using Eq. (2.76) and simplifying, we get

$$(\mathbf{T} - \mu_3 \mathbf{B}_3).\mathbf{D} + (\mu_3 \mathbf{B}_3 - \mu_2 \mathbf{B}_2).\mathbf{D}_G + \mu_2 \mathbf{B}_2.\mathbf{D}_1 = \eta_1 \mathbf{D}_1.\mathbf{D}_1 + \eta_G \mathbf{D}_G.\mathbf{D}_G. \tag{2.80}$$

Since, the right hand side of Eq. (2.80) does not depend on $\mathbf{D}$, the incompressibility

constraint, $tr(\mathbf{D}) = 0$, leads to

$$\mathbf{T} = -p\mathbf{I} + \mu_3\mathbf{B}_3, \tag{2.81}$$

where $-p\mathbf{I}$ is the reaction stress due to the incompressibility constraint. Using, Eq. (2.81) in (2.80), we must have

$$(\mu_3\mathbf{B}_3 - \mu_2\mathbf{B}_2).\mathbf{D}_G + \mu_2\mathbf{B}_2.\mathbf{D}_1 = \eta_1\mathbf{D}_1.\mathbf{D}_1 + \eta_G\mathbf{D}_G.\mathbf{D}_G. \tag{2.82}$$

Now, we maximize the rate of dissipation by varying $\mathbf{D}_1, \mathbf{D}_G$ for fixed $\mathbf{B}_2, \mathbf{B}_3$ with the constraints

$$tr(\mathbf{D}_1) = 0, \quad tr(\mathbf{D}_G) = 0. \tag{2.83}$$

Finally, we arrive at the following set of equations:

$$\begin{aligned} \mathbf{T} &= -p\mathbf{I} + \mu_3\mathbf{B}_3, \\ \mu_3\mathbf{B}_3 - \mu_2\mathbf{B}_2 &= -p'\mathbf{I} + \eta_G\mathbf{D}_G, \\ \mu_2\mathbf{B}_2 &= -p''\mathbf{I} + \eta_1\mathbf{D}_1, \end{aligned} \tag{2.84}$$

where $p,\ p',\ p''$ are the Lagrange multipliers with

$$\begin{aligned} p' &= -\frac{1}{3}\left[\mu_3 tr(\mathbf{B}_3) - \mu_2 tr(\mathbf{B}_2)\right], \\ p'' &= -\frac{1}{3}\mu_2 tr(\mathbf{B}_2). \end{aligned} \tag{2.85}$$

Pre-multiplying and post-multiplying Eqs. $(2.84)_b$, $(2.84)_c$ by $\mathbf{V}_3$ and $\mathbf{V}_2$ respectively, Eq. (2.84) reduces to

$$\begin{aligned} \mathbf{T} &= -p\mathbf{I} + \mu_3\mathbf{B}_3, \\ \mu_3\mathbf{B}_3^2 - \mu_2\mathbf{V}_3\mathbf{B}_2\mathbf{V}_3 &= -p'\mathbf{B}_3 - \frac{\eta_G}{2}\overset{\nabla}{\mathbf{B}}_3, \\ \mu_2\mathbf{B}_2^2 &= -p''\mathbf{B}_2 - \frac{\eta_1}{2}\overset{\nabla_G}{\mathbf{B}}_2, \end{aligned} \tag{2.86}$$

with Eq. (2.85). If we denote $\mu_2\mathbf{B}_2, \mu_3\mathbf{B}_3$ by $\mathbf{S}_1, \mathbf{S}_2$ respectively, then the final con-

stitutive relations for this model are

$$\begin{aligned} \mathbf{T} &= -p\mathbf{I} + \mathbf{S}_2, \\ \mathbf{S}_1^2 &= \frac{1}{3} tr(\mathbf{S}_1)\mathbf{S}_1 - \frac{\eta_1}{2} \overset{\nabla_G}{\mathbf{S}_1}, \\ \mathbf{S}_2^2 - \sqrt{\mathbf{S}_2}\mathbf{S}_1\sqrt{\mathbf{S}_2} &= \frac{1}{3}\left[tr(\mathbf{S}_2) - tr(\mathbf{S}_1)\right]\mathbf{S}_2 - \frac{\eta_G}{2} \overset{\nabla}{\mathbf{S}_2}\,. \end{aligned} \tag{2.87}$$

3. Reduction of the model to one dimensional Burgers' model

For simplicity, we shall use Eq. (2.84) for the reduction. Now, Eqs. $(2.84)_{b,c}$ can be re-written as

$$\begin{aligned} \mu_3\left(\mathbf{B}_3 - \mathbf{I}\right) - \mu_2\left(\mathbf{B}_2 - \mathbf{I}\right) &= \frac{1}{3}\left[\mu_3\left(tr(\mathbf{B}_3) - 3\right) - \mu_2\left(tr(\mathbf{B}_2) - 3\right)\right]\mathbf{I} + \eta_G\mathbf{D}_G, \\ \mu_2\left(\mathbf{B}_2 - \mathbf{I}\right) &= \frac{1}{3}\mu_2\left(tr(\mathbf{B}_2) - 3\right)\mathbf{I} + \eta_1\mathbf{D}_1. \end{aligned} \tag{2.88}$$

Assuming that the displacement gradient associated with elastic response is small, leads to

$$\|\mathbf{B}_i - \mathbf{I}\| = \mathbf{O}(\gamma), \quad \gamma \ll 1, \quad i = 2, 3. \tag{2.89}$$

The first term on the right hand sides of Eq. $(2.88)_{b,c}$ can be neglected. Then, Eq. (2.88) reduces to

$$\begin{aligned} \mu_3\left(\mathbf{B}_3 - \mathbf{I}\right) - \mu_2\left(\mathbf{B}_2 - \mathbf{I}\right) &= \eta_G\mathbf{D}_G, \\ \mu_2\left(\mathbf{B}_2 - \mathbf{I}\right) &= \eta_1\mathbf{D}_1. \end{aligned} \tag{2.90}$$

In one dimension, Eq. (2.90) becomes

$$\mu_3(\lambda_3^2 - 1) - \mu_2(\lambda_2^2 - 1) = \eta_G\frac{\dot{\lambda_G}}{\lambda_G}, \quad \mu_2(\lambda_2^2 - 1) = \eta_1\frac{\dot{\lambda_1}}{\lambda_1}, \tag{2.91}$$

where λ_i ($i = 1, 2, 3, G$ or no subscript) is the stretch, in one dimension, corresponding to the right stretch tensor $\mathbf{V}_i$. Using $ln\lambda_i = \epsilon_i$ (ϵ is the true strain), with the

assumption of $\epsilon_i \ll 1$, Eq. (2.91) reduces to

$$2\mu_3\epsilon_3 - 2\mu_2\epsilon_2 = \eta_G\dot{\epsilon_G}, \quad 2\mu_2\epsilon_2 = \eta_1\dot{\epsilon}_1. \tag{2.92}$$

In addition, Eq. $(2.84)_a$ reduces to

$$\sigma = 2\mu_3\epsilon_3. \tag{2.93}$$

Eq. (2.73) together with Eq. (2.71), in one dimension, reduces to

$$\epsilon = \epsilon_G + \epsilon_3, \text{ or}, \quad \epsilon_G = \epsilon_2 + \epsilon_1. \tag{2.94}$$

The spring-dashpot arrangement in Fig. 6(b) also yields Eqs. (2.92), (2.93) along with Eqs. (2.61), (2.94). These equations on simplification reduce to

$$\sigma + \left(\frac{\eta_1}{2\mu_2} + \frac{\eta_1}{2\mu_3} + \frac{\eta_G}{2\mu_3}\right)\dot{\sigma} + \frac{\eta_1\eta_G}{4\mu_2\mu_3}\ddot{\sigma} = (\eta_1 + \eta_G)\,\dot{\epsilon} + \frac{\eta_1\eta_G}{2\mu_2}\ddot{\epsilon}, \tag{2.95}$$

which is same as the Burgers' one dimensional model (Eq. (2.1)), with

$$p_1 = \frac{\eta_1}{2\mu_2} + \frac{\eta_1}{2\mu_3} + \frac{\eta_G}{2\mu_3}, \quad p_2 = \frac{\eta_1\eta_G}{4\mu_2\mu_3}, \quad q_1 = \eta_1 + \eta_G, \quad q_2 = \frac{\eta_1\eta_G}{2\mu_2}. \tag{2.96}$$

E. Model 3

1. Preliminaries

As with models 1 and 2, for this model we shall assume that the body has two evolving natural configurations ($\kappa_{p_1(t)}, \kappa_{p_1(t)}$, see Fig. 8). We shall also use the definition of $\mathbf{F}_i, i = 1, 2, 3$ used for the previous models in addition to the definitions in Eqs. (2.16), (2.17) and the relation Eq. (2.18). Further, we shall also choose $\mathbf{F}_2 = \mathbf{V}_2$ and $\mathbf{F}_3 = \mathbf{V}_3$. We recall from the preliminary discussion concerning models 1 and 2,

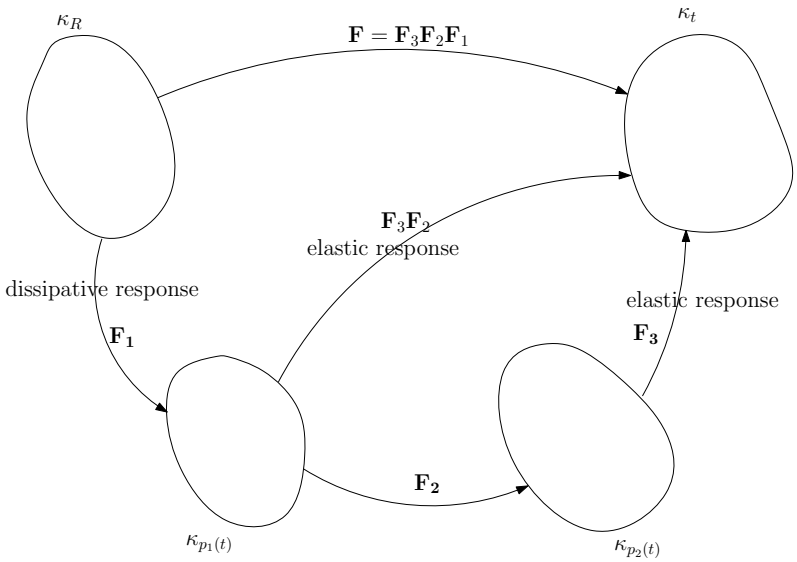

Fig. 8.: Schematic to illustrate the natural configurations for model 3. The body's response is viscous fluid-like and elastic solid-like, during its motion from, κ_R to $\kappa_{p_t(t)}$, and $\kappa_{p_2(t)}$ to κ_t respectively. From $\kappa_{p_1(t)}$ to $\kappa_{p_2(t)}$, the response is Kelvin-Voigt solid-like.

that

$$\mathbf{D}_2 = -\frac{1}{2}\mathbf{V}_3^{-1}\overset{\nabla_p}{\mathbf{B}}_3\,\mathbf{V}_3^{-1}, \quad \mathbf{D}_1 = -\frac{1}{2}\mathbf{V}_2^{-1}\overset{\nabla_G}{\mathbf{B}}_2\,\mathbf{V}_2^{-1}. \tag{2.97}$$

These definitions and relations shall be used in the following analysis.

2. Constitutive assumptions

For this model, we shall assume the specific stored energy, ψ and the rate of dissipation, ξ to be of the form

$$\psi \equiv \psi(\mathbf{B}_2, \mathbf{B}_3), \quad \xi \equiv \xi(\mathbf{D}_1, \mathbf{D}_2). \tag{2.98}$$

Specifically, in virtue of the body being incompressible and isotropic, we choose,

$$\psi(\mathbf{B}_2, \mathbf{B}_3) = \frac{\mu_2}{2\rho}(\mathbf{I}.\mathbf{B}_2 - 3) + \frac{\mu_3}{2\rho}(\mathbf{I}.\mathbf{B}_3 - 3), \tag{2.99}$$

and

$$\xi(\mathbf{D}_1, \mathbf{D}_2) = \eta_1' \mathbf{D}_1.\mathbf{D}_1 + \eta_2' \mathbf{D}_2.\mathbf{D}_2, \tag{2.100}$$

i.e., the body possesses instantaneous elastic response from the current configuration κ_t to the natural configuration $\kappa_{p_2(t)}$ and stores energy like a neo-Hookean solid. Also, the response of the body between $\kappa_{p_1(t)}$ to $\kappa_{p_2(t)}$ is similar to that of a Kelvin-Voigt solid. The body also dissipates like a linear viscous fluid during its motion from κ_R to $\kappa_{p_1(t)}$.

On substituting Eq. (2.99) into Eq. (2.13) and using Eq. (2.33) we get,

$$\mathbf{T}.\mathbf{D} - \mu_2 \mathbf{B}_2.\mathbf{D}_2 - \mu_3 \mathbf{B}_3.\left[\mathbf{D} - \mathbf{D}_2 - \frac{1}{2}\left(\mathbf{F}_2 \mathbf{L}_1 \mathbf{F}_2^{-1} + \mathbf{F}_2^{-T} \mathbf{L}_1^T \mathbf{F}_2^T\right)\right] = \eta_1' \mathbf{D}_1.\mathbf{D}_1 + \eta_2' \mathbf{D}_2.\mathbf{D}_2, \tag{2.101}$$

which reduces to

$$(\mathbf{T} - \mu_3 \mathbf{B}_3).\mathbf{D} + (\mu_3 \mathbf{B}_3 - \mu_2 \mathbf{B}_2).\mathbf{D}_2 + \frac{\mu_3}{2} \mathbf{B}_3.\left(\mathbf{F}_2 \mathbf{L}_1 \mathbf{F}_2^{-1} + \mathbf{F}_2^{-T} \mathbf{L}_1^T \mathbf{F}_2^T\right) = \eta_1' \mathbf{D}_1.\mathbf{D}_1 + \eta_2' \mathbf{D}_2.\mathbf{D}_2. \tag{2.102}$$

Using Eq. (2.102), we maximize the rate of dissipation with incompressibility as a constraint, i.e.,

$$tr(\mathbf{D}) = tr(\mathbf{D}_1) = tr(\mathbf{D}_2) = 0, \tag{2.103}$$

by varying $\mathbf{D}, \mathbf{D}_1, \mathbf{D}_2$ for fixed $\mathbf{B}_2, \mathbf{B}_3$ and get:

$$\begin{aligned} \mathbf{T} &= -p\mathbf{I} + \mu_3 \mathbf{B}_3, \\ \mu_3 \mathbf{B}_3 - \mu_2 \mathbf{B}_2 &= -p'\mathbf{I} + \eta_2 \mathbf{D}_2, \\ \frac{\mu_3}{2}\left(\mathbf{F}_2^T \mathbf{B}_3 \mathbf{F}_2^{-T} + \mathbf{F}_2^{-1} \mathbf{B}_3 \mathbf{F}_2\right) &= -p''\mathbf{I} + \eta_1 \mathbf{D}_1, \end{aligned} \tag{2.104}$$

where $p,\ p',\ p''$ are the Lagrange multipliers with

$$\begin{aligned} -p' &= \frac{1}{3}\left[\mu_3 tr(\mathbf{B}_3) - \mu_2 tr(\mathbf{B}_2)\right], \\ -p'' &= \frac{1}{3}\mu_3 tr(\mathbf{B}_3), \end{aligned} \tag{2.105}$$

and

$$\eta_i = \eta_i' \left(1 - \frac{\mu_3 \mathbf{B}_3 . \mathbf{F}_2 \mathbf{W}_1 \mathbf{F}_2^{-1}}{\eta_1' \mathbf{D}_1 . \mathbf{D}_1 + \eta_2' \mathbf{D}_2 . \mathbf{D}_2} \right), \quad i = 1, 2. \tag{2.106}$$

Pre-multiplying and post-multiplying Eq. $(2.104)_b$ by $\mathbf{V}_3$, pre-multiplying and post-multiplying Eq. $(2.104)_c$ by $\mathbf{V}_2$ and using Eq. (2.97), we find that

$$\begin{aligned} \mathbf{T} &= -p\mathbf{I} + \mu_3 \mathbf{B}_3, \\ \mu_3 \mathbf{B}_3^2 - \mu_2 \mathbf{V}_3 \mathbf{B}_2 \mathbf{V}_3 &= -p' \mathbf{B}_3 - \frac{\eta_2}{2} \overset{\nabla_p}{\mathbf{B}}_3, \\ \frac{\mu_3}{2} \left(\mathbf{B}_2 \mathbf{B}_3 + \mathbf{B}_3 \mathbf{B}_2 \right) &= -p'' \mathbf{B}_2 - \frac{\eta_1}{2} \overset{\nabla_G}{\mathbf{B}}_2, \end{aligned} \tag{2.107}$$

along with Eq. (2.105).

If we call $\mu_3 \mathbf{B}_3, \mu_2 \mathbf{B}_2$ by $\mathbf{S}_1, \mathbf{S}_2$ respectively, then, the final form for the constitutive relation can be given as

$$\begin{aligned} \mathbf{T} &= -p\mathbf{I} + \mathbf{S}_1, \\ \mathbf{S}_1^2 - \sqrt{\mathbf{S}_1} \mathbf{S}_2 \sqrt{\mathbf{S}_1} &= \frac{1}{3} \left[tr(\mathbf{S}_1) - tr(\mathbf{S}_2) \right] \mathbf{S}_1 - \frac{\eta_2}{2} \overset{\nabla_p}{\mathbf{S}}_1, \\ \frac{1}{2} \left(\mathbf{S}_2 \mathbf{S}_1 + \mathbf{S}_1 \mathbf{S}_2 \right) &= \frac{1}{3} tr(\mathbf{S}_1) \mathbf{S}_2 - \frac{\eta_1}{2} \overset{\nabla_G}{\mathbf{S}}_2 . \end{aligned} \tag{2.108}$$

3. Reduction of the model to one dimensional Burgers' model

Following the method used in D.3, Eq. (2.104), in one dimension, reduces to

$$\begin{aligned} \sigma &= 2\mu_3 \epsilon_3, \\ 2\mu_3 \epsilon_3 - 2\mu_2 \epsilon_2 &= \eta_2 \dot{\epsilon}_2, \\ 2\mu_3 \epsilon_3 &= \eta_1 \dot{\epsilon}_1. \end{aligned} \tag{2.109}$$

The above set of equations, can also be obtained from the spring-dashpot arrangement in Fig. 6(c).

Now, Eq. (2.109) can be re-written as

$$\sigma = 2\mu_3\epsilon_3, \quad \sigma = 2\mu_2\epsilon_2 + \eta_2\dot{\epsilon}_2, \quad \sigma = \eta_1\dot{\epsilon}_1. \tag{2.110}$$

Also, differentiating Eq. (2.61) with respect to time and using Eqs. $(2.110)_{a,c}$, we obtain

$$\dot{\epsilon} = \frac{\sigma}{\eta_1} + \frac{\dot{\sigma}}{2\mu_3} + \dot{\epsilon}_2. \tag{2.111}$$

Now, multiplying Eq. (2.111) with $2\mu_2$, multiplying the derivative of Eq. (2.111) with respect to time with η_2; then, adding these two equations, along with Eq. $(2.110)_b$, we get

$$\frac{2\mu_2}{\eta_1}\sigma + \left(1 + \frac{\eta_2}{\eta_1} + \frac{\mu_2}{\mu_3}\right)\dot{\sigma} + \frac{\eta_2}{2\mu_3}\ddot{\sigma} = 2\mu_2\dot{\epsilon} + \eta_2\ddot{\epsilon}, \tag{2.112}$$

re-written as

$$\sigma + \left(\frac{\eta_1}{2\mu_2} + \frac{\eta_2}{2\mu_2} + \frac{\eta_1}{2\mu_3}\right)\dot{\sigma} + \frac{\eta_1\eta_2}{4\mu_2\mu_3}\ddot{\sigma} = \eta_1\dot{\epsilon} + \frac{\eta_1\eta_2}{2\mu_2}\ddot{\epsilon}. \tag{2.113}$$

Thus, Eq. (2.113) has the same form as Eq. (2.1), with

$$p_1 = \frac{\eta_1}{2\mu_2} + \frac{\eta_2}{2\mu_2} + \frac{\eta_1}{2\mu_3}, \quad p_2 = \frac{\eta_1\eta_2}{4\mu_2\mu_3}, \quad q_1 = \eta_1, \quad q_2 = \frac{\eta_1\eta_2}{2\mu_2}. \tag{2.114}$$

F. Model 4

1. Preliminaries

Once again, we shall assume that the body has two natural configurations associated with it, denoted by $\kappa_{p_1(t)}, \kappa_{p_2(t)}$. However, in this model, the evolution equations of the two natural configurations are not coupled and they evolve independently (see Fig. 9). We shall denote the gradients of the motion from κ_R to $\kappa_{p_1(t)}$ and from $\kappa_{p_1(t)}$ to κ_t by $\mathbf{F}_1, \mathbf{F_2}$. We shall also denote the gradients of the motion from κ_R to $\kappa_{p_2(t)}$

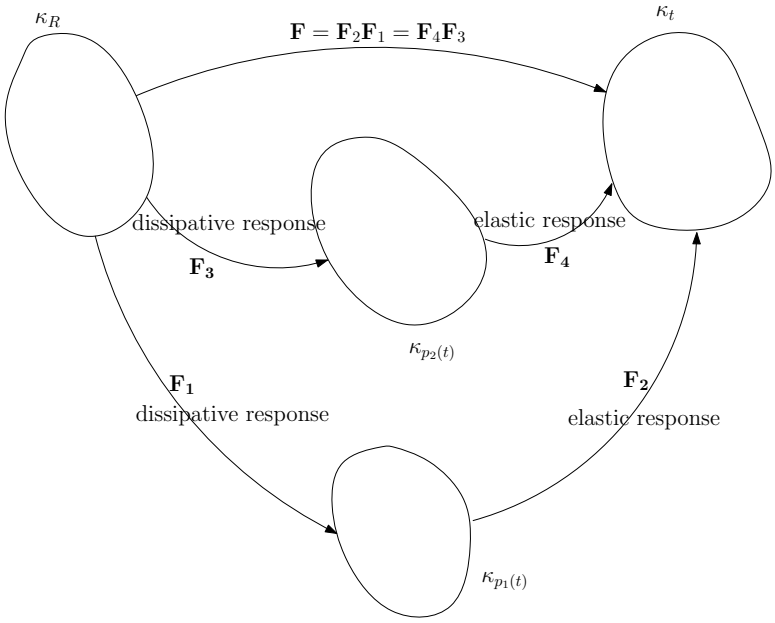

Fig. 9.: Schematic to illustrate the natural configurations for model 4. The body's response is similar to that of a "mixture" of two Maxwell-like fluids with different relaxation times.

and from $\kappa_{p_2(t)}$ to κ_t by $\mathbf{F}_3, \mathbf{F_4}$. It follows that

$$\mathbf{F} = \mathbf{F}_2\mathbf{F}_1 = \mathbf{F}_4\mathbf{F}_3. \tag{2.115}$$

The left stretch tensor, velocity gradient and its corresponding symmetric part are denoted by

$$\mathbf{B}_i := \mathbf{F}_i\mathbf{F}_i^T, \quad \mathbf{L}_i := \dot{\mathbf{F}}_i\mathbf{F}_i^{-1}, \quad \mathbf{D}_i := \frac{1}{2}\left(\mathbf{L}_i + \mathbf{L}_i^T\right), \quad i = 1, 2, 3, 4. \tag{2.116}$$

Also, a straightforward calculation leads to

$$\overset{\nabla}{\mathbf{B}}_2 = -2\mathbf{F}_2\mathbf{D}_1\mathbf{F}_2^T, \quad \overset{\nabla}{\mathbf{B}}_4 = -2\mathbf{F}_4\mathbf{D}_3\mathbf{F}_4^T. \tag{2.117}$$

2. Constitutive assumptions

Here, we shall assume the specific stored energy, ψ and the rate of dissipation, ξ to be of the form

$$\psi \equiv \psi(\mathbf{B}_2, \mathbf{B}_4), \quad \xi \equiv \xi(\mathbf{D}_1, \mathbf{D}_3). \tag{2.118}$$

As the material is isotropic and incompressible, we choose,

$$\psi(\mathbf{B}_2, \mathbf{B}_4) = \frac{\mu_2}{2\rho}(\mathbf{I}.\mathbf{B}_2 - 3) + \frac{\mu_4}{2\rho}(\mathbf{I}.\mathbf{B}_4 - 3), \tag{2.119}$$

and

$$\xi(\mathbf{D}_1, \mathbf{D}_3) = \eta_1 \mathbf{D}_1.\mathbf{D}_1 + \eta_3 \mathbf{D}_3.\mathbf{D}_3. \tag{2.120}$$

This means that the response of the natural configurations $(\kappa_{p_1(t)}, \kappa_{p_2(t)})$ from the current configuration is like that of a neo-Hookean solid and the response from the reference configuration to the natural configurations is similar to that of a linear viscous fluid. Thus, Burgers' fluid can also be perceived as a "mixture" of two Maxwell-like fluids with different relaxation times.

We shall set

$$\mathbf{F}_2 = \mathbf{V}_2, \quad \mathbf{F}_4 = \mathbf{V}_4, \tag{2.121}$$

where $\mathbf{V}_2, \mathbf{V}_4$ are the right stretch tensors in the polar decomposition of $\mathbf{F}_2, \mathbf{F}_4$, based on the assumption of isotropic elastic response. Hence, from Eq. (2.117) and Eq. (2.121), we have

$$\mathbf{I}.\dot{\mathbf{B}}_2 = 2\mathbf{B}_2.(\mathbf{D} - \mathbf{D}_1), \quad \mathbf{I}.\dot{\mathbf{B}}_4 = 2\mathbf{B}_4.(\mathbf{D} - \mathbf{D}_3). \tag{2.122}$$

On entering Eqs. (2.119), (2.120) in Eq. (2.13) and using Eq. (2.122), we get

$$(\mathbf{T} - \mu_2 \mathbf{B}_2 - \mu_4 \mathbf{B}_4).\mathbf{D} + \mu_2 \mathbf{B}_2.\mathbf{D}_1 + \mu_4 \mathbf{B}_4.\mathbf{D}_3 = \eta_1 \mathbf{D}_1.\mathbf{D}_1 + \eta_3 \mathbf{D}_3.\mathbf{D}_3. \tag{2.123}$$

Using the constraint of incompressibility

$$tr(\mathbf{D}) = tr(\mathbf{D}_1) = tr(\mathbf{D}_3) = 0, \tag{2.124}$$

and Eq. (2.123), we maximize the rate of dissipation by varying $\mathbf{D}, \mathbf{D}_1, \mathbf{D}_3$ for fixed $\mathbf{B}_2, \mathbf{B}_4$ and get:

$$\begin{aligned} \mathbf{T} &= -p\mathbf{I} + \mu_2\mathbf{B}_2 + \mu_4\mathbf{B}_4, \\ \mu_2\mathbf{B}_2 &= -p'\mathbf{I} + \eta_1\mathbf{D}_1, \\ \mu_4\mathbf{B}_4 &= -p''\mathbf{I} + \eta_3\mathbf{D}_3, \end{aligned} \tag{2.125}$$

where $p,\ p',\ p''$ are the Lagrange multipliers with

$$-p' = \frac{1}{3}\mu_2 tr(\mathbf{B}_2), \quad -p'' = \frac{1}{3}\mu_4 tr(\mathbf{B}_4). \tag{2.126}$$

Pre-multiplying and post-multiplying, Eq. $(2.125)_b$ by $\mathbf{V}_2$, and Eq. $(2.125)_c$ by $\mathbf{V}_4$; then, using Eq. (2.117), we arrive at

$$\begin{aligned} \mu_2\mathbf{B}_2^2 &= -p'\mathbf{B}_2 - \frac{\eta_1}{2}\overset{\nabla}{\mathbf{B}}_2, \\ \mu_4\mathbf{B}_4^2 &= -p''\mathbf{B}_4 - \frac{\eta_3}{2}\overset{\nabla}{\mathbf{B}}_4, \end{aligned} \tag{2.127}$$

Eqs. $(2.127)_{a,b}$ represents the evolution equations of the natural configurations ($\kappa_{p_1(t)}, \kappa_{p_2(t)}$ respectively). If we denote $\mu_2\mathbf{B}_2, \mu_4\mathbf{B}_4$ by $\mathbf{S}_1, \mathbf{S}_2$ respectively, then the final constitutive relations, for model 4, are

$$\begin{aligned} \mathbf{T} &= -p\mathbf{I} + \mathbf{S}_1 + \mathbf{S}_2, \\ \mathbf{S}_1^2 &= \frac{1}{3}tr(\mathbf{S}_1)\mathbf{S}_1 - \frac{\eta_1}{2}\overset{\nabla}{\mathbf{S}}_1, \\ \mathbf{S}_2^2 &= \frac{1}{3}tr(\mathbf{S}_2)\mathbf{S}_2 - \frac{\eta_1}{2}\overset{\nabla}{\mathbf{S}}_2\ . \end{aligned} \tag{2.128}$$

This model is a variation of the model proposed by Murali Krishnan and Rajagopal [33]. They considered stretch dependent dissipation, in contrast to our linear viscous

fluid type dissipation.

3. Reduction of the model to the one dimensional Burgers' model

For this model, we shall once again assume that the displacement gradient associated with the elastic response is small, and thus

$$\|\mathbf{B}_i - \mathbf{I}\| = \mathbf{O}(\gamma), \quad \gamma \ll 1, \quad i = 2, 4. \tag{2.129}$$

Then, Eq. (2.125) becomes

$$\begin{aligned} \mathbf{T} &= -p\mathbf{I} + \mu_2\mathbf{B}_2 + \mu_4\mathbf{B}_4, \\ \mu_2\left(\mathbf{B}_2 - \mathbf{I}\right) &= \eta_1\mathbf{D}_1, \\ \mu_4\left(\mathbf{B}_4 - \mathbf{I}\right) &= \eta_3\mathbf{D}_3, \end{aligned} \tag{2.130}$$

which in one dimension reduces to

$$\begin{aligned} \sigma &= 2\mu_2\epsilon_2 + 2\mu_4\epsilon_4, \\ 2\mu_2\epsilon_2 &= \eta_1\dot{\epsilon}_1, \\ 2\mu_4\epsilon_4 &= \eta_3\dot{\epsilon}_3. \end{aligned} \tag{2.131}$$

Further, Eq. (2.115), in one dimension, reduces to

$$\epsilon = \epsilon_2 + \epsilon_1 = \epsilon_3 + \epsilon_4. \tag{2.132}$$

In fact, the spring-dashpot arrangement Fig. 6(d) leads to Eq. (2.131), (2.132). We shall now show that these two equations, on simplification lead to Eq. (2.1). Differentiating Eq. (2.132) with respect to time and using Eq. $(2.131)_{b,c}$, we have

$$\begin{aligned} \dot{\epsilon} &= \frac{2\mu_2}{\eta_1}\epsilon_2 + \dot{\epsilon}_2, \\ \dot{\epsilon} &= \frac{2\mu_4}{\eta_3}\epsilon_4 + \dot{\epsilon}_4. \end{aligned} \tag{2.133}$$

Eliminating ϵ_4 from Eq. $(2.131)_a$ and Eq. $(2.133)_b$ leads to

$$\dot{\epsilon} = \frac{\sigma}{\eta_3} + \frac{\dot{\sigma}}{2\mu_4} - \frac{2\mu_2}{\eta_3}\epsilon_2 - \frac{\mu_2}{\mu_4}\dot{\epsilon}_2. \tag{2.134}$$

Solving Eq. $(2.133)_a$ and Eq. (2.134) simultaneously, we get

$$\begin{aligned} \epsilon_2 &= \frac{\left(1+\frac{\mu_2}{\mu_4}\right)\dot{\epsilon} - \frac{\sigma}{\eta_3} - \frac{\dot{\sigma}}{2\mu_4}}{\frac{2\mu_2}{\eta_1}\left(\frac{\mu_2}{\mu_4} - \frac{\eta_1}{\eta_3}\right)}, \\ \dot{\epsilon}_2 &= \frac{\left(1+\frac{\eta_1}{\eta_3}\right)\dot{\epsilon} - \frac{\sigma}{\eta_3} - \frac{\dot{\sigma}}{2\mu_4}}{\frac{\eta_1}{\eta_3} - \frac{\mu_2}{\mu_4}}. \end{aligned} \tag{2.135}$$

Now, differentiating Eq. $(2.135)_a$ with respect to time and equating it to Eq. $(2.135)_b$, we get

$$\sigma + \left(\frac{\eta_1}{2\mu_2} + \frac{\eta_3}{2\mu_4}\right)\dot{\sigma} + \frac{\eta_1\eta_3}{4\mu_3\mu_4}\ddot{\sigma} = (\eta_1+\eta_3)\,\dot{\epsilon} + \frac{\eta_1\eta_3}{2\mu_2}\left(1+\frac{\mu_2}{\mu_4}\right)\ddot{\epsilon}. \tag{2.136}$$

This is of the same form as Eq. (2.1) with

$$p_1 = \frac{\eta_1}{2\mu_2} + \frac{\eta_3}{2\mu_4}, \quad p_2 = \frac{\eta_1\eta_3}{4\mu_3\mu_4}, \quad q_1 = \eta_1+\eta_3, \quad q_2 = \frac{\eta_1\eta_3}{2\mu_2}\left(1+\frac{\mu_2}{\mu_4}\right). \tag{2.137}$$

G. Final remarks

We have shown four sets of energy storage and rate of dissipation which lead to four different three dimensional constitutive relations, which reduce in one dimension to the model developed by Burgers (Eq. (2.1)). Each of these three dimensional models can claim equal status as representing the three dimensional generalization of Burgers' model. We have chosen two natural configurations instead of one in all of these models. This is to incorporate two relaxation times possessed by Burgers-like fluid bodies. For example, in an asphalt concrete mixture (which has been shown to exhibit Burgers-like fluid behavior), the aggregate matrix has a small relaxation time whereas the asphalt mortar matrix has relatively larger relaxation time (see

[33]) and the choice of two natural configurations seems natural. It is possible that several other choices for the stored energy and the rate of dissipation could lead to the same one dimensional model due to Burgers. Interestingly, the structure of the three dimensional models that we have developed are quite distinct.

CHAPTER III

A THERMODYNAMIC FRAMEWORK TO DEVELOP RATE-TYPE MODELS FOR FLUIDS WITHOUT INSTANTANEOUS ELASTICITY*

In this chapter, we apply the thermodynamic framework recently put into place by Rajagopal and co-workers, to develop rate-type models for viscoelastic fluids which do not possess instantaneous elasticity. To illustrate the capabilities of such models we make a specific choice for the specific Helmholtz potential and the rate of dissipation and consider the creep and stress relaxation response associated with the model. Given specific forms for the Helmholtz potential and the rate of dissipation, the rate of dissipation is maximized with the constraint that the difference between the stress power and the rate of change of Helmholtz potential is equal to the rate of dissipation and any other constraint that may be applicable such as incompressibility. We show that the model that is developed exhibits fluid-like characteristics and is incapable of instantaneous elastic response. It also includes Maxwell-like and Kelvin-Voigt-like viscoelastic materials (when certain material moduli take special values).

A. Introduction

Recently, a thermodynamic framework has been put into place to describe the response of dissipative bodies that includes a large class of viscoelastic bodies (see Rajagopal and Srinivasa [40, 29], for details of the framework). With regard to the response of viscoelastic bodies, they consider the response to be that of a class of elastic bodies from an evolving set of configurations which they refer to as natural

*With kind permission from Springer Science + Business Media: Acta Mechanica, A thermodynamic framework to develop rate-type models for fluids without instantaneous elasticity, 205(1), 2009, 105–119, Satish Karra and K. R. Rajagopal.

configurations (also see Eckart [41], Rajagopal [34]). The evolution of the natural configuration is determined by the rate of dissipation, or to be more precise, the maximization of the rate of dissipation. In a purely mechanical context, the response of the material is characterized by constitutively prescribing the stored energy (or Helmholtz potential) and the rate of dissipation functions. Since in a closed system the entropy increases to achieve its maximum equilibrium value, the quickest way in which the maximum could be reached is by maximizing the rate of dissipation. Of course, this is a plausible assumption and not a "principle". Also, to require such a criterion for an open system is not on very sound footing. However, it is surprising how well such a requirement works. Using such a thermodynamic framework a variety of material responses such as viscoelasticity [6, 20], twinning [42], solid-solid phase transition [43], plasticity [44], crystallization of polymers [45, 46], single crystal super alloys [47, 48], response of multi-network polymers [49] and anisotropic liquids [50] have been modelled. Particularly in viscoelasticity, this framework has been used to generalize one dimensional models due to Maxwell [2], Kelvin [3] and Voigt [4], Burgers [32], and the standard linear solid to three dimensions [6, 51, 33, 52]. Moreover, recently, it has been shown within the context of Maxwell fluid [31] that by choosing different forms for the stored energy and the rate of dissipation, one can obtain the same constitutive relation for stress. It has also been shown (see [53]) that this framework leads to more than one three dimensional model that reduce within the context of one dimension to Burgers' fluid model.

Based on the aforementioned general framework, Rajagopal and Srinivasa [6] have developed a methodology to obtain rate-type models for fluids which possess instantaneous elasticity and in particular have derived a three dimensional generalization for the one dimensional Maxwell model (with the mechanical analog – a spring and a dashpot in series). When one assumes that the displacement gradients

are small, this non-linear model leads to the classical upper convected Maxwell model. The aim of this chapter is to use the framework to develop rate-type models for fluids which do not possess instantaneous elasticity. Specifically, we shall assume that the response from the natural configuration to the current configuration is akin to that of a generalized Kelvin-Voigt solid. Upon removal of external load, the body moves to the natural configuration with some "relaxation time" which is greater than the intrinsic time t_m (also see [38]). By setting this relaxation time to a value less than t_m, one can obtain the class of models that can be generated using the framework in [6] and thus our work here can be viewed as a generalization of the analysis in [6]. As an example, using our framework, we develop constitutive relations which in one dimension reduces to a dashpot and a Kelvin-Voigt element (which is a spring and a dashpot in parallel), in series (see section (E)). In carrying out the maximization of the rate of entropy production, one needs to decide what one maximizes with respect to. In most of the studies that have been cited, the maximization is with respect to appropriate kinematical variables and determining a constitutive representation for the stress. On the other hand, one could maximize with respect to the stress. In all the problems considered thus far, both methods lead to the same answer in explicit constitutive theories. However, it is possible to obtain a much larger class of constitutive relations following the latter procedure (see [37]). Also, from a philosophical perspective it is preferable to use the latter procedure. We shall not get into these issues here. In this chapter we maximize with respect to the kinematical variables and obtain a constitutive expression for the stress.

While the idea of maximizing the rate of dissipation was also enunciated by Ziegler [54], Wehrli and Ziegler [55] our philosophy, interpretation and use of the maximization of the rate of entropy production is quite different, and the difference is not minor. We have discussed the differences in our approach in some detail in [37].

In fact, Ziegler's approach cannot be used to obtain a whole host of models including a whole class of implicit constitutive relations (see [37]). Also, the original work of Ziegler contains certain mathematical errors as pointed out in [29].

It is appropriate to remark that the procedure adopted here, namely maximizing the rate of entropy production does not stand in contradiction with the procedure of minimizing entropy production that was introduced by Onsager [56] (see also Glansdorff and Prigogine [57], Prigogine [58]) as they refer to totally different circumstances. Maximization of the rate of entropy production leads to a constitutive choice amongst a competing class of constitutive relations. It leads to a rate of entropy production that is non-negative that can be viewed as a Lyapunov function. In time, this Lyapunov function reaches a minimum as the system or body under consideration tends towards equilibrium in time. It is this latter minimum that Onsager appeals to and is referred to as Onsager's "principle". This "principle" is however not a general principle and holds for special materials undergoing special processes. Rajagopal and Srinivasa [38] discuss how the ideas of Onsager can be generalized to include non-linear phenomenological laws.

After a discussion of the preliminaries in the next section, we develop a general framework for the development of constitutive models for viscoelastic bodies that do not possess instantaneous elastic response in sub-section (C.1). Within our general framework, we derive a specific model in sub-section (C.2) which stores energy like a neo-Hookean solid with a rate of dissipation which depends on the stretching tensor of the natural configuration and the stretching tensor between the natural configuration and the current configuration. In sub-section (C.3), we show that our model reduces to either the Maxwell-like fluid or the Kelvin-Voigt-like solid under certain restrictions on the material parameters. We shall solve the problem of uniaxial extension in section (D), followed by some remarks on the application of our framework to develop models

for visco-elasto-plastic response in section (F).

B. Preliminaries

Let $\kappa_R(\mathcal{B})$ and $\kappa_t(\mathcal{B})$ denote the reference configuration and the configuration of the body $\mathcal{B}$ at time t (or the current configuration), respectively. Let $\mathbf{X}$ denote a typical point belonging to $\kappa_R(\mathcal{B})$ and $\mathbf{x}$ the same material point at time t, belonging to $\kappa_t(\mathcal{B})$. Let χ_{κ_R} denote a one to one mapping that assigns to each $\mathbf{X} \in \kappa_R(\mathcal{B})$, a point $\mathbf{x} \in \kappa_t(\mathcal{B})$, i.e.,

$$\mathbf{x} := \chi_{\kappa_R}(\mathbf{X}, t)\,. \tag{3.1}$$

We shall assume that χ_{κ_R} is a sufficiently smooth mapping. The velocity $\mathbf{v}$, the velocity gradient $\mathbf{L}$ and the deformation gradient $\mathbf{F}_{\kappa_R}$ are defined through

$$\mathbf{v} := \frac{\partial \chi_{\kappa_R}}{\partial t}, \quad \mathbf{L} := \frac{\partial \mathbf{v}}{\partial \mathbf{x}}, \quad \mathbf{F}_{\kappa_R} := \frac{\partial \chi_{\kappa_R}}{\partial \mathbf{X}}. \tag{3.2}$$

It immediately follows that

$$\mathbf{L} = \dot{\mathbf{F}}_{\kappa_R} \mathbf{F}_{\kappa_R}^{-1}, \tag{3.3}$$

and the symmetric part of the velocity gradient $\mathbf{D}$ is given by

$$\mathbf{D} := \frac{1}{2}\left(\mathbf{L} + \mathbf{L}^T\right), \tag{3.4}$$

where $(.)^T$ denotes transpose of a second order tensor. The left and right Cauchy-Green stretch tensors $\mathbf{B}_{\kappa_R}$ and $\mathbf{C}_{\kappa_R}$ are defined through

$$\mathbf{B}_{\kappa_R} := \mathbf{F}_{\kappa_R} \mathbf{F}_{\kappa_R}^T, \quad \mathbf{C}_{\kappa_R} := \mathbf{F}_{\kappa_R}^T \mathbf{F}_{\kappa_R}. \tag{3.5}$$

Let $\kappa_{p(t)}$ denote the natural configuration associated with the configuration κ_t. We define $\mathbf{F}_{\kappa_{p(t)}}$ as the mapping from the tangent space at a material point in $\kappa_{p(t)}$ to the tangent space at the same material point at κ_t (see Fig. 10). Similar to

Eq. (3.5), we can also define the left and right Cauchy-Green tensors from the natural configuration to the current configuration[1]

$$\mathbf{B}_{\kappa_{p(t)}} := \mathbf{F}_{\kappa_{p(t)}}\mathbf{F}^{T}_{\kappa_{p(t)}}, \quad \mathbf{C}_{\kappa_{p(t)}} := \mathbf{F}^{T}_{\kappa_{p(t)}}\mathbf{F}_{\kappa_{p(t)}}. \tag{3.6}$$

The mapping $\mathbf{G}$ is defined through (see Fig. 10)

$$\mathbf{G} := \mathbf{F}_{\kappa_R \to \kappa_{p(t)}} := \mathbf{F}^{-1}_{\kappa_{p(t)}}\mathbf{F}_{\kappa_R}. \tag{3.7}$$

$\mathbf{F}_{\kappa_{p(t)}}$ and hence $\mathbf{B}_{\kappa_{p(t)}}$ can be determined if one knows the current configuration and the natural configuration corresponding to the current configuration. This natural configuration is attained by removing the external stimuli present in the current configuration. For instance, in classical plasticity where one has infinity of natural configurations from which one has a one-parameter family of elastic responses, the natural configuration and hence $\mathbf{F}_{\kappa_{p(t)}}$ is determined by instantaneously elastically unloading. The same can be done for viscoelastic fluids which are capable of instantaneous elastic response. In our case, the material does not posses an instantaneous elastic response and the natural configuration is obtained by removing the external stimuli consistent with the class of thermodynamic processes that are allowable.

We define the tensors $\mathbf{B}_G$, $\mathbf{L}_G$ and $\mathbf{D}_G$ through

$$\mathbf{B}_G := \mathbf{B}_{\kappa_R \to \kappa_{p(t)}} = \mathbf{G}\mathbf{G}^{T}, \quad \mathbf{L}_G := \dot{\mathbf{G}}\mathbf{G}^{-1}, \quad \mathbf{D}_G := \frac{1}{2}\left(\mathbf{L}_G + \mathbf{L}_G^{T}\right). \tag{3.8}$$

In addition, let the tensors $\mathbf{L}_{p(t)}$ and $\mathbf{D}_{p(t)}$ be defined by

$$\mathbf{L}_{p(t)} := \dot{\mathbf{F}}_{\kappa_{p(t)}}\mathbf{F}^{-1}_{\kappa_{p(t)}}, \quad \mathbf{D}_{p(t)} := \frac{1}{2}\left(\mathbf{L}_{p(t)} + \mathbf{L}^{T}_{p(t)}\right). \tag{3.9}$$

[1]In this chapter, henceforth we shall suppress κ and denote $\mathbf{B}_{\kappa_{p(t)}}$ by $\mathbf{B}_{p(t)}$.

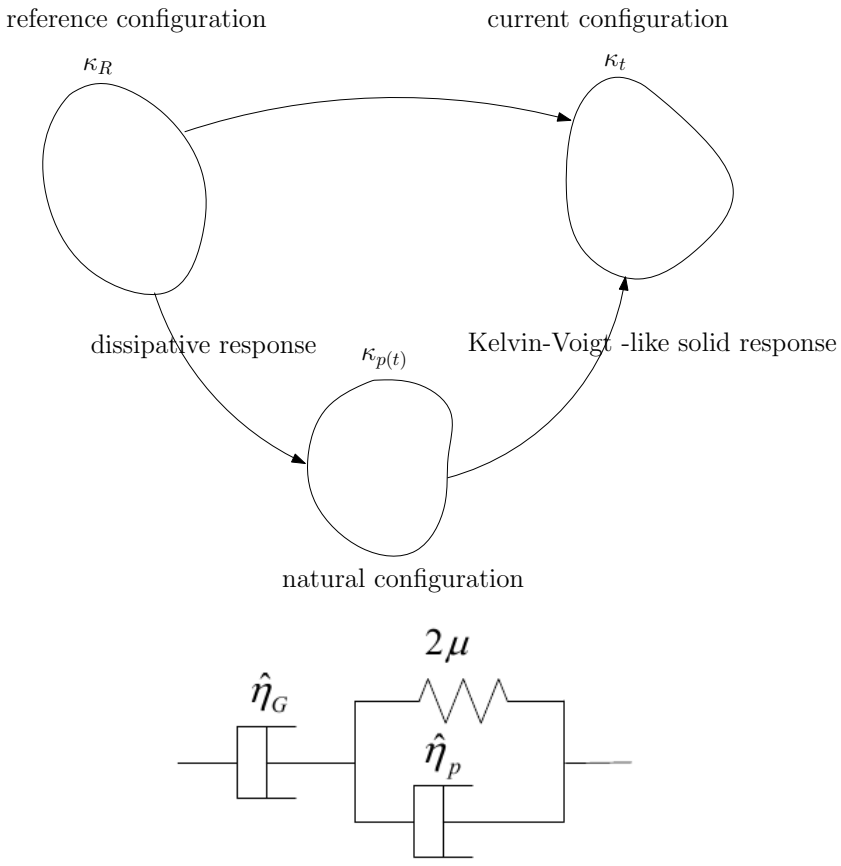

Fig. 10.: Schematic of the natural configuration $\kappa_{p(t)}$ corresponding to the current configuration κ_t and the relevant mappings from the tangent spaces of the same material point in κ_R, κ_t and $\kappa_{p(t)}$ (above). The response from the natural configuration $\kappa_{p(t)}$ is like a Kelvin-Voigt solid and the response of $\kappa_{p(t)}$ from the reference configuration κ_R is purely dissipative. The corresponding one-dimensional spring dashpot analogy where a dashpot is in series with a Kelvin-Voigt element (below).

Also, the principal invariants of $\mathbf{B}_{p(t)}$ are denoted by

$$I_{\mathbf{B}_{p(t)}} = tr(\mathbf{B}_{p(t)}), \quad II_{\mathbf{B}_{p(t)}} = \frac{1}{2}\left[(tr(\mathbf{B}_{p(t)}))^2 - tr(\mathbf{B}^2_{p(t)})\right], \quad III_{\mathbf{B}_{p(t)}} = det(\mathbf{B}_{p(t)}), \tag{3.10}$$

where $tr(.)$ is the trace operator for a second order tensor and $det(.)$ is the determinant of a second order tensor.

Now, from Eq. (3.7):

$$\begin{aligned} &\dot{\mathbf{F}}_{\kappa_R} = \dot{\mathbf{F}}_{\kappa_{p(t)}}\mathbf{G} + \mathbf{F}_{\kappa_{p(t)}}\dot{\mathbf{G}} \\ &\Rightarrow \dot{\mathbf{F}}_{\kappa_R}\mathbf{F}^{-1}_{\kappa_R} = \dot{\mathbf{F}}_{\kappa_{p(t)}}\mathbf{G}\mathbf{G}^{-1}\mathbf{F}^{-1}_{\kappa_{p(t)}} + \mathbf{F}_{\kappa_{p(t)}}\dot{\mathbf{G}} \\ &\Rightarrow \mathbf{L} = \mathbf{L}_{p(t)} + \mathbf{F}_{\kappa_{p(t)}}\mathbf{L}_G\mathbf{F}^{-1}_{\kappa_{p(t)}}. \end{aligned} \tag{3.11}$$

where $\dot{(.)}$ is the material time derivative of the second order tensor given by

$$\dot{\mathbf{A}} := \frac{\partial(\mathbf{A})}{\partial t} + grad(\mathbf{A})[\mathbf{v}], \tag{3.12}$$

for a second order tensor $\mathbf{A}$ with $grad(.)$ being the gradient of a second order tensor with respect to the current configuration κ_t. Hence, from Eq. (3.11),

$$\mathbf{L}^T = \mathbf{L}^T_{p(t)} + \mathbf{F}^{-T}_{\kappa_{p(t)}}\mathbf{L}^T_G\mathbf{F}^T_{\kappa_{p(t)}}, \tag{3.13}$$

and so

$$\mathbf{D} = \mathbf{D}_{p(t)} + \frac{1}{2}\left[\mathbf{F}_{\kappa_{p(t)}}\mathbf{L}_G\mathbf{F}^{-1}_{\kappa_{p(t)}} + \mathbf{F}^{-T}_{\kappa_{p(t)}}\mathbf{L}^T_G\mathbf{F}^T_{\kappa_{p(t)}}\right]. \tag{3.14}$$

Further, we note that the upper convected Oldroyd derivative [36] (also see [44] for the interpretation of Oldroyd derivative within the context of theory of multiple natural configurations) of $\mathbf{B}_{p(t)}$ can be related to $\mathbf{D}_G$ through (see [6])

$$\overset{\nabla}{\mathbf{B}}_{p(t)} := \dot{\mathbf{B}}_{p(t)} - \mathbf{L}\mathbf{B}_{p(t)} - \mathbf{B}_{p(t)}\mathbf{L}^T = -2\mathbf{F}_{\kappa_{p(t)}}\mathbf{D}_G\mathbf{F}^T_{\kappa_{p(t)}}. \tag{3.15}$$

Assuming that the body under consideration is incompressible, we shall record

the balance of mass, and the balance of linear and angular momentum (in the absence of body couples):

$$div(\mathbf{v}) = 0, \quad \rho\dot{\mathbf{v}} = div(\mathbf{T}^T) + \rho\mathbf{b}, \quad \mathbf{T} = \mathbf{T}^T, \tag{3.16}$$

where ρ is the density, $\mathbf{v}$ is the velocity, $\mathbf{T}$ is the Cauchy stress tensor, $\mathbf{b}$ is the specific body force and $div(.)$ is the divergence operator with respect to current configuration κ_t. In addition, the local form of balance of energy is

$$\rho\dot{\epsilon} = \mathbf{T}.\mathbf{L} - div(\mathbf{q}) + \rho r, \tag{3.17}$$

where ϵ denotes the specific internal energy, $\mathbf{q}$ denotes the heat flux vector and r denotes the specific radiant heating.

Finally, we shall assume that the body under consideration undergoes isothermal processes. It is easy to modify the procedure to take into account non-isothermal processes. We shall invoke the second law of thermodynamics in the form of the *reduced energy dissipation equation*, given by (see [29]):

$$\mathbf{T}.\mathbf{D} - \rho\dot{\psi} = \rho\theta\zeta := \xi \geq 0, \tag{3.18}$$

where $\mathbf{T}$ is the Cauchy stress, ψ is the specific Helmholtz free energy, ζ is the rate of entropy production and ξ is the rate of dissipation[2].

[2]The terminology rate of dissipation usually refers to the conversion of working into energy in thermal form (heat). However, while considering general non-isothermal processes one uses the term to the product of the density, temperature and entropy production.

C. Constitutive assumptions

1. General framework

In this sub-section, we shall first constitutively specify general forms for the specific Helmholtz potential ψ and the rate of dissipation ξ. Using Eq. (3.18) and incompressibility as constraints, we shall maximize the rate of dissipation ξ, to obtain our constitutive relations.

We shall assume that during its motion from $\kappa_{p(t)}$ to κ_t, the body stores energy as well as dissipates. The storage is due to elongation of the polymer networks. Now, assuming that the response of the body from $\kappa_{p(t)}$ to κ_t is that of an isotropic body along with the assumption of incompressibility, we shall choose the specific Helmholtz free energy to be a function of the Cauchy-Green left stretch tensor $\mathbf{B}_{p(t)}$, i.e.,

$$\psi = \psi(\mathbf{B}_{p(t)}) = \hat{\psi}(I_{\mathbf{B}_{p(t)}}, II_{\mathbf{B}_{p(t)}}). \tag{3.19}$$

The prescription of the stored energy as shown in Eq. (3.19) is no different for instance from finite plasticity theory wherein the stored energy of the elastic response has such a form. Of course, one cannot determine the exact form of any function from any number of experiments as infinity of function could pass through any finite number of points, and it is only this information one can obtain from experiments. All one can do is to make a reasonable choice based on experimental data.

Eq. (3.19) implies that,

$$\dot{\psi} = 2\left[\left(\frac{\partial\hat{\psi}}{\partial I_{\mathbf{B}_{p(t)}}} + I_{\mathbf{B}_{p(t)}}\frac{\partial\hat{\psi}}{\partial II_{\mathbf{B}_{p(t)}}}\right)\mathbf{B}_{p(t)} - \frac{\partial\hat{\psi}}{\partial II_{\mathbf{B}_{p(t)}}}\mathbf{B}^2_{p(t)}\right].\mathbf{D}_{p(t)}. \tag{3.20}$$

Also, we shall assume the rate of dissipation to be a function of the stretching tensor and Cauchy-Green left stretch tensor between the $\kappa_{p(t)}$ to κ_t, the stretching tensor

between κ_R and $\kappa_{p(t)}$, i.e.,

$$\xi_m = \xi_m(\mathbf{B}_{p(t)}, \mathbf{D}_{p(t)}, \mathbf{D}_G). \tag{3.21}$$

In other words, the body dissipates energy during its motion from $\kappa_{p(t)}$ to κ_t (due to continuous scission and healing of polymer networks) and also dissipates energy during its motion from κ_R to $\kappa_{p(t)}$ (due to sliding of polymer strands over one another).

Due to the assumption of isotropic elastic response, the stored energy remains unchanged under any rotation. Hence, for our calculations, we shall assume that the natural configuration is rotated such that[3]

$$\mathbf{F}_{\kappa_{p(t)}} = \mathbf{V}_{\kappa_{p(t)}}, \tag{3.22}$$

and therefore

$$\begin{aligned} \mathbf{D}_{p(t)} &= \frac{1}{2}\left(\dot{\mathbf{V}}_{\kappa_{p(t)}}\mathbf{V}^{-1}_{\kappa_{p(t)}} + \mathbf{V}^{-1}_{\kappa_{p(t)}}\dot{\mathbf{V}}_{\kappa_{p(t)}}\right) \\ &= \frac{1}{2}\mathbf{V}^{-1}_{\kappa_{p(t)}}\dot{\mathbf{B}}_{p(t)}\mathbf{V}^{-1}_{\kappa_{p(t)}}. \end{aligned} \tag{3.23}$$

On substituting Eq. (3.20) into Eq. (3.18), we get

$$\mathbf{T}.\mathbf{D} - \mathbf{T}_{p(t)}.\mathbf{D}_{p(t)} = \xi_m(\mathbf{B}_{p(t)}, \mathbf{D}_{p(t)}, \mathbf{D}_G), \tag{3.24}$$

where

$$\mathbf{T}_{p(t)} := 2\rho\left[\left(\frac{\partial\hat{\psi}}{\partial I_{B_{p(t)}}} + I_{B_{p(t)}}\frac{\partial\hat{\psi}}{\partial II_{B_{p(t)}}}\right)\mathbf{B}_{p(t)} - \frac{\partial\hat{\psi}}{\partial II_{B_{p(t)}}}\mathbf{B}^2_{p(t)}\right]. \tag{3.25}$$

[3]For the application of this thermodynamic framework to anisotropic fluids the reader should refer to [50].

Substituting Eq. (3.14) into Eq. (3.24), we obtain that

$$\frac{1}{2}\mathbf{T}.\left(\mathbf{F}_{\kappa_{p(t)}}\mathbf{L}_G\mathbf{F}^{-1}_{\kappa_{p(t)}}+\mathbf{F}^{-T}_{\kappa_{p(t)}}\mathbf{L}^T_G\mathbf{F}^T_{\kappa_{p(t)}}\right)+\left(\mathbf{T}-\mathbf{T}_{p(t)}\right).\mathbf{D}_{p(t)}=\xi_m(\mathbf{B}_{p(t)},\mathbf{D}_{p(t)},\mathbf{D}_G). \tag{3.26}$$

Since $\mathbf{T}$ is symmetric, Eq. (3.26) reduces to

$$\mathbf{F}^T_{\kappa_{p(t)}}\mathbf{T}\mathbf{F}^{-T}_{\kappa_{p(t)}}.\mathbf{L}_G+\left(\mathbf{T}-\mathbf{T}_{p(t)}\right).\mathbf{D}_{p(t)}=\xi_m(\mathbf{B}_{p(t)},\mathbf{D}_{p(t)},\mathbf{D}_G). \tag{3.27}$$

Also the assumption of incompressibility leads to

$$tr(\mathbf{D})=tr(\mathbf{D}_{p(t)})=tr(\mathbf{D}_G)=0. \tag{3.28}$$

Now, following Rajagopal and Srinivasa [6], we maximize the rate of dissipation ξ_m by varying $\mathbf{L}_G,\mathbf{D}_{p(t)}$ for fixed $\mathbf{B}_{p(t)}$ with Eqs. (3.27), (3.28) as constraints. We maximize the auxiliary function Φ given by

$$\begin{aligned}\Phi:=\xi_m+\lambda_1\left[\xi_m-\mathbf{F}^T_{\kappa_{p(t)}}\mathbf{T}\mathbf{F}^{-T}_{\kappa_{p(t)}}.\mathbf{L}_G-\left(\mathbf{T}-\mathbf{T}_{p(t)}\right).\mathbf{D}_{p(t)}\right]\\ +\lambda_2(\mathbf{I}.\mathbf{D}_G)+\lambda_3(\mathbf{I}.\mathbf{D}_{p(t)}),\end{aligned} \tag{3.29}$$

where $\lambda_1,\lambda_2,\lambda_3$ are Lagrange multipliers. By setting, $\partial\Phi/\partial\mathbf{D}_{p(t)}=0$ and $\partial\Phi/\partial\mathbf{L}_G=0$, we get

$$\mathbf{T}=\mathbf{T}_{p(t)}+\frac{\lambda_3}{\lambda_1}\mathbf{I}+\left(\frac{\lambda_1+1}{\lambda_1}\right)\frac{\partial\xi_m}{\partial\mathbf{D}_{p(t)}}, \tag{3.30}$$

and

$$\mathbf{T}=\frac{\lambda_2}{\lambda_1}\mathbf{I}+\left(\frac{\lambda_1+1}{\lambda_1}\right)\mathbf{F}^{-T}_{\kappa_{p(t)}}\frac{\partial\xi_m}{\partial\mathbf{L}_G}\mathbf{F}^T_{\kappa_{p(t)}}. \tag{3.31}$$

At this juncture it is worth recalling the comments in the introduction concerning maximization with respect to the kinematical quantities. On substituting in Eq. (3.27), we finally obtain

$$\left(\frac{\lambda_1+1}{\lambda_1}\right)=\frac{\xi_m}{\frac{\partial\xi_m}{\partial\mathbf{L}_G}.\mathbf{L}_G+\frac{\partial\xi_m}{\partial\mathbf{D}_{p(t)}}.\mathbf{D}_{p(t)}}, \tag{3.32}$$

Hence, from Eqs. (3.30), (3.31), the final constitutive equations reduce to

$$\begin{aligned}\mathbf{T} &= p\mathbf{I} + 2\rho\left[\left(\frac{\partial\hat{\psi}}{\partial I_{B_{p(t)}}} + I_{B_{p(t)}}\frac{\partial\hat{\psi}}{\partial II_{B_{p(t)}}}\right)\mathbf{B}_{p(t)} - \frac{\partial\hat{\psi}}{\partial II_{B_{p(t)}}}\mathbf{B}^2_{p(t)}\right] \\ &\quad + \left(\frac{\xi_m}{\frac{\partial\xi_m}{\partial\mathbf{L}_G}.\mathbf{L}_G + \frac{\partial\xi_m}{\partial\mathbf{D}_{p(t)}}.\mathbf{D}_{p(t)}}\right)\frac{\partial\xi_m}{\partial\mathbf{D}_{p(t)}}, \\ \mathbf{T} &= \hat{\lambda}\mathbf{I} + \left(\frac{\xi_m}{\frac{\partial\xi_m}{\partial\mathbf{L}_G}.\mathbf{L}_G + \frac{\partial\xi_m}{\partial\mathbf{D}_{p(t)}}.\mathbf{D}_{p(t)}}\right)\mathbf{F}^{-T}_{\kappa_{p(t)}}\frac{\partial\xi_m}{\partial\mathbf{L}_G}\mathbf{F}^{T}_{\kappa_{p(t)}},\end{aligned} \tag{3.33}$$

where $\hat{\lambda} := \frac{\lambda_2}{\lambda_1}, p := \frac{\lambda_3}{\lambda_1}$ are Lagrange multipliers due to the constraint of incompressibility. At this point it appears that there are two constitutive relations – $(3.33)_a$, $(3.33)_b$ – for stress instead of just one! We would like to note that the two expressions – $(3.33)_a$, $(3.33)_b$ – have to be equated and simplified to obtain one expression for stress and an evolution equation for $\mathbf{B}_{p(t)}$. This will become clear within the context of the specific choices of ψ and ξ that are made in the next sub-section. Furthermore, expression $(3.33)_b$ appears at first glance non-symmetric but is in fact symmetric for the specific form chosen for ξ as we shall show in the next sub-section.

2. Specific model

We now derive constitutive expression for the stress by choosing the stored energy to be

$$\hat{\psi}(I_{\mathbf{B}_{p(t)}}, II_{\mathbf{B}_{p(t)}}) = \frac{\mu}{2\rho}\left(I_{\mathbf{B}_{p(t)}} - 3\right), \tag{3.34}$$

and rate of dissipation to be of the form

$$\xi_m(\mathbf{B}_{p(t)}, \mathbf{D}_{p(t)}, \mathbf{D}_G) = \eta_p\mathbf{D}_{p(t)}.\mathbf{B}_{p(t)}\mathbf{D}_{p(t)} + \eta_G\mathbf{D}_G.\mathbf{B}_{p(t)}\mathbf{D}_G. \tag{3.35}$$

The stored energy chosen here is that for a neo-Hookean material with μ being its elastic modulus, whereas the rate of dissipation is similar to that of a "mixture" of two Newtonian-like fluids (in the sense that the dissipation is quadratic in the symmetric

part of velocity gradient), whose dissipation also depends on the stretch (specifically the stretch from the natural configuration to the current configuration), with viscosities η_G and η_p[4]. The former term on the right hand side of expression (3.35) is due to the dissipation during the motion from κ_R to $\kappa_{p(t)}$ and the latter term is due to dissipation during the motion from $\kappa_{p(t)}$ to κ_t. Note that with the above choices for ψ and ξ, as the body moves from the $\kappa_{p(t)}$ to κ_t, there is both storage (like a neo-Hookean solid) and dissipation (like a Newtonian-like fluid) of energy simultaneously and hence, $\kappa_{p(t)}$ evolves like the natural configuration of a Kelvin-Voigt-like solid (also see [51]) with respect to κ_t. Now, with this choice for ψ and ξ, the constitutive relations given by Eq. (3.33) reduce to

$$\mathbf{T} = p\mathbf{I} + \mu\mathbf{B}_{p(t)} + \frac{\eta_p}{2}\left(\mathbf{B}_{p(t)}\mathbf{D}_{p(t)} + \mathbf{D}_{p(t)}\mathbf{B}_{p(t)}\right), \tag{3.36}$$

and

$$\mathbf{T} = \hat{\lambda}\mathbf{I} + \frac{\eta_G}{2}\mathbf{F}^{-T}_{\kappa_{p(t)}}\left(\mathbf{B}_{p(t)}\mathbf{D}_G + \mathbf{D}_G\mathbf{B}_{p(t)}\right)\mathbf{F}^{T}_{\kappa_{p(t)}}. \tag{3.37}$$

Now, from Eq. (3.36) and Eq. (3.37)

$$\left(p - \hat{\lambda}\right)\mathbf{I} + \mu\mathbf{B}_{p(t)} + \frac{\eta_p}{2}\left(\mathbf{B}_{p(t)}\mathbf{D}_{p(t)} + \mathbf{D}_{p(t)}\mathbf{B}_{p(t)}\right) = \frac{\eta_G}{2}\mathbf{V}^{-1}_{\kappa_{p(t)}}\left(\mathbf{B}_{p(t)}\mathbf{D}_G + \mathbf{D}_G\mathbf{B}_{p(t)}\right)\mathbf{V}_{\kappa_{p(t)}}, \tag{3.38}$$

and using Eq. (3.15) and Eq. (3.23) in Eq. (3.38), we get

$$\left(p - \hat{\lambda}\right)\mathbf{I} + \mu\mathbf{B}_{p(t)} + \frac{\eta_p}{4}\left(\mathbf{V}_{\kappa_{p(t)}}\dot{\mathbf{B}}_{p(t)}\mathbf{V}^{-1}_{\kappa_{p(t)}} + \mathbf{V}^{-1}_{\kappa_{p(t)}}\dot{\mathbf{B}}_{p(t)}\mathbf{V}_{\kappa_{p(t)}}\right) = \frac{\eta_G}{4}\mathbf{V}^{-1}_{\kappa_{p(t)}}\left[-\mathbf{V}_{\kappa_{p(t)}}\overset{\nabla}{\mathbf{B}}_{p(t)}\mathbf{V}^{-1}_{\kappa_{p(t)}} - \mathbf{V}^{-1}_{\kappa_{p(t)}}\overset{\nabla}{\mathbf{B}}_{p(t)}\mathbf{V}_{\kappa_{p(t)}}\right]\mathbf{V}_{\kappa_{p(t)}}. \tag{3.39}$$

[4]Of course, one can choose the rate of dissipation to be quadratic in the symmetric part of velocity gradient without any stretch dependence, for example, $\xi = \eta_p\mathbf{D}_{p(t)}.\mathbf{D}_{p(t)} + \eta_G\mathbf{D}_G.\mathbf{D}_G$. The resulting model would be a variation of the current model.

Pre-multiplying and post-multiplying Eq. (3.39) by $\mathbf{V}_{\kappa_{p(t)}}$, we have

$$\left(p-\hat{\lambda}\right)\mathbf{B}_{p(t)}+\mu\mathbf{B}_{p(t)}^{2}+\frac{\eta_p}{4}\left(\mathbf{B}_{p(t)}\dot{\mathbf{B}}_{p(t)}+\dot{\mathbf{B}}_{p(t)}\mathbf{B}_{p(t)}\right)= \frac{\eta_G}{4}\mathbf{V}_{\kappa_{p(t)}}^{-1}\left(-\mathbf{B}_{p(t)}\overset{\nabla}{\mathbf{B}}_{p(t)}-\overset{\nabla}{\mathbf{B}}_{p(t)}\mathbf{B}_{p(t)}\right)\mathbf{V}_{\kappa_{p(t)}}. \tag{3.40}$$

Also, from Eq. (3.39)

$$\left(p-\hat{\lambda}\right)=-\frac{1}{3}\left[\frac{\eta_G}{2}tr\left(\overset{\nabla}{\mathbf{B}}_{p(t)}\right)+\frac{\eta_p}{2}tr\left(\dot{\mathbf{B}}_{p(t)}\right)+\mu tr\left(\mathbf{B}_{p(t)}\right)\right]. \tag{3.41}$$

Eq. (3.37) can be re-written as

$$\mathbf{T}=\hat{\lambda}\mathbf{I}+\frac{\eta_G}{4}\mathbf{V}_{\kappa_{p(t)}}^{-1}\left[-\mathbf{V}_{\kappa_{p(t)}}\overset{\nabla}{\mathbf{B}}_{p(t)}\mathbf{V}_{\kappa_{p(t)}}^{-1}-\mathbf{V}_{\kappa_{p(t)}}^{-1}\overset{\nabla}{\mathbf{B}}_{p(t)}\mathbf{V}_{\kappa_{p(t)}}\right]\mathbf{V}_{\kappa_{p(t)}}. \tag{3.42}$$

Eq. (3.40) and Eq. (3.42) are the final constitutive relations with Eq. (3.40) together with Eq. (3.41) being the evolution equation for the natural configuration $\kappa_{p(t)}$.

In what follows, we shall also show that our model can be reduced to both the Maxwell-like fluid model and Kelvin-Voigt-like solid model under certain assumptions for the material parameters that are involved. We shall solve the problems of creep and stress relaxation by considering homogeneous uniaxial extension. Based on the results for creep and stress relaxation, and following the definitions given in [11] for a fluid-like body and a solid-like body, we shall show that our model is a fluid-like model when none of the material parameters are ignored.

3. Limiting cases

By setting η_p to zero, one can see from Eq. (3.38) that $\mathbf{B}_{p(t)}$ and $\mathbf{D}_G$ have the same eigen-vectors and hence commute. Using this fact, Eq. (3.36) and Eq. (3.40) reduce to the Maxwell-like fluid model developed by Rajagopal and Srinivasa (see Eqs. 40–42 in [6]). On the other hand, if we assume η_G goes to infinity, with η_p, μ and all other

kinematical quantities remaining finite, then as the deviatoric part of Eq. (3.37) is finite, from Eqs. (3.37), (3.28), we must have $\mathbf{D}_G \to 0$. This also implies that $\mathbf{G}$ is pure rotation and hence $\mathbf{B}_{p(t)} \to \mathbf{B}_{\kappa_R}$, $\mathbf{D}_{p(t)} \to \mathbf{D}$. Thus, Eq. (3.36) reduces to

$$\mathbf{T} = p\mathbf{I} + \mu\mathbf{B}_{\kappa_R} + \frac{\eta_p}{2}\left(\mathbf{B}_{\kappa_R}\mathbf{D} + \mathbf{D}\mathbf{B}_{\kappa_R}\right). \tag{3.43}$$

This is a generalized Kelvin-Voigt solid model.

D. Application of the model

1. Creep

In this sub-section we shall solve the problem of homogeneous extension under constant stress and show that our model is a fluid-like model when none of the material moduli are ignored. Before we go into the details of the problem, we would like to note that for steady problems wherein the deformation is homogeneous, the results for our model would be same as that for a Maxwell-like fluid with stretch dependent relaxation as formulated in [6]. This is because $\dot{\mathbf{B}}_{p(t)} = 0$ (since $\frac{\partial \mathbf{B}_{p(t)}}{\partial t} = 0$, due to the assumption that the deformation is steady and $grad(\mathbf{B}_{p(t)}) = 0$ as the deformation is homogeneous) and the constitutive relations in Eqs. (3.40), (3.42) reduce to Eqs. (36), (39) in [6].

Now, in the case of time dependent homogeneous extension:

$$x = \lambda(t)X, \quad y = \frac{1}{\sqrt{\lambda(t)}}Y, \quad z = \frac{1}{\sqrt{\lambda(t)}}Z, \tag{3.44}$$

the deformation gradient with respect to the reference configuration is given by

$$\mathbf{F}_{\kappa_R} = \mathrm{diag}\left\{\lambda(t), \frac{1}{\sqrt{\lambda(t)}}, \frac{1}{\sqrt{\lambda(t)}}\right\}. \tag{3.45}$$

Hence, the velocity gradient is given by

$$\mathbf{L} = \text{diag}\left\{\frac{\dot{\lambda}}{\lambda}, -\frac{\dot{\lambda}}{2\lambda}, -\frac{\dot{\lambda}}{2\lambda}\right\}. \tag{3.46}$$

Now, we shall assume that

$$\mathbf{B}_{p(t)} = \text{diag}\left\{B(t), \frac{1}{\sqrt{B(t)}}, \frac{1}{\sqrt{B(t)}}\right\}, \tag{3.47}$$

and hence

$$\dot{\mathbf{B}}_{p(t)} = \text{diag}\left\{\dot{B}(t), -\frac{\dot{B}(t)}{2B^{3/2}(t)}, -\frac{\dot{B}(t)}{2B^{3/2}(t)}\right\}, \tag{3.48}$$

$$\overset{\nabla}{\mathbf{B}}_{p(t)} = \text{diag}\left\{\dot{B}(t) - \frac{2B(t)\dot{\lambda}(t)}{\lambda(t)}, -\frac{\dot{B}(t)}{2B^{3/2}(t)} + \frac{\dot{\lambda}(t)}{\sqrt{B}(t)\lambda(t)}, -\frac{\dot{B}(t)}{2B^{3/2}(t)} + \frac{\dot{\lambda}(t)}{\sqrt{B}(t)\lambda(t)}\right\}, \tag{3.49}$$

and

$$\mathbf{V}_{\kappa_{p(t)}} = \text{diag}\left\{\sqrt{B}(t), \frac{1}{B^{1/4}(t)}, \frac{1}{B^{1/4}(t)}\right\}. \tag{3.50}$$

For the case of homogeneous extension, Eq. (3.36) and Eq. (3.37) reduce to

$$\begin{aligned}\mathbf{T} &= p\mathbf{I} + \mu\mathbf{B}_{p(t)} + \eta_p\mathbf{B}_{p(t)}\mathbf{D}_{p(t)},\\ \mathbf{T} &= \hat{\lambda}\mathbf{I} + \eta_G\mathbf{B}_{p(t)}\mathbf{D}_G,\end{aligned} \tag{3.51}$$

and the final constitutive relations Eq. (3.40) and Eq. (3.42) become

$$\mathbf{T} = \hat{\lambda}\mathbf{I} - \frac{\eta_G}{2}\mathbf{V}_{\kappa_{p(t)}}\ \overset{\nabla}{\mathbf{B}}_{p(t)}\ \mathbf{V}^{-1}_{\kappa_{p(t)}}, \tag{3.52}$$

$$(p - \hat{\lambda})\mathbf{I} + \mu\mathbf{B}_{p(t)} = -\frac{\eta_G}{2}\ \overset{\nabla}{\mathbf{B}}_{p(t)} - \frac{\eta_p}{2}\dot{\mathbf{B}}_{p(t)}, \tag{3.53}$$

where

$$(p - \hat{\lambda}) = -\frac{3\mu}{tr(\mathbf{B}^{-1}_{p(t)})}. \tag{3.54}$$

On substituting Eqs. (3.48), (3.49) into Eq. (3.53), we arrive at

$$\dot{B}(t) = \frac{2\eta_G}{\eta_G + \eta_p} \frac{B(t)\dot{\lambda}(t)}{\lambda(t)} - \frac{4\mu}{\eta_G + \eta_p} \left[\frac{B^{5/2}(t) - B(t)}{1 + 2B^{3/2}(t)} \right]. \tag{3.55}$$

Using Eqs. (3.49), (3.50) in Eq. (3.52) and using the fact that lateral surfaces are traction free, we find that

$$T_{11} = \frac{\eta_G}{2} \left(1 + \frac{1}{2B^{3/2}(t)} \right) \left(\frac{2B(t)\dot{\lambda}(t)}{\lambda(t)} - \dot{B}(t) \right). \tag{3.56}$$

Solving Eqs. (3.55), (3.56) simultaneously, we obtain

$$\dot{B}(t) = \frac{2T_{11}}{\eta_p \left(1 + \frac{1}{2B^{3/2}(t)} \right)} - \frac{4\mu}{\eta_p} \left(\frac{B^{5/2}(t) - B(t)}{1 + 2B^{3/2}(t)} \right), \tag{3.57}$$

$$\frac{\dot{\lambda}(t)}{\lambda(t)} = \frac{2\left(\eta_p + \eta_G\right)}{\eta_G \eta_p} \left(\frac{T_{11} B^{1/2}(t)}{1 + 2B^{3/2}(t)} \right) - \frac{2\mu}{\eta_p} \left(\frac{B^{3/2}(t) - 1}{1 + 2B^{3/2}(t)} \right), \tag{3.58}$$

which can be re-written as

$$\frac{dB}{d\bar{t}} = \frac{2\bar{T}_{11}}{\left(1 + \frac{1}{2B^{3/2}(t)} \right)} - 4 \left(\frac{B^{5/2}(t) - B(t)}{1 + 2B^{3/2}(t)} \right), \tag{3.59}$$

$$\frac{1}{\lambda} \frac{d\lambda}{d\bar{t}} = 2 \left(\frac{1}{\bar{\eta}} + 1 \right) \left(\frac{\bar{T}_{11} B^{1/2}(t)}{1 + 2B^{3/2}(t)} \right) - 2 \left(\frac{B^{3/2}(t) - 1}{1 + 2B^{3/2}(t)} \right), \tag{3.60}$$

where $\bar{t} = \frac{t\mu}{\eta_p}$ is a non-dimensional time, $\bar{T}_{11} = \frac{T_{11}}{\mu}$ is a non-dimensional stress, and $\bar{\eta} = \frac{\eta_p}{\eta_G}$ is the ratio of viscosities (η_p, η_G). With known values for $\bar{T}_{11}$ and $\bar{\eta}$, the ODEs – Eqs. (3.59), (3.60) – were solved simultaneously using "ode45" solver in Matlab. The initial conditions $B(0) = \lambda(0) = 1$ were used for the loading process. In the case of unloading, the initial values were set to the values of $B,\ \lambda$ evaluated at the end of loading process. Before we discuss our results, the reader should note that B is the square of the stretch from the natural configuration to the current configuration and λ is the stretch from the reference configuration to the current configuration or the

total stretch.

We shall now discuss the numerical results obtained for the problem of creep. Fig. (11) portrays the results (specifically, B as a function of $\bar{t}$ and λ as function of $\bar{t}$) for $\bar{T}_{11} = 1$ for various values of $\bar{\eta}$. For all the cases of $\bar{\eta}$, the evolution of the natural configuration with respect to the current configuration (or B as a function of $\bar{t}$) is the same. This can also be seen from Eqs. (3.59),(3.60) as the evolution of B in time depends only on the value of $\bar{T}_{11}$, and does not depend on $\bar{\eta}$. Also, as seen in Fig. (11)(a), on removal of the load, the stretch in the body does not return to unity but exhibits a permanent residual stretch, which is the typical behavior of a fluid-like body (see [11]). In addition, from Fig. (11) and Fig. (12), by increasing $\bar{T}_{11}$ (from 1 to 5) for fixed $\bar{\eta}$ (here the value is 10) – the maximum value of B increases, the maximum value for λ increases and the permanent residual stretch also increases.

Now, as discussed earlier in section 2, the natural configuration evolves like a Kelvin-Voigt-like solid with respect to the current configuration. Fig. (11)(b) reiterates this fact since B varies with t in a fashion similar to the stretch as a function of time for a Kelvin-Voigt solid in a creep experiment. Fig. (11)(a) also shows that, as $\bar{\eta}$ increases, the maximum value for total stretch (λ) decreases. This shows that for a fixed amount of loading time (for instance for $\bar{t} = 10$) as the value for $\bar{\eta}$ increases, the value for maximum total stretch decreases and so the rate of relaxation decreases. As $\bar{\eta}$ increases one would expect that our model would tend to a solid model in the limit of $\bar{\eta} \to \infty$. To see this, in our numerical simulations, we set $\bar{\eta}$ to a very large number (specifically $\bar{\eta} = 100000$), with $\bar{T}_{11} = 1$, and we found $\sqrt{B}$ and λ to follow the same trend in time (see Fig. 13). This is an extreme case when the natural configuration and the reference configuration tend to being the same, reducing our model to Kelvin-Voigt-like solid model.

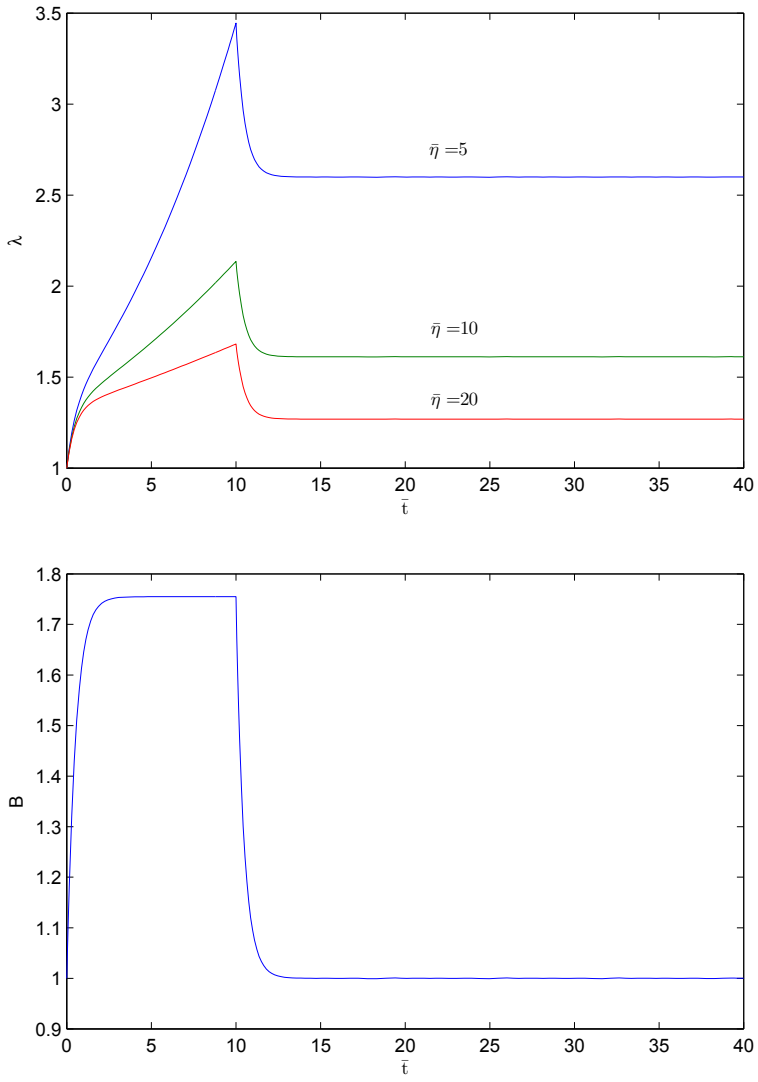

Fig. 11.: Overall stretch of the current configuration from the reference configuration (λ) and square of the stretch from the natural configuration to the current configuration (B) as a function of non-dimensional time $\bar{t}$ for the creep experiment. For the loading process, $\bar{T}_{11} = 1$ and the unloading starts at $t = 10$. Plots for $\bar{\eta} = 5,\ 10,\ 20$ are shown.

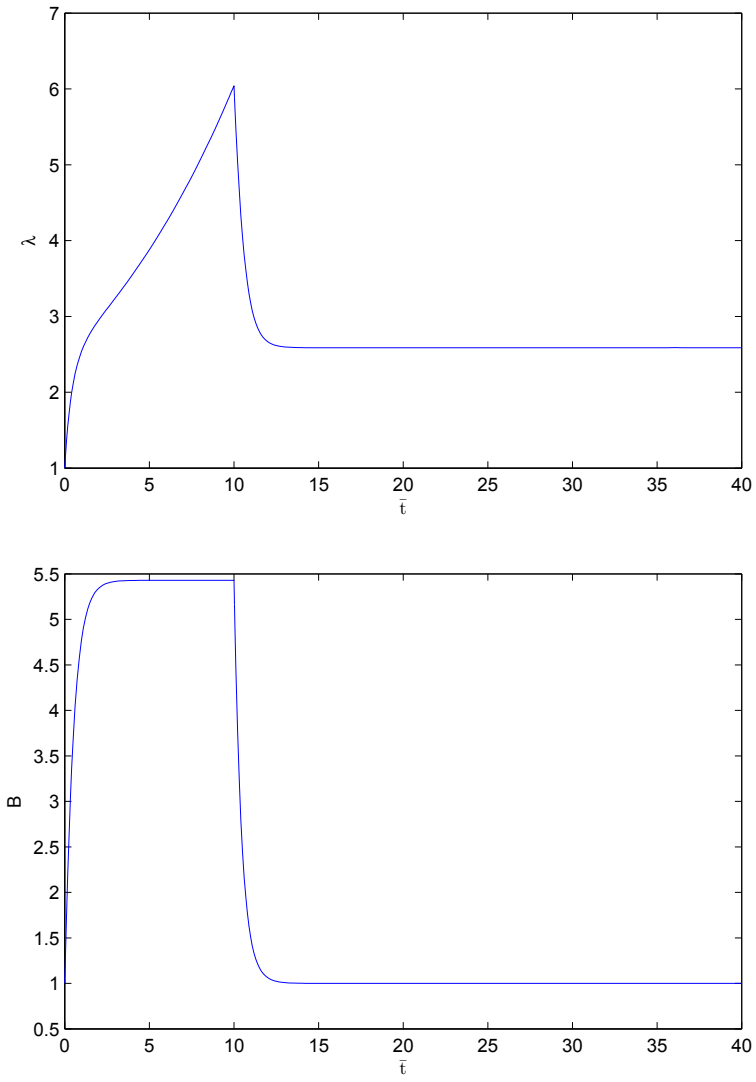

Fig. 12.: Overall stretch of the current configuration from the reference configuration (λ) and square of the stretch from the natural configuration to the current configuration (B) as a function of non-dimensional time $\bar{t}$ for the creep experiment. For this case, the non-dimensional stress $\bar{T}_{11} = 5$ and the ratio of the viscosities $\bar{\eta} = 10$. The unloading for the creep experiment starts at $t = 10$.

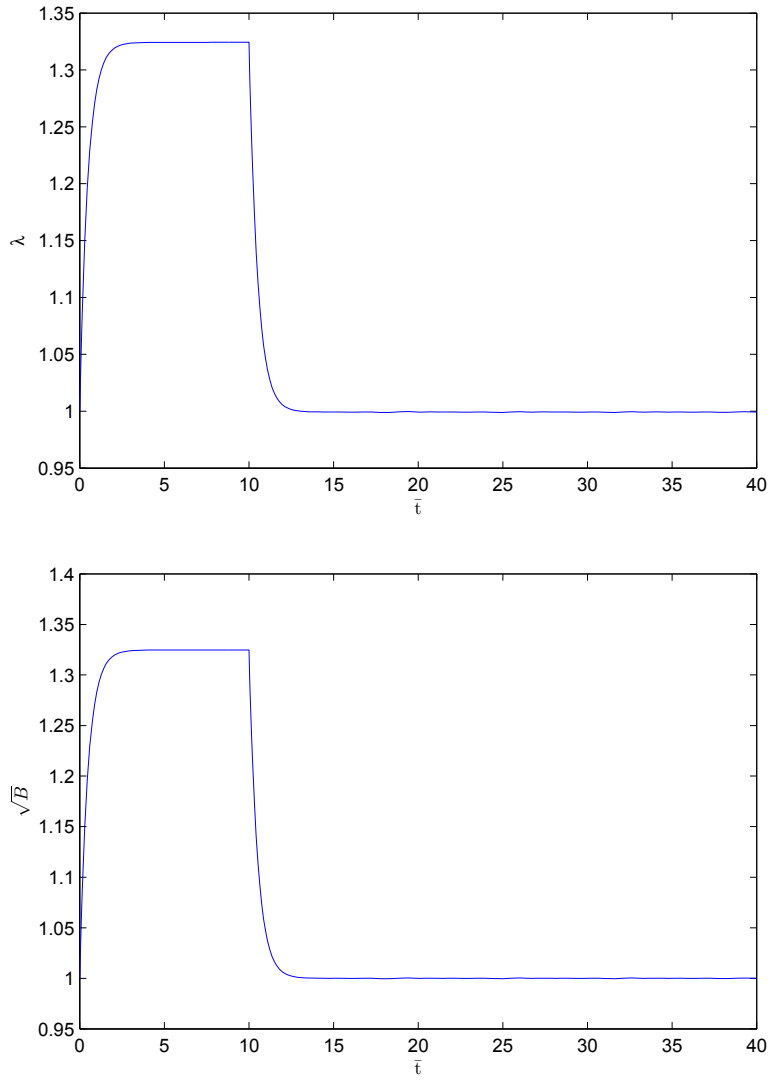

Fig. 13.: Overall stretch of the current configuration from the reference configuration (λ) and stretch from the natural configuration to the current configuration ($\sqrt{\bar{B}}$) as a function of non-dimensional time $\bar{t}$ for the creep experiment. For this case, the non-dimensional stress $\bar{T}_{11} = 1$ and the ratio of the viscosities $\bar{\eta} = 100000$. Unloading for the creep experiment starts at $t = 10$.

2. Stress under constant strain rate

If we define $\epsilon := ln\lambda$ as our strain measure, then Eq. (3.55) reduces to

$$\dot{B}(t) = \frac{2\eta_G}{\eta_G + \eta_p} B(t)\dot{\epsilon} - \frac{4\mu}{\eta_G + \eta_p}\left[\frac{B^{5/2}(t) - B(t)}{1 + 2B^{3/2}(t)}\right]. \tag{3.61}$$

Using Eq. (3.61) in Eq. (3.56), we get

$$T_{11} = \eta_G\left(1 + \frac{1}{2B^{3/2}(t)}\right)\left[\frac{\eta_p}{\eta_p + \eta_G} B(t)\dot{\epsilon} + \frac{2\mu}{\eta_G + \eta_p}\frac{B^{5/2}(t) - B(t)}{1 + 2B^{3/2}(t)}\right]. \tag{3.62}$$

Upon non-dimensionalizing Eqs. (3.61), (3.62), we arrive at

$$\frac{dB}{d\bar{t}} = \frac{2\bar{\eta}B}{\bar{\eta} + 1}\frac{d\epsilon}{d\bar{t}} - \frac{4}{\bar{\eta} + 1}\left(\frac{B^{5/2} - B}{1 + 2B^{3/2}}\right), \tag{3.63}$$

$$\bar{T}_{11} = \left(1 + \frac{1}{2B^{3/2}}\right)\left[\frac{B\bar{\eta}}{1 + \bar{\eta}}\frac{d\epsilon}{d\bar{t}} + \frac{2}{1 + \bar{\eta}}\left(\frac{B^{5/2} - B}{1 + 2B^{3/2}}\right)\right]. \tag{3.64}$$

With known values for $\frac{d\epsilon}{d\bar{t}}$, B can be evaluated using Eq. (3.63) and then from Eq. (3.64), $\bar{T}_{11}$ can be calculated. For stress relaxation, we set $\frac{d\epsilon}{d\bar{t}}$ to zero and solved the ODEs – Eqs. (3.63), (3.64) – numerically using the solver "ode45" in Matlab. Fig. (14) displays the plots for B, and $\bar{T}_{11}$ as functions of $\bar{t}$ for various values of $\bar{\eta}$. The initial condition for B was chosen to be 2. Fig. (14)(b) also shows that the stress finally relaxes to zero. This is a characteristic of a fluid-like material. In addition, one can also see from Fig. (14) that as the ratio of viscosities $\bar{\eta}$ increases, the time of relaxation increases. Also from Eq. (3.64), as $\bar{\eta} \to \infty$, $\bar{T}_{11} \to 0$ and hence cannot stress relax. This is because as $\bar{\eta} \to \infty$, the model behaves like a Kelvin-Voigt-like solid model as can be gleaned from the creep response discussed in section (1) . In addition, one can also notice from Fig. (14)(b) that the initial value for $\bar{T}_{11}$ decreases as $\bar{\eta}$ increases.

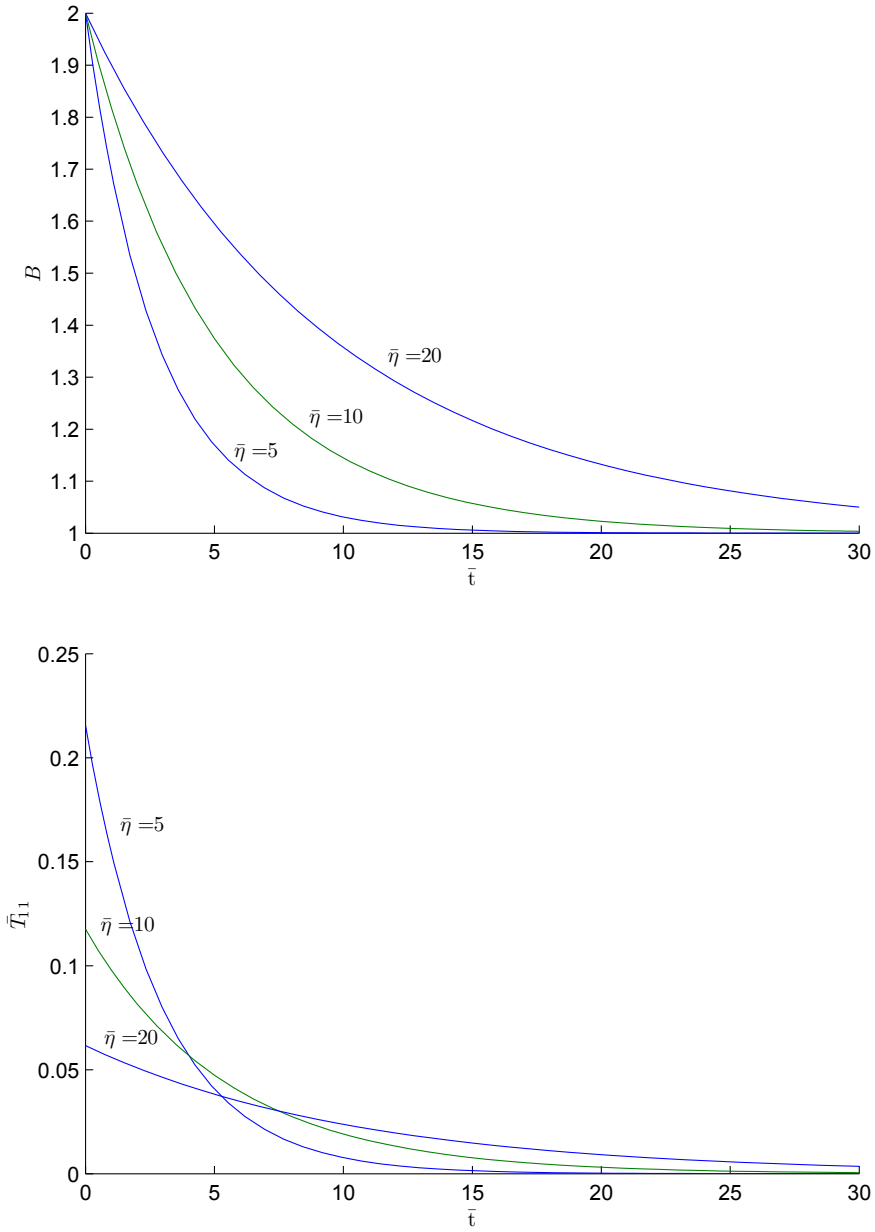

Fig. 14.: Square of the stretch from the natural configuration to the current configuration (B), non-dimensional stress ($\bar{T}_{11}$) plotted as functions of non-dimensional time $\bar{t}$ for various values of $\bar{\eta}$, in the stress relaxation experiment. The initial condition for B was chosen as 2.

E. Model reduction in one dimension

If the elastic strain is small in the sense that

$$\|\mathbf{B}_{p(t)} - \mathbf{I}\| = O(\epsilon), \quad \epsilon \ll 1, \tag{3.65}$$

then Eq. (3.54) reduces to (see [6])

$$\left(p - \hat{\lambda}\right) = -\mu, \tag{3.66}$$

and hence Eq. (3.51) reduce to

$$\begin{aligned} &\mathbf{T} = \hat{\lambda}\mathbf{I} + \eta_G \mathbf{B}_{p(t)}\mathbf{D}_G, \\ &\mu\left(\mathbf{B}_{p(t)} - \mathbf{I}\right) = \mathbf{B}_{p(t)}\left(\eta_G \mathbf{D}_G - \eta_p \mathbf{D}_{p(t)}\right). \end{aligned} \tag{3.67}$$

If λ_i $(i = G, p)$ is the one-dimensional stretch and $\epsilon = ln\lambda_i$ is the true strain, then in one dimension, Eq. (3.67) reduces to

$$\begin{aligned} &\sigma = \hat{\eta}_G \frac{\dot{\lambda}_G}{\lambda_G}, \\ &\mu\left(\lambda_p^2 - 1\right) = \hat{\eta}_G \frac{\dot{\lambda}_G}{\lambda_G} - \hat{\eta}_p \frac{\dot{\lambda}_p}{\lambda_p}, \end{aligned} \tag{3.68}$$

where $\hat{\eta}_i = \eta_i \lambda_p^2$ $(i = G, p)$ are the stretch dependent viscosities and σ is the one dimensional stress. Eq. (3.68) under the assumption that $\epsilon_i \ll 1$ $(i = G, p)$ reduces to

$$\sigma = \hat{\eta}_G \dot{\epsilon}_G, \quad 2\mu\epsilon_p = \hat{\eta}_G \dot{\epsilon}_G - \hat{\eta}_p \dot{\epsilon}_p. \tag{3.69}$$

Eqn. (3.69) can also be obtained if we have a dashpot with $\hat{\eta}_G$ as the viscosity and a Kelvin-Voigt element, with a spring constant 2μ and viscosity $\hat{\eta}_p$, in series (see Fig. 10). Thus, our model in section 2 reduces to a dashpot and a Kelvin-Voigt element in series whose viscosities are stretch dependent.

F. Concluding remarks

For the model developed in this chapter, we solved the problems of creep and stress relaxation and based on the results showed that our model is a fluid-like model. We have also shown that under certain idealizations, our model reduces to both a Maxwell-like fluid and a Kelvin-Voigt-like solid. We have also shown that our model is a three dimensional generalization of the one dimensional model with a dashpot and Kelvin-Voigt element in series. We would also like to note that the general framework developed in section 1 can be extended to model visco-elasto-plastic response by choosing the rate of dissipation for the motion from κ_R to $\kappa_{p(t)}$ to be of the form given in Eq. (39) or Eq. (40) in [44]. For example, one can choose the rate of dissipation to be of the form

$$\xi_m(\mathbf{B}_{p(t)}, \mathbf{D}_{p(t)}, \mathbf{D}_G) = Y \left(\mathbf{D}_{p(t)}.\mathbf{B}_{p(t)}\mathbf{D}_{p(t)}\right)^{1/2} + \eta_G \mathbf{D}_G.\mathbf{B}_{p(t)}\mathbf{D}_G, \tag{3.70}$$

where Y is a material constant, along with the stored energy in Eq. (3.34), and then maximize the rate of dissipation under appropriate constraints.

CHAPTER IV

DEGRADATION AND HEALING IN A GENERALIZED NEO-HOOKEAN SOLID DUE TO INFUSION OF A FLUID

The mechanical response and load bearing capacity of high performance polymer composites changes due to degradation or healing associated with diffusion of a fluid, temperature, oxidation or the extent of the deformation. Hence, there is a need to study the response of bodies under such degradation mechanisms. In this chapter, we study the effect of degradation and healing due to the diffusion of a fluid on the response of a solid which prior to the diffusion can be described by the generalized neo-Hookean model. We show that a generalized neo-Hookean solid - which behaves like an elastic body (i.e., it does not produce entropy) within a purely mechanical context - creeps and stress relaxes due to degradation/healing when infused with a fluid and behaves like a body whose material properties are time dependent. We specifically investigate the torsion of a degrading/healing generalized neo-Hookean circular cylindrical annulus infused with a fluid. The equations of equilibrium for a generalized neo-Hookean solid are solved together with the convection-diffusion equation for the fluid concentration. Different boundary conditions for the fluid concentration are also considered. We also solve the problem for the case when the diffusivity of the fluid depends on the deformation of the generalized neo-Hookean solid.

A. Introduction

As elastic bodies are incapable of producing any entropy, this would be the proper definition of an elastic body within a thermodynamic context. Elastic bodies also cannot stress relax, i.e., when the strain is kept constant in time the stresses within the body cannot change with time. However, the stresses in a body that is initially

elastic, which subsequently undergoes chemical reactions due to interactions with the environment or which is subject to the effects of electro-magnetic radiation such as ultra-violet rays, could change with time and the body's response ceases to be that of an elastic body. The chemical reactions or the interactions with the environment invariably produce entropy. However, it could happen that when the chemical reactions cease and the body is isolated from the environment the body ceases to produce entropy, that is, it becomes a different elastic body. The body, due to its exposure to the environment can undergo deterioration or enhancement with respect to its load carrying capacity or other properties. While moisture diffusion in a polymer can cause degradation of the body in that its load carrying capacity goes down, a body such as biological matter can be strengthened due to a drug that is being injected. Though the stress in the body might decrease when the strain is held constant in bodies that are undergoing degradation, this phenomenon is quite different from the stress relaxation observed in viscoelastic solids (see [59], [11]).

There is need for a good understanding of the degradation of materials as this is relevant to a plethora of applications. For instance, the mechanical properties of high performance polymer composites (like polyimides) used in hypersonic vehicles vary due to the effect of high temperature, diffusion of moisture and the subsequent oxidation. Chen and Tyler [60] have recently shown that polymers can also degrade due to deformation. In this chapter we are interested in studying the response of a body whose properties are changing due to the presence of a fluid, the extent of the change depending on the concentration of the fluid.

There has been considerable interest in the damage and degradation of polymeric solids and polymer composites. However, most of these studies appeal to ad hoc constitutive equations. Also, many studies appeal to the notion of a hygrothermal expansion coefficient (see [61], [62]) and such an approach would not be appropriate

when large deformations due to swelling are involved. A general thermodynamic framework has been developed to describe damage in composites by Weitsman [63]. This work introduces the notion of a damage tensor which is essentially a tensor internal variable. While the study is very detailed and has a thermodynamic basis, the theory however involves several material moduli that depend on as many as 32 invariants in the case of transversely isotropic materials, making it impractical to put the theory to use as it is impossible to develop an experimental program to determine the numerous material functions that characterize the body. Moreover, such theories lead to intractable mathematical equations. While there have been several other studies concerning the diffusion of moisture in composites (e.g., [64], [65], [66], and [67]), they are primarily parametric studies in which the material moduli are allowed to depend on the moisture content according to some pre-assigned manner and not as a consequence of a reasonable convection-diffusion equation; that is the coupled problem for the deformation of the composite and the diffusion of moisture is not solved simultaneously. In general, the diffusivity depends on the temperature, moisture content, strain, and stress. In fact, the diffusivity can depend on the history of these quantities. Weitsman [68] and Roy et al. [69] have also addressed damage due to diffusion but not in the manner advocated here.

Using ideas in multi-network theories for polymeric materials (see [70], [71]), Wineman and Rajagopal [72] and Rajagopal and Wineman [49] developed a theory applicable to the large deformation of polymeric solids that exhibit scisson and healing and permanent set, within a purely mechanical context. This work was extended in a series of papers by Huntley (see [73, 74, 75]) to deal with a variety of deformations involving elastomeric solids that undergo permanent set. The scission and healing that takes place can be viewed within the context of deformation induced damage and due to cross-linkings that take place. These works within a purely mechanical

context were later generalized to include thermal effects (see [76], [77]).

A general thermodynamic framework which takes into account chemical reactions (with chemical kinetics), diffusion and thermal effects needs to be put into place in order to develop constitutive relations to study the degradation of materials (like polyimides) due to chemical reactions. As a first step towards such a goal, in this chapter, we shall first solve the problem of torsion of a degrading body, which when there is no degradation taking place responds like a generalized neo-Hookean body. We also look at healing (or strengthening) of a generalized neo-Hookean body when a fluid is infused. We assume the body to be a cylindrical annulus of finite length. We shall study the torsion of a cylindrical annulus through which a fluid is infusing. We will assume that the infusion of the fluid is radial and thus the degradation or healing takes place radially. We introduce a parameter that is a measure of the degradation or healing which in virtue of the diffusion being radial also varies radially. The material parameters are assumed to be functions of the variables that quantify the degradation or healing. We need to then solve the convection-diffusion equation that governs the diffusion of the fluid in tandem with the equilibrium equations for the torsion problem; we look at how the moment varies with time when the angle of twist of the cylinder is kept constant in time, and how the angle of twist of the cylinder varies when the moment applied to the cylinder is kept constant. We find that the moment that is needed to maintain the angular displacement decreases with time, that is the body stress relaxes, when the material is degrading, but as we observed earlier such a decrease of stress is very different from the stress relaxation observed in viscoelastic bodies. The stresses can decrease in the body due to a variety of reasons such as degradation of properties of the body due to chemical reactions, aging, etc., and it is important to recognize the reason for the "stress relaxation". Rajagopal and Wineman [78] have studied stress relaxation due to aging and they find that in

marked contrast to the stress relaxation observed in viscoelastic bodies, the decrease in stress is dependent on the geometry of the body. This aspect related to stress relaxation, namely its dependence on the geometry is what sets stress relaxation in viscoelastic materials apart from stress relaxation that manifests itself due to most degradation theories. In order to highlight this difference, Rajagopal and Wineman [78] considered the torsion of a viscoelastic cylinder that ages. They found that the stress relaxation can be split into two parts, one that is a consequence of the body being viscoelastic, which is independent of the size of the specimen, and another part due to the aging of the cylindrical specimen, this being dependent on the radius of the cylinder undergoing torsion. In this current chapter, we also find that the angular displacement undergone by the body increases with time for the applied moment, when the material is degrading. When one looks at healing due to diffusion of a fluid, we find that that the moment needed to maintain a given angular displacement increases with time, whereas the body's angular displacement decreases with time when one applies a constant moment.

We will now turn to a discussion of the response characteristics of the undamaged elastic solid, namely the power-law neo-Hookean solid. The generalized (or power-law) neo-Hookean elastic model (see [79]) allows for softening and stiffening under simple shear when the power-law parameter (n) is lesser or greater than unity, respectively. Softening and stiffening which are seen in real materials cannot be explained using the classical neo-Hookean model while some of it possibly can be explained in terms of the generalized neo-Hookean solid. In any event, one should recognize that such models are merely caricatures of reality and in this study we are mainly interested in obtaining some understanding of the degradation due to the infusion of fluid. On setting the power-law parameter (n) to 1, one obtains the classical neo-Hookean model. Knowles [79] studied the anti-plane shear of a power-law neo-Hookean body

that has a crack, and noted that for $n \geq \frac{1}{2}$, the equation of equilibrium for anti-plane shear is always elliptic and that the ellipticity is lost when $n < \frac{1}{2}$. Hou and Zhang [80] have studied the stability of a power-law neo-Hookean cylinder under axial stretching and constant radial traction. The power-law model has also been used in several subsequent studies (see [81]).

Rajagopal and Tao [82] studied inhomogeneous deformations in a wedge of a generalized neo-Hookean material numerically, and later, Mcleod and Rajagopal [83] re-investigated the same problem with a view towards establishing existence of solutions to the governing equations. Tao et al. [84] have analyzed the problem of inhomogeneous circular shear combined with torsion for a generalized neo-Hookean material and have obtained exact solutions for certain values of the material constants. This study was followed by an analysis by Zhang and Rajagopal [85] concerning steady and unsteady inhomogeneous shear of a slab and a cylindrical annulus. The reason for citing these studies is that in all of [82, 83, 84, 85], "boundary layer" type solutions (that is, close to the boundary the deformations are inhomogeneous while the deformations are mainly homogeneous in the inner core region of the body) have been observed for certain values of the material parameters and also the strain is concentrated in these boundary layers in that the strain gradients are very large in these layers. Thus, one would expect damage, degradation and failure to occur in these boundary layers. A systematic method to obtain approximate equations within the boundary layer of a generalized neo-Hookean solid similar to the boundary layer theory in fluid mechanics has been discussed by Rajagopal [86]. To show the efficacy of this method, the approximate boundary layer equations were solved for the circumferential shear problem and were compared to the full solution.

While there have been several studies concerning generalized neo-Hookean materials within the context of a purely mechanical setting, as noted above, there is

no study concerning the degradation or enhancement of the properties of generalized neo-Hookean materials. Such a study would be important since materials like elastomers, for which the generalized neo-Hookean model is used, degrade or heal due to the diffusion of moisture or other chemicals.

Recently, there have been a few investigations of the deformation of an elastic solid that is undergoing degradation due to the influence of a diffusant. Muliana et al. [87] analyzed the response of a composite cylinder that is undergoing degradation due to the diffusion of a fluid, and Darbha and Rajagopal [88] studied unsteady motions of a slab through which a fluid is diffusing. They investigated the unsteady shear of an infinite slab of finite thickness and a cylindrical annulus of infinite length under degradation due to diffusion of a chemical species. In both the studies the body was assumed to be a linearized elastic body and the material moduli were assumed to vary linearly with the concentration of the diffusing species.

Rajagopal [89] assumed the shear modulus of a generalized neo-Hookean material to depend on temperature and solved the problem of inhomogeneous shear of an infinite slab. Boundary layer type solutions were obtained based on the nature of the boundary conditions for the temperature. Although, this paper was not written within the context of understanding degradation due to temperature, one can extend this work by assuming that all the material moduli depend on temperature in a certain fashion and study the effect of temperature on the response of the body. It is expected that boundary layers would develop due to degradation and the failure of the body would be determined by the stresses in this boundary layer.

The current chapter is organized as follows. In section B, the problem of torsion of a finite cylindrical annulus comprised of a generalized neo-Hookean material through which a fluid is diffusing, is set up. In section C, we specifically assume that the degradation or healing is due to diffusion and also assume that material moduli

vary linearly with the concentration of the diffusant, and obtain the solutions to the convection-diffusion equation for the diffusing species as well as the equilibrium equations. We also obtain an expression for the moment that is applied in terms of the the angular displacement and the material parameters. In section D, the results are discussed in detail, followed by final conclusions in section E.

B. Torsion of a cylindrical annulus undergoing degradation

Let κ_R and κ_t denote the reference and the current configuration of a body, respectively. The motion χ_{κ_R} is a one-one mapping that assigns to each point $\mathbf{X} \in \kappa_R$, a point $\mathbf{x} \in \kappa_t$, at a time t, i.e.,

$$\mathbf{x} = \chi_{\kappa_R}(\mathbf{X}, t). \tag{4.1}$$

The gradient of motion (or the deformation gradient) $\mathbf{F}$ is defined by

$$\mathbf{F} := \frac{\partial \chi_{\kappa_R}}{\partial \mathbf{X}}, \tag{4.2}$$

with the velocity $\mathbf{v}$ defined as

$$\mathbf{v} := \frac{\partial \chi_{\kappa_R}}{\partial t}. \tag{4.3}$$

Let (R, Θ, Z) and (r, θ, z) be cylindrical co-ordinates in the reference and current configuration, respectively. Consider a cylindrical annulus of height H with inner radius R_i and outer radius R_o under torsion, whose motion is given by

$$r = R, \quad \theta = \Theta + f(z, t), \quad z = Z. \tag{4.4}$$

The deformation gradient $\mathbf{F}$ and the left Cauchy-Green stretch tensor $\mathbf{B}$ associated with Eq. (4.4) are given by

$$\mathbf{F} = \begin{bmatrix} 1 & 0 & 0 \\ 0 & 1 & rf_z \\ 0 & 0 & 1 \end{bmatrix}, \quad \mathbf{B} := \mathbf{F}\mathbf{F}^T = \begin{bmatrix} 1 & 0 & 0 \\ 0 & \left(1 + (rf_z)^2\right) & rf_z \\ 0 & rf_z & 1 \end{bmatrix}. \tag{4.5}$$

Thus, the first invariant of $\mathbf{B}$ is, $I_1 = tr(\mathbf{B}) = 3 + (rf_z)^2$, where $f_z := \dfrac{\partial f(z,t)}{\partial z}$, and $tr(.)$ is the trace of a second order tensor.

The Cauchy stress tensor $\mathbf{T}$ in an incompressible generalized neo-Hookean material, is given by

$$\mathbf{T} = -p\mathbf{I} + \mu \left[1 + \frac{b}{n}\left(I_1 - 3\right)\right]^{n-1} \mathbf{B}, \tag{4.6}$$

where $-p\mathbf{I}$ is the spherical part due to the constraint of incompressibility, and $\mu \times \left[1 + \frac{b}{n}\left(I_1 - 3\right)\right]^{n-1}$ is the generalized shear modulus, μ being the shear modulus at zero stretch. In general, the degradation or healing of the generalized neo-Hookean material can be caused by diffusion, temperature, electromagnetic radiation, etc. We shall denote the variable that is a measure of the degradation or healing by α, i.e., when degradation due to diffusion is considered, α would be the concentration of the diffusing species; α would be temperature if we have degradation or healing due to temperature, etc., with an appropriate governing equation for the variable. We shall refer to α as the degradation/healing parameter. We shall assume that the material moduli are functions of the degradation/healing parameter i.e., $n = n(\alpha)$, $\mu = \mu(\alpha)$, $b = b(\alpha)$, which leads to changes in the response characteristics of the body. In view of the geometry of the body, and the assumed form for the deformation field, we shall further assume that the degradation/healing parameter varies only with the radius and time, i.e., $\alpha = \alpha(r,t)$. Then, the material moduli would be functions of the radius

and time and Eq. (4.6) reduces to the form

$$\mathbf{T} = -p\mathbf{I} + \Phi(r, z, t)\mathbf{B}, \tag{4.7}$$

where $\Phi(r, z, t) := \mu(r, t)\left[1 + \frac{b(r,t)}{n(r,t)}\left(rf_z\right)^2\right]^{n(r,t)-1}$.

We shall consider the diffusion to be reasonably slow and that the inertial effects in the solid can be neglected. It is important to bear in mind that the temporal effects are not being ignored. One could choose to view time as a parameter. Neglecting the body force, the balance of linear momentum reduces to the equations of equilibrium,

$$\text{div } \mathbf{T} = 0, \tag{4.8}$$

where div(.) denotes the divergence operator in the current configuration. We assume that the concentration of the diffusing species (c) is governed by the following convection-diffusion equation

$$\frac{\partial c}{\partial t} + \text{div}\left(c\mathbf{v}\right) = \text{div}\left(D\,\text{grad}(c)\right), \tag{4.9}$$

where D is the diffusivity and in general it could depend on the deformation as well as the concentration, grad(.) is the gradient based on the current configuration. In this study, we assume that the diffusion is very slow so that the velocity of the fluid that is diffusing can be neglected. The second term on the left side of Eq. (4.9) involves the derivative of the velocity and of course it is possible that even if the velocity is small its spatial derivatives need not be small. We shall however assume that the derivatives of the velocity are small and thus we neglect the second term in Eq. (4.9). We shall assume that D depends on the deformation, thus the equation governing the diffusion of the fluid is coupled with the balance of linear momentum. Since the concentration is only a function of the radius r and time t, equation Eq. (4.9) reduces

to

$$\frac{\partial c(r,t)}{\partial t} = \frac{1}{r}\frac{\partial}{\partial r}\left(Dr\frac{\partial c(r,t)}{\partial r}\right). \tag{4.10}$$

Next, we shall document the balance of energy for the generalized neo-Hookean solid and fluid as follows (see [90]):

$$\rho^i \frac{d\varepsilon^i}{dt} = \mathbf{T}^i.\mathbf{L}^i - \mathrm{div}\mathbf{q}^i + \rho^i r^i + E^i, \quad i = \mathrm{solid}, \mathrm{fluid}, \tag{4.11}$$

where ε^i, $\mathbf{q}^i$, r^i are the specific internal energy, heat flux, radiant heating associated with the i-th component and E^i is the energy supplied to the i-th constituent from the other constituents. We shall ignore the energy equation associated with the fluid and the contributions due to the interactions between the fluid and the solid (E^s) in the energy balance for the solid. We shall however later on incorporate the energy associated with fluid indirectly by assuming that the internal energy of the solid depends on the concentration of the diffusing fluid. In such a case, the energy equation is merely,

$$\rho\dot{\varepsilon} = \mathbf{T}.\mathbf{L} - \mathrm{div}\mathbf{q} + \rho r, \tag{4.12}$$

where ε is the internal energy of the solid, $\mathbf{L}$ is the velocity gradient of the solid, $\mathbf{q}$ is the heat flux, and r is the specific radiant heating. Further assumption that the internal energy of the solid depends on the temperature (T), concentration of the diffusing fluid and the deformation gradient of the solid, i.e.,

$$\varepsilon = \varepsilon\left(T, c, \mathbf{F}\right), \tag{4.13}$$

leads to

$$\rho\frac{\partial\varepsilon}{\partial T}\dot{T} + \rho\frac{\partial\varepsilon}{\partial c}\dot{c} + \rho\frac{\partial\varepsilon}{\partial\mathbf{F}}\mathbf{F}^T.\mathbf{L} = \mathbf{T}.\mathbf{L} - \mathrm{div}\mathbf{q} + \rho r, \tag{4.14}$$

where $(.)^T$ is the transpose of a second-order tensor. We shall define the specific Helmholtz potential as $\Psi = \varepsilon - T\eta$, where η is the specific entropy. Then Eq. (4.14) reduces to

$$\rho\frac{\partial\varepsilon}{\partial T}\dot{T} + \rho\frac{\partial\Psi}{\partial\mathbf{F}}\mathbf{F}^T.\mathbf{L} - \rho T\frac{\partial^2\Psi}{\partial T\partial\mathbf{F}}\mathbf{F}^T.\mathbf{L} + \rho\frac{\partial\Psi}{\partial c}\dot{c} - \rho T\frac{\partial^2\Psi}{\partial T\partial c}\dot{c} = \mathbf{T}.\mathbf{L} - \text{div}\mathbf{q} + \rho r. \tag{4.15}$$

where we have also used that $\eta = -\dfrac{\partial\Psi}{\partial T}$. Now, if we set $\mathbf{T} = -\pi\mathbf{I} + \rho\dfrac{\partial\Psi}{\partial\mathbf{F}}\mathbf{F}^T$, where π is the Lagrange multiplier due to the constraint of incompressibility (given by $tr(\mathbf{L}) = 0$), then in the absence of radiation along with the assumption of Fourier's relation for heat conduction,

$$\mathbf{q} = -k\ \text{grad}(T), \tag{4.16}$$

Eq. (4.15) reduces to

$$\rho C_v\dot{T} - \rho T\frac{\partial^2\Psi}{\partial T\partial\mathbf{F}}\mathbf{F}^T.\mathbf{L} + \rho\frac{\partial\Psi}{\partial c}\dot{c} - \rho T\frac{\partial^2\Psi}{\partial T\partial c}\dot{c} = \text{div}\left(k\ \text{grad}(T)\right), \tag{4.17}$$

where $C_v = \dfrac{\partial\varepsilon}{\partial T} = -T\dfrac{\partial^2\Psi}{\partial T^2}$ is the specific heat capacity and k is the heat conductivity, both of which could depend on the deformation, temperature as well as concentration of the diffusing fluid (in general, it could depend on the degradation/healing parameter α). We also note that for a generalized neo-Hookean body, the specific Helmholtz potential is given by

$$\Psi = \frac{\mu}{2\rho b}\left\{\left[1 + \frac{b}{n}\left(I_1 - 3\right)\right]^n - 1\right\}. \tag{4.18}$$

In general, along with infusion of a fluid, the body could be subject to high temperature which could cause additional degradation, and so the material parameters could depend on temperature as well i.e., $n = n(c,T)$, $\mu = \mu(c,T)$, $b = b(c,T)$. In

such a case, one ought to solve Eqs. (4.8), (4.10), (4.17), simultaneously along with Eq. (4.18). In what follows, we shall ignore the thermal effects and study the problem of degradation or healing only due to the diffusion of a fluid.

C. Degradation and healing due to diffusion

It follows from Eq. (4.7) and Eq. (4.8) that

$$\frac{\partial}{\partial r}\left(-p+\Phi(r,z,t)\right)-r\Phi(r,z,t)\left(f_z\right)^2=0, \tag{4.19}$$

$$\frac{1}{r}\frac{\partial}{\partial\theta}\left(-p+\Phi(r,z,t)\right)+\frac{\partial}{\partial z}\left(\Phi(r,z,t)rf_z\right)=0, \tag{4.20}$$

$$\frac{\partial}{\partial z}\left(-p+\Phi(r,z,t)\right)=0. \tag{4.21}$$

In solving Eqs. (4.19), (4.20) and (4.21), time t is treated as a parameter i.e., we are solving the balance of linear momentum Eq. (4.8) at every instant of time assuming that the problem is quasi-static.

Next, from Eq. (4.21), it follows that

$$-p+\Phi(r,z,t)=g(\theta,r). \tag{4.22}$$

Taking the derivative of Eq. (4.19) with respect to θ, and using Eq. (4.22), we obtain that

$$\begin{aligned}&\frac{\partial}{\partial r}\left(\frac{\partial g(r,\theta)}{\partial\theta}\right)=0,\\ \Rightarrow&\frac{\partial g(r,\theta)}{\partial\theta}=h(\theta),\end{aligned} \tag{4.23}$$

and therefore Eqs. (4.22), (4.23) reduce to

$$\frac{\partial}{\partial\theta}\left(-p+\Phi(r,z,t)\right)=h(\theta), \tag{4.24}$$

where h is a function of θ. From Eqs. (4.20) and (4.24), we obtain that

$$-\frac{\partial}{\partial\theta}\left(-p+\Phi(r,z,t)\right)=r\frac{\partial}{\partial z}\left(\Phi(r,z,t)rf_z\right)=E, \tag{4.25}$$

where E is a constant. On the basis of periodicity, we can assume that $\dfrac{\partial p}{\partial\theta}=0$, and hence from Eq. (4.25) it follows that E must be zero. Using the definition of Φ in Eq. (4.25), we obtain that

$$\left\{\left[1+\frac{b}{n}\left(rf_z\right)^2\right]^{n-1}+\frac{2b(n-1)}{n}\left(rf_z\right)^2\left[1+\frac{b}{n}\left(rf_z\right)^2\right]^{n-2}\right\}f_{zz}=\frac{E}{\mu r^2}=0, \tag{4.26}$$

where $f_{zz}:=\dfrac{\partial^2 f(z,t)}{\partial z^2}$. Thus, Eq. (4.26) reduces to either

$$f_{zz}=0, \tag{4.27}$$

or

$$\left\{\left[1+\frac{b}{n}\left(rf_z\right)^2\right]^{n-1}+\frac{2b(n-1)}{n}\left(rf_z\right)^2\left[1+\frac{b}{n}\left(rf_z\right)^2\right]^{n-2}\right\}=0. \tag{4.28}$$

Eq. (4.27) implies that

$$f(z,t)=C_1(t)z+C_2(t), \tag{4.29}$$

and Eq. (4.28) reduces to

$$1+\frac{b(2n-1)}{n}\left(rf_z\right)^2=0, \tag{4.30}$$

which has no solution[1]. Hence, Eq. (4.29) is the solution to Eq. (4.8). Interestingly, the solution Eq. (4.29) does not depend on the material parameters n, b or μ.

If we assume that the angle of twist at $z=0$ is zero, i.e., if we assume that the

[1]Here, we are assuming that b is non-negative, and $n\geq\frac{1}{2}$. As discussed previously if $n<\frac{1}{2}$, then the equations of equilibrium for anti-plane shear lose their ellipticity.

bottom of the cylinder is fixed, then we obtain that

$$f(z,t) = \psi(t)z, \tag{4.31}$$

where $\psi(t)$ is the angle of twist per unit length of the cylinder which is the time dependent generalization of the classical torsion solution. The twisting moment is given by

$$\begin{aligned} M(t) &= 2\pi \int_{R_i}^{R_0} T_{z\theta} r^2 dr \\ &= 2\pi \int_{R_i}^{R_0} \mu(c(r,t)) \left[1 + \frac{b(c(r,t))}{n(c(r,t))} \left(r\psi(t)\right)^2\right]^{n(c(r,t))-1} \psi(t) r^3 dr. \end{aligned} \tag{4.32}$$

In our work, we shall enforce the following two sets of initial and boundary conditions for the concentration of the diffusing species:

Case 1:

$$c(r,0) = 0, \ R_i \leq r \leq R_0, \tag{4.33}$$

$$\frac{\partial c}{\partial r}(R_i,t) = 0, \ \forall t > 0, \tag{4.34}$$

$$c(R_o,t) = 1, \ \forall t > 0. \tag{4.35}$$

That is, initially, the body is assumed to be in its virgin state and there is no diffusant in the body. Also, the boundary condition Eq. (4.34) implies that the gradient of the concentration is zero at the inner boundary of the annular cylinder. This can be achieved by having some sort of a membrane on the inside of the annulus which is impermeable to the diffusing species. The boundary condition Eq. (4.35) means that the outer cylinder is always exposed to the diffusant.

Case 2:

$$c(r,0) = 0,\ R_i \leq r \leq R_0, \tag{4.36}$$

$$c(R_i,t) = c_0,\ \forall t > 0, \tag{4.37}$$

$$c(R_o,t) = 1,\ \forall t > 0. \tag{4.38}$$

Here, as opposed to case 1, the inner boundary of the annular cylinder is held at a constant diffusant concentration (as reflected by Eq. (4.37)). By constructing a mechanism which continuously removes the diffusing species from the inside of the cylindrical annulus, a constant concentration boundary condition can be maintained. For example, if the diffusing species is moisture, then by blowing air inside the annulus continuously, one can control the concentration of the moisture. For convenience, we shall set c_0 to zero for this case.

In addition, we shall assume that the material moduli change in a linear fashion due to the diffusion, that is the material parameters change with c as follows:

$$\mu = \mu_0 \pm \mu_1 c, \quad 0 < \mu_1 < \mu_0, \tag{4.39}$$

$$b = b_0 \pm b_1 c, \quad 0 < b_1 < b_0, \tag{4.40}$$

$$n = n_0 \pm n_1 c, \quad 0 < n_1 < n_0, \tag{4.41}$$

with the minus sign chosen when degradation is considered and plus sign for healing. The restrictions on the ranges of μ_1, b_1, n_1 are being enforced to ensure that μ, b, n are positive, in the case of degradation.

Before proceeding with the solutions, we render the governing equations dimensionless. The non-dimensionalization is carried out in the following manner. We

define

$$\bar{t} = \frac{t}{t_0}, \bar{r} = \frac{r}{R_o}, \bar{z} = \frac{z}{H}, \bar{\psi} = \frac{\psi H}{\theta_0}, \bar{\mu} = \frac{\mu}{\mu_0}, \tag{4.42}$$

where t_0, θ_0 are characteristic time and angle. Then Eqs. (4.32) and (4.10) reduce to

$$\underbrace{\frac{MH}{2\pi R_o^4 \theta_0 \mu_0}}_{\bar{M}} = \int_0^1 \bar{\mu} \left[1 + \frac{b}{n} \underbrace{\frac{R_o^2 \theta_0^2}{H^2}}_{\bar{q}} (\bar{r}\bar{\psi})^2 \right]^{n-1} \bar{\psi}\bar{r}^3 d\bar{r}, \tag{4.43}$$

$$\frac{\partial c(\bar{r},\bar{t})}{\partial \bar{t}} = \frac{1}{\bar{r}} \frac{\partial}{\partial \bar{r}} \left(\bar{r} \underbrace{\left(\frac{Dt_0}{R_o^2} \right)}_{\bar{D}} \frac{\partial c(\bar{r},\bar{t})}{\partial \bar{r}} \right), \tag{4.44}$$

where $\bar{\mu} = 1 \pm \bar{\mu}_1 c$, with $\bar{\mu}_1 = \dfrac{\mu_1}{\mu_0}$.

The initial and boundary conditions for c after non-dimensionalization reduce to

Case 1:

$$c(\bar{r}, 0) = 0, \ \bar{r}_i \leq \bar{r} \leq 1, \tag{4.45}$$

$$\frac{\partial c}{\partial \bar{r}}(\bar{r}_i, \bar{t}) = 0, \ \forall \bar{t} > 0, \tag{4.46}$$

$$c(1, \bar{t}) = 1, \ \forall \bar{t} > 0. \tag{4.47}$$

Case 2:

$$c(\bar{r}, 0) = 0, \ \bar{r}_i \leq \bar{r} \leq 1, \tag{4.48}$$

$$c(\bar{r}_i, \bar{t}) = 0, \ \forall \bar{t} > 0, \tag{4.49}$$

$$c(1, \bar{t}) = 1, \ \forall \bar{t} > 0, \tag{4.50}$$

where $\bar{r}_i = \dfrac{R_i}{R_o}$.

D. Discussion of results

We now proceed to solve the non-dimensionalized problem, numerically. Fig. (15)(a) shows the solution to the convection-diffusion equation Eq. (4.44) for $\bar{D} = 0.01$, which has been solved using `pdepe` solver in MATLAB. We notice that after a certain time, the concentration profile reaches a steady state which implies that no further healing or degradation of the body takes place. For a given value of $\bar{\psi}$, the values of concentration thus obtained at various radii and times were used to numerically integrate (4.43) using composite trapezoidal rule to find $\bar{M}$. On the other hand for a given value of $\bar{M}$, $\bar{\psi}$ was calculated using a combination of the bisection method and the composite trapezoidal rule of integration on (4.43). The numerical values chosen for the non-dimensional quantities are shown in the figures.

The solution depicted in Fig. (15)(b) was obtained by setting n_0 to 1 along with n_1 to 0 when degradation is assumed. Under these conditions the model reduces to a neo-Hookean model as $n = 1$; furthermore, note that $\bar{\mu}_1 = 0$ corresponds to case when the neo-Hookean body is neither degrading nor healing. Notice that as $\bar{\mu}_1$ increases, the stress required to maintain the angular displacement decreases, i.e., the higher the degradation of the material, the greater is the stress relaxation in that less moment is necessary to maintain the angular displacement. Of course, since the moment is related to the shear stress through Eq. (4.32), we can call this stress relaxation due to degradation. In Figs. (15), (16) the non-dimensional moment is portrayed as a function of non-dimensional time by varying μ_1, b_1 and n_1 along with other quantities as indicated. In all these cases, it is seen that as the degradation increases, less moment is needed to maintain the deformation, as is to be expected. Next, we assume that the material is healing as the fluid diffuses (see Fig. (17)), and the non-dimensional moment is observed as a function of time for a fixed value of

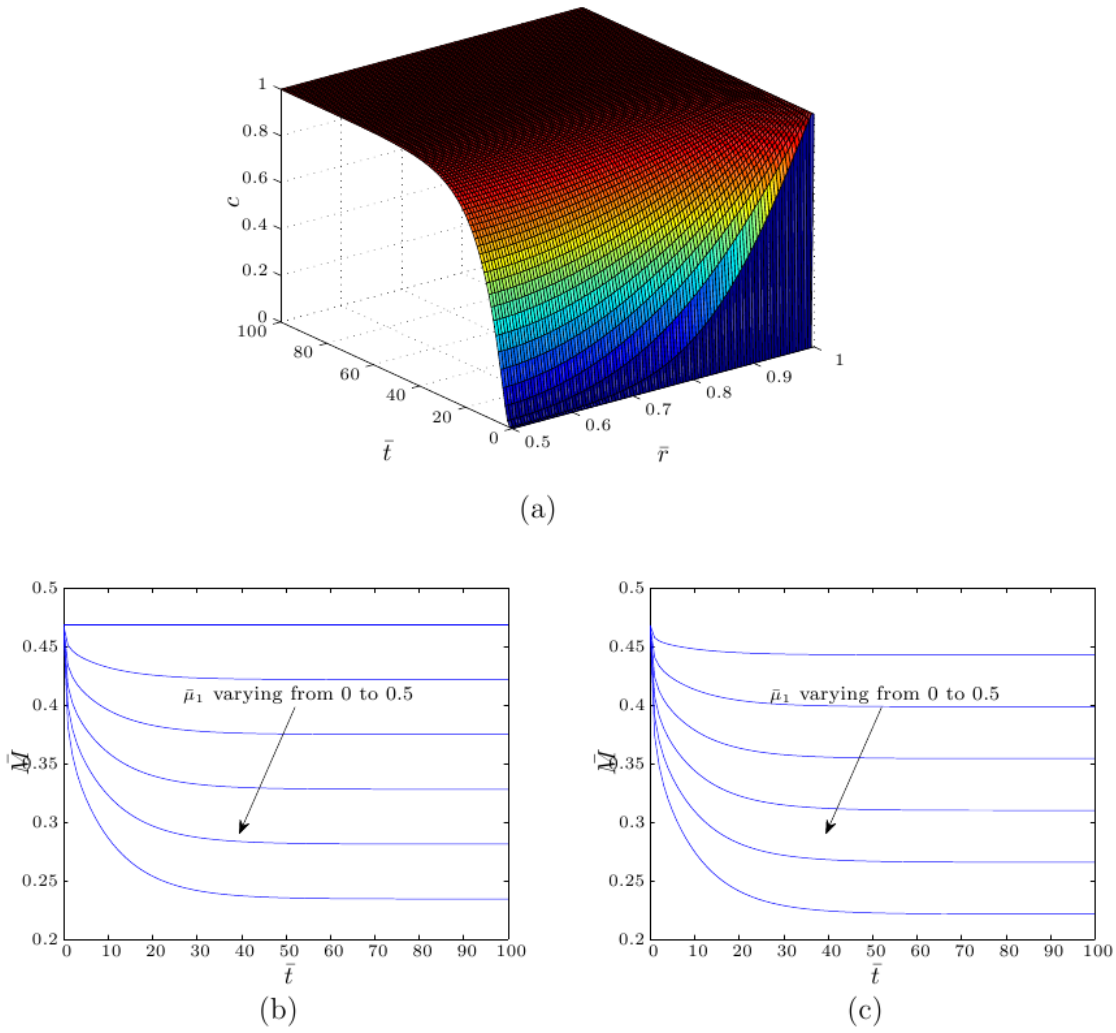

Fig. 15.: (a) Solution to the convection diffusion equation given in Eq. (4.44). (b) Non-dimensional moment ($\bar{M}$) as a function of non-dimensional time ($\bar{t}$) for various values of $\bar{\mu}_1$ starting from 0 to 0.5 in increments of 0.1 for the degradation case. Values chosen were $R_i/R_o = 0.5$, $\bar{q} = 1$, $\bar{\psi} = 1$, $\bar{D} = 0.01$, $b_0 = n_0 = 1$, $b_1 = 0$, $n_1 = 0$. This corresponds to the neo-Hookean model since $n = 1$. (c) Non-dimensional moment ($\bar{M}$) as a function of non-dimensional time ($\bar{t}$) with $\bar{\mu}_1$ varying from 0 to 0.5 in increments of 0.1 for the degradation case. Values chosen were $R_i/R_o = 0.5$, $\bar{q} = 1$, $\bar{\psi} = 1$, $\bar{D} = 0.01$, $b_0 = n_0 = 1$, $b_1 = 0.1$, $n_1 = 0.1$.

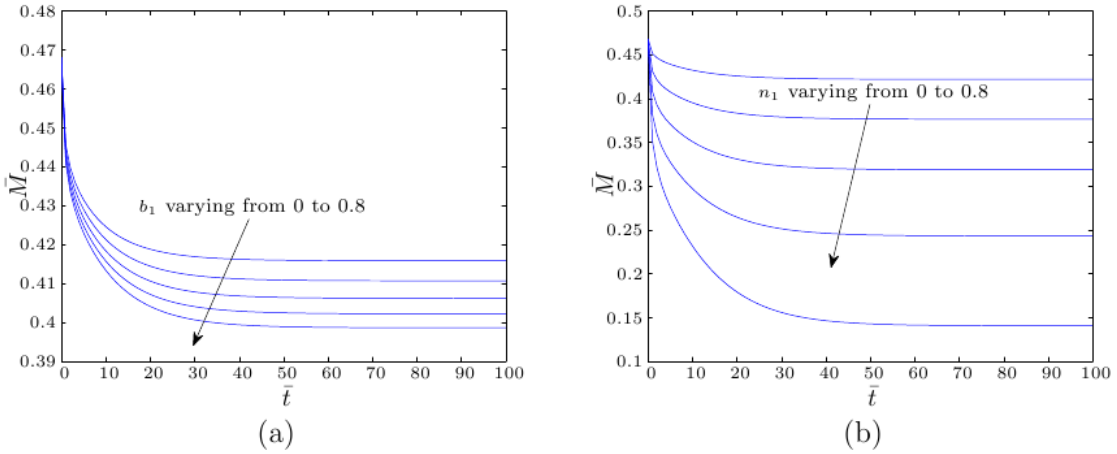

Fig. 16.: (a) Non-dimensional moment ($\bar{M}$) as a function of non-dimensional time ($\bar{t}$) for various values of b_1 varying from 0 to 0.8 in increments of 0.2 for the degradation case. Here, $R_i/R_o = 0.5$, $\bar{q} = 1$, $\bar{\psi} = 1$, $\bar{D} = 0.01$, $b_0 = n_0 = 1$, $\bar{\mu}_1 = 0.1$, $n_1 = 0.1$. (b) Non-dimensional moment ($\bar{M}$) as a function of non-dimensional time ($\bar{t}$) for various values of n_1 starting at 0 to 0.8 in increments of 0.2 for the degradation case. Here, $R_i/R_o = 0.5$, $\bar{q} = 1$, $\bar{\psi} = 1$, $\bar{D} = 0.01$, $b_0 = n_0 = 1$, $b_1 = 0.1$, $\bar{\mu}_1 = 0.1$.

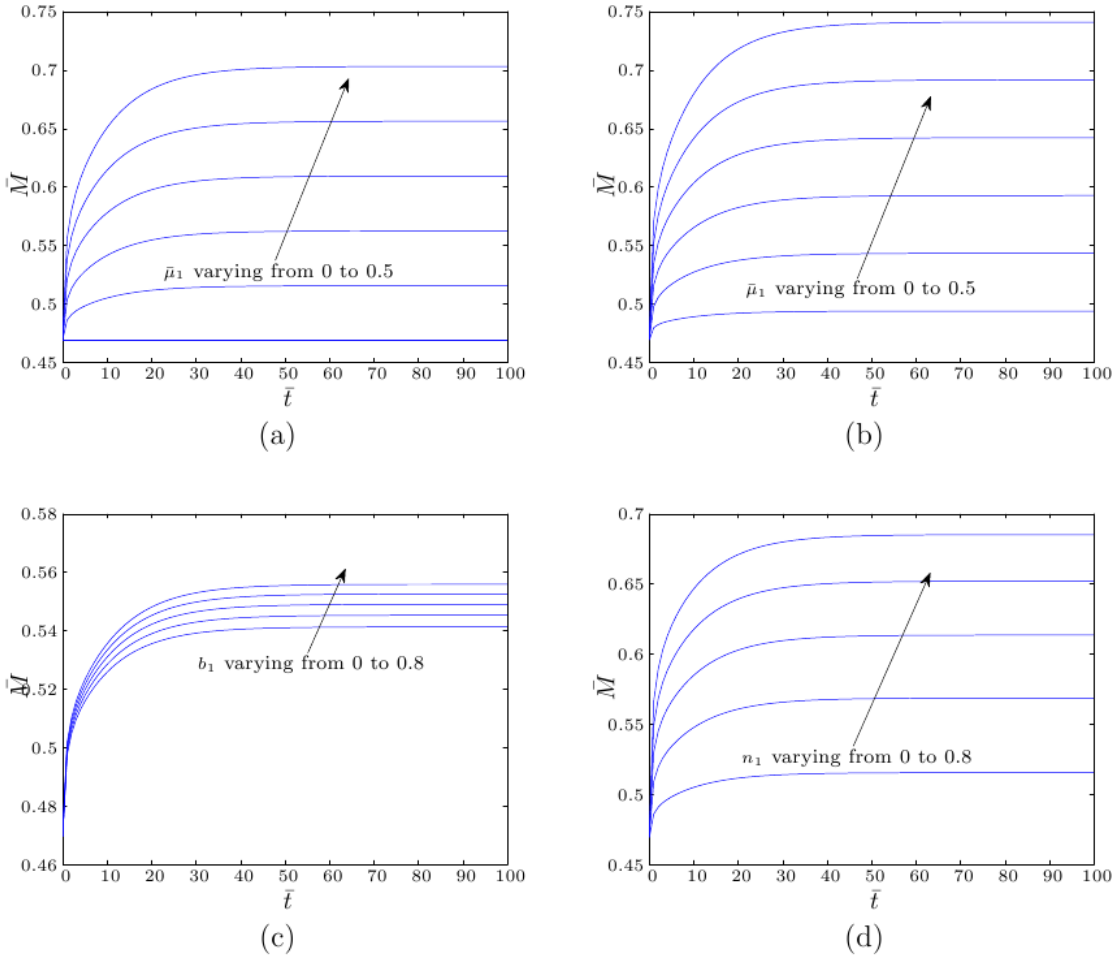

Fig. 17.: Non-dimensional moment ($\bar{M}$) as a function of non-dimensional time ($\bar{t}$) for various values of the material parameters when the body is healing. (a) $\bar{\mu}_1$ varying from 0 to 0.5 in increments of 0.1 with $b_0 = n_0 = 1$, $b_1 = 0$, $n_1 = 0$ (neo-Hookean model). (b) $\bar{\mu}_1$ varying from 0 to 0.5 in increments of 0.1 with $b_0 = n_0 = 1$, $b_1 = 0.1$, $n_1 = 0.1$. (c) b_1 varying from 0 to 0.8 in increments of 0.2 with $b_0 = n_0 = 1$, $\bar{\mu}_1 = 0.1$, $n_1 = 0.1$. (d) n_1 varying from 0 to 0.8 in increments of 0.2 with $b_0 = n_0 = 1$, $b_1 = 0.1$, $\bar{\mu}_1 = 0.1$. Other values chosen in (a), (b), (c), (d) were $R_i/R_o = 0.5$, $\bar{q} = 1$, $\bar{\psi} = 1$, $\bar{D} = 0.01$.

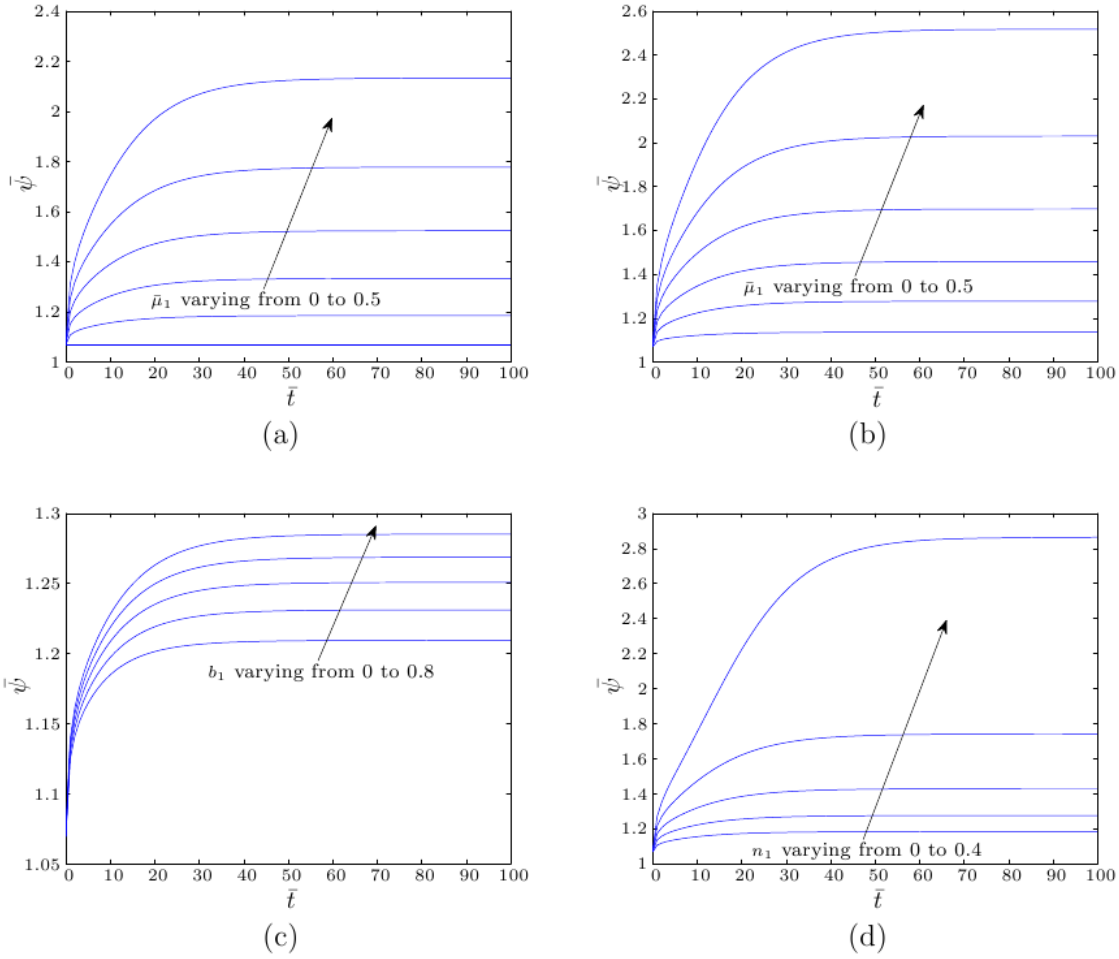

Fig. 18.: Non-dimensional angular displacement ($\bar{\psi}$) as a function of non-dimensional time ($\bar{t}$) for various values of the material parameters when the body is degrading. (a) $\bar{\mu}_1$ varying from 0 to 0.5 in increments of 0.1 with $b_0 = n_0 = 1$, $b_1 = 0$, $n_1 = 0$ (neo-Hookean model). (b) $\bar{\mu}_1$ varying from 0 to 0.5 in increments of 0.1 with $b_0 = n_0 = 1$, $b_1 = 0.1$, $n_1 = 0.1$. (c) b_1 varying from 0 to 0.8 in increments of 0.2 with $b_0 = n_0 = 1$, $\bar{\mu}_1 = 0.1$, $n_1 = 0.1$. (d) n_1 varying from 0 to 0.4 in increments of 0.1 with $b_0 = n_0 = 1$, $b_1 = 0.1$, $\bar{\mu}_1 = 0.1$. Other values chosen in (a), (b), (c), (d) were $R_i/R_o = 0.5$, $\bar{q} = 1$, $\bar{M} = 0.5$, $\bar{D} = 0.01$.

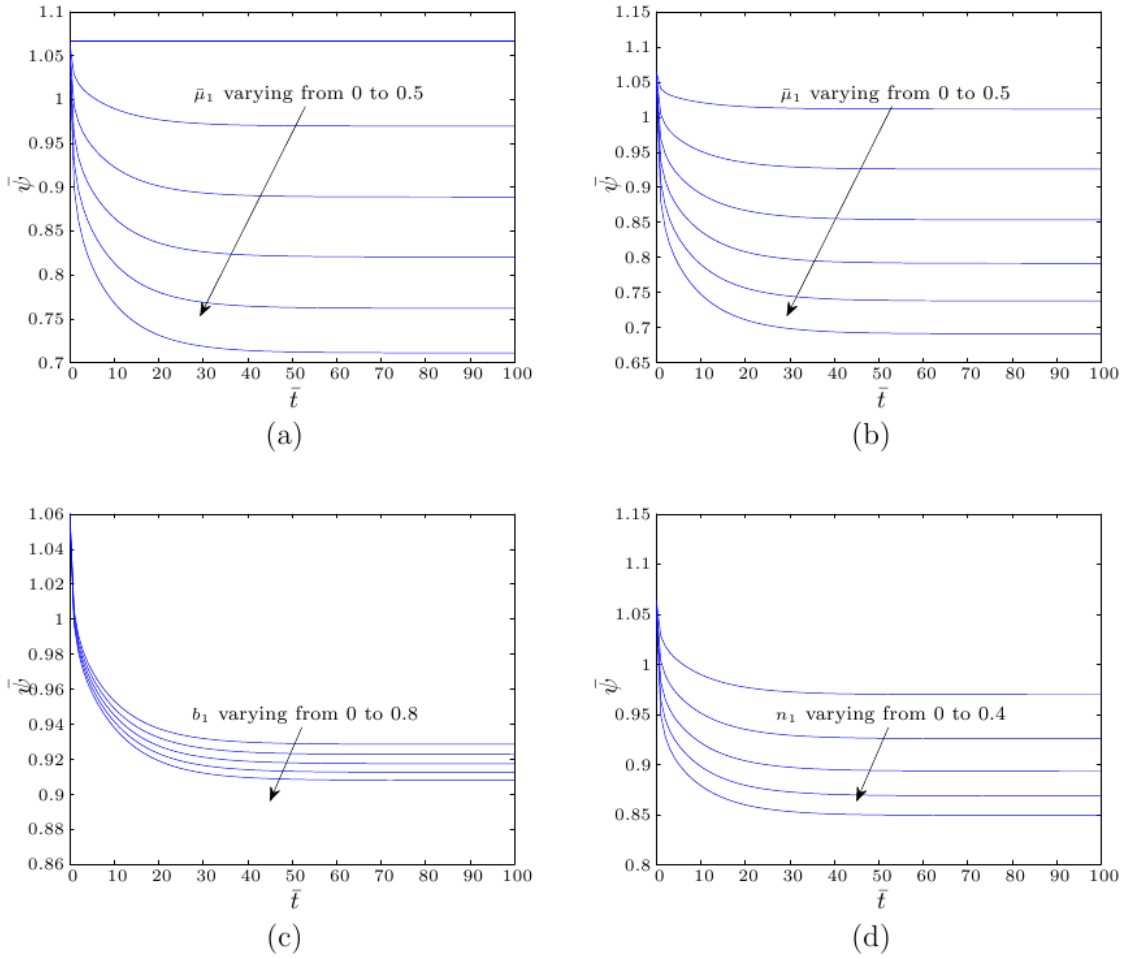

Fig. 19.: Non-dimensional angular displacement ($\bar{\psi}$) as a function of non-dimensional time ($\bar{t}$) for various values of the material parameters when the body is healing. (a) $\bar{\mu}_1$ varying from 0 to 0.5 in increments of 0.1 with $b_0 = n_0 = 1$, $b_1 = 0$, $n_1 = 0$ (neo-Hookean model). (b) $\bar{\mu}_1$ varying from 0 to 0.5 in increments of 0.1 with $b_0 = n_0 = 1$, $b_1 = 0.1$, $n_1 = 0.1$. (c) b_1 varying from 0 to 0.8 in increments of 0.2 with $b_0 = n_0 = 1$, $\bar{\mu}_1 = 0.1$, $n_1 = 0.1$. (d) n_1 varying from 0 to 0.4 in increments of 0.1 with $b_0 = n_0 = 1$, $b_1 = 0.1$, $\bar{\mu}_1 = 0.1$. Other values chosen in (a), (b), (c), (d) were $R_i/R_o = 0.5$, $\bar{q} = 1$, $\bar{M} = 0.5$, $\bar{D} = 0.01$.

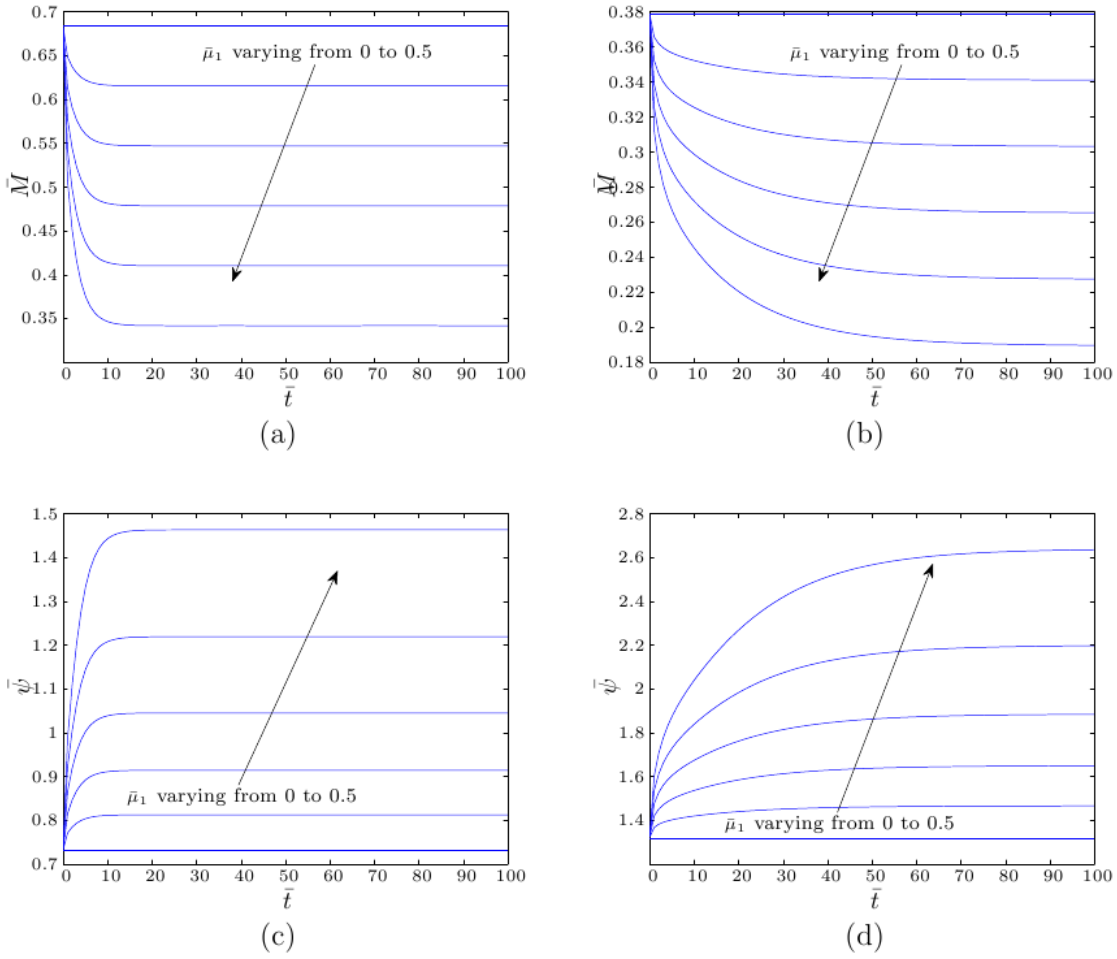

Fig. 20.: (a) Non-dimensional moment ($\bar{M}$) as a function of non-dimensional time ($\bar{t}$) for various values of $\bar{\mu}_1$ starting from 0 to 0.5 in increments of 0.1 for the degradation case with $R_i/R_o = 0.75$.

Fig. 20.: continued. (b) Non-dimensional moment ($\bar{M}$) as a function of non-dimensional time ($\bar{t}$) for various values of $\bar{\mu}_1$ starting from 0 to 0.5 in increments of 0.1 for the degradation case with $R_i/R_o = 0.35$. (c) Non-dimensional angular displacement ($\bar{\psi}$) as a function of non-dimensional time ($\bar{t}$) for various values of $\bar{\mu}_1$ starting from 0 to 0.5 in increments of 0.1 for the degradation case with $R_i/R_o = 0.75$. (d) Non-dimensional angular displacement ($\bar{\psi}$) as a function of non-dimensional time ($\bar{t}$) for various values of $\bar{\mu}_1$ starting from 0 to 0.5 in increments of 0.1 for the degradation case with $R_i/R_o = 0.35$. In all cases, $\bar{q} = 1$, $b_0 = n_0 = 1$, $b_1 = 0.0$, $n_1 = 0.0$. Initial and boundary conditions considered are given by Eqs. (4.45–4.47).

non-dimensional angular displacement. As the body heals with time, the moment required to maintain the deformation increases. Furthermore, as seen from Figs. (15), (16), (17) the non-dimensional moment reaches a steady value to maintain the angular displacement since the concentration of the diffusant reaches a steady value after which there is no further degradation or healing.

Fig. (18) shows that the non-dimensional angular displacement of the cylinder increases with time for an applied non-dimensional moment when the generalized neo-Hookean body is degrading i.e., the body "creeps" for sometime, and then the angular displacement reaches a steady value. This is very different from the creep in a viscoelastic solid, wherein the angular displacement continuously increases with time when an external moment is applied. This is one way of determining if the creep undergone by a body is either due to the viscoelastic nature of the body or due to degradation. Now, when one considers healing, the non-dimensional angular displacement of the body decreases with time as shown in Fig. (19) for an applied moment, and then remains steady.

As mentioned in the introduction, Rajagopal and Wineman [78] showed that the stress relaxation due to aging depends on the material geometry, and this characteristic differentiates the stress relaxation due to aging/degradation from the stress relaxation due to viscoelasticity. To illustrate this phenomenon in our work, results were obtained at the ratio of the inner radius of the annulus to the outer radius ($\bar{r}_i$) being 0.35 and 0.75 (see Fig. (20)), and it is seen that not only stress relaxation but also creep due to degradation depends on the geometry. Comparing Figs. (20)(a) and (20)(b), Figs. (20)(c) and (20)(d), one can also see that the steady state values are attained at a faster rate when $\bar{r}_i = 0.75$. This is because the annulus has a smaller thickness for this case and so the concentration reaches steady state faster.

To see how the stress relaxation and creep depend on the diffusivity, we changed

the non-dimensional diffusivity ($\bar{D}$) from 0.01 to 0.1. As can be seen in Fig. (21) the moment relaxes faster as the diffusivity increases, and the angular displacement undergone by the body increases faster as the diffusivity increases. This is because higher diffusivity means that the concentration at any given location increases faster as it tends towards the steady state value, and as the material parameters decrease or increase (based on degradation or healing) in value with increasing concentration, the material degrades or heals faster. Also, notice that the steady state non-dimensional moment and the non-dimensional angular displacement values are the same for the three values of the non-dimensional diffusivity. This is due to the fact that the steady state solution for concentration of the diffusant is the same in all the cases, which is $c(r,t) = 1$, for t sufficiently large so that steady state is reached.

Next, we shall look at how the results vary when the diffusivity depends on the strain; we choose the Almansi-Hamel strain as the measure of the non-linear strain. This is to capture the fact that the pore structure in the body depends on the strain and hence will lead to a change in the diffusivity. However, a priori, it is not clear whether the diffusivity has to increase or decrease. In this study, we shall assume that the diffusivity increases with the strain.

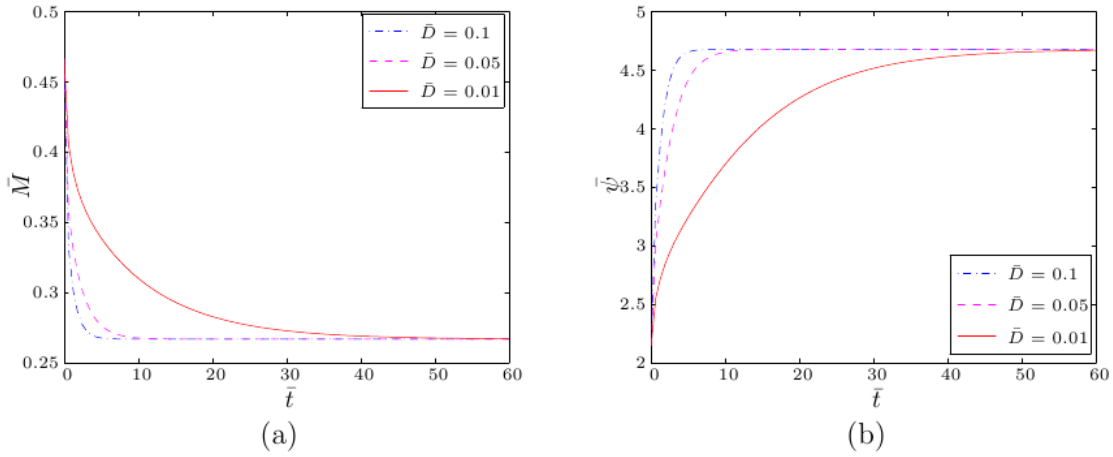

Fig. 21.: (a) Comparison of non-dimensional moment ($\bar{M}$) as a function of non-dimensional time ($\bar{t}$) for various constant diffusivity values for $\bar{\psi} = 1$. (b) Comparison of non-dimensional angular displacement ($\bar{\psi}$) as a function of non-dimensional time ($\bar{t}$) for various constant diffusivity values for $\bar{M} = 1$. Also, $R_i/R_o = 0.5$, $\bar{q} = 1$, $b_0 = n_0 = 1$, $b_1 = 0.1$, $n_1 = 0.1$, $\bar{\mu}_1 = 0.4$. Initial and boundary conditions considered are given by Eqs. (4.45–4.47).

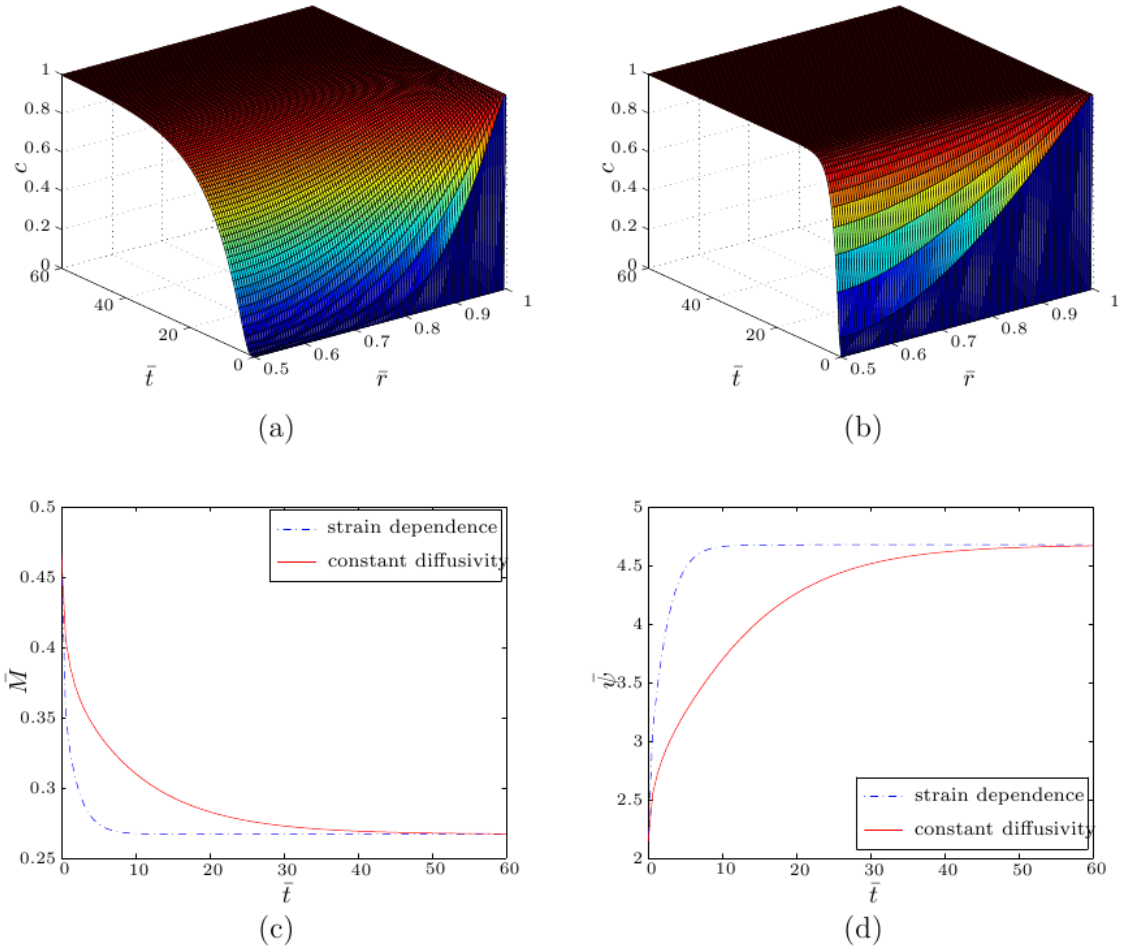

Fig. 22.: (a) Solution to the convection-diffusion equation Eq. (4.44) when the diffusivity is held constant. (b) Solution to Eq. (4.44) when the diffusivity depends on the Almansi-Hamel strain.

Fig. 22.: continued. (c) Non-dimensional moment ($\bar{M}$) as a function of non-dimensional time ($\bar{t}$) with and without diffusivity depending on the Almansi-Hamel strain for $\bar{\psi} = 1$. (d) Non-dimensional angular displacement ($\bar{\psi}$) as a function of non-dimensional time ($\bar{t}$) with and without diffusivity depending on the Almansi-Hamel strain for $\bar{M} = 1$. Here, $R_i/R_o = 0.5$, $\bar{q} = 1$, $b_0 = n_0 = 1$, $b_1 = 0.1$, $n_1 = 0.1$, $\bar{\mu}_1 = 0.4$. For constant diffusivity case $\bar{D} = 0.01$, and for diffusivity depending on the Almansi-strain, relation Eq. (4.53) is assumed with $\bar{D}_0 = 0.01$, $\bar{D}_\infty = 0.1$, $\lambda = 1$. Initial and boundary conditions considered are given by Eqs. (4.45–4.47).

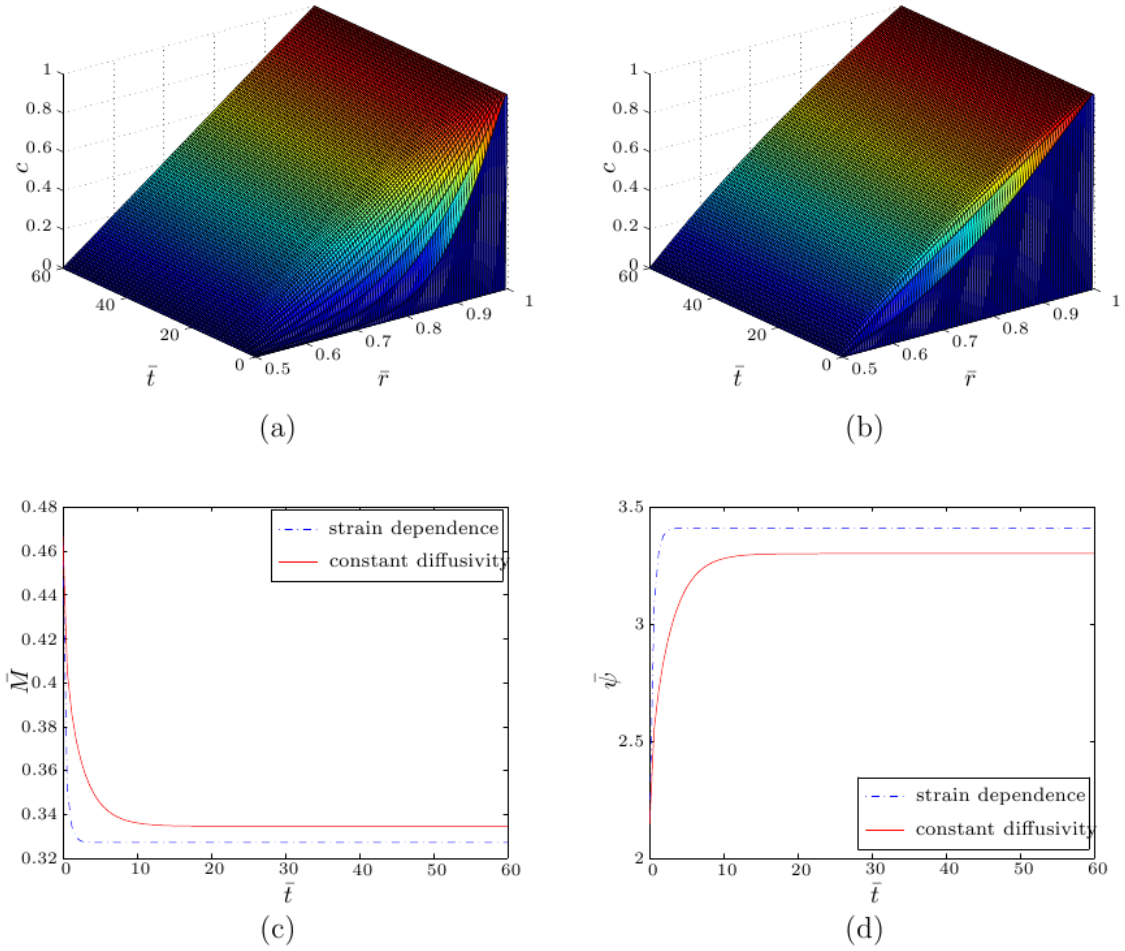

Fig. 23.: (a) Solution to the convection-diffusion equation Eq. (4.44) when the diffusivity is held constant. (b) Solution to Eq. (4.44) when the diffusivity depends on the Almansi-Hamel strain.

Fig. 23.: continued. (c) Non-dimensional moment ($\bar{M}$) as a function of non-dimensional time ($\bar{t}$) with and without diffusivity depending on the Almansi-Hamel strain for $\bar{\psi} = 1$. (d) Non-dimensional displacement ($\bar{\psi}$) as a function of non-dimensional time ($\bar{t}$) with and without diffusivity depending on the Almansi-Hamel strain for $\bar{M} = 1$. Here, $R_i/R_o = 0.5$, $\bar{q} = 1$, $b_0 = n_0 = 1$, $b_1 = 0.1$, $n_1 = 0.1$, $\bar{\mu}_1 = 0.4$. For constant diffusivity case $\bar{D} = 0.01$, and for diffusivity depending on the Almansi-strain, relation Eq. (4.53) is assumed with $\bar{D}_0 = 0.01$, $\bar{D}_\infty = 0.1$, $\lambda = 1$. Initial and boundary conditions considered are given by Eqs. (4.48–4.50).

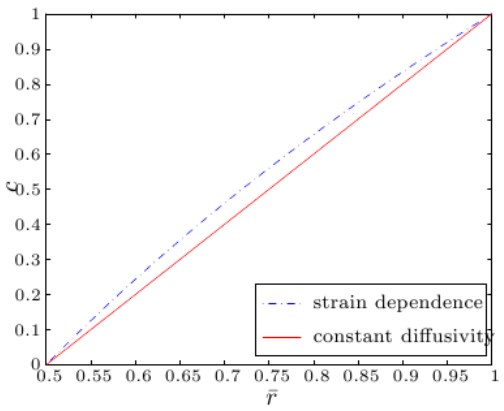

Fig. 24.: Comparison of the steady state solutions ($\bar{t} = 40$) to Eq. (4.44) with constant diffusivity and when the diffusivity depends on the Almansi-Hamel strain, with initial and boundary conditions given by Eqs. (4.48–4.50). $R_i/R_o = 0.5$, $\bar{q} = 1$, $\bar{\psi} = 1$, $b_0 = n_0 = 1$, $b_1 = 0.1$, $n_1 = 0.1$, $\bar{\mu}_1 = 0.4$. For constant diffusivity case $\bar{D} = 0.01$, and for diffusivity depending on the Almansi-strain, relation Eq. (4.53) is assumed with $\bar{D}_0 = 0.01$, $\bar{D}_\infty = 0.1$, $\lambda = 1$.

Now, the Almansi-Hamel strain is given by

$$\mathbf{e} = \frac{1}{2}\left(\mathbf{I} - \mathbf{B}^{-1}\right) = \begin{bmatrix} 0 & 0 & 0 \\ 0 & 0 & \left(\frac{1}{2}r\psi\right) \\ 0 & \left(\frac{1}{2}r\psi\right) & \left(-\frac{1}{2}r^2\psi^2\right) \end{bmatrix}. \tag{4.51}$$

The Frobenius norm of $\mathbf{e}$ is given by

$$\begin{aligned} \|\mathbf{e}\| := \sqrt{tr\left(\mathbf{e}^{\mathrm{T}}\mathbf{e}\right)} &= \sqrt{\frac{1}{4}(r\psi)^4 + \frac{1}{2}(r\psi)^2} \\ &= \sqrt{\frac{1}{4}\bar{q}^2\left(\bar{r}\bar{\psi}\right)^4 + \frac{1}{2}\bar{q}\left(\bar{r}\bar{\psi}\right)^2}. \end{aligned} \tag{4.52}$$

We shall assume that the diffusivity $\bar{D}$ depends on the Almansi-Hamel strain in the following manner

$$\bar{D} = \bar{D}_0 + \left(\bar{D}_\infty - \bar{D}_0\right)\left(1 - e^{-\lambda\|\mathbf{e}\|}\right). \tag{4.53}$$

Figs. (22)(c), (22)(d) compare the stress relaxation and creep for the case with constant diffusivity against the case when the diffusivity depends on the Almansi-Hamel strain with the initial and boundary conditions considered are given by Eqs. (4.45–4.47). The stress relaxation and creep are faster when diffusivity is assumed to be a function of the Almansi-Hamel strain, as the diffusivity is higher in this case and hence the degradation is faster.

Next, we shall consider the situation when we have the initial and boundary conditions given by Eqs. (4.48–4.50). Here too, the stress relaxation and creep are faster when the diffusivity depends on the Almansi-Hamel strain is assumed (see Figs. (23)(c), (23)(d)). However, the steady state values of the non-dimensional moment and non-dimensional angular displacement when the diffusivity is maintained constant is not the same as that when the diffusivity depends on the Almansi-Hamel

strain. One can explain this by looking at the steady state solutions for the convection-diffusion equation in Fig. (24). Unlike the situation corresponding to Eqs. (4.45–4.47), the steady state solutions for the concentration are not the same and the steady state concentrations when the diffusivity depends on the strain are higher than the steady state values when the diffusivity is constant. This induces the stresses to relax to a lower value in (23)(c) and the angular diplacement to reach a higher value in (23)(d). These values are also attained faster as the steady state solution is reached faster when the diffusivity depends on the strain.

E. Conclusions

Using the generalized neo-Hookean solid as a vehicle to illustrate the effects of degradation of a body that is initially elastic we have shown that degradation due to the infusion of a fluid can cause stress relaxation and creep until a steady state is reached. In contrast to a viscoelastic body which creeps continuously upon application of a load, the body considered here stops to creep after a certain steady state value is attained. This is one important characteristic that can be used to differentiate the creep due to the viscoelastic nature of a body, and the creep due to degradation. We have also shown the geometric dependence of the stress relaxation and creep due to degradation. We have also considered the case of healing or strengthening of a generalized neo-Hookean body due to the infusion of a fluid. One can easily extend this work to other forms of degradation in a generalized neo-Hookean material or for that matter in any elastic body whose properties change due to the infusion of a fluid, by providing an appropriate equation that governs the evolution of the degradation parameter.

CHAPTER V

MODELING THE NON-LINEAR VISCOELASTIC RESPONSE OF HIGH TEMPERATURE POLYIMIDES

A constitutive model is developed to predict the viscoelastic response of polyimide resins that are used in high temperature applications. This model is based on a thermodynamic framework that uses the notion that the 'natural configuration' of a body evolves as the body undergoes a process and the evolution is determined by maximizing the rate of entropy production in general and the rate of dissipation within purely mechanical considerations. We constitutively prescribe forms for the specific Helmholtz potential and the rate of dissipation (which is the product of density, temperature and the rate of entropy production), and the model is derived by maximizing the rate of dissipation with the constraint of incompressibility, and the reduced energy dissipation equation is also regarded as a constraint in that it is required to be met in every process that the body undergoes. The efficacy of the model is ascertained by comparing the predictions of the model with the experimental data for PMR-15 and HFPE-II-52 polyimide resins.

A. Introduction

Polyimides are well known to be extremely stable at high temperatures and also have a glass transition temperature that is greater than 300°C. Due to their good performance at high temperature ranges they are used by aircraft and automobile industries to fashion their products. They are also used in wafer fabrication due to their excellent high temperature resistance and adhesive properties (see [25]). The mechanical properties of polyimides and polyimide composites used in several applications especially in the aerospace industry are affected by high temperature, diffusion of moisture

and subsequent oxidation. Hence, there is need for a good understanding of the various degradation mechanisms that are operational when such materials are subject to hostile environment. Recent experimental evidence shows that the response of polyimide resins is solid-like viscoelastic response (see [91], [92]). Moreover, the response of such bodies is non-linear (For a detailed description concerning how to differentiate between viscoelastic solid-like and fluid-like response we refer the reader to [11], [93]). A thermodynamic framework which takes into account the viscoelastic solid-like response of the polyimides along with the various degradation processes needs to be developed. As a first step, our aim in this chapter is to develop a model based on a thermodynamic framework that can predict the non-linear viscoelastic solid-like response of polyimides at various temperatures. This first step is non-trivial and presents interesting challenges. Subsequently, we shall extend this model to include degradation due to moisture diffusion, and chemical reactions, specifically oxidation.

While the thermal response of linear viscoelastic solids have been studied in great detail, there has been no systematic study of non-linear viscoelastic solids. Standard techniques like superposition that are valid in linear response are no longer valid, thus making the study much more complicated. A single integral model has been proposed by Pipkin and Rogers [14] who have assumed that a linear combination of responses to single step strain histories can be used as an approximation to the response to an arbitrary strain history. Unfortunately, such a model does not have a sound thermodynamic basis, and moreover the model is too general to be of use. Later on, Fung [15] developed a quasi-linear viscoelastic model that has been shown to predict the behavior of several biological materials, though not adequately when the strains are large. This model by Fung can be shown to be a special case of the model by Pipkin and Rogers. For further details on the various viscoelastic models for solids that have been reported in the literature, see the review articles by Drapaca

et al. [16] and Wineman [17].

Most of the literature concerning the modeling of the response of polyimides use a viscoelastic model proposed by Schapery [94]. Muliana and Sawant [95] used Schapery's model and obtained material parameters for PMR-15[1] using the experiments carried out by Marais and Villoutreix [96]. They used these material parameters in their 'micromechanical' model to predict the behavior of Kevlar/PMR-15 composites. Ahci and Talreja [97] performed experiments on a composite made of graphite fiber in a HFPE-II[2]. They have extended the framework developed by Schapery to include a 'damage tensor' as an internal variable, and have also included anisotropy to model the composite behavior. Recently, Falcone and Ruggles-Wrenn performed experiments on PMR-15 at the service temperature of an aircraft, 288°C, and compared the predictions of Schapery's model for the problem of creep with experimental data. Bhargava [91] has also used Schapery's model to predict the behavior of HFPE-II-52. More recently, Hall [98] developed a thermodynamic framework for finite anisotropic viscoplastic models to study the response of polymers subject to extreme thermal environment.

Given its extensive use some comments on Schapery's model are warranted: Schapery developed a viscoelastic model using linear phenomenological relations based on Onsager's reciprocity theorem (see [56]) which states that the forces are linearly related to the fluxes near equilibrium (see for instance, equation 11 in [99]). Next, he introduced nonlinearity by assuming that the coefficient matrix relating the forces and fluxes depends on generalized coordinates and temperature. Furthermore, the free energy expression was obtained using a Taylor series expansion and by neglecting

[1]PMR polymerization of monomer reactant.

[2]HFPE stands for hydrofluoropolyether.

higher order terms. Thus, while the model might be able to describe slight deviation from linear response, one cannot expect it to be capable of describing truly non-linear response that is thermodynamically compatible. Thus, if one is interested in describing the non-linear response of viscoelastic solids that takes into account its thermodynamic effects, a different model is necessary. In this chapter we develop a viscoelastic solid model based on a thermodynamic framework that can be used to describe the non-linear response exhibited by a class of polymers. The framework has been recently developed and is used to describe the response of bodies that produce entropy in a variety of ways. In order to derive meaningful physical models they require that amongst the class of processes that are possible the process which is actually taken by the body is one that maximizes the rate of entropy production. One can find details concerning this approach in the review article by Rajagopal and Srinivasa [20]. In this approach, one need not assume near-equilibrium behavior and linear phenomenological relations between forces and fluxes, the approach is much more general. Also, one need not use a Taylor series expansion of the free energy, and neglect higher order terms. Recently, Rajagopal and Srinivasa [38] have shown that if one uses an expression for entropy production which is quadratic in the fluxes, one can arrive at Onsager's relations upon maximizing the rate of entropy production along with appropriate constraints. As mentioned earlier such a thermodynamic framework has also been used to model various material responses such as viscoelastic solid-like and fluid-like behavior, traditional plasticity, twinning, crystallization and so on (see the review article by Rajagopal and Srinivasa [20] for the references and for the details of the framework).

In this chapter, a viscoelastic solid model is derived by assuming forms for the Helmholtz potential and the rate of dissipation, and maximizing the rate of dissi-

pation[3] with incompressibility and the reduced energy dissipation equation as constraints. This model is shown to predict the viscoelastic response of polyimide resin. Experimental data for PMR-15 polyimide resin from [92], and for HFPE-II-52 from [91] are used to evaluate the efficacy of the model.

The current chapter is organized as follows. In section (B), the kinematics that is required in this chapter are documented. In sub-sections (C.1), (C.2), a viscoelastic solid model is developed using a thermodynamic framework. We show that the viscoelastic solid model that is developed is a generalization of the one-dimensional standard linear solid model in (C.3). In sub-section (C.4) the problem of uniaxial extension is set up using our model, and the creep solution obtained by using the model is compared with experimental data for PMR-15 and HFPE-II-52 polyimide resins in sub-section (C.5). We find that the theoretical predictions agree quite well with the experimental results.

B. Preliminaries

Let $\kappa_R(\mathcal{B})$ and $\kappa_t(\mathcal{B})$ denote the reference configuration and the current configuration, respectively. The motion χ_{κ_R} is defined as the one-one mapping that assigns to each point $\boldsymbol{X} \in \kappa_R$, a point $\boldsymbol{x} \in \kappa_t$, at a time t, i.e.,

$$\boldsymbol{x} = \chi_{\kappa_R}(\boldsymbol{X}, t). \tag{5.1}$$

The mapping $\chi_{\kappa_R}(\boldsymbol{X}, t)$ is assumed to be sufficiently smooth and invertible. Let $\kappa_{p(t)}$ be the stress-free configuration instantaneously reached by the body upon removal of the external stimuli (see Fig. (25)). We assume that the body can be instantaneously

[3] In case of isothermal processes, the rate of dissipation is the rate of conversion of mechanical working into heat (energy in thermal form), and in general it is the product of density, temperature and the rate of entropy production.

unloaded. We shall call this configuration as the natural configuration corresponding to κ_t. The natural configuration that underlies the current configuration depends on the process class that is admissible. Thus underlying natural configuration corresponding to isothermal and adiabatic processes could be different. Let $\boldsymbol{F}$ be gradient of motion $\chi_{\kappa_R}(\boldsymbol{X}, t)$ (usually known as the deformation gradient), defined by

$$\boldsymbol{F} := \frac{\partial \chi_{\kappa_R}}{\partial \boldsymbol{X}}, \tag{5.2}$$

and let the left and right Cauchy-Green tensors be defined through

$$\boldsymbol{B} = \boldsymbol{F}\boldsymbol{F}^T, \quad \boldsymbol{C} = \boldsymbol{F}^T\boldsymbol{F}. \tag{5.3}$$

Let $\boldsymbol{F}_{\kappa_{p(t)}}$ be the gradient of the mapping from $\kappa_{p(t)}$ to κ_t, and let $\boldsymbol{G}$ be defined by

$$\boldsymbol{G} := \boldsymbol{F}_{\kappa_R \to \kappa_{p(t)}} = \boldsymbol{F}^{-1}_{\kappa_{p(t)}}\boldsymbol{F}. \tag{5.4}$$

Similar to Eq. (5.3), we shall denote the left Cauchy-Green stretch tensors $\boldsymbol{B}_G$ and $\boldsymbol{B}_{p(t)}$ as

$$\boldsymbol{B}_G = \boldsymbol{G}\boldsymbol{G}^T, \quad \boldsymbol{B}_{p(t)} = \boldsymbol{F}_{\kappa_{p(t)}}\boldsymbol{F}^T_{\kappa_{p(t)}}. \tag{5.5}$$

We shall also define the velocity gradients

$$\boldsymbol{L}_G = \dot{\boldsymbol{G}}\boldsymbol{G}^{-1}, \quad \boldsymbol{L} = \dot{\boldsymbol{F}}\boldsymbol{F}^{-1}, \quad \boldsymbol{L}_p = \dot{\boldsymbol{F}}_{\kappa_{p(t)}}\boldsymbol{F}^{-1}_{\kappa_{p(t)}}, \tag{5.6}$$

and their symmetric parts by

$$\boldsymbol{D}_i = \frac{1}{2}\left(\boldsymbol{L}_i + \boldsymbol{L}_i^T\right), \quad i = p(t), G \quad \text{or no subscript.} \tag{5.7}$$

Also, we define the principal invariants through

$$\mathrm{I}_{\boldsymbol{B}_l} = \mathrm{tr}(\boldsymbol{B}_l), \quad \mathrm{II}_{\boldsymbol{B}_l} = \frac{1}{2}\left\{[\mathrm{tr}(\boldsymbol{B}_l)]^2 - \mathrm{tr}(\boldsymbol{B}_l^2)\right\}, \quad \mathrm{III}_{\boldsymbol{B}_l} = \det(\boldsymbol{B}_l) \quad l = G, p(t), \tag{5.8}$$

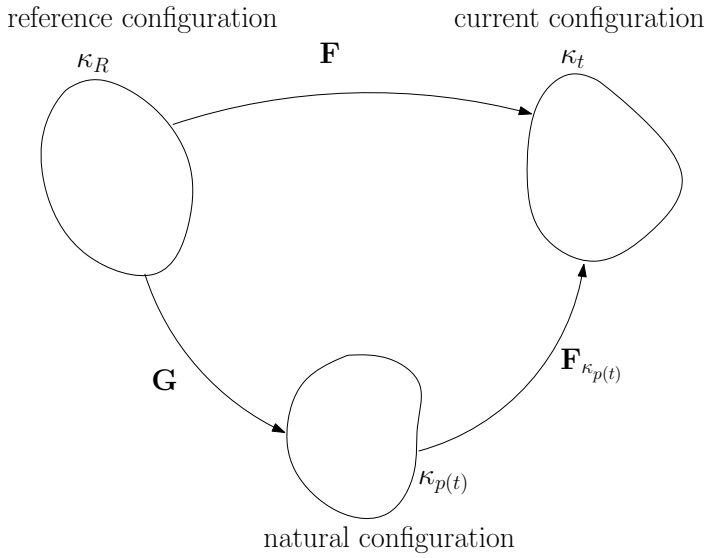

Fig. 25.: Illustration of various configurations of the body.

where tr(.) is the trace operator for a second order tensor and det(.) is the determinant. Now, from Eq. (5.4)

$$\begin{aligned} &\dot{\boldsymbol{F}} = \dot{\boldsymbol{F}}_{\kappa_{p(t)}}\boldsymbol{G} + \boldsymbol{F}_{\kappa_{p(t)}}\dot{\boldsymbol{G}} \\ &\Rightarrow \dot{\boldsymbol{F}}\boldsymbol{F}^{-1} = \dot{\boldsymbol{F}}_{\kappa_{p(t)}}\boldsymbol{G}\boldsymbol{G}^{-1}\boldsymbol{F}^{-1}_{\kappa_{p(t)}} + \boldsymbol{F}_{\kappa_{p(t)}}\dot{\boldsymbol{G}} \\ &\Rightarrow \boldsymbol{L} = \boldsymbol{L}_{p(t)} + \boldsymbol{F}_{\kappa_{p(t)}}\boldsymbol{L}_G\boldsymbol{F}^{-1}_{\kappa_{p(t)}}, \end{aligned} \tag{5.9}$$

where $\dot{(.)}$ is the material time derivative of the second order tensor. In addition,

$$\begin{aligned} \dot{\boldsymbol{B}}_{p(t)} &= \dot{\boldsymbol{F}}_{\kappa_{p(t)}}\boldsymbol{F}^T + \boldsymbol{F}\dot{\boldsymbol{F}}^T_{\kappa_{p(t)}} \\ &= \boldsymbol{L}_{p(t)}\boldsymbol{B}_{p(t)} + \boldsymbol{B}_{p(t)}\boldsymbol{L}^T_{p(t)}, \end{aligned} \tag{5.10}$$

and similarly

$$\dot{\boldsymbol{B}}_G = \boldsymbol{L}_G\boldsymbol{B}_G + \boldsymbol{B}_G\boldsymbol{L}^T_G. \tag{5.11}$$

Hence, from Eq. (5.9) and Eq. (5.10), we have

$$\dot{\boldsymbol{B}}_{p(t)} = \boldsymbol{L}\boldsymbol{B}_{p(t)} + \boldsymbol{B}_{p(t)}\boldsymbol{L}^T_{p(t)} - \boldsymbol{F}_{\kappa_{p(t)}}\left(\boldsymbol{L}_G + \boldsymbol{L}^T_G\right)\boldsymbol{F}^T_{\kappa_{p(t)}}, \tag{5.12}$$

and so

$$\overset{\nabla}{\boldsymbol{B}}_{p(t)} = -2\boldsymbol{F}_{\kappa_{p(t)}}\boldsymbol{D}_G\boldsymbol{F}^T_{\kappa_{p(t)}}, \tag{5.13}$$

where $\overset{\nabla}{(.)}$ is the usual Oldroyd derivative defined through $\overset{\nabla}{\boldsymbol{A}} := \dot{\boldsymbol{A}} - \boldsymbol{L}\boldsymbol{A} - \boldsymbol{A}\boldsymbol{L}^T$. When one considers non-isothermal processes the local form of the second law of thermodynamics takes the following form:

$$\boldsymbol{T}\cdot\boldsymbol{D} - \varrho\dot{\psi} - \varrho s\dot{\theta} - \frac{\boldsymbol{q}_h\cdot\operatorname{grad}(\theta)}{\theta} = \varrho\theta\zeta := \xi \geq 0, \tag{5.14}$$

where $\boldsymbol{T}$ is the Cauchy stress, ψ is the specific Helmholtz potential, ϱ is the density, θ is the temperature, s is the specific entropy, $\boldsymbol{q}_h$ is the heat flux, ζ is the rate of entropy production and ξ is the rate of dissipation.

C. Constitutive assumptions and maximization of the rate of dissipation

1. General results

We shall assume that the viscoelastic solid is isotropic and incompressible with the specific Helmholtz potential of the form

$$\psi = \psi(\boldsymbol{B}_{p(t)}, \boldsymbol{B}_G, \theta) = \hat{\psi}(\mathrm{I}_{\boldsymbol{B}_{p(t)}}, \mathrm{II}_{\boldsymbol{B}_{p(t)}}, \mathrm{I}_{\boldsymbol{B}_G}, \mathrm{II}_{\boldsymbol{B}_G}, \theta). \tag{5.15}$$

Since the elastic response is isotropic, without loss of generality, we choose $\kappa_{p(t)}$ such that

$$\boldsymbol{F}_{\kappa_{p(t)}} = \boldsymbol{V}_{\kappa_{p(t)}}, \tag{5.16}$$

where $\boldsymbol{V}_{\kappa_{p(t)}}$ is the right stretch tensor in the polar decomposition of $\boldsymbol{F}_{\kappa_{p(t)}}$. We shall also assume that the total rate of dissipation can be split additively as follows

$$\boldsymbol{T}\cdot\boldsymbol{D} - \varrho\dot{\psi} - \varrho s\dot{\theta} = \xi_m \geq 0, \quad -\frac{\boldsymbol{q}_h\cdot\operatorname{grad}(\theta)}{\theta} = \xi_c \geq 0, \tag{5.17}$$

where ξ_m, ξ_c are the rates of mechanical dissipation (conversion of working into thermal energy) and dissipation due to heat conduction, respectively. Now, we constitutively choose

$$\boldsymbol{q}_h = -k(\theta)\,\mathrm{grad}(\theta), \quad k(\theta) \geq 0, \tag{5.18}$$

where k is the thermal conductivity, so that Eq. $(5.17)_{(b)}$ is automatically satisfied.

Next,

$$\begin{aligned}\dot{\psi} = &\left[\left(\frac{\partial\hat{\psi}}{\partial \mathrm{I}_{B_{p(t)}}} + \mathrm{I}_{B_{p(t)}}\frac{\partial\hat{\psi}}{\partial \mathrm{II}_{B_{p(t)}}}\right)\boldsymbol{I} - \frac{\partial\hat{\psi}}{\partial \mathrm{II}_{B_{p(t)}}}\boldsymbol{B}_{p(t)}\right]\cdot\dot{\boldsymbol{B}}_{p(t)} \\ &+ \left[\left(\frac{\partial\hat{\psi}}{\partial \mathrm{I}_{B_G}} + \mathrm{I}_{B_G}\frac{\partial\hat{\psi}}{\partial \mathrm{II}_{B_G}}\right)\boldsymbol{I} - \frac{\partial\hat{\psi}}{\partial \mathrm{II}_{B_G}}\boldsymbol{B}_G\right]\cdot\dot{\boldsymbol{B}}_G + \frac{\partial\hat{\psi}}{\partial\theta}\dot{\theta},\end{aligned} \tag{5.19}$$

and using Eqs. (5.10), (5.11) along with Eq. (5.16) in Eq. (5.19), we obtain

$$\begin{aligned}\dot{\psi} = &\,2\left[\left(\frac{\partial\hat{\psi}}{\partial \mathrm{I}_{B_{p(t)}}} + \mathrm{I}_{B_{p(t)}}\frac{\partial\hat{\psi}}{\partial \mathrm{II}_{B_{p(t)}}}\right)\boldsymbol{B}_{p(t)} - \frac{\partial\hat{\psi}}{\partial \mathrm{II}_{B_{p(t)}}}\boldsymbol{B}^2_{p(t)}\right]\cdot(\boldsymbol{D} - \boldsymbol{D}_G) \\ &+ 2\left[\left(\frac{\partial\hat{\psi}}{\partial \mathrm{I}_{B_G}} + \mathrm{I}_{B_G}\frac{\partial\hat{\psi}}{\partial \mathrm{II}_{B_G}}\right)\boldsymbol{B}_G - \frac{\partial\hat{\psi}}{\partial \mathrm{II}_{B_G}}\boldsymbol{B}^2_G\right]\cdot\boldsymbol{D}_G + \frac{\partial\hat{\psi}}{\partial\theta}\dot{\theta}.\end{aligned} \tag{5.20}$$

Next, we shall assume the rate of mechanical dissipation to be of the form

$$\xi_m = \xi_m(\theta, \boldsymbol{B}_{p(t)}, \boldsymbol{D}_G). \tag{5.21}$$

On substituting Eq. (5.20) into Eq. $(5.17)_{(a)}$, we arrive at

$$\begin{aligned}
&\left[\boldsymbol{T} - 2\varrho\left(\frac{\partial\hat{\psi}}{\partial \mathrm{I}_{B_{p(t)}}} + \mathrm{I}_{B_{p(t)}}\frac{\partial\hat{\psi}}{\partial \mathrm{II}_{B_{p(t)}}}\right)\boldsymbol{B}_{p(t)} + 2\varrho\frac{\partial\hat{\psi}}{\partial \mathrm{II}_{B_{p(t)}}}\boldsymbol{B}^2_{p(t)}\right]\cdot\boldsymbol{D} \\
&\quad + 2\varrho\left[\left(\frac{\partial\hat{\psi}}{\partial \mathrm{I}_{B_{p(t)}}} + \mathrm{I}_{B_{p(t)}}\frac{\partial\hat{\psi}}{\partial \mathrm{II}_{B_{p(t)}}}\right)\boldsymbol{B}_{p(t)} - \frac{\partial\hat{\psi}}{\partial \mathrm{II}_{B_{p(t)}}}\boldsymbol{B}^2_{p(t)}\right]\cdot\boldsymbol{D}_G \\
&\quad - 2\varrho\left[\left(\frac{\partial\hat{\psi}}{\partial \mathrm{I}_{B_G}} + \mathrm{I}_{B_G}\frac{\partial\hat{\psi}}{\partial \mathrm{II}_{B_G}}\right)\boldsymbol{B}_G - \frac{\partial\hat{\psi}}{\partial \mathrm{II}_{B_G}}\boldsymbol{B}^2_G\right]\cdot\boldsymbol{D}_G \\
&\quad - \varrho\left[\frac{\partial\hat{\psi}}{\partial\theta} + s\right]\dot{\theta} \\
&\quad = \xi_m(\theta, \boldsymbol{B}_{p(t)}, \boldsymbol{D}_G).
\end{aligned} \tag{5.22}$$

We shall set

$$s = -\frac{\partial\hat{\psi}}{\partial\theta}, \tag{5.23}$$

and define

$$\boldsymbol{T}_{p(t)} := 2\varrho\left[\left(\frac{\partial\hat{\psi}}{\partial \mathrm{I}_{B_{p(t)}}} + \mathrm{I}_{B_{p(t)}}\frac{\partial\hat{\psi}}{\partial \mathrm{II}_{B_{p(t)}}}\right)\boldsymbol{B}_{p(t)} - \frac{\partial\hat{\psi}}{\partial \mathrm{II}_{B_{p(t)}}}\boldsymbol{B}^2_{p(t)}\right], \tag{5.24}$$

$$\boldsymbol{T}_G := 2\varrho\left[\left(\frac{\partial\hat{\psi}}{\partial \mathrm{I}_{B_G}} + \mathrm{I}_{B_G}\frac{\partial\hat{\psi}}{\partial \mathrm{II}_{B_G}}\right)\boldsymbol{B}_G - \frac{\partial\hat{\psi}}{\partial \mathrm{II}_{B_G}}\boldsymbol{B}^2_G\right]. \tag{5.25}$$

Using Eqs. (5.23)–(5.25) in Eq. (5.22), we obtain

$$\begin{aligned}
&\left(\boldsymbol{T} - \boldsymbol{T}_{p(t)}\right)\cdot\boldsymbol{D} + \left(\boldsymbol{T}_{p(t)} - \boldsymbol{T}_G\right)\cdot\boldsymbol{D}_G \\
&\qquad = \xi_m(\theta, \boldsymbol{B}_{p(t)}, \boldsymbol{D}_G).
\end{aligned} \tag{5.26}$$

From constraint of incompressibility, we have

$$\mathrm{tr}(\boldsymbol{D}) = \mathrm{tr}(\boldsymbol{D}_{p(t)}) = \mathrm{tr}(\boldsymbol{D}_G) = 0. \tag{5.27}$$

Since, RHS of Eq. (5.26) does not depend on $\boldsymbol{D}$, using Eq. (5.27),

$$\boldsymbol{T} = p\boldsymbol{I} + \boldsymbol{T}_{p(t)}, \tag{5.28}$$

where p is the Lagrange multiplier due to the constraint of incompressibility, with

$$\left(\boldsymbol{T}_{p(t)} - \boldsymbol{T}_G\right) \cdot \boldsymbol{D}_G = \xi_m(\theta, \boldsymbol{B}_{p(t)}, \boldsymbol{D}_G), \tag{5.29}$$

which can be re-written as

$$(\boldsymbol{T} - \boldsymbol{T}_G) \cdot \boldsymbol{D}_G = \xi_m(\theta, \boldsymbol{B}_{p(t)}, \boldsymbol{D}_G), \tag{5.30}$$

using Eqs. (5.27) and (5.28).

Now, we shall maximize the rate of dissipation ξ_m by varying $\boldsymbol{D}_G$ for fixed $\boldsymbol{B}_{p(t)}$. That is, we maximize the function[4]

$$\Phi := \xi_m + \lambda_1 \left[\xi_m - (\boldsymbol{T} - \boldsymbol{T}_G) \cdot \boldsymbol{D}_G\right] + \lambda_2(\boldsymbol{I} \cdot \boldsymbol{D}_G), \tag{5.31}$$

where λ_1, λ_2 are the Lagrange multipliers. By setting, $\partial\Phi/\partial\boldsymbol{D}_G = 0$, we get

$$\boldsymbol{T} = \boldsymbol{T}_G + \frac{\lambda_2}{\lambda_1}\boldsymbol{I} + \left(\frac{\lambda_1 + 1}{\lambda_1}\right)\frac{\partial \xi_m}{\partial \boldsymbol{D}_G}. \tag{5.32}$$

We need to determine the Lagrange multipliers. On substituting Eq. (5.32) into Eq. (5.30), we get

$$\left(\frac{\lambda_1 + 1}{\lambda_1}\right) = \frac{\xi_m}{\frac{\partial \xi_m}{\partial \boldsymbol{D}_G} \cdot \boldsymbol{D}_G}, \tag{5.33}$$

and so Eq. (5.32) with Eq. (5.25) becomes

$$\boldsymbol{T} = 2\varrho\left[\left(\frac{\partial \hat{\psi}}{\partial \mathrm{I}_{B_G}} + \mathrm{I}_{B_G}\frac{\partial \hat{\psi}}{\partial \mathrm{II}_{B_G}}\right)\boldsymbol{B}_G - \frac{\partial \hat{\psi}}{\partial \mathrm{II}_{B_G}}\boldsymbol{B}_G^2\right] + \left(\frac{\xi_m}{\frac{\partial \xi_m}{\partial \boldsymbol{D}_G} \cdot \boldsymbol{D}_G}\right)\frac{\partial \xi_m}{\partial \boldsymbol{D}_G} + \hat{\lambda}\boldsymbol{I}, \tag{5.34}$$

where $\hat{\lambda} := \frac{\lambda_2}{\lambda_1}$ is the Lagrange multiplier due to the constraint of incompressibility.

---

[4]Though we only document that the first derivative is zero here, it can be shown that the extremum is a maximum.

Finally, the constitutive relations for the viscoelastic solid are given by

$$\boldsymbol{T} = p\boldsymbol{I} + 2\varrho\left[\left(\frac{\partial\hat{\psi}}{\partial \mathrm{I}_{B_{p(t)}}} + \mathrm{I}_{B_{p(t)}}\frac{\partial\hat{\psi}}{\partial \mathrm{II}_{B_{p(t)}}}\right)\boldsymbol{B}_{p(t)} - \frac{\partial\hat{\psi}}{\partial \mathrm{II}_{B_{p(t)}}}\boldsymbol{B}^2_{p(t)}\right], \tag{5.35a}$$

$$\boldsymbol{T} = \hat{\lambda}\boldsymbol{I} + 2\varrho\left[\left(\frac{\partial\hat{\psi}}{\partial \mathrm{I}_{B_G}} + \mathrm{I}_{B_G}\frac{\partial\hat{\psi}}{\partial \mathrm{II}_{B_G}}\right)\boldsymbol{B}_G - \frac{\partial\hat{\psi}}{\partial \mathrm{II}_{B_G}}\boldsymbol{B}^2_G\right] + \left(\frac{\xi_m}{\frac{\partial\xi_m}{\partial \boldsymbol{D}_G}\cdot\boldsymbol{D}_G}\right)\frac{\partial\xi_m}{\partial \boldsymbol{D}_G}, \tag{5.35b}$$

$$\boldsymbol{q}_h = -k(\theta)\mathrm{grad}(\theta), \quad s = -\frac{\partial\hat{\psi}}{\partial\theta}. \tag{5.35c}$$

2. Specific case

Specifically, we choose the specific Helmholtz potential as

$$\begin{aligned}\hat{\psi} = A^s + \left(B^s + c^s_2\right)(\theta-\theta_s) - \frac{c^s_1}{2}(\theta-\theta_s)^2 - c^s_2\theta\ln\left(\frac{\theta}{\theta_s}\right) + \frac{\mu_{G0}-\mu_{G1}\theta}{2\varrho\theta_s}(\mathrm{I}_{B_G}-3)\\ + \frac{\mu_{p0}-\mu_{p1}\theta}{2\varrho\theta_s}(\mathrm{I}_{B_{p(t)}}-3),\end{aligned} \tag{5.36}$$

where μ_G, μ_p are elastic constants, θ_s is a reference temperature for the viscoelastic solid, and the rate of dissipation as

$$\xi_m = \eta(\theta)\left(\boldsymbol{D}_G\cdot\boldsymbol{B}_{p(t)}\boldsymbol{D}_G\right), \tag{5.37}$$

where η is the viscosity.

Now,

$$\begin{aligned}s &= -\frac{\partial\hat{\psi}}{\partial\theta}\\ &= -(B^s + c^s_2) + c^s_1(\theta-\theta_s) + c^s_2\ln\left(\frac{\theta}{\theta_s}\right) + c^s_2 + \frac{\mu_{G1}}{2\varrho\theta_s}(\mathrm{I}_{B_G}-3) + \frac{\mu_{p1}}{2\varrho\theta_s}(\mathrm{I}_{B_{p(t)}}-3).\end{aligned} \tag{5.38}$$

The internal energy ϵ is given by

$$\begin{aligned}\epsilon &= \hat{\psi} + \theta s \\ &= A^s - B^s\theta_s + c_2^s\left(\theta - \theta_s\right) + \frac{c_1^s}{2}\left(\theta^2 - \theta_s^2\right) + \frac{\mu_{G0}}{2\varrho\theta_s}(\mathrm{I}_{B_G} - 3) + \frac{\mu_{p0}}{2\varrho\theta_s}(\mathrm{I}_{B_{p(t)}} - 3).\end{aligned} \tag{5.39}$$

and the specific heat capacity C_v is

$$C_v = \frac{\partial\epsilon}{\partial\theta} = c_1^s\theta + c_2^s. \tag{5.40}$$

Also, Eqs. (5.35a), (5.35b) reduce to

$$\boldsymbol{T} = p\boldsymbol{I} + \bar{\mu}_p\boldsymbol{B}_{p(t)}, \tag{5.41a}$$

$$\boldsymbol{T} = \lambda\boldsymbol{I} + \bar{\mu}_G\boldsymbol{B}_G + \frac{\eta}{2}\left(\boldsymbol{B}_{p(t)}\boldsymbol{D}_G + \boldsymbol{D}_G\boldsymbol{B}_{p(t)}\right), \tag{5.41b}$$

where $\bar{\mu}_p = \frac{\mu_{p0}-\mu_{p1}\theta}{\theta_s}$, $\bar{\mu}_G = \frac{\mu_{G0}-\mu_{G1}\theta}{\theta_s}$. From Eq. (5.41)

$$(p-\lambda)\boldsymbol{I} + \bar{\mu}_p\boldsymbol{B}_{p(t)} = \bar{\mu}_G\boldsymbol{B}_G + \frac{\eta}{2}\left(\boldsymbol{B}_{p(t)}\boldsymbol{D}_G + \boldsymbol{D}_G\boldsymbol{B}_{p(t)}\right), \tag{5.42}$$

and so by pre-multiplying the above equation by $\boldsymbol{B}_{p(t)}^{-1}$ and taking the trace, we get

$$(p-\lambda) = \frac{\bar{\mu}_G\mathrm{tr}(\boldsymbol{B}_{p(t)}^{-1}\boldsymbol{B}_G) - 3\bar{\mu}_p}{\mathrm{tr}(\boldsymbol{B}_{p(t)}^{-1})}. \tag{5.43}$$

Using Eq. (5.43) in Eq. (5.42), we arrive at the following equation that holds:

$$\left[\frac{\bar{\mu}_G\mathrm{tr}(\boldsymbol{B}_{p(t)}^{-1}\boldsymbol{B}_G) - 3\bar{\mu}_p}{\mathrm{tr}(\boldsymbol{B}_{p(t)}^{-1})}\right]\boldsymbol{I} + \bar{\mu}_p\boldsymbol{B}_{p(t)} = \bar{\mu}_G\boldsymbol{B}_G + \frac{\eta}{2}\left(\boldsymbol{B}_{p(t)}\boldsymbol{D}_G + \boldsymbol{D}_G\boldsymbol{B}_{p(t)}\right), \tag{5.44}$$

which can be re-written as

$$\begin{aligned}&\left[\frac{\bar{\mu}_G\mathrm{tr}(\boldsymbol{B}_{p(t)}^{-1}\boldsymbol{B}_G) - 3\bar{\mu}_p}{\mathrm{tr}(\boldsymbol{B}_{p(t)}^{-1})}\right]\boldsymbol{I} + \bar{\mu}_p\boldsymbol{B}_{p(t)} \\ &= \bar{\mu}_G\boldsymbol{B}_G - \frac{\eta}{4}\left(\boldsymbol{V}_{p(t)}\overset{\nabla}{\boldsymbol{B}}_{p(t)}\boldsymbol{V}_{\kappa_{p(t)}}^{-1} + \boldsymbol{V}_{\kappa_{p(t)}}^{-1}\overset{\nabla}{\boldsymbol{B}}_{p(t)}\boldsymbol{V}_{p(t)}\right),\end{aligned} \tag{5.45}$$

where we have used Eqs. (5.13) and (5.44). Thus, with the current choice of the specific Helmholtz potential and the rate of dissipation, we arrive at the following constitutive equations:

$$\boldsymbol{T} = p\boldsymbol{I} + \bar{\mu}_p \boldsymbol{B}_{p(t)}, \tag{5.46}$$

where the evolution of the natural configuration is given by Eq. (5.45). Also, note that the above model reduces to the generalized Maxwell fluid model derived by Rajagopal and Srinivasa [6] when $\bar{\mu}_G = 0$. This is interesting, but not totally surprising, that we obtain a fluid model by eliminating a energy storage mechanism. In the corresponding one dimensional model this is tantamount to a spring being removed.

3. Relationship to the standard linear solid

Now, Eqs. (5.46), (5.45) can be re-written as

$$\boldsymbol{T} = (p + \bar{\mu}_p)\boldsymbol{I} + \bar{\mu}_p(\boldsymbol{B}_{p(t)} - \boldsymbol{I}), \tag{5.47a}$$

$$\begin{aligned} &\left[\frac{\bar{\mu}_G \mathrm{tr}(\boldsymbol{B}_{p(t)}^{-1}\boldsymbol{B}_G) - 3\bar{\mu}_p}{\mathrm{tr}(\boldsymbol{B}_{p(t)}^{-1})} + \bar{\mu}_p - \bar{\mu}_G\right]\boldsymbol{I} + \bar{\mu}_p(\boldsymbol{B}_{p(t)} - \boldsymbol{I}) \\ &= \bar{\mu}_G(\boldsymbol{B}_G - \boldsymbol{I}) - \frac{\eta}{4}\left(\boldsymbol{V}_{p(t)}\ \overset{\nabla}{\boldsymbol{B}}_{p(t)}\ \boldsymbol{V}^{-1}_{\kappa_{p(t)}} + \boldsymbol{V}^{-1}_{\kappa_{p(t)}}\ \overset{\nabla}{\boldsymbol{B}}_{p(t)}\ \boldsymbol{V}_{p(t)}\right). \end{aligned} \tag{5.47b}$$

If λ_i $(i = G, p)$ is the one-dimensional stretch and $\varepsilon_i = \ln\lambda_i$ $(i = G, p)$ is the logarithmic strain, when one is restricted to one-dimension, Eq. (5.47) reduces to

$$\sigma = \bar{\mu}_p(\lambda_p^2 - 1), \tag{5.48a}$$

$$\bar{\mu}_p(\lambda_p^2 - 1) = \bar{\mu}_G(\lambda_G^2 - 1) + \eta\lambda_p^2\frac{\dot{\lambda}_G}{\lambda_G}, \tag{5.48b}$$

where σ is the one dimensional stress. Eq. (5.48) under the assumption that $\varepsilon_i \ll 1$ $(i = G, p)$ reduces to

$$\sigma = 2\bar{\mu}_p \varepsilon_p, \tag{5.49a}$$

$$2\bar{\mu}_p \varepsilon_p = 2\bar{\mu}_G \varepsilon_G + \hat{\eta}\dot{\varepsilon}_G, \tag{5.49b}$$

where $\hat{\eta} = \eta\lambda_p^2$ is the stretch dependent viscosity. Eq. (5.49) can also be obtained by using a Kelvin-Voigt element (with spring constant $2\bar{\mu}_G$, viscosity of $\hat{\eta}$) and a spring (of spring constant $2\bar{\mu}_p$) in series, which is the spring-dashpot analogy for the standard linear solid. However, in this model the viscosity is stretch dependent and hence the model is a generalization of the classical standard linear solid as the viscosity in the standard linear solid model is assumed to be a constant. Hence, the viscoelastic solid model given by Eqs. (5.46), (5.45) is a three-dimensional generalization of the standard linear solid. Of course, there can be infinity of three dimensional generalizations of a one dimensional model (see [53]). Recently, Kannan and Rajagopal [52] have also derived a three-dimensional viscoelastic solid model, that is different from the model developed in this chapter, that also reduces to the standard linear solid. That more than one, in fact, infinity of generalizations are possible is akin to the situation in elementary mathematics and stems from the fact that infinity of three dimensional functions can have the same one dimensional projection. In fact, even when one considers the thermodynamical formulation that is used in this chapter, using different forms for the specific Helmholtz potential and the rate of dissipation, and by maximizing the rate of dissipation with the necessary constraints more than one three-dimensional model reduces to the same one-dimensional model (see [53] for details of an example).

4. Application of the model

Let us study the uniaxial extension, given by

$$x = \lambda(t)X, \quad y = \frac{1}{\sqrt{\lambda(t)}}Y, \quad z = \frac{1}{\sqrt{\lambda(t)}}Z, \tag{5.50}$$

within the context of this model. The velocity gradient is given by

$$\boldsymbol{L} = \operatorname{diag}\left\{\frac{\dot{\lambda}}{\lambda}, -\frac{\dot{\lambda}}{2\lambda}, -\frac{\dot{\lambda}}{2\lambda}\right\}. \tag{5.51}$$

We shall assume that the stretch $\boldsymbol{B}_{p(t)}$ is given by

$$\boldsymbol{B}_{p(t)} = \operatorname{diag}\left\{B, \frac{1}{\sqrt{B}}, \frac{1}{\sqrt{B}}\right\}. \tag{5.52}$$

So,

$$\dot{\boldsymbol{B}}_{p(t)} = \operatorname{diag}\left\{\dot{B}, -\frac{\dot{B}}{2B^{3/2}}, -\frac{\dot{B}}{2B^{3/2}}\right\}, \tag{5.53}$$

$$\overset{\nabla}{\boldsymbol{B}}_{p(t)} = \operatorname{diag}\left\{\dot{B} - \frac{2B\dot{\lambda}}{\lambda}, -\frac{\dot{B}}{2B^{3/2}} + \frac{\dot{\lambda}}{\lambda\sqrt{B}}, -\frac{\dot{B}}{2B^{3/2}} + \frac{\dot{\lambda}}{\lambda\sqrt{B}}\right\}, \tag{5.54}$$

$$\boldsymbol{V}_{\kappa_{p(t)}} = \operatorname{diag}\left\{\sqrt{B}, \frac{1}{B^{1/4}}, \frac{1}{B^{1/4}}\right\}, \tag{5.55}$$

and

$$\boldsymbol{D}_G = -\frac{1}{2}\operatorname{diag}\left\{\frac{\dot{B}}{B} - \frac{2\dot{\lambda}}{\lambda}, \frac{\dot{\lambda}}{\lambda} - \frac{\dot{B}}{2B}, \frac{\dot{\lambda}}{\lambda} - \frac{\dot{B}}{2B}\right\}. \tag{5.56}$$

Also,

$$\begin{aligned} \boldsymbol{G} &= \boldsymbol{V}^{-1}_{\kappa_{p(t)}}\boldsymbol{F} \\ &= \operatorname{diag}\left\{\frac{\lambda}{\sqrt{B}}, \frac{B^{1/4}}{\sqrt{\lambda}}, \frac{B^{1/4}}{\sqrt{\lambda}}\right\}, \end{aligned} \tag{5.57}$$

which yields

$$\boldsymbol{B}_G = \operatorname{diag}\left\{\frac{\lambda^2}{B}, \frac{\sqrt{B}}{\lambda}, \frac{\sqrt{B}}{\lambda}\right\}. \tag{5.58}$$

and

$$\boldsymbol{B}_{p(t)}^{-1}\boldsymbol{B}_G = \text{diag}\left\{\frac{\lambda^2}{B^2}, \frac{B}{\lambda}, \frac{B}{\lambda}\right\}. \tag{5.59}$$

Substituting Eqs. (5.52), (5.54)), (5.59) into Eq. (5.44)

$$\frac{\dot{B}}{2} = \frac{B\dot{\lambda}}{\lambda} + \frac{\bar{\mu}_G}{\eta}\frac{\lambda^2}{B} - \frac{\bar{\mu}_p}{\eta}B - \left\{\frac{\frac{\bar{\mu}_G}{\eta}\left(\lambda^3 + 2B^3\right) - 3\frac{\bar{\mu}_p}{\eta}\lambda B^2}{\lambda B\left(1 + 2B^{3/2}\right)}\right\}, \tag{5.60}$$

which can be re-written in the following form:

$$\dot{\lambda} = \lambda\left\{\frac{\dot{B}}{2B} - \left[\frac{1}{\eta B}\left(\bar{\mu}_G\frac{\lambda^2}{B} - \bar{\mu}_p B - \left(\frac{\bar{\mu}_G\left(\lambda^3 + 2B^3\right) - 3\bar{\mu}_p B^2\lambda}{B\lambda(1 + 2B^{3/2})}\right)\right)\right]\right\}. \tag{5.61}$$

Now, from Eqs. (5.52), (5.46), and using the fact that lateral surfaces are traction free, we conclude that

$$T_{11} = \bar{\mu}_p\left(B - \frac{1}{\sqrt{B}}\right). \tag{5.62}$$

We shall also use logarithmic strain (or true strain) $\varepsilon = \ln\lambda$ as our strain measure in what follows.

5. Comparison with experimental creep data

For the loading process, with known constant applied stress T_{11} and material properties, Eq. (5.62) was first solved for $B(t)$. Then, Eq. (5.60) was solved with the initial condition $\lambda(0) = \sqrt{B(0)}$. For the unloading process, T_{11} was set to zero and $B(t)$ was evaluated using Eq. (5.62). Then, using $\lambda(t_u^+) = \frac{\lambda(t_u^-)}{\lambda(0)}$ as the initial condition (where t_u is the time when unloading starts), $\lambda(t)$ during the unloading process is evaluated using Eq. (5.60). All the ODEs were solved in MATLAB using the `ode45` solver.

In order to obtain the material parameters for a given set of experimental creep data, `fminsearch` function in MATLAB (which uses Nedler-Mead simplex method)

was used to minimize the error defined by

$$error = w \times \sqrt{\frac{\sum \left(\varepsilon_{theo,load} - \varepsilon_{exp,load}\right)^2}{\sum \left(\varepsilon_{exp,load}\right)^2}} + (1-w) \times \sqrt{\frac{\sum \left(\varepsilon_{theo,unload} - \varepsilon_{exp,unload}\right)^2}{\sum \left(\varepsilon_{exp,unload}\right)^2}}, \tag{5.63}$$

where ε_{theo} denotes the theoretical strain values, ε_{exp} denotes the experimental strain values, the suffixes *load*, *unload* denote the values during loading and unloading processes respectively, w is a weight. The material parameters for the model was obtained for HFPE-II-52 polyimide resin using the experimental creep data from [91] at different temperatures (285°C, 300°C, 315°C and 330°C). To determine the efficacy of the model the following process was followed. At 285°C, the experimental data values for the loading of 0.45 UTS were used to obtain the material parameters by minimizing the error in Eq. (5.63). Then, these material parameters were used for the model prediction at the other loadings of 0.30 UTS and 0.15 UTS. The loading values corresponding to the sets of experimental data which were used to obtain the material parameters at the other temperatures are shown in table (I). Similar to the process described above for 285°C, the material parameters shown in table (I) were used to predict the creep at other temperatures. The model predictions compare well with the experimental data as shown in Figs. (26), (27).

Next, the creep solution that stems from our model is compared to the experimental creep data of Falcone and Ruggles-Wrenn [92] for PMR-15 resin at 288°C in Fig. (28). The best-fit values of the parameters for were found to be $\bar{\mu}_G = 4.42 \times 10^8$ Pa, $\bar{\mu}_p = 3.76 \times 10^8$ Pa, $\eta = 6.22 \times 10^{12}$ Pa.s. A weight of $w = 0.75$ was used since there are fewer data points for the unloading process. As it can be seen from Fig. (28), our model shows a good fit with the experiment. However, there is no additional experiment with which the predictive capability of the model can be tested.

It is seen in the experiments that at a loading close to the failure values, the

experimental data shows permanent set in the body, and there seems to be 'yielding'. Our model being a viscoelastic solid model it cannot predict such a permanent set. Thus, the model should be generalized to take into account the inelastic response of the polymer, but this is a daunting problem that requires a careful and separate study.

In conclusion, a viscoelastic model has been developed which predicts the behavior of polyimide resins, that takes into account the thermal response, quite well. Our work can be extended to include anisotropy, and inelasticity to predict the response of polyimide composites and one can include various degradation mechanisms as well.

Table I.: Table showing values for the ultimate tensile strength (UTS) and various material parameters ($\bar{\mu}_p$, $\bar{\mu}_G$, η). The table also shows the loading value data set that was used to obtain the optimum set of material parameters.

Temperature	UTS (MPa)	$\bar{\mu}_p$ ($\times 10^8$ Pa)	$\bar{\mu}_G$ ($\times 10^9$ Pa)	η ($\times 10^{13}$ Pa.s)	Parameter loading value
285°C	43.0	4.79	1.43	3.95	0.45 UTS
300°C	40.2	4.12	0.51	2.23	0.45 UTS
315°C	36.3	4.19	0.79	4.04	0.30 UTS
330°C	23.8	5.07	0.79	3.19	0.20 UTS

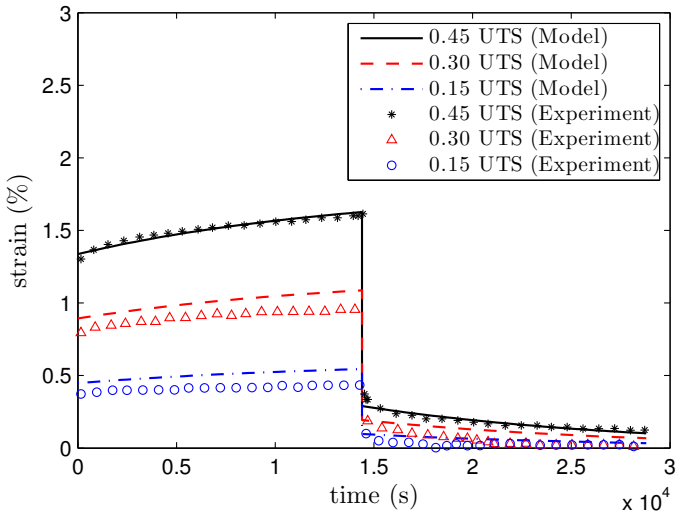

(a) 285°C

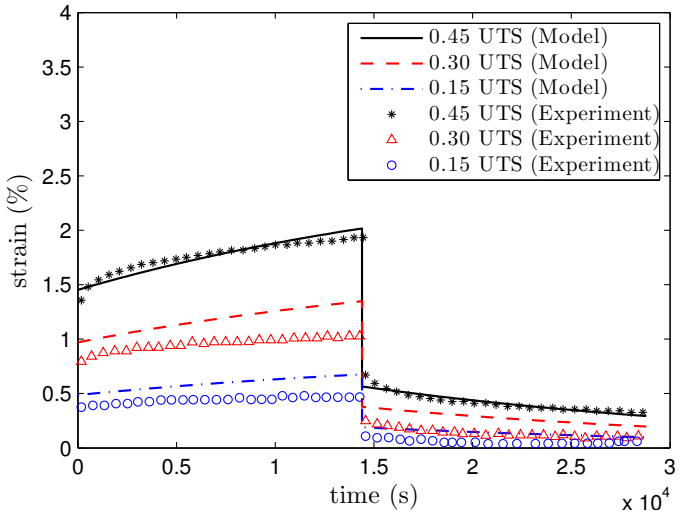

(b) 300°C

Fig. 26.: Comparison of the model predictions with experimental creep data of Bhargava [91] at different loadings. The polyimide in this case is HFPE-II-52 at 285°C and 300°C. The parameters chosen and the values for the ultimate tensile strength (UTS) are shown in table (I). A weight of $w = 0.5$ was used for these two cases to obtain the optimum set of parameters.

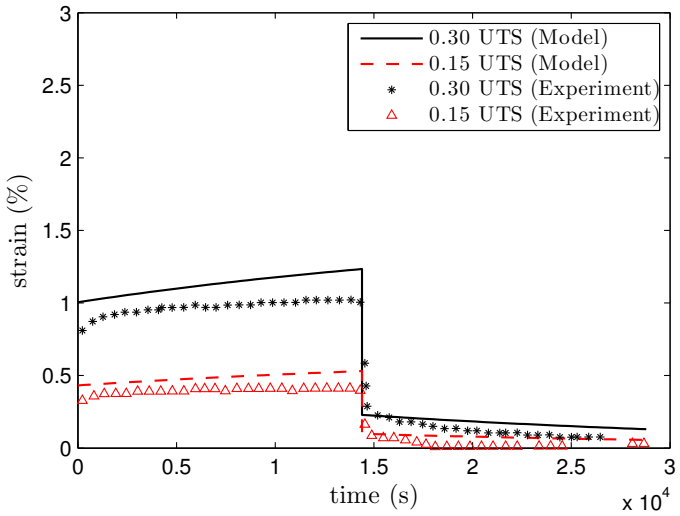

(a) 315°C

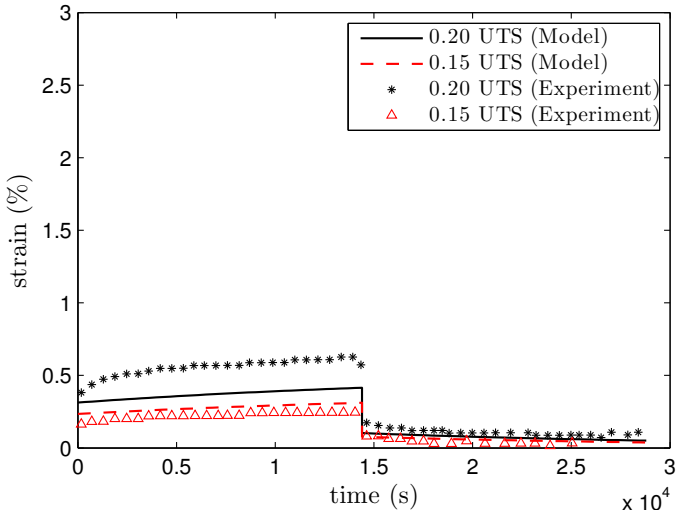

(b) 330°C

Fig. 27.: Comparison of the model predictions with experimental creep data of Bhargava [91] at different loadings. The polyimide in this case is HFPE-II-52 at 315°C and 330°C. The parameters chosen and the values for the ultimate tensile strength (UTS) are shown in table (I). A weight of $w = 0.75$ was used for these two cases to obtain the optimum set of parameters.

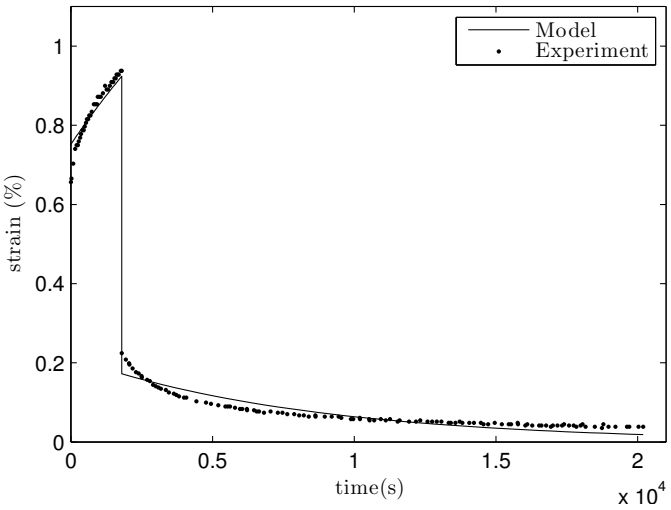

Fig. 28.: Comparison of the model with experimental creep data of Falcone and Ruggles-Wrenn [92] for a loading of 10 MPa. The polyimide in this case is PMR-15 at a temperature of 288°C. The parameter values used were $\bar{\mu}_G = 4.42 \times 10^8$ Pa, $\bar{\mu}_p = 3.76 \times 10^8$ Pa, $\eta = 6.22 \times 10^{12}$ Pa.

CHAPTER VI

DIFFUSION OF A FLUID THROUGH A VISCOELASTIC SOLID

This chapter is concerned with the diffusion of a fluid through a viscoelastic solid undergoing large deformations. The constitutive relations for a mixture of a viscoelastic solid and a fluid (specifically Newtonian fluid) are derived using ideas from the classical theory of mixtures and a thermodynamic framework based on the notion of maximization of the rate of entropy production. We prescribe forms for the specific Helmholtz potential and the rate of dissipation and the relations for the partial stress in the solid, the partial stress in the fluid, the interaction force between the solid and the fluid, and the evolution equation of the natural configuration of the solid are derived. We also use the assumption that the volume of the mixture is equal to the sum of the volumes of the two constituents in their natural state as a constraint. Results from the developed model are shown to be in good agreement with the experimental data for the diffusion of various solvents through high temperature polyimides that are used in the aircraft industry. We also study the swelling of a viscoelastic solid under the application of an external force.

A. Introduction

Several materials in the areas of of polymer mechanics, asphalt mechanics, and biomechanics that show non-linear viscoelastic behavior swell in the presence of a fluid. For instance, polyimides which are known to show viscoelastic solid-like response (see [91], [92]) are used in the aerospace industry due to their good performance at high temperatures (also see [25]). These materials in their service environment are known to swell in the presence of moisture. In addition, asphalt based materials (that are well know to show non-linear viscoelastic fluid-like behavior) degrade in the presence

of moisture [100]. Diffusion of biological fluids through biological materials is another application wherein typically nutrition is provided by the fluid that diffuses, and the amount of the stress or strain in the solid can control the chemicals that are released [101]. Thus, there is a considerable interest to understand how such viscoelastic materials deform and swell due to diffusion of a fluid. Study of such a phenomenon is also of interest in geomechanics [102] and food industry [103].

It is well known that the Darcy's and Fick's equations ([104, 105]) that are extensively used cannot predict swelling of the solid as well as the stresses in the solid. In fact, Darcy's equation is an approximation of the balance of linear momentum of the fluid going through a rigid solid. To capture the swelling phenomena, several works have been done using mixture theory (see review article [106]) and using variational principles [107]. These models have been shown to match experimental swelling data well for rubber materials (that show elastic response) due to the diffusion of various organic solvents.

In the area of diffusion of a fluid through viscoelastic materials, some of the earliest works were by Biot [108] and Weitsman [68], who have used linear viscoelasticity. In deriving their models, they have used the fact that the fluxes and affinities are related through linear phenomenonological relations. Later on, Cohen and co-workers [109, 110], and Durning and co-workers [111, 112] have also recognized the importance of studying diffusion of solvents through polymeric materials showing viscoelastic bodies. They have coupled diffusion and viscoelasticity by adding terms to the flux of the diffusing fluid that depend on the stress in the solid. Such an approach does not have a thermodynamic basis. Furthermore, these models developed are only one-dimensional in nature. Recently, Liu et al. [113] have used the model developed by Cohen and co-workers to study the effect of various viscoelastic parameters on diffusion. They have shown that comparable relaxation times of polymer viscoelasticity

and diffusion of a fluid results in non-Fickian behavior.

1. Main contributions of this work

Our main goal in this chapter is to develop a thermodynamic framework to model diffusion of a fluid through a viscoelastic solid and we shall mainly focus on the swelling of polyimides. We use ideas from mixture theory (see [90], [114], [115], [116], [117], [118], [119], [120], [121] for details) and irreversible thermodynamics to build such a framework. In Chapter V, we developed a framework that can be used to predict the non-linear viscoelastic response of polyimides under various temperature and loading conditions. We extend this work in Chapter V to incorporate diffusion of a fluid and to model the swelling phenomenon.

The thermodynamic framework in the current work uses the notion of *evolving natural configuration* that has been used to model a variety of phenomena including classical plasticity, viscoelasticity, multi-network theory, superplasticity, twinning, etc. (see [20] for details). The evolution of such a natural configuration is determined by maximizing the rate of entropy production (with any additional constraints). We constitutively prescribe forms for the Helmholtz potential of the mixture and the rate of dissipation (which is the product of density, temperature and the rate of entropy production) due to mechanical working, diffusion, heat conduction, and the final constitutive relations are derived by maximizing the rate of dissipation under appropriate constraints. In such an approach, one need not assume linear phenomenonological relations between the flux and the affinites, and thus our framework is more general. It has also been shown recently that if one chooses quadratic form for the rate of entropy production in terms of affinities, and maximizes the rate of entropy production with respect to the affinities, one can arrive at the Onsager's relations (see [38] for further details).

An initial boundary value problem is solved where a viscoelastic solid held between two rigid walls, and immersed in a fluid is considered. Using the model developed in this chapter, free swelling of a viscoelastic solid and swelling under the application of external force i.e., stress-assisted swelling are studied. The numerical results for free swelling of the viscoelastic solid are compared with experimental data for diffusion of different solvents through polyimides.

2. Organization of the work

In section (B), the kinematics required in this chapter are documented. In section (C), the constitutive assumptions are specified and the constitutive relations are derived. We shall also show that our constitutive relations reduces to the equations for diffusion through an elastic solid derived using theory of mixtures when certain parameters take special values. An initial boundary value problem is set up using our model in section (D). The boundary conditions used, the non-dimensionalization scheme, and comparison of the numerical results with experimental data are given in (D.1), (D.2), and (D.3), respectively. Final concluding remarks are given in section (E).

B. Preliminaries

Let us consider a mixture of a fluid and a viscoelastic solid. We shall assume co-occupancy of the constituents, which is the central idea in theory of mixtures and is based on the notion that at each point $\boldsymbol{x}$ in the mixture at some time t, the two constituents exist together in a homogenized fashion and are capable of moving relative to each other. We shall denote the quantities associated with the fluid through the superscript f and use the superscript s for the solid. Now, we shall define the

motion $\boldsymbol{\chi}^i$ for the i-th constituent of the mixture through

$$\boldsymbol{x} = \boldsymbol{\chi}^i \left(\boldsymbol{X}^i, t \right), \quad i = f, s, \tag{6.1}$$

where $\boldsymbol{X}^i$ is the material point of the i-th constituent in its reference configuration. We shall assume that the mapping $\boldsymbol{\chi}^i$ is sufficiently smooth and invertible at each time t. The velocity associated with the i-th constituent is defined as

$$\boldsymbol{v}^i = \frac{\partial \boldsymbol{\chi}^i}{\partial t}, \tag{6.2}$$

and the deformation gradient through

$$\boldsymbol{F}^i = \frac{\partial \boldsymbol{\chi}^i}{\partial \boldsymbol{x}}. \tag{6.3}$$

Let κ_t denote the current configuration of the mixture and let κ_R, κ_r denote the reference configurations of the solid and the fluid respectively. Also, let $\kappa_{p(t)}$ denote the *natural configuration* of the viscoelastic solid (see Fig. (29)). Such a configuration is attained by the body upon instantaneous removal of external loading. For a Navier-Stokes fluid, the natural configuration is same as the current configuration of the fluid [34]. Now, if $\boldsymbol{F}^i$, $i = f, s$ is the gradient of the motion (usually known as deformation gradient) $\boldsymbol{\chi}^{\boldsymbol{i}} \left(\boldsymbol{X}^{\boldsymbol{i}}, t \right)$, and if $\boldsymbol{F}^s_{\kappa_{p(t)}}$ is the gradient of the motion of the viscoelastic solid from $\kappa_{p(t)}$ to κ_t, then

$$\boldsymbol{G}^s = \left(\boldsymbol{F}^s_{\kappa_{p(t)}} \right)^{-1} \boldsymbol{F}^s. \tag{6.4}$$

The density ρ and the average velocity (also known as *barycentric* velocity) $\boldsymbol{v}$ of the mixture are defined by

$$\rho = \sum_i \rho^i, \quad \boldsymbol{v} = \frac{1}{\rho} \sum_i \rho^i \boldsymbol{v}^i. \tag{6.5}$$

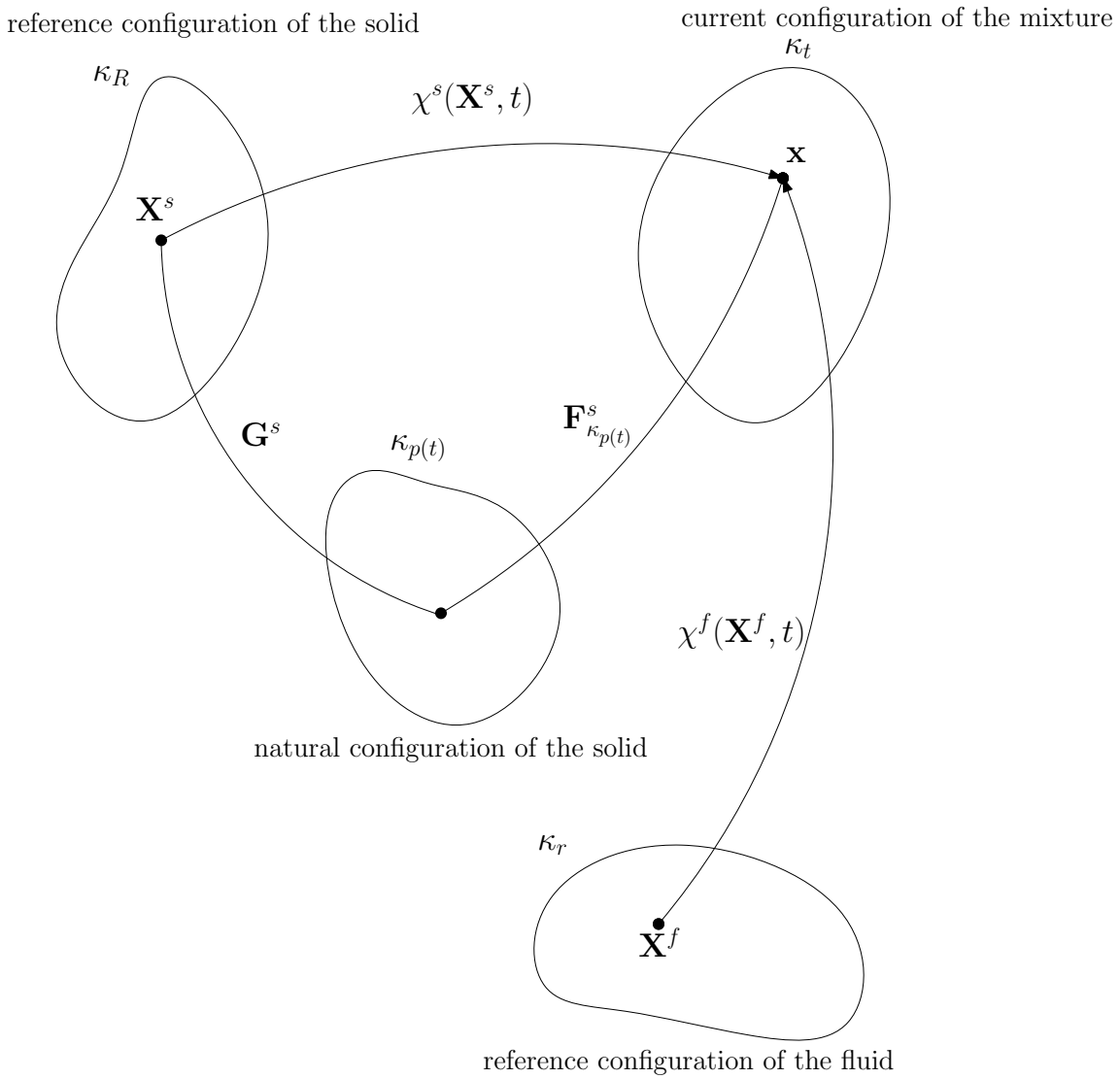

Fig. 29.: Illustration of the various configurations of the viscoelastic solid and fluid components in the mixture.

We define the following derivatives for any scalar quantity ϕ^i by

$$\frac{\partial \phi^i}{\partial t} = \frac{\partial \tilde{\phi}^i}{\partial t}, \quad \frac{d^i \phi^i}{dt} = \frac{\partial \hat{\phi}^i}{\partial t}, \quad \text{grad}(\phi^i) = \frac{\partial \tilde{\phi}^i}{\partial \boldsymbol{x}}, \quad \frac{\partial \phi^i}{\partial \boldsymbol{X}^i} = \frac{\partial \hat{\phi}^i}{\partial \boldsymbol{X}^i}, \tag{6.6}$$

where

$$\phi^i = \tilde{\phi}^i(\boldsymbol{x}, t) = \hat{\phi}^i\left(\boldsymbol{X}^i, t\right). \tag{6.7}$$

Hence,

$$\frac{d^i \phi^i}{dt} = \frac{\partial \phi^i}{\partial t} + \text{grad}(\phi^i) \cdot \boldsymbol{v}^i, \tag{6.8}$$

and we shall also define the following

$$\frac{d\phi}{dt} = \frac{\partial \phi}{\partial t} + \text{grad}(\phi) \cdot \boldsymbol{v}. \tag{6.9}$$

The velocity gradient for the i-th component $\boldsymbol{L}^i$ and the velocity gradient for the total mixture $\boldsymbol{L}$ are defined by

$$\boldsymbol{L}^i = \text{grad}(\boldsymbol{v}^i), \quad \boldsymbol{L} = \text{grad}(\boldsymbol{v}). \tag{6.10}$$

The symmetric and anti-symmetric parts for the velocity gradients $\boldsymbol{L}^i$, $\boldsymbol{L}$ are

$$\begin{aligned} \boldsymbol{D}^i &= \frac{1}{2}\left[\boldsymbol{L}^i + \left(\boldsymbol{L}^i\right)^T\right], \quad \boldsymbol{W}^i = \frac{1}{2}\left[\boldsymbol{L}^i - \left(\boldsymbol{L}^i\right)^T\right], \\ \boldsymbol{D} &= \frac{1}{2}\left[\boldsymbol{L} + (\boldsymbol{L})^T\right], \quad \boldsymbol{W} = \frac{1}{2}\left[\boldsymbol{L} - (\boldsymbol{L})^T\right]. \end{aligned} \tag{6.11}$$

The left Cauchy-Green stretch tensor $\boldsymbol{B}_p^s$, $\boldsymbol{B}_{p(t)}^s$ and their principal invariants are defined as

$$\boldsymbol{B}_G^s = \boldsymbol{F}_G^s \left(\boldsymbol{F}_G^s\right)^T, \quad \boldsymbol{B}_{p(t)}^s = \boldsymbol{F}_{\kappa_{p(t)}}^s \left(\boldsymbol{F}_{\kappa_{p(t)}}^s\right)^T, \tag{6.12}$$

$$\mathrm{I}_{B_j^s} = \mathrm{tr}\left(\boldsymbol{B}_j^s\right), \quad \mathrm{II}_{B_j^s} = \frac{1}{2}\left\{\left[\mathrm{tr}\left(\boldsymbol{B}_j^s\right)\right]^2 - \mathrm{tr}\left[\left(\boldsymbol{B}_j^s\right)^2\right]\right\}, \quad \mathrm{III}_{B_j^s} = \det\left(\boldsymbol{B}_j^s\right), \quad j = G, p(t). \tag{6.13}$$

where det(.) is the determinant of a second order tensor. We shall now note the balance laws.

The balance of mass for the i-th constituent without any mass production is given by

$$\frac{\partial \rho^i}{\partial t} + \mathrm{div}\left(\rho^i \boldsymbol{v}^i\right) = 0, \tag{6.14}$$

where ρ^i is the mass density of the i-th constituent and div(.) := tr(grad(.)) is the divergence operator with tr(.) meaning the trace of a second order tensor. The summation of Eq. (6.14) over i along with Eq. (6.5) leads to

$$\frac{\partial \rho}{\partial t} + \mathrm{div}\left(\rho \boldsymbol{v}\right) = 0. \tag{6.15}$$

The balance of linear momentum for i-th constituent is

$$\rho^i \frac{d^i \boldsymbol{v}^i}{dt} = \mathrm{div}\left[\left(\boldsymbol{T}^i\right)^T\right] + \rho^i \boldsymbol{b}^i + \boldsymbol{m}^i, \tag{6.16}$$

where $\boldsymbol{m}^i$ is the interaction force on the i-th constituent due to the other constituents, $\boldsymbol{b}^i$ is the external body force on the i-th constituent, $\boldsymbol{T}^i$ is the partial Cauchy stress tensor associated with the i-th constituent related to the surface traction on the i-th constituent $\boldsymbol{t}^i$ through

$$\boldsymbol{t}^i = \left(\boldsymbol{T}^i\right)^T \boldsymbol{n}, \tag{6.17}$$

where $\boldsymbol{n}$ is the surface outward normal. From Newton's third law, we have

$$\sum_i \boldsymbol{m}^i = 0. \tag{6.18}$$

For mixtures, the balance of angular momentum, in the absence of body couples requires that the total Cauchy stress of the mixture be symmetric i.e.,

$$\boldsymbol{T} = \boldsymbol{T}^T, \quad \text{where} \quad \boldsymbol{T} = \sum_i \boldsymbol{T}^i, \tag{6.19}$$

although the individual partial stresses $\boldsymbol{T}^i$ could be non-symmetric. Now, the balance of energy for the i-th constituent is given by

$$\rho^i \frac{d}{dt}\left(\epsilon^i + \frac{\boldsymbol{v}^i.\boldsymbol{v}^i}{2}\right) = \operatorname{div}\left(\boldsymbol{T}^i \cdot \boldsymbol{v}^i - \boldsymbol{q}^i\right) + \rho^i r^i + \rho^i \boldsymbol{b}^i \cdot \boldsymbol{v}^i + E^i + \boldsymbol{m}^i \cdot \boldsymbol{v}^i, \tag{6.20}$$

where ϵ^i, $\boldsymbol{q}^i$, r^i are the specific internal energy, heat flux, radiant heating associated with the i-th component and E^i is the energy supplied to the i-th constituent from the other constituents.

Now, taking the scalar multiplication of Eq. (6.16) and $\boldsymbol{v}^i$ and subtracting the resulting equation from Eq. (6.20), we arrive at

$$\rho^i \frac{d\epsilon^i}{dt} = \boldsymbol{T}^i \cdot \boldsymbol{L}^i - \operatorname{div}(\boldsymbol{q}^i) + \rho^i r^i + E^i, \tag{6.21}$$

Using $\epsilon^i = \psi^i + \theta\eta^i$, where ψ^i, η^i are the Helmholtz potential and specific entropy of the i-th constituent, with θ being the common temperature of the constituents at a point in the mixture, Eq. (6.21) along with Eq. (6.14) results in

$$\begin{aligned}\frac{\partial}{\partial t}\left(\rho^i\eta^i\right) + \operatorname{div}\left(\rho^i\eta^i\boldsymbol{v}^i\right) = \frac{1}{\theta}\boldsymbol{T}^i \cdot \boldsymbol{L}^i - \operatorname{div}\left(\frac{\boldsymbol{q}^i}{\theta}\right) - \frac{1}{\theta^2}\boldsymbol{q}^i \cdot \operatorname{grad}(\theta) + \frac{1}{\theta}\rho^i r^i + \frac{1}{\theta}E^i \\ - \frac{\rho^i}{\theta}\left(\frac{d^i\psi^i}{dt} + \eta^i\frac{d^i\theta}{dt}\right).\end{aligned} \tag{6.22}$$

Now, using the fact that $\eta^i = -\frac{\partial\psi^i}{\partial\theta}$, we can establish the following result:

$$\begin{aligned}\frac{d^i\psi^i}{dt} + \eta^i\frac{d^i\theta}{dt} = \frac{d^i\psi^i}{dt} - \frac{\partial\psi^i}{\partial\theta}\frac{d^i\theta}{dt} = \left(\frac{\partial\psi^i}{\partial t} - \frac{\partial\psi^i}{\partial\theta}\frac{\partial\theta}{\partial t}\right) + \boldsymbol{v}^i \cdot \left(\operatorname{grad}(\psi^i) - \frac{\partial\psi^i}{\partial\theta}\operatorname{grad}(\theta)\right) \\ = \left(\frac{d^i\psi^i}{dt}\right)_{\theta\,\text{fixed}},\end{aligned} \tag{6.23}$$

where the subscript "θ fixed" means that the derivative is to be taken keeping θ fixed. We shall define

$$\boldsymbol{q} = \sum_i \boldsymbol{q^i}, \quad r = \frac{1}{\rho}\sum_i \rho^i r^i. \tag{6.24}$$

Using the relation Eq. (6.23) in Eq. (6.22) and summing over i, along with Eq. (6.24), we get

$$\frac{\partial}{\partial t}\left(\sum_i \rho^i \eta^i\right) + \operatorname{div}\left(\sum_i \rho^i \eta^i \boldsymbol{v}^i\right) = \frac{1}{\theta}\sum_i \boldsymbol{T}^i.\boldsymbol{L}^i - \operatorname{div}\left(\frac{\boldsymbol{q}}{\theta}\right) - \frac{1}{\theta^2}\boldsymbol{q}\cdot\operatorname{grad}(\theta) + \rho\left(\frac{r}{\theta}\right) + \frac{1}{\theta}\sum_i E^i - \frac{1}{\theta}\sum_i \rho^i \left(\frac{d^i\psi^i}{dt}\right)_{\theta \text{ fixed}}. \tag{6.25}$$

Eq. (6.25) is the balance of entropy with the rate of entropy production ζ being

$$\zeta = \frac{1}{\theta}\sum_i \boldsymbol{T}^i \cdot \boldsymbol{L}^i - \frac{1}{\theta^2}\boldsymbol{q}\cdot\operatorname{grad}(\theta) + \frac{1}{\theta}\sum_i E^i - \frac{1}{\theta}\sum_i \rho^i \left(\frac{d^i\psi^i}{dt}\right)_{\theta \text{ fixed}}. \tag{6.26}$$

We shall assume that the total entropy production can be additively split into entropy production due to thermal effects i.e., conduction (ζ_c), and entropy production due to internal working and mixing (ζ_m). We shall also require that each of these quantities be non-negative, so that the rate of entropy production ζ is non-negative and the second law of thermodynamics is satisfied automatically. This implies that

$$\zeta_c := -\frac{\boldsymbol{q}\cdot\operatorname{grad}(\theta)}{\theta^2} \geq 0, \tag{6.27a}$$

$$\zeta_m := \frac{1}{\theta}\sum_i \boldsymbol{T}^i \cdot \boldsymbol{L}^i + \frac{1}{\theta}\sum_i E^i - \frac{1}{\theta}\sum_i \rho^i \left(\frac{d^i\psi^i}{dt}\right)_{\theta \text{ fixed}} \geq 0. \tag{6.27b}$$

We shall choose $\boldsymbol{q} = -k(\rho,\theta)\operatorname{grad}(\theta)$, $k \geq 0$, so that Eq. (6.27b) automatically satisfies. Also, if we define the rate of dissipation $\xi_m := \theta\zeta_m$, then

$$\sum_i \boldsymbol{T}^i \cdot \boldsymbol{L}^i + \sum_i E^i - \sum_i \rho^i \left(\frac{d^i\psi^i}{dt}\right)_{\theta \text{ fixed}} = \xi_m \geq 0. \tag{6.28}$$

Assuming

$$\sum_i E^i + \sum_i \boldsymbol{m}^i \cdot \boldsymbol{v}^i = 0, \tag{6.29}$$

Eq. (6.28) can be re-written as

$$\sum_i \boldsymbol{T}^i \cdot \boldsymbol{L}^i - \sum_i \boldsymbol{m}^i \cdot \boldsymbol{v}^i - \sum_i \rho^i \left(\frac{d^i \psi^i}{dt} \right)_{\theta \text{ fixed}} = \xi_m. \tag{6.30}$$

Now,

$$\begin{aligned} \sum_i \rho^i \left(\frac{d^i \psi^i}{dt} \right) &= \frac{\partial}{\partial t} \left(\sum_i \rho^i \psi^i \right) + \operatorname{div} \left(\sum_i \rho^i \psi^i \boldsymbol{v}^i \right) \\ &= \rho \frac{d\psi}{dt} + \operatorname{div} \left(\sum_i \rho^i \psi^i \left(\boldsymbol{v}^i - \boldsymbol{v} \right) \right), \end{aligned} \tag{6.31}$$

where $\psi := \frac{1}{\rho} \sum_i \rho^i \psi^i$ is the average Helmholtz potential of the mixture.

Finally, from Eqs. (6.31) and (6.30), we arrive at

$$\sum_i \boldsymbol{T}^i \cdot \boldsymbol{L}^i - \sum_i \boldsymbol{m}^i \cdot \boldsymbol{v}^i - \left[\rho \frac{d\psi}{dt} + \operatorname{div} \left(\sum_i \rho^i \psi^i \left(\boldsymbol{v}^i - \boldsymbol{v} \right) \right) \right]_{\theta \text{ fixed}} = \xi_m. \tag{6.32}$$

Assuming that all the components have the same Helmholtz potential Eq. (6.32) reduces to

$$\sum_i \boldsymbol{T}^i \cdot \boldsymbol{L}^i - \sum_i \boldsymbol{m}^i \cdot \boldsymbol{v}^i - \left(\rho \frac{d\psi}{dt} \right)_{\theta \text{ fixed}} = \xi_m, \tag{6.33}$$

where we have used Eq. (6.5). The second law of thermodynamics is invoked by ensuring $\xi_m \geq 0$. The preliminaries discussed so far are sufficient for the derivation of the constitutive equations in section (C).

C. Constitutive assumptions

We shall assume that the specific Helmholtz potential for the mixture is of the form

$$\psi = \hat{\psi}\left(\theta, \mathrm{I}_{B^s_G}, \mathrm{II}_{B^s_G}, \mathrm{III}_{B^s_G}, \mathrm{I}_{B^s_{p(t)}}, \mathrm{II}_{B^s_{p(t)}}, \mathrm{III}_{B^s_{p(t)}}\right), \tag{6.34}$$

and so

$$\begin{aligned}
&\frac{d\psi}{dt} = \frac{d^s\psi}{dt} + (\boldsymbol{v} - \boldsymbol{v}^s)\cdot\operatorname{grad}(\psi) \qquad (6.35)\\
&\Rightarrow \left(\frac{d\psi}{dt}\right)_{\theta\,\text{fixed}} = \\
&\left[\left(\frac{\partial\hat{\psi}}{\partial \mathrm{I}_{B^s_{p(t)}}} + \mathrm{I}_{B^s_{p(t)}}\frac{\partial\hat{\psi}}{\partial \mathrm{II}_{B^s_{p(t)}}}\right)\boldsymbol{I} - \frac{\partial\hat{\psi}}{\partial \mathrm{II}_{B^s_{p(t)}}}\boldsymbol{B}^s_{p(t)} + \mathrm{III}_{B^s_{p(t)}}\frac{\partial\hat{\psi}}{\partial \mathrm{III}_{B^s_{p(t)}}}(\boldsymbol{B}^s_{p(t)})^{-1}\right]\cdot\dot{\boldsymbol{B}}^s_{p(t)}\\
&\quad + \left[\left(\frac{\partial\hat{\psi}}{\partial \mathrm{I}_{B^s_G}} + \mathrm{I}_{B^s_G}\frac{\partial\hat{\psi}}{\partial \mathrm{II}_{B^s_G}}\right)\boldsymbol{I} - \frac{\partial\hat{\psi}}{\partial \mathrm{II}_{B^s_G}}\boldsymbol{B}^s_G + \mathrm{III}_{B^s_G}\frac{\partial\hat{\psi}}{\partial \mathrm{III}_{B^s_G}}(\boldsymbol{B}^s_G)^{-1}\right]\cdot\dot{\boldsymbol{B}}^s_G\\
&\quad + (\boldsymbol{v} - \boldsymbol{v}^s)\cdot(\operatorname{grad}(\psi))_{\theta\,\text{fixed}}\,, \qquad (6.36)
\end{aligned}$$

where $\dot{(\,)}$ is $\frac{d^s(\,)}{dt}$ for the sake of convenience.

Now,

$$\begin{aligned}
&\dot{\boldsymbol{F}}^s = \dot{\boldsymbol{F}}^s_{\kappa_{p(t)}}\boldsymbol{G}^s + \boldsymbol{F}^s_{\kappa_{p(t)}}\dot{\boldsymbol{G}}^s\\
&\Rightarrow \dot{\boldsymbol{F}}^s(\boldsymbol{F}^s)^{-1} = \dot{\boldsymbol{F}}^s_{\kappa_{p(t)}}\boldsymbol{G}^s(\boldsymbol{G}^s)^{-1}(\boldsymbol{F}^s_{\kappa_{p(t)}})^{-1} + \boldsymbol{F}^s_{\kappa_{p(t)}}\dot{\boldsymbol{G}}^s(\boldsymbol{G}^s)^{-1}(\boldsymbol{F}^s_{\kappa_{p(t)}})^{-1}\\
&\Rightarrow \boldsymbol{L}^s = \boldsymbol{L}^s_{p(t)} + \boldsymbol{F}^s_{\kappa_{p(t)}}\boldsymbol{L}^s_G(\boldsymbol{F}^s_{\kappa_{p(t)}})^{-1}\\
&\Rightarrow \boldsymbol{D}^s = \boldsymbol{D}^s_{p(t)} + \frac{1}{2}\left[\boldsymbol{F}^s_{\kappa_{p(t)}}\boldsymbol{L}^s_G(\boldsymbol{F}^s_{\kappa_{p(t)}})^{-1} + (\boldsymbol{F}^s_{\kappa_{p(t)}})^{-T}(\boldsymbol{L}^s_G)^T(\boldsymbol{F}^s_{\kappa_{p(t)}})^T\right].
\end{aligned} \tag{6.37}$$

In addition,

$$\begin{aligned}
\dot{\boldsymbol{B}}^s_{p(t)} &= \dot{\boldsymbol{F}}^s_{\kappa_{p(t)}}(\boldsymbol{F}^s)^T + \boldsymbol{F}^s(\dot{\boldsymbol{F}}^s_{\kappa_{p(t)}})^T\\
&= \boldsymbol{L}^s_{p(t)}\boldsymbol{B}^s_{p(t)} + \boldsymbol{B}^s_{p(t)}(\boldsymbol{L}^s_{p(t)})^T,
\end{aligned} \tag{6.38}$$

and similarly

$$\dot{\boldsymbol{B}}^s_G = \boldsymbol{L}^s_G\boldsymbol{B}^s_G + \boldsymbol{B}^s_G(\boldsymbol{L}^s_G)^T. \tag{6.39}$$

Assuming that the response of the viscoelastic solid from the current configuration to its natural configuration is isotropic elastic, we choose $\kappa_{p(t)}$ such that

$$\boldsymbol{F}^s_{\kappa_{p(t)}} = \boldsymbol{V}^s_{\kappa_{p(t)}}, \tag{6.40}$$

where $\boldsymbol{V}^s_{\kappa_{p(t)}}$ is the right stretch tensor in the polar decomposition of $\boldsymbol{F}^s_{\kappa_{p(t)}}$.

Using Eqs. (6.37), (6.38), (6.39), (6.40) in Eq. (6.36), we get

$$\begin{aligned}
&\left(\frac{d\psi}{dt}\right)_{\theta\,\text{fixed}} = \\
&2\left[\left(\frac{\partial\hat{\psi}}{\partial \mathrm{I}^s_{B_{p(t)}}} + \mathrm{I}_{B^s_{p(t)}}\frac{\partial\hat{\psi}}{\partial \mathrm{II}_{B^s_{p(t)}}}\right)\boldsymbol{B}^s_{p(t)} - \frac{\partial\hat{\psi}}{\partial \mathrm{II}_{B^s_{p(t)}}}(\boldsymbol{B}^s_{p(t)})^2 + \mathrm{III}_{B^s_{p(t)}}\frac{\partial\hat{\psi}}{\partial \mathrm{III}^s_{B_{p(t)}}}\boldsymbol{I}\right]\cdot(\boldsymbol{L}^s - \boldsymbol{L}^s_G) \\
&+2\left[\left(\frac{\partial\hat{\psi}}{\partial \mathrm{I}^s_{B_G}} + \mathrm{I}_{B^s_G}\frac{\partial\hat{\psi}}{\partial \mathrm{II}_{B^s_G}}\right)\boldsymbol{B}^s_G - \frac{\partial\hat{\psi}}{\partial \mathrm{II}^s_{B_G}}(\boldsymbol{B}^s_G)^2 + \mathrm{III}_{B^s_G}\frac{\partial\hat{\psi}}{\partial \mathrm{III}_{B^s_G}}\boldsymbol{I}\right]\cdot\boldsymbol{L}^s_G \\
&+(\boldsymbol{v}-\boldsymbol{v}^s)\cdot(\mathrm{grad}(\psi))_{\theta\,\text{fixed}}\,,
\end{aligned} \tag{6.41}$$

In what follows, we shall assume that the reference configurations (subscript o) of the constituents are same as their natural states (subscript R) and so $\phi^i := \dfrac{\rho^i}{\rho^i_R} = \dfrac{\rho^i_o}{\det\boldsymbol{F}^i\rho^i_R} = \dfrac{1}{\det\boldsymbol{F}^i}$, $i = s, f$, where we have used the fact that $\rho^i_o = \rho^i_R$. This need not be true in general.

We shall also assume the volume additivity constraint that is based on the fact that the volume of the swollen viscoelastic solid is equal to the sum of the volumes of the unswollen viscoelastic solid and the fluid [122]. In our case this constraint is given by,

$$\phi^s + \phi^f = 1, \tag{6.42}$$

and so Eq. (6.14) can be re-written as

$$\frac{\partial\phi^i}{\partial t} + \mathrm{div}\left(\phi^i\boldsymbol{v}^i\right) = 0, \tag{6.43}$$

which implies

$$\frac{\partial \sum_i \phi^i}{\partial t} + \operatorname{div}\left(\sum_i \phi^i \boldsymbol{v}^i\right) = 0 \tag{6.44}$$

$$\Rightarrow \operatorname{div}\left(\phi^f \boldsymbol{v}^f + \phi^s \boldsymbol{v}^s\right) = 0 \quad \text{(using Eq. (6.42))}. \tag{6.45}$$

Eq. (6.45) can be re-written as

$$\phi^s \operatorname{tr}(\boldsymbol{L}^s) + \phi^f \operatorname{tr}(\boldsymbol{L}^f) + \boldsymbol{v}^s \cdot \operatorname{grad}(\phi^s) + \boldsymbol{v}^f \cdot \operatorname{grad}(\phi^f) = 0. \tag{6.46}$$

Again from Eq. (6.42), we have

$$\operatorname{grad}(\phi^s) + \operatorname{grad}(\phi^f) = 0, \tag{6.47}$$

and hence, using Eq. (6.47) in Eq. (6.46), we arrive at

$$\phi^s \operatorname{tr}(\boldsymbol{L}^s) + \phi^f \operatorname{tr}(\boldsymbol{L}^f) + \boldsymbol{v}_{s,f} \cdot \operatorname{grad}(\phi^s) = 0, \tag{6.48}$$

where $\boldsymbol{v}_{s,f} = \boldsymbol{v}^s - \boldsymbol{v}^f$, is the velocity of the solid with respect to the fluid.

Next, we shall assume that the rate of entropy production is of the form

$$\xi_m = \xi_m\left(\boldsymbol{L}^s_G, \boldsymbol{F}^s_{p(t)}, \boldsymbol{L}^f, \theta, \boldsymbol{v}_{s,f}\right). \tag{6.49}$$

and so Eq. (6.33) along with Eq. (6.18) reduces to

$$\boldsymbol{T}^s \cdot \boldsymbol{L}^s + \boldsymbol{T}^f \cdot \boldsymbol{L}^f - \boldsymbol{m}^s \cdot \boldsymbol{v}_{s,f} - \left(\rho \frac{d\psi}{dt}\right)_{\theta \text{ fixed}} = \xi_m\left(\boldsymbol{L}^s_G, \boldsymbol{F}^s_{p(t)}, \boldsymbol{L}^f, \theta, \boldsymbol{v}_{s,f}\right). \tag{6.50}$$

Using Eq. (6.41) in Eq. (6.50), we get

$$\begin{aligned}\boldsymbol{T}^s \cdot \boldsymbol{L}^s + \boldsymbol{T}^f \cdot \boldsymbol{L}^f - \boldsymbol{m}^s \cdot \boldsymbol{v}_{s,f} - \boldsymbol{T}^s_{p(t)} \cdot (\boldsymbol{L}^s - \boldsymbol{L}^s_G) - \boldsymbol{T}^s_G \cdot \boldsymbol{L}^s_G - \rho(\boldsymbol{v} - \boldsymbol{v}^s) \cdot (\operatorname{grad}(\psi))_{\theta \text{ fixed}} \\ = \xi_m\left(\boldsymbol{L}^s_G, \boldsymbol{F}^s_{p(t)}, \boldsymbol{L}^f, \theta, \boldsymbol{v}_{s,f}\right),\end{aligned} \tag{6.51}$$

where

$$\boldsymbol{T}^s_{p(t)} := 2\rho\left[\left(\frac{\partial\hat{\psi}}{\partial \mathrm{I}_{B^s_{p(t)}}} + \mathrm{I}_{B^s_{p(t)}}\frac{\partial\hat{\psi}}{\partial \mathrm{II}_{B^s_{p(t)}}}\right)\boldsymbol{B}^s_{p(t)} - \frac{\partial\hat{\psi}}{\partial \mathrm{II}_{B^s_{p(t)}}}(\boldsymbol{B}^s_{p(t)})^2 + \mathrm{III}_{B^s_{p(t)}}\frac{\partial\hat{\psi}}{\partial \mathrm{III}_{B_{p(t)}}}\boldsymbol{I}\right], \tag{6.52}$$

$$\boldsymbol{T}^s_{G} := 2\rho\left[\left(\frac{\partial\hat{\psi}}{\partial \mathrm{I}_{B^s_{G}}} + \mathrm{I}_{B^s_{G}}\frac{\partial\hat{\psi}}{\partial \mathrm{II}_{B^s_{G}}}\right)\boldsymbol{B}^s_{G} - \frac{\partial\hat{\psi}}{\partial \mathrm{II}_{B^s_{G}}}(\boldsymbol{B}^s_{G})^2 + \mathrm{III}_{B^s_{G}}\frac{\partial\hat{\psi}}{\partial \mathrm{III}_{B^s_{G}}}\boldsymbol{I}\right]. \tag{6.53}$$

Eq. (6.51) with the constraint Eq. (6.48) can be written as

$$\begin{aligned}\boldsymbol{T}^s\cdot\boldsymbol{L}^s + \boldsymbol{T}^f\cdot\boldsymbol{L}^f - \boldsymbol{m}^s\cdot\boldsymbol{v}_{s,f} - \boldsymbol{T}^s_{p(t)}\cdot(\boldsymbol{L}^s - \boldsymbol{L}^s_G) - \boldsymbol{T}^s_G\cdot\boldsymbol{L}^s_G - \rho(\boldsymbol{v}-\boldsymbol{v}^s)\cdot(\mathrm{grad}\psi)_{\theta\,\text{fixed}}\\ + \lambda\left(\phi^s\mathrm{tr}(\boldsymbol{L}^s) + \phi^f\mathrm{tr}(\boldsymbol{L}^f) + \boldsymbol{v}_{s,f}\cdot\mathrm{grad}(\phi^s)\right) = \xi_m\left(\boldsymbol{L}^s_G, \boldsymbol{F}^s_{p(t)}, \boldsymbol{L}^f, \theta, \boldsymbol{v}_{s,f}\right),\end{aligned} \tag{6.54}$$

where λ is a Lagrange multiplier.

We shall further assume that the rate of dissipation can be additively split into the rate of dissipation due to mechanical working of the viscoelastic solid, the rate of dissipation due to the fluid and the rate of dissipation due to diffusion of the fluid, with specific forms as follows:

$$\xi_m\left(\boldsymbol{L}^s_G, \boldsymbol{F}^s_{p(t)}, \boldsymbol{L}^f, \theta, \boldsymbol{v}_{s,f}\right) = \xi\left(\boldsymbol{L}^s_G, \boldsymbol{B}^s_{p(t)}, \theta\right) + \nu\boldsymbol{D}^f\cdot\boldsymbol{D}^f + \alpha(\theta)\boldsymbol{v}_{s,f}\cdot\boldsymbol{v}_{s,f}. \tag{6.55}$$

Then, from Eq. (6.55) and Eq. (6.54), we arrive at

$$\begin{aligned}\boldsymbol{T}^s\cdot\boldsymbol{L}^s + \boldsymbol{T}^f\cdot\boldsymbol{L}^f - \boldsymbol{m}^s\cdot\boldsymbol{v}_{s,f} - \boldsymbol{T}^s_{p(t)}\cdot(\boldsymbol{L}^s - \boldsymbol{L}^s_G) - \boldsymbol{T}^s_G\cdot\boldsymbol{L}^s_G - \rho(\boldsymbol{v}-\boldsymbol{v}^s)\cdot(\mathrm{grad}(\psi))_{\theta\,\text{fixed}}\\ + \lambda\left(\phi^s\mathrm{tr}(\boldsymbol{L}^s) + \phi^f\mathrm{tr}(\boldsymbol{L}^f) + \boldsymbol{v}_{s,f}\cdot\mathrm{grad}(\phi^s)\right) = \xi\left(\boldsymbol{L}^s_G, \boldsymbol{B}^s_{p(t)}, \theta\right) + \nu\boldsymbol{D}^f\cdot\boldsymbol{D}^f\\ + \alpha(\theta)\boldsymbol{v}_{s,f}\cdot\boldsymbol{v}_{s,f},\end{aligned} \tag{6.56}$$

which can be re-written as

$$\boldsymbol{L}^s \cdot \left[\boldsymbol{T}^s + \lambda\phi^s\boldsymbol{I} - \boldsymbol{T}^s_{p(t)}\right] + \boldsymbol{L}^f \cdot \left[\boldsymbol{T}^f + \lambda\phi^f\boldsymbol{I} - \nu\boldsymbol{D}^f\right] + \left(\boldsymbol{T}^s_{p(t)} - \boldsymbol{T}^s_G\right) \cdot \boldsymbol{L}^s_G$$
$$+ \boldsymbol{v}_{s,f} \cdot \left[-\boldsymbol{m}^s + \lambda\ \mathrm{grad}(\phi^s) - \alpha(\theta)\boldsymbol{v}_{s,f} + \rho^f\left(\mathrm{grad}(\psi)\right)_{\theta\,\mathrm{fixed}}\right] = \xi\left(\boldsymbol{L}^s_G, \boldsymbol{B}^s_{p(t)}, \theta\right), \tag{6.57}$$

using the fact that $\rho\left(\boldsymbol{v} - \boldsymbol{v}^s\right) = -\rho^f\boldsymbol{v}_{s,f}$. Since, the right hand side of Eq. (6.57) does not depend on $\boldsymbol{L}^s$, $\boldsymbol{L}^f$ and $\boldsymbol{v}_{s,f}$, we have

$$\boldsymbol{T}^s = -\lambda\phi^s\boldsymbol{I} + \boldsymbol{T}^s_{p(t)}, \tag{6.58}$$

$$\boldsymbol{T}^f = -\lambda\phi^f\boldsymbol{I} + \nu\boldsymbol{D}^f, \tag{6.59}$$

$$\boldsymbol{m}^s = \lambda\ \mathrm{grad}(\phi^s) - \alpha(\theta)\boldsymbol{v}_{s,f} + \rho^f\left(\mathrm{grad}(\psi)\right)_{\theta\,\mathrm{fixed}}, \tag{6.60}$$

and so Eq. (6.57) reduces to

$$\left(\boldsymbol{T}^s_{p(t)} - \boldsymbol{T}^s_G\right) \cdot \boldsymbol{L}^s_G = \xi\left(\boldsymbol{L}^s_G, \boldsymbol{B}^s_{p(t)}, \theta\right). \tag{6.61}$$

Next, we shall maximize the rate of dissipation ξ with Eq. (6.61). We shall maximize the auxiliary function

$$\Phi := \xi + \beta\left[\xi - \left(\boldsymbol{T}^s_{p(t)} - \boldsymbol{T}^s_G\right) \cdot \boldsymbol{L}^s_G\right]. \tag{6.62}$$

Now,

$$\frac{\partial\Phi}{\partial\boldsymbol{L}^s_G} = 0 \Rightarrow \frac{(\beta+1)}{\beta}\frac{\partial\xi}{\partial\boldsymbol{L}^s_G} - \left(\boldsymbol{T}^s_{p(t)} - \boldsymbol{T}^s_G\right) = 0. \tag{6.63}$$

Taking the scalar product of Eq. (6.63) with $\boldsymbol{L}^s_G$ and using Eq. (6.61), we arrive at

$$\frac{(\beta+1)}{\beta} = \frac{\xi}{\dfrac{\partial\xi}{\partial\boldsymbol{L}^s_G} \cdot \boldsymbol{L}^s_G}. \tag{6.64}$$

and hence the evolution equation for the natural configuration of the solid is given by

$$\left(\boldsymbol{T}^s_{p(t)} - \boldsymbol{T}^s_G\right) = \frac{\xi}{\dfrac{\partial \xi}{\partial \boldsymbol{L}^s_G} \cdot \boldsymbol{L}^s_G} \frac{\partial \xi}{\partial \boldsymbol{L}^s_G}. \tag{6.65}$$

1. Specific constitutive assumptions

We shall assume the following specific form for the specific Helmholtz potential of the mixture

$$\begin{aligned}\hat{\psi} = {} & A^s + \left(B^s + c^s_2\right)(\theta - \theta_s) - \frac{c^s_1}{2}(\theta - \theta_s)^2 - c^s_2 \theta \ln\left(\frac{\theta}{\theta_s}\right) + \frac{\mu_{G0} - \mu_{G1}\theta}{\rho^s \theta_s}(\mathrm{I}_{B^s_G} - 3) \\ & + \frac{\mu_{p0} - \mu_{p1}\theta}{\rho^s \theta_s}(\mathrm{I}_{B^s_{p(t)}} - 3) + \frac{R\theta}{\rho^f_R V_0 \phi^s}\left[(1-\phi^s)\ln(1-\phi^s) - \chi(\phi^s)^2\right], \end{aligned} \tag{6.66}$$

where $\mu_{G0}, \mu_{G1}, \mu_{p0}, \mu_{p1}$ are material parameters, θ_s is a reference temperature for the viscoelastic solid, R is the gas constant, θ the absolute temperature of mixture, V_0 the molar volume of the fluid, and χ a mixing parameter for the particular solid-fluid combination. The last term in Eq. (6.66) is the term added to the specific Helmholtz in Chapter V to capture the swelling phenomenon in the solid.

Now,

$$\begin{aligned}\eta = {} & -\frac{\partial \hat{\psi}}{\partial \theta} \\ = {} & -(B^s + c^s_2) + c^s_1(\theta - \theta_s) + c^s_2 \ln\left(\frac{\theta}{\theta_s}\right) + c^s_2 + \frac{\mu_{G1}}{\rho \theta_s}(\mathrm{I}_{B^s_G} - 3) + \frac{\mu_{p1}}{\rho \theta_s}(\mathrm{I}_{B^s_{p(t)}} - 3) \\ & - \frac{R}{\rho^f_R V_0 \phi^s}\left[(1-\phi^s)\ln(1-\phi^s) - \chi(\phi^s)^2\right]. \end{aligned} \tag{6.67}$$

The internal energy ϵ is given by

$$\begin{aligned}\epsilon = {} & \psi + \theta\eta \\ = {} & A^s - B^s\theta_s + c^s_2(\theta - \theta_s) + \frac{c^s_1}{2}\left(\theta^2 - \theta^2_s\right) + \frac{\mu_{G0}}{\rho \theta_s}(\mathrm{I}_{B^s_G} - 3) + \frac{\mu_{p0}}{\rho \theta_s}(\mathrm{I}_{B^s_{p(t)}} - 3), \end{aligned} \tag{6.68}$$

and the specific heat capacity C_v is

$$C_v = \frac{\partial \epsilon}{\partial \theta} = c_1^s \theta + c_2^s. \tag{6.69}$$

From Eq. (6.66) and Eq. (6.52)

$$\begin{aligned}\boldsymbol{T}^s_{p(t)} = &\frac{\rho J^s_p J^s_G}{\rho^s_R}\left[2\bar{\mu}_p \boldsymbol{B}^s_{p(t)} + \bar{\mu}_p\left(\mathrm{I}_{B^s_{p(t)}} - 3\right)\boldsymbol{I} + \bar{\mu}_G\left(\mathrm{I}_{B^s_G} - 3\right)\boldsymbol{I}\right] \\ &+ \frac{\rho R\theta J^s_p J^s_G}{\rho^f_R V_0}\left[\ln(1-\phi^s) + \phi^s + \chi(\phi^s)^2\right]\boldsymbol{I},\end{aligned} \tag{6.70}$$

and from Eq. (6.66) and Eq. (6.53),

$$\begin{aligned}\boldsymbol{T}^s_G = &\frac{\rho J^s_p J^s_G}{\rho^s_R}\left[2\bar{\mu}_G \boldsymbol{B}^s_G + \bar{\mu}_p\left(\mathrm{I}_{B^s_{p(t)}} - 3\right)\boldsymbol{I} + \bar{\mu}_G\left(\mathrm{I}_{B^s_G} - 3\right)\boldsymbol{I}\right] \\ &+ \frac{\rho R\theta J^s_p J^s_G}{\rho^f_R V_0}\left[\ln(1-\phi^s) + \phi^s + \chi(\phi^s)^2\right]\boldsymbol{I},\end{aligned} \tag{6.71}$$

where $\bar{\mu}_G = \frac{\bar{\mu}_{G0} - \bar{\mu}_{G1}\theta}{\theta_s}$, $\bar{\mu}_p = \frac{\bar{\mu}_{p0} - \bar{\mu}_{p1}\theta}{\theta_s}$, $J^s_G = \det(\boldsymbol{G}^s)$, $J^s_p = \det(\boldsymbol{F}^s_{\kappa_{p(t)}})$.

We shall further assume that the rate of dissipation ξ is of the form

$$\xi = \gamma(\theta)\boldsymbol{D}^s_G \cdot \boldsymbol{D}^s_G, \tag{6.72}$$

then Eq. (6.58) becomes

$$\begin{aligned}\boldsymbol{T}^s = &-\lambda\phi^s\boldsymbol{I} + \frac{\rho}{\rho^s}\left[2\bar{\mu}_p \boldsymbol{B}_{p(t)} + \bar{\mu}_p\left(\mathrm{I}_{B^s_{p(t)}} - 3\right)\boldsymbol{I} + \bar{\mu}_G\left(\mathrm{I}_{B^s_G} - 3\right)\boldsymbol{I}\right] \\ &+ \frac{\rho R\theta J^s_p J^s_G}{\rho^f_R V_0}\left[\ln(1-\phi^s) + \phi^s + \chi(\phi^s)^2\right]\boldsymbol{I},\end{aligned} \tag{6.73}$$

and Eq. (6.65) reduces to

$$\frac{2\rho}{\rho^s}\left[\bar{\mu}_p \boldsymbol{B}^s_{p(t)} - \bar{\mu}_G \boldsymbol{B}^s_G\right] = \gamma(\theta)\boldsymbol{D}^s_G. \tag{6.74}$$

The final constitutive equations are

$$\boldsymbol{T}^s = -\lambda\phi^s\boldsymbol{I} + \frac{\rho}{\rho^s}\left[2\bar{\mu}_p\boldsymbol{B}^s_{p(t)} + \bar{\mu}_p\left(\mathrm{I}_{B^s_{p(t)}} - 3\right)\boldsymbol{I} + \bar{\mu}_G\left(\mathrm{I}_{B^s_G} - 3\right)\boldsymbol{I}\right] + \frac{\rho R\theta J^s_p J^s_G}{\rho^f_R V_0}\left[\ln(1-\phi^s) + \phi^s + \chi(\phi^s)^2\right]\boldsymbol{I}, \tag{6.75a}$$

$$\boldsymbol{T}^f = -\lambda\phi^f\boldsymbol{I} + \nu\boldsymbol{D}^f, \tag{6.75b}$$

$$\boldsymbol{m}^s = \lambda\ \mathrm{grad}\phi^s - \alpha(\theta)\boldsymbol{v}_{s,f} + \rho^f\left(\mathrm{grad}\psi\right)_{\theta\,\text{fixed}}, \tag{6.75c}$$

and

$$\frac{2\rho}{\rho^s}\left[\bar{\mu}_p\boldsymbol{B}^s_{p(t)} - \bar{\mu}_G\boldsymbol{B}^s_G\right] = \gamma(\theta)\boldsymbol{D}^s_G, \tag{6.76}$$

being the evolution equation of the natural configuration of the solid.

Notice that when $\bar{\mu}_G = 0$ and $\gamma \to \infty$, for the LHS of Eq. (6.76) to be finite, we must have $\boldsymbol{D}^s_G = 0$. This implies that $\boldsymbol{G}^s = \boldsymbol{I}$, and hence $\boldsymbol{B}^s_{p(t)} = \boldsymbol{B}^s$ and the solid is now an elastic solid. In such a case, the constitutive equations Eq. (6.75), with additional assumption of $\nu = 0$, reduce to

$$\boldsymbol{T}^s = -\lambda\phi^s\boldsymbol{I} + 2\rho\left[\left(\frac{\partial\hat{\psi}}{\partial\mathrm{I}_{B^s}} + \mathrm{I}_{B^s}\frac{\partial\hat{\psi}}{\partial\mathrm{II}_{B^s}}\right)\boldsymbol{B}^s - \frac{\partial\hat{\psi}}{\partial\mathrm{II}_{B^s}}(\boldsymbol{B}^s)^2 + \mathrm{III}_{B^s}\frac{\partial\hat{\psi}}{\partial\mathrm{III}_{B^s}}\boldsymbol{I}\right], \tag{6.77a}$$

$$\boldsymbol{T}^f = -\lambda\phi^f\boldsymbol{I}, \tag{6.77b}$$

$$\boldsymbol{m}^s = \lambda\ \mathrm{grad}\phi^s - \alpha(\theta)\boldsymbol{v}_{s,f} + \rho^f\left(\mathrm{grad}\psi\right)_{\theta\,\text{fixed}}. \tag{6.77c}$$

These equations are same as the equations derived using theory of mixtures for the diffusion of a fluid through an elastic solid (see equations 3.15–3.17 in [123]).

D. Initial boundary value problem

Let us consider the problem of compression of the viscoelastic solid body inside rigid walls as shown in Fig. (30). Let us assume that the motion of the swollen solid body is given by

$$x = X, \quad y = Y, \quad z = f(Z,t). \tag{6.78}$$

In this case, the deformation gradient of the solid ($\boldsymbol{F}^s$) is given by

$$\boldsymbol{F}^s = \operatorname{diag}\{1,1,p\}, \tag{6.79}$$

where $p := \dfrac{\partial f}{\partial Z}$. Let us assume a form for $\boldsymbol{G}^s$ as follows

$$\boldsymbol{G}^s = \operatorname{diag}\{1,1,g(Z,t)\}, \tag{6.80}$$

and the velocity of the fluid be of the form

$$\boldsymbol{v}^f = (0,0,v(Z,t)). \tag{6.81}$$

Then,

$$\boldsymbol{B}^s_{\kappa_{p(t)}} = \operatorname{diag}\left\{1,1,\left(\frac{p}{g}\right)^2\right\}, \tag{6.82}$$

$$\mathrm{I}_{B^s_{p(t)}} = 2 + \left(\frac{p}{g}\right)^2, \quad \mathrm{I}_{B^s_G} = 2 + g^2, \quad J^s_p = \frac{p}{g}, \quad J^s_G = g. \tag{6.83}$$

The balance of mass for the solid gives

$$\phi^s = \frac{1}{\det(\boldsymbol{F}^s)} = \frac{1}{p}, \tag{6.84}$$

and hence from volume additivity constraint

$$\rho^f = \rho_R^f \left(1 - \frac{1}{p}\right). \tag{6.85}$$

Also, we note the following relations

$$\frac{\rho}{\rho^s} = 1 + \frac{\rho_R^f}{\rho_R^s}(p-1), \tag{6.86a}$$

$$\frac{\rho}{\rho_R^f} = 1 + \frac{1}{p}\left(\frac{\rho_R^s}{\rho_R^f} - 1\right). \tag{6.86b}$$

The balance of mass for the fluid reduces to

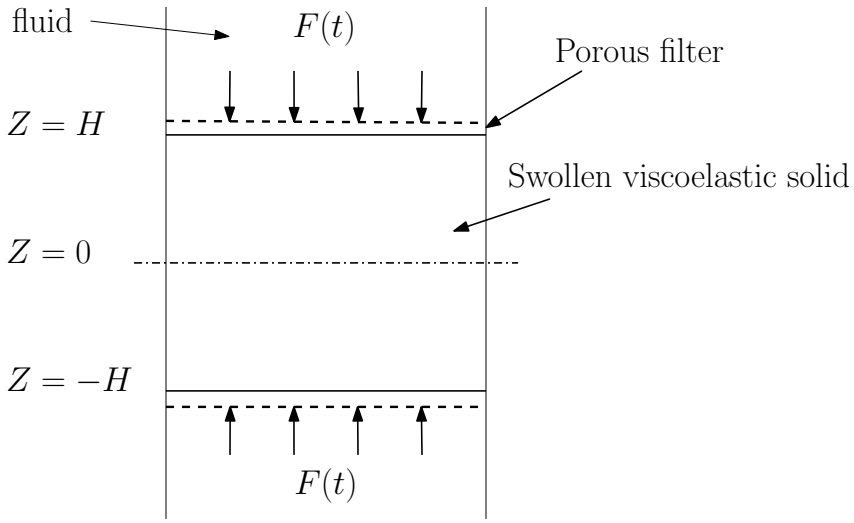

Fig. 30.: Schematic of the initial boundary value problem

$$\frac{\partial p}{\partial t} + \frac{v}{p}\frac{\partial p}{\partial Z} + (p-1)\frac{\partial v}{\partial Z} = 0. \tag{6.87}$$

Setting $\nu = 0$, zz-component of the total stress tensor for the mixture reduces to

$$\begin{aligned} T_{zz} &= T^s_{zz} + T^f_{zz} \qquad (6.88)\\ &= -\lambda + \left(1 + \frac{\rho^f_R}{\rho^s_R}(p-1)\right)\left[2\bar{\mu}_p\left(\frac{p}{g}\right)^2 + \bar{\mu}_p\left(\frac{p^2}{g^2} - 1\right) + \bar{\mu}_G\left(g^2 - 1\right)\right] \\ &\quad + \left(1 + \frac{1}{p}\left(\frac{\rho^s_R}{\rho^f_R} - 1\right)\right)\frac{R\theta p}{V_0}\left[\ln\left(1 - \frac{1}{p}\right) + \frac{1}{p} + \chi\frac{1}{p^2}\right]. \qquad (6.89) \end{aligned}$$

The balance of linear momentum for the solid and the fluid after assuming zero body forces reduce to

$$\rho^s \frac{\partial^2 f}{\partial t^2} = \frac{\partial T^s_{zz}}{\partial z} + m^s_z, \qquad (6.90a)$$

$$\rho^f \frac{\partial v}{\partial t} = \frac{\partial T^f_{zz}}{\partial z} - m^s_z. \qquad (6.90b)$$

Now, adding Eqs. (6.90a), (6.90b), we arrive at the balance of linear momentum for the mixture

$$\begin{aligned} \rho^s \frac{\partial^2 f}{\partial t^s} + \rho^f \frac{\partial v}{\partial t} &= \frac{\partial}{\partial z}(T^s_{zz} + T^f_{zz}) \\ \Rightarrow \rho^s \frac{\partial^2 f}{\partial t^s} + \rho^f \frac{\partial v}{\partial t} &= -\frac{\partial \lambda}{\partial z} + \frac{\partial T^{sf}_{zz}}{\partial z}, \qquad (6.91) \end{aligned}$$

where

$$\begin{aligned} T^{sf}_{zz} &= \left(1 + \frac{\rho^f_R}{\rho^s_R}(p-1)\right)\left[2\bar{\mu}_p\left(\frac{p}{g}\right)^2 + \bar{\mu}_p\left(\frac{p^2}{g^2} - 1\right) + \bar{\mu}_G\left(g^2 - 1\right)\right] \\ &\quad + \left(1 + \frac{1}{p}\left(\frac{\rho^s_R}{\rho^f_R} - 1\right)\right)\frac{R\theta p}{V_0}\left[\ln\left(1 - \frac{1}{p}\right) + \frac{1}{p} + \chi\frac{1}{p^2}\right]. \qquad (6.92) \end{aligned}$$

Now, Eq. (6.90b) along with volume additivity constraint reduces to

$$\rho^f \frac{\partial v}{\partial t} = -\phi^f \frac{\partial \lambda}{\partial z} + \alpha\left(\frac{\partial f}{\partial t} - v\right) - \rho^f \left(\frac{\partial \psi}{\partial z}\right)_{\theta \text{ fixed}}, \qquad (6.93)$$

where we have used the fact that the velocity of the solid is $(0, 0, \dfrac{\partial f}{\partial t})$.

Multiplying Eq. (6.91) with ϕ^f and subtracting Eq. (6.93) from the resulting equation we get

$$\phi^f \rho^s \frac{\partial^2 f}{\partial t^2} + (\phi^f - 1)\rho^f \frac{\partial v}{\partial t} = -\alpha \left(\frac{\partial f}{\partial t} - v \right) + \phi^f \frac{\partial T_{zz}^{sf}}{\partial z} + \rho^f \left(\frac{\partial \psi}{\partial z} \right)_{\theta \text{ fixed}}, \tag{6.94}$$

which reduces to

$$\phi^f \rho^s \frac{\partial^2 f}{\partial t^2} + (\phi^f - 1)\rho^f \frac{\partial v}{\partial t} = -\alpha \left(\frac{\partial f}{\partial t} - v \right) + \phi^f \frac{\partial T_{zz}^{sf}}{\partial z} + \rho^f \left(\frac{\partial \tilde{\psi}}{\partial z} \right), \tag{6.95}$$

where

$$\tilde{\psi} = \frac{\bar{\mu}_G p}{\rho_R^s} \left(g^2 - 1 \right) + \frac{p \bar{\mu}_p}{\rho_R^s} \left(\frac{p^2}{g^2} - 1 \right) + \frac{R\theta p}{\rho_R^f V_0} \left[\left(1 - \frac{1}{p} \right) \ln \left(1 - \frac{1}{p} \right) - \chi \frac{1}{p^2} \right]. \tag{6.96}$$

Now, assuming that the velocity and acceleration of the solid are small compared to that of the fluid, we shall drop $\dfrac{\partial f}{\partial t}$ and $\dfrac{\partial^2 f}{\partial t^2}$ in Eq. (6.95), we get

$$(\phi^f - 1)\rho^f \frac{\partial v}{\partial t} = \alpha v + \phi^f \frac{\partial T_{zz}^{sf}}{\partial z} + \rho^f \left(\frac{\partial \tilde{\psi}}{\partial z} \right). \tag{6.97}$$

Next, we shall also assume that the acceleration of the fluid is also small and we shall drop $\dfrac{\partial v}{\partial t}$ term in Eq. (6.97), to get

$$v = -\frac{1}{\alpha} \left[\phi^f \frac{\partial T_{zz}^{sf}}{\partial z} + \rho^f \left(\frac{\partial \tilde{\psi}}{\partial z} \right) \right]. \tag{6.98}$$

Using Eq. (6.98) in Eq. (6.87), we arrive at

$$\frac{\partial p}{\partial t} = \frac{1}{\alpha p^2} \frac{\partial p}{\partial Z} \left[\phi^f \frac{\partial T_{zz}^{sf}}{\partial Z} + \rho^f \left(\frac{\partial \tilde{\psi}}{\partial Z} \right) \right] + \frac{p-1}{\alpha} \frac{\partial}{\partial Z} \left[\frac{\phi^f}{p} \frac{\partial T_{zz}^{sf}}{\partial Z} + \frac{\rho^f}{p} \left(\frac{\partial \tilde{\psi}}{\partial Z} \right) \right]. \tag{6.99}$$

Also, note that

$$\boldsymbol{D}_G = \boldsymbol{L}_G = \text{diag} \left\{ 0, 0, \frac{1}{g} \frac{\partial g}{\partial t} \right\}, \tag{6.100}$$

and so the evolution equation of the natural configuration reduces to

$$\gamma \frac{1}{g}\frac{\partial g}{\partial t} = 2\left(1 + \frac{\rho_R^f}{\rho_R^s}(p-1)\right)\left[\bar{\mu}_p\left(\frac{p}{g}\right)^2 - \bar{\mu}_G g^2\right]. \tag{6.101}$$

1. Boundary conditions

Applying boundary conditions in an initial boundary value problem has been an issue in mixture theory due to its basic assumption of co-occupancy. For instance, if traction is applied on the boundary, a natural question is how is the traction to be split between the solid and the fluid. To this end, the method of spitting the traction based on the volume fraction of the solid and the fluid was proposed [121]. Later on, Baek and Srinivasa [107] derived the relations for swelling of an elastic body based on variational principles and the boundary conditions were derived *naturally*. However, this approach assumes that the swelling is *slow*, and that the relative velocity between the solid and the diffusing fluid is small. Recently, Prasad and Rajagopal [124] have compared the solutions of diffusion of a fluid through a elastic slab using various boundary conditions like saturation boundary condition, traction splitting boundary condition, the natural boundary condition derived by Baek and Srinivasa, and the condition that the chemical potential is continuous across the boundary. Interestingly, they show that the results are *insensitive* to these different forms of boundary conditions.

For our problem, let $F(t)$ be the compressive force applied on the solid at $Z = \pm H$ as shown in Fig. (30) and let P_∞ be the pressure in the fluid at the boundaries $Z = \pm H$, then we shall apply the following boundary conditions:

$$T_{zz}^s = -F(t) - \phi^s P_\infty, \quad Z = \pm H, \tag{6.102a}$$

$$T_{zz}^f = -\phi^f P_\infty, \quad Z = \pm H, \tag{6.102b}$$

that is, we are assuming that the external force is borne by the solid only, while the fluid pressure is borne by both the solid and the fluid, and this pressure is split proportional to the volume fraction of the constituents. Based on these assumptions, Eq. (6.102b) reduces to

$$\lambda = P_\infty, \quad Z = \pm H. \tag{6.103}$$

Eq. (6.102a) and Eq. (6.103) reduce to

$$-F(t) = T^{sf}_{zz}, \quad Z = \pm H. \tag{6.104}$$

Note that $F(t)$ is zero under free-swelling.

2. Non-dimensionalization

We shall use the following non-dimensionalization scheme:

$$Z^\star = \frac{Z}{L},\ t^\star = \frac{t}{T},\ v^\star = \frac{vT}{L},\ p^\star = p,\ g^\star = g,\ \bar{\mu}^\star_p = \frac{\bar{\mu}_p}{\mu},\ \gamma^\star = \frac{\gamma V}{\mu L}, \tag{6.105}$$

where T, L are characteristic time and length respectively. If we pick $\mu = \frac{R\theta}{V_0}$ and define the non-dimensionalization quantities $\beta_1 := \frac{\rho^s_R}{\rho^f_R}$, $\beta_2 := \frac{L^2 V_0 \alpha}{R\theta T}$ then Eqs. (6.99), (6.101) become

$$\begin{aligned}\beta_2 \frac{\partial p\star}{\partial t} &= \frac{1}{(p^\star)^2}\left(1 - \frac{1}{p^\star}\right)\frac{\partial p^\star}{\partial Z^\star}\left[\frac{\partial T^{sf\star}_{zz}}{\partial Z^\star} + \frac{\partial \tilde{\psi}^\star}{\partial Z^\star}\right] \\ &\quad + (p^\star - 1)\frac{\partial}{\partial Z^\star}\left[\left(1 - \frac{1}{p^\star}\right)\frac{1}{p^\star}\left(\frac{\partial T^{sf\star}_{zz}}{\partial Z^\star} + \frac{\partial \tilde{\psi}^\star}{\partial Z^\star}\right)\right], \qquad (6.106a)\\ \gamma^\star \frac{1}{g^\star}\frac{\partial g^\star}{\partial t^\star} &= 2\left(1 + \frac{1}{\beta_1}(p^\star - 1)\right)\left[\bar{\mu}^\star_p\left(\frac{p^\star}{g^\star}\right)^2 - \bar{\mu}^\star_G (g^\star)^2\right], \qquad (6.106b)\end{aligned}$$

where

$$T_{zz}^{sf\star} = \left(1+\frac{1}{\beta_1}(p^\star-1)\right)\left[2\bar{\mu}_p^\star\left(\frac{p^\star}{g^\star}\right)^2+\bar{\mu}_p^\star\left(\frac{(p^\star)^2}{(g^\star)^2}-1\right)+\bar{\mu}_G^\star\left((g^\star)^2-1\right)\right]$$
$$+\left(1+\frac{1}{p^\star}\left(\beta_1-1\right)\right)p^\star\left[\ln\left(1-\frac{1}{p^\star}\right)+\frac{1}{p^\star}+\chi\frac{1}{(p^\star)^2}\right], \tag{6.107a}$$

$$\tilde{\psi}^\star = \frac{\bar{\mu}_G^\star p^\star}{\beta_1}\left((g^\star)^2-1\right)+\frac{p^\star\bar{\mu}_p^\star}{\beta_1}\left(\frac{(p^\star)^2}{(g^\star)^2}-1\right)+p^\star\left[\left(1-\frac{1}{p^\star}\right)\ln\left(1-\frac{1}{p^\star}\right)-\chi\frac{1}{(p^\star)^2}\right]. \tag{6.107b}$$

The boundary conditions Eq. (6.104) reduce to

$$-F^\star(t^\star) = T_{zz}^{sf\star}, \quad Z^\star = \pm H^\star, \tag{6.108}$$

with $F^\star = \frac{F}{\mu}$, $P_\infty^\star = \frac{P_\infty^\star}{\mu}$. If we pick H as the characteristic length L, then $H^\star = 1$. The coupled equations Eqs. (6.106a), (6.106b) are solved using the staggered scheme shown in algorithm 1.

The ratio of the mass of the swollen solid to its original unswollen mass can be calculated as follows:

$$\begin{aligned}\frac{m}{m_0} &= \frac{\int \rho\, dV}{\int \rho_R^s\, dV}\\ &= \frac{\int_{z=-1}^{z=1}\frac{\rho}{\rho_R^s}\, dz}{\int_{z=-1}^{z=1} dz}\\ &= \frac{1}{2\beta_1}\int_{z=-1}^{z=1}\left[1+\frac{1}{p^\star}\left(\beta_1-1\right)\right] dz.\end{aligned} \tag{6.109}$$

Once, the value of $p^\star(Z^\star, t^\star)$ is evaluated on the domain at various times, Eq. (6.109) is integrated numerically to get the mass ratio.

Algorithm 1 A staggered procedure for solving the coupled equations

1: Input: β_1, β_2, χ, $F^\star$, $P^\star_\infty$, $\bar{\mu}^\star_p$, $\bar{\mu}^\star_G$, $\gamma^\star$; Time of integration $t^\star_f$; Time step $\Delta t^\star$; No. of divisions along $Z^\star$ direction N; TOLERANCE.

2: Output: $\boldsymbol{p}^\star$.

3: Set $\boldsymbol{p}^{\star 0} = 1$, $\boldsymbol{g}^{\star 0} = 1$.

4: **while** $t < t_f$ **do**

5: $t^\star = t^\star + \Delta t^\star$.

6: **while** true **do**

7: Using $\boldsymbol{p}^{\star i(l)}$, $\boldsymbol{g}^{\star i(l)}$, N, Δt, β_1, β_2, χ, $F^\star$, $P^\star_\infty$, $\bar{\mu}^\star_p$, $\bar{\mu}^\star_G$, $\gamma^\star$, Solve for $\boldsymbol{p}^{\star i(l+1)}$ using Eq. (6.106a) in MATLAB's `pdepe` solver with the $\boldsymbol{p}^{\star i(l+1)}$ at the boundaries ($Z^\star = \pm 1$) obtained by solving the non-linear algebraic equation in Eq. (6.108). This non-linear algebraic equation is solved using the `fsolve` solver in MATLAB.

8: Using $\boldsymbol{p}^{\star i(l+1)}$, $\boldsymbol{g}^{\star i(l)}$ and Δt, β_1, β_2, χ, $F^\star$, $P^\star_\infty$, $\bar{\mu}^\star_p$, $\bar{\mu}^\star_G$, $\gamma^\star$, Solve for $\boldsymbol{g}^{\star i(l)}$ using Eq. (6.106b) in MATLAB's `ode45` solver.

9: **if** $\|\boldsymbol{p}^{\star i(l+1)} - \boldsymbol{p}^{\star i(l)}\|_2 <$ TOLERANCE **then**

10: Return.

11: **end if**

12: **end while**

13: $\boldsymbol{p}^{\star i+1} \leftarrow \boldsymbol{p}^{\star i}$, $\boldsymbol{g}^{\star i+1} \leftarrow \boldsymbol{g}^{\star i}$.

14: **end while**

3. Comparison with experimental data

Fig. (31) shows comparison of the numerical results to the experimental data for the ratio of swollen to unswollen (see Eq. (6.109)) PMDA-ODA (poly(N, N'- bisphenoxyphenylpyromellitimide)) due to diffusion of the solvents DMSO (dimethylsulfoxide) and NMP (N-methyl-2-pyrollidinone). In case of DMSO diffusing through PMDA-ODA the following material parameters were chosen: Density of DMSO was chosen to be $1.096\,g/cc$ [125] and density of PMDA-ODA to be $1.42\,g/cc$ [126], and so $\beta_1 = 1.3$. Also, $\chi = 0.425$, $\beta_2 = 0.018$, $\bar{\mu}_p^\star = 0.1$, $\bar{\mu}_G^\star = 0.1$, $\gamma^\star = 20$ were chosen. The characteristic time (T) chosen was $10500\,min$. For the diffusion of NMP, the material parameters chosen were: density of NMP is taken to be $1.02\,g/cc$ [125] and so $\beta_1 = 1.4$. Next, $\chi = 0.6$, $\beta_2 = 0.016$, $\bar{\mu}_p^\star = 0.1$, $\bar{\mu}_G^\star = 0.1$, $\gamma^\star = 20$ and the characteristic time chosen was $245\,min$. The numerical results show good agreement with the experimental data taken from [127].

Next, we shall consider the diffusion of water through HPFE-II-52. The material parameters were assumed to be: $\chi = 0.425$, $\beta_1 = 1.3$, $\beta_2 = 0.018$, $\bar{\mu}_p^\star = 0.1$, $\bar{\mu}_G^\star = 0.1$, $\gamma^\star = 20$. The characteristic time chosen was $2800\,s$. Even in this case the numerical results and experimental data taken from [91] match well (see Fig. (32)). In all the numerical calculations TOLERANCE was chosen to be 10^{-4}.

We shall now consider the problem of compression of the viscoelastic solid and study its effects on swelling due to diffusion of a fluid. In this numerical experiment, the solid is allowed to swell freely first till it saturates with fluid (upto $t^\star = 0.5$). Then, the swollen solid is subjected to constant compressive force of $F^\star = 1$ is applied for a time period of $t^\star = 0.5$ and then the load is removed, and the solid is allowed to swell freely again for another time period of $t^\star = 0.5$. Fig. (33a) shows that the volume of the solid gradually increases with time and then reaches a steady state

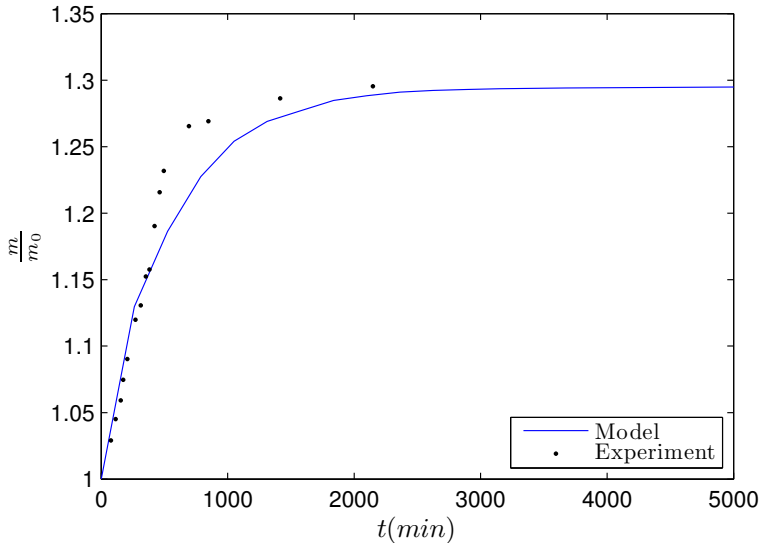

(a) DMSO

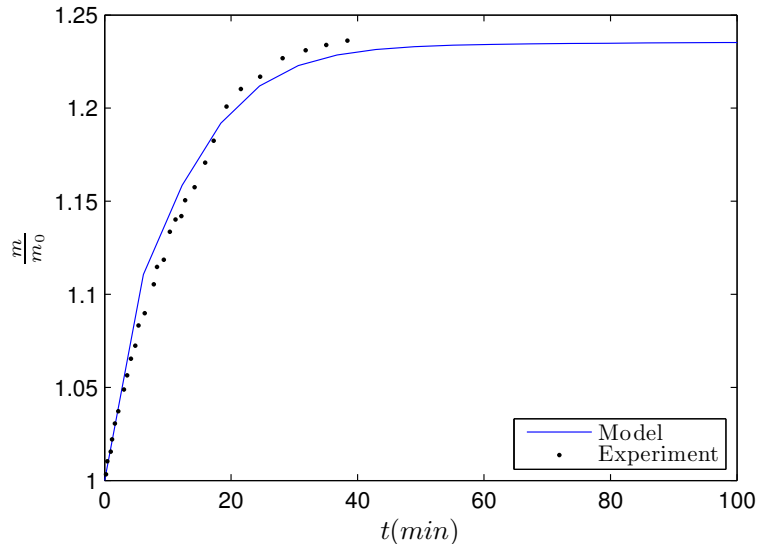

(b) NMP

Fig. 31.: Comparison of the model with the experimental data from [127] for the diffusion of DMSO and NMP through PMDA-ODA (imidized at 300^{o}C) under free-swelling condition. The characteristic times chosen were 10500 min and 245 min for DMSO and NMP, respectively. Here, 301 spatial points were used for the calculations, non-dimensional time step chosen is $\Delta t^\star = 0.025$.

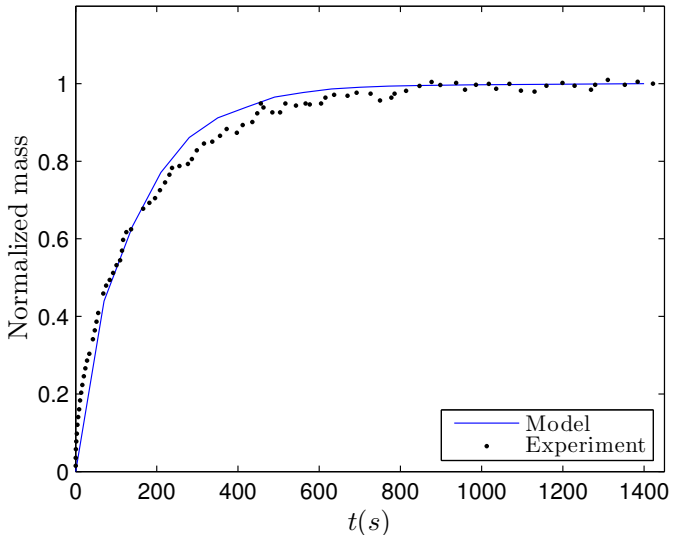

Fig. 32.: Comparison of the model with the experimental data from [91] (pg. 27) for the diffusion of water through HFPE-II-52 under free-swelling condition. The characteristic time chosen was 2800 s. The parameters chosen are $\chi = 0.425$, $\beta_1 = 1.3$, $\beta_2 = 0.018$, $\bar{\mu}_p^\star = 0.1$, $\bar{\mu}_G^\star = 0.1$, $\gamma^\star = 20$. Here, 301 spatial points were used for the calculations, $\Delta t^\star = 0.025$. The normalized mass is defined by $\dfrac{m(t) - m_0}{m_\infty - m_0}$, where m_0 is the mass of the dry solid, m_∞ is the steady state mass of the swollen solid, $m(t)$ is the mass of the swollen solid at a given time t.

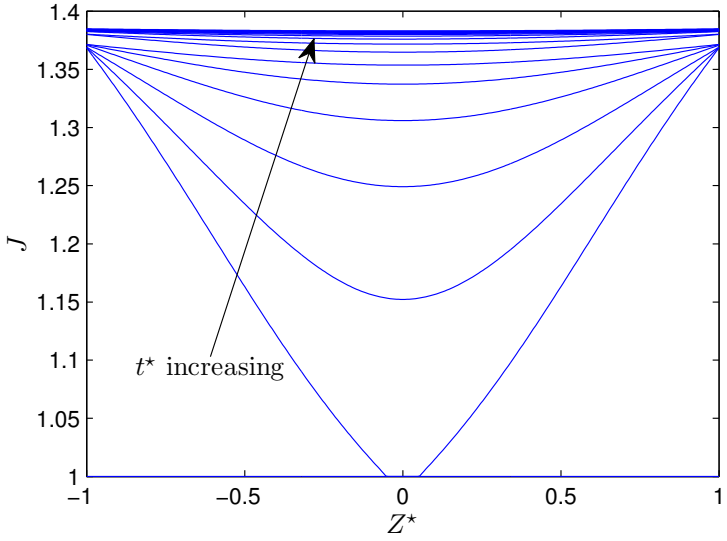

(a) free swelling

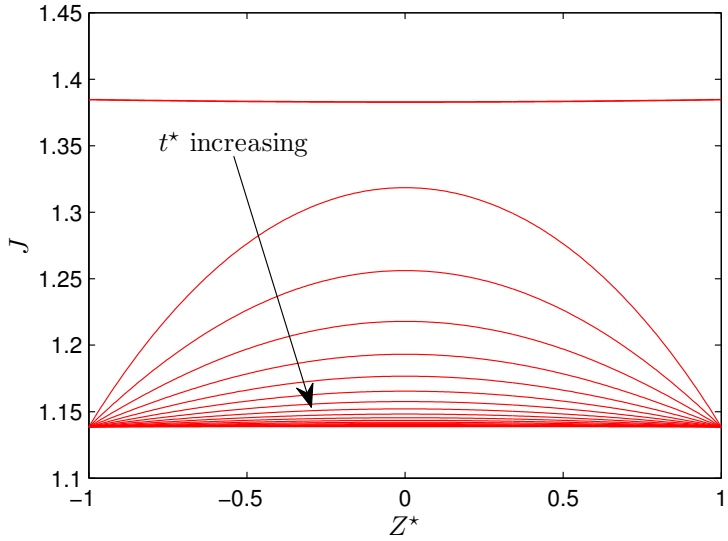

(b) compression after free swelling

Fig. 33.: Ratio of volume of the swollen solid to volume of unswollen solid ($J = \det(\boldsymbol{F}^s)$) as a function of time for (a) free swelling and (b) compressive force $F^\star = 1$ is applied after the swollen solid reaches a saturated state due to free swelling. The parameters chosen are $\chi = 0.425$, $\beta_1 = 1.3$, $\beta_2 = 0.018$, $\bar{\mu}_p^\star = 0.1$, $\bar{\mu}_G^\star = 0.1$, $\gamma^\star = 20$. Here, 301 spatial points were used for the calculations, non-dimensional time step chosen is $\Delta t^\star = 0.025$.

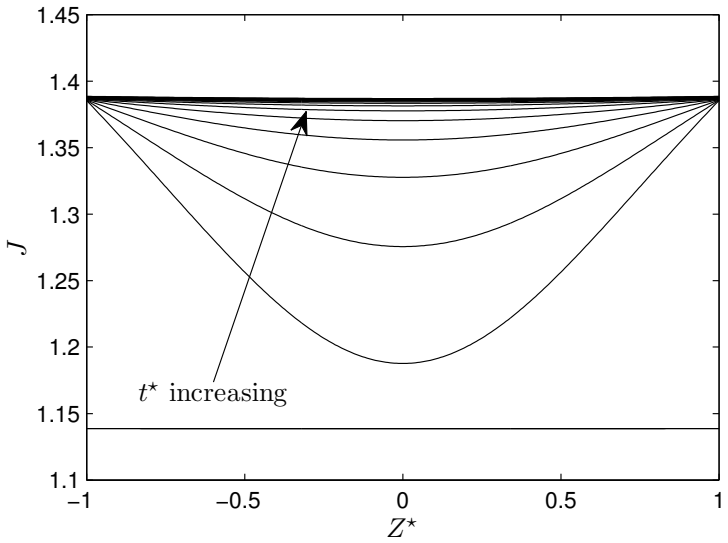

Fig. 34.: Ratio of volume of the swollen solid to volume of unswollen solid ($J = \det(\boldsymbol{F}^s)$) as a function of time for free- swelling after the compressive force is removed. The parameters chosen are $\chi = 0.425$, $\beta_1 = 1.3$, $\beta_2 = 0.018$, $\mu_p^\star = 0.1$, $\mu_G^\star = 0.1$, $\gamma^\star = 20$. Here, 301 spatial points were used for the calculations, non-dimensional time step chosen is $\Delta t^\star = 0.025$.

where the volume of the solid is same everywhere and there is no further swelling. Also, the volume of the solid near the boundary increases faster than that of the inner solid. Upon application of a constant compressive load in Fig. (33b), the fluid diffuses out of the swollen solid and the volume of the solid gradually decreases until the volume of the solid is same everywhere. Next, upon removal of the compressive load in Fig. (34), the solid absorbs the fluid and swells freely back to its original swollen saturation state.

E. Conclusions

We developed a systematic framework with a thermodynamic basis to develop constitutive relations for the diffusion of a fluid through a viscoelastic solid. A model was also derived using this framework by choosing specific forms for the Helmholtz potential and the rate of dissipation, and by maximizing the rate of dissipation. An initial boundary value problem was solved where we considered free swelling and swelling under the application of external force. We also showed that the model fits well with the experimental data for diffusion of fluids through polyimides. Furthermore, our work in this chapter can be easily extended to study the diffusion of fluids in biological materials as well as in studying moisture-induced damage in asphalt mixes and other geomaterials that show viscoelastic behavior.

Finally, here we shall summarize the assumptions made in this chapter:

1. the specific Helmholtz potential of the constituents is the same,

2. the temperature of the constituents is the same,

3. the specific Helmholtz potential of the mixture depends on the temperature of the mixture, and the deformation of the solid,

4. the volume of the mixture is sum of the volumes of the constituents in their natural state,

5. the response of the solid from the current configuration to its natural configuration is isotropic and elastic,

6. the reference configurations of the constituents are same as their natural states,

7. the rate of dissipation of the mixture is assumed to be the sum of the rates of dissipation due to mechanical working of the viscoelastic solid, due to the fluid (i.e, due to the friction between the layers of the fluid), and due to the drag between the solid and the fluid.

The following additional assumptions are made to solve the problem of compression:

1. the viscosity of the fluid is zero i.e., we are assuming that the dissipation due to the friction between the layers of the fluid is much smaller than that due to the drag between the solid and the fluid,

2. the velocity and acceleration of the solid are small compared to that of the fluid,

3. acceleration of the fluid is small,

4. the external loading is applied on the solid only, whereas the fluid pressure at the boundary is borne by both the solid and the fluid.

CHAPTER VII

A MODEL FOR THE DEGRADATION OF POLYIMIDES DUE TO OXIDATION

Polyimides, due to their superior mechanical behavior at high temperatures, are used in a variety of applications that include aerospace, automobile and electronic packaging industries, as matrices for composites, as adhesives etc. In this chapter, we extend our previous model in Chapter V, which was shown to be a three-dimensional extension of the standard linear solid model, to include oxidative degradation of these high temperature polyimides. The forms for the Helmholtz potential and the rate of dissipation are modified to incorporate the degradation. The results for specific boundary value problem, using our model compare well with the experimental creep data for PMR-15 resin that is aged in air.

A. Introduction

Polyimide and polyimide composites are used in a variety of applications due to the high glass transition temperature of above 300^oC. These polymers and their composite components undergo degradation in a variety of ways including degradation due to oxidation. Thus, there is a need to understand how the mechanical behavior of these materials is affected by oxidation. Several experimental studies have been carried out which show that there is: (a) weight loss in the polyimides, and (b) an oxidized layer is formed on the surface of the material (see [128, 129], also see references in [130]) due to oxidation. The loss of weight due to oxidation is observed to be due to chemical bond breakage and escape of volatile lower molecular weight gaseous products. In addition, it has been observed that the brittle oxidized layer formed on the surface of the polyimide acts as a crack initiation site, which leads to the failure of the materials. These cracks also provide more surface area for further degradation

and damage due to oxidation. Recently, Tandon et al. [131], Pochiraju and Tandon [130], Roy et al. [132] have looked at oxidative degradation of polymer composites from a modeling perspective. However, most of the works either do not consider the coupling between chemical reactions and deformation or assume that the coupling is between the small strain in a linearized elastic solid model (which does not correctly describe the mechanical behavior of these high temperature polymers since it has been experimentally shown that they exhibit non-linear viscoelastic response, see [92]) and an advection-diffusion-reaction equation.

A thermodynamic framework that considers the coupling between chemical reactions (including stoichiometry and chemical kinetics) and deformation of polyimides that show non-linear viscoelastic response, is needed. Such a framework can also be used in modeling similar coupling in areas like asphalt mechanics, biomechanics and geomechanics. Some of the earlier works in areas of stoichiometry and thermochemistry are by Prigogine [58], de Donder and Van Rysselberghe [133], Van Rysselberghe [134], Bowen [135, 136], Samohýl [137], Nunziato and Walsh [138], Björnbom [139], Fishtik and Datta [140], Germain et al. [141], Pekar [142], Zeleznik [143], and Kannan and Rajagopal [144].

In this chapter, we shall extend our constitutive theory that has been used to model the non-linear response of viscoelastic solids (see Chapter V) to include degradation due to chemical reactions (specifically, oxidation). This theory is based on the thermodynamic framework of Rajagopal and co-workers (we refer the reader to [20] for details of this framework) that has been shown to be able to capture a plethora of phenomena. We extend our previous work by introducing a variable α that represents the extent of oxidation in the polyimide. Our approach should not be thought of as merely other internal variable theories that are in vogue; we are able to assign a clear meaning to this variable and thus it is a variable that goes towards specifying the

state of the body. The forms for the Helmholtz ψ potential and the rate of dissipation ξ in Chapter V are modified to incorporate the changes in the response of the body due to oxidative degradation. Our approach is similar to that of Rajagopal et al. [145] who have modeled the degradation due to deformation and chain scission in polymers using a variable to quantify the degradation.

The current chapter is organized as follows. The preliminaries that are required are documented in section (B). In sub-sections (C.1), (C.2), the constitutive relations for the degradation due to oxidation are derived. In sub-section (C.3), the predictions of our proposed model are compared with the experimental creep data for oxidative degradation of PMR-15 given in [146]. In the final section, we make some remarks concerning the limitations of the approach, the scope for its improvement and future work that needs to be carried out.

B. Preliminaries

The local form of the balance of mass, linear momentum, angular momentum (in the absence of internal couples), and energy are given by

$$\dot{\varrho} = -\varrho \operatorname{div}(\boldsymbol{v}), \tag{7.1a}$$

$$\varrho \dot{\boldsymbol{v}} = \operatorname{div}\left(\boldsymbol{T}^T\right) + \varrho \boldsymbol{b}, \tag{7.1b}$$

$$\boldsymbol{T} = \boldsymbol{T}^T, \tag{7.1c}$$

$$\varrho \dot{\epsilon} = \boldsymbol{T}.\mathbf{L} + \varrho r - \operatorname{div}(\boldsymbol{q}). \tag{7.1d}$$

where $\boldsymbol{T}$ is the Cauchy stress, ϱ is the density, $\boldsymbol{b}$ is the specific body force, ϵ is the specific internal energy, r is the radiant heating, $\boldsymbol{q}$ is the heat flux, div(.) stands for the divergence operator in the current configuration. The kinematics presented in this section in addition to the preliminaries in Chapter V are sufficient for the work

that follows.

C. Constitutive assumptions

1. General results

We shall assume that the viscoelastic solid is isotropic and incompressible with the specific Helmholtz potential of the form

$$\psi = \psi(\boldsymbol{B}_{p(t)}, \boldsymbol{B}_G, \theta, \alpha) = \hat{\psi}(\mathrm{I}_{\boldsymbol{B}_{p(t)}}, \mathrm{II}_{\boldsymbol{B}_{p(t)}}, \mathrm{I}_{\boldsymbol{B}_G}, \mathrm{II}_{\boldsymbol{B}_G}, \theta, \alpha), \tag{7.2}$$

where α is a variable that accounts for the extent of oxidation. α equal to zero implies the body is in its virgin state and $\alpha = 1$ means that the material is completely oxidized, and no further oxidation is possible. The rate of change of the variable α is related to the rate of the oxidation reaction that takes place in the polyimide. In general, $\boldsymbol{\alpha}$ can be taken to be a tensor which represents the degree of oxidation in different directions i.e., anisotropic oxidation. Although it is seen in experiments that oxidation mostly occurs on the surface of the polyimide, we shall assume that oxidation occurs at every point in the body. One can model the motion of the surface of oxidation in the polyimide using a mixture theory approach such as that used by Rajagopal and Tao [121] which can take into effect the diffusion of a singular surface, which in the case of the problem under consideration would be the surface that separates the region of the virgin and oxidized body; however such an approach would make the problem too complicated to be amenable to a meaningful study of a initial-boundary value problem. We are also assuming that oxygen, polyimide and the products of oxidation together constitute a constrained mixture i.e., there is no relative velocity between these constituents, and hence our approach does not capture the diffusion process. In order to model the diffusion phenomenon, one can follow the

approach shown in Chapter VI.

Next, assuming that the elastic response from the current configuration κ_t to the natural configuration $\kappa_{p(t)}$ is isotropic, without loss of generality, we choose $\kappa_{p(t)}$ such that

$$\boldsymbol{F}_{\kappa_{p(t)}} = \boldsymbol{V}_{\kappa_{p(t)}}, \tag{7.3}$$

where $\boldsymbol{V}_{\kappa_{p(t)}}$ is the right stretch tensor in the polar decomposition of $\boldsymbol{F}_{\kappa_{p(t)}}$. We shall also assume that the total rate of dissipation can be split additively as follows

$$\boldsymbol{T}\cdot\boldsymbol{D} - \varrho\dot{\psi} - \varrho s\dot{\theta} = \xi_{m,d} \geq 0, \quad -\frac{\boldsymbol{q}_h\cdot\operatorname{grad}(\theta)}{\theta} = \xi_c \geq 0, \tag{7.4}$$

where $\xi_{m,d}$ is the rate of dissipation due to the conversion of mechanical working into thermal energy and due to degradation, ξ_c is the rate of dissipation due to heat conduction. Now, if we constitutively choose

$$\boldsymbol{q}_h = -\mathcal{K}(\theta)\operatorname{grad}(\theta), \quad \mathcal{K}(\theta) \geq 0, \tag{7.5}$$

where $\mathcal{K}$ is the thermal conductivity, then Eq. $(7.4)_{(b)}$ is automatically satisfied.

Now,

$$\begin{aligned}\dot{\psi} = &\left[\left(\frac{\partial\hat{\psi}}{\partial \mathrm{I}_{B_{p(t)}}} + \mathrm{I}_{B_{p(t)}}\frac{\partial\hat{\psi}}{\partial \mathrm{II}_{B_{p(t)}}}\right)\boldsymbol{I} - \frac{\partial\hat{\psi}}{\partial \mathrm{II}_{B_{p(t)}}}\boldsymbol{B}_{p(t)}\right]\cdot\dot{\boldsymbol{B}}_{p(t)} \\ &+ \left[\left(\frac{\partial\hat{\psi}}{\partial \mathrm{I}_{B_G}} + \mathrm{I}_{B_G}\frac{\partial\hat{\psi}}{\partial \mathrm{II}_{B_G}}\right)\boldsymbol{I} - \frac{\partial\hat{\psi}}{\partial \mathrm{II}_{B_G}}\boldsymbol{B}_G\right]\cdot\dot{\boldsymbol{B}}_G + \frac{\partial\hat{\psi}}{\partial\theta}\dot{\theta} + \frac{\partial\hat{\psi}}{\partial\alpha}\dot{\alpha},\end{aligned} \tag{7.6}$$

and using Eqs. (5.10), (5.11) along with Eq. (7.3) in Eq. (7.6), we obtain that

$$\begin{aligned}\dot{\psi} = &\,2\left[\left(\frac{\partial\hat{\psi}}{\partial \mathrm{I}_{B_{p(t)}}} + \mathrm{I}_{B_{p(t)}}\frac{\partial\hat{\psi}}{\partial \mathrm{II}_{B_{p(t)}}}\right)\boldsymbol{B}_{p(t)} - \frac{\partial\hat{\psi}}{\partial \mathrm{II}_{B_{p(t)}}}\boldsymbol{B}_{p(t)}^2\right]\cdot(\boldsymbol{D}-\boldsymbol{D}_G) \\ &+ 2\left[\left(\frac{\partial\hat{\psi}}{\partial \mathrm{I}_{B_G}} + \mathrm{I}_{B_G}\frac{\partial\hat{\psi}}{\partial \mathrm{II}_{B_G}}\right)\boldsymbol{B}_G - \frac{\partial\hat{\psi}}{\partial \mathrm{II}_{B_G}}\boldsymbol{B}_G^2\right]\cdot\boldsymbol{D}_G + \frac{\partial\hat{\psi}}{\partial\theta}\dot{\theta} + \frac{\partial\hat{\psi}}{\partial\alpha}\dot{\alpha}.\end{aligned} \tag{7.7}$$

Next, we shall assume the rate of dissipation $\xi_{m,d}$ to be of the form

$$\xi_{m,d} = \xi_{m,d}(\theta, \alpha, \dot{\alpha}, \boldsymbol{B}_{p(t)}, \boldsymbol{D}_G). \tag{7.8}$$

On substituting Eq. (7.7) into Eq. $(7.4)_{(a)}$, we arrive at

$$\begin{aligned}
&\left[\boldsymbol{T} - 2\varrho\left(\frac{\partial\hat{\psi}}{\partial \mathrm{I}_{B_{p(t)}}} + \mathrm{I}_{B_{p(t)}}\frac{\partial\hat{\psi}}{\partial \mathrm{II}_{B_{p(t)}}}\right)\boldsymbol{B}_{p(t)} + 2\varrho\frac{\partial\hat{\psi}}{\partial \mathrm{II}_{B_{p(t)}}}\boldsymbol{B}^2_{p(t)}\right]\cdot\boldsymbol{D}\\
&\quad + 2\varrho\left[\left(\frac{\partial\hat{\psi}}{\partial \mathrm{I}_{B_{p(t)}}} + \mathrm{I}_{B_{p(t)}}\frac{\partial\hat{\psi}}{\partial \mathrm{II}_{B_{p(t)}}}\right)\boldsymbol{B}_{p(t)} - \frac{\partial\hat{\psi}}{\partial \mathrm{II}_{B_{p(t)}}}\boldsymbol{B}^2_{p(t)}\right]\cdot\boldsymbol{D}_G\\
&\quad - 2\varrho\left[\left(\frac{\partial\hat{\psi}}{\partial \mathrm{I}_{B_G}} + \mathrm{I}_{B_G}\frac{\partial\hat{\psi}}{\partial \mathrm{II}_{B_G}}\right)\boldsymbol{B}_G - \frac{\partial\hat{\psi}}{\partial \mathrm{II}_{B_G}}\boldsymbol{B}^2_G\right]\cdot\boldsymbol{D}_G - \varrho\frac{\partial\hat{\psi}}{\partial\alpha}\dot{\alpha}\\
&\quad - \varrho\left[\frac{\partial\hat{\psi}}{\partial\theta} + s\right]\dot{\theta}\\
&\quad = \xi_{m,d}(\theta, \alpha, \dot{\alpha}, \boldsymbol{B}_{p(t)}, \boldsymbol{D}_G).
\end{aligned} \tag{7.9}$$

We shall set

$$s = -\frac{\partial\hat{\psi}}{\partial\theta}, \tag{7.10}$$

and define

$$\boldsymbol{T}_{p(t)} := 2\varrho\left[\left(\frac{\partial\hat{\psi}}{\partial \mathrm{I}_{B_{p(t)}}} + \mathrm{I}_{B_{p(t)}}\frac{\partial\hat{\psi}}{\partial \mathrm{II}_{B_{p(t)}}}\right)\boldsymbol{B}_{p(t)} - \frac{\partial\hat{\psi}}{\partial \mathrm{II}_{B_{p(t)}}}\boldsymbol{B}^2_{p(t)}\right], \tag{7.11}$$

$$\boldsymbol{T}_G := 2\varrho\left[\left(\frac{\partial\hat{\psi}}{\partial \mathrm{I}_{B_G}} + \mathrm{I}_{B_G}\frac{\partial\hat{\psi}}{\partial \mathrm{II}_{B_G}}\right)\boldsymbol{B}_G - \frac{\partial\hat{\psi}}{\partial \mathrm{II}_{B_G}}\boldsymbol{B}^2_G\right]. \tag{7.12}$$

Using Eqs. (7.10)–(7.12) in Eq. (7.9), we obtain

$$\begin{aligned}
&\big(\boldsymbol{T} - \boldsymbol{T}_{p(t)}\big)\cdot\boldsymbol{D} + \big(\boldsymbol{T}_{p(t)} - \boldsymbol{T}_G\big)\cdot\boldsymbol{D}_G - \varrho\frac{\partial\hat{\psi}}{\partial\alpha}\dot{\alpha}\\
&\quad = \xi_{m,d}(\theta, \alpha, \dot{\alpha}, \boldsymbol{B}_{p(t)}, \boldsymbol{D}_G).
\end{aligned} \tag{7.13}$$

By virtue of the constraint of incompressibility, we have

$$\mathrm{tr}(\boldsymbol{D}) = \mathrm{tr}(\boldsymbol{D}_{p(t)}) = \mathrm{tr}(\boldsymbol{D}_G) = 0. \tag{7.14}$$

Since, the right hand side of Eq. (7.13) does not depend on $\boldsymbol{D}$, using Eq. (7.14),

$$\boldsymbol{T} = p\boldsymbol{I} + \boldsymbol{T}_{p(t)}, \tag{7.15}$$

where p is the Lagrange multiplier due to the constraint of incompressibility[1], with

$$\left(\boldsymbol{T}_{p(t)} - \boldsymbol{T}_G\right) \cdot \boldsymbol{D}_G - \varrho \frac{\partial \hat{\psi}}{\partial \alpha} \dot{\alpha} = \xi_{m,d}(\theta, \alpha, \dot{\alpha}, \boldsymbol{B}_{p(t)}, \boldsymbol{D}_G), \tag{7.16}$$

which can be re-written as

$$(\boldsymbol{T} - \boldsymbol{T}_G) \cdot \boldsymbol{D}_G - \varrho \frac{\partial \hat{\psi}}{\partial \alpha} \dot{\alpha} = \xi_{m,d}(\theta, \alpha, \dot{\alpha}, \boldsymbol{B}_{p(t)}, \boldsymbol{D}_G), \tag{7.17}$$

using Eqs. (7.14) and (7.15).

We shall further assume that $\xi_{m,d}$ can be further additively split as follows:

$$\xi_{m,d}(\theta, \dot{\alpha}, \boldsymbol{B}_{p(t)}, \boldsymbol{D}_G) = \xi_m(\theta, \alpha, \boldsymbol{B}_{p(t)}, \boldsymbol{D}_G) + \xi_d(\theta, \alpha, \dot{\alpha}), \tag{7.18}$$

with each of ξ_m, ξ_d being non-negative, so that the second law is automatically satisfied. Noting that the first term and second terms on the left hand side of Eq. (7.17) are the contributions to dissipation[2] due to mechanical working and degradation, respectively, we shall further assume that

$$(\boldsymbol{T} - \boldsymbol{T}_G) \cdot \boldsymbol{D}_G = \xi_m(\theta, \alpha, \boldsymbol{B}_{p(t)}, \boldsymbol{D}_G), \tag{7.19a}$$

$$-\varrho \frac{\partial \hat{\psi}}{\partial \alpha} \dot{\alpha} = \xi_d(\theta, \alpha, \dot{\alpha}). \tag{7.19b}$$

---

[1]The standard method in continuum mechanics to obtain constraints appeals to the notion that the constraint response does not work. It has been shown recently by Rajagopal and Srinivasa [147] that such an assumption is in general incorrect.

[2]The term dissipation is used to refer to the mechanical working being converted into energy in thermal form, and associated with this dissipation we have entropy production. We shall abuse the use of the term dissipation and refer to other entropy producing mechanism such as degradation as also dissipation.

Now, we shall maximize the rate of dissipation ξ_m by varying $\boldsymbol{D}_G$ for fixed $\boldsymbol{B}_{p(t)}$. That is, we maximize the function

$$\Phi := \xi_m + \lambda_1 \left[\xi_m - (\boldsymbol{T} - \boldsymbol{T}_G) \cdot \boldsymbol{D}_G\right] + \lambda_2(\boldsymbol{I} \cdot \boldsymbol{D}_G), \tag{7.20}$$

where λ_1, λ_2 are the Lagrange multipliers. By setting, $\partial\Phi/\partial\boldsymbol{D}_G = 0$, we get

$$\boldsymbol{T} = \boldsymbol{T}_G + \frac{\lambda_2}{\lambda_1}\boldsymbol{I} + \left(\frac{\lambda_1 + 1}{\lambda_1}\right)\frac{\partial \xi_m}{\partial \boldsymbol{D}_G}. \tag{7.21}$$

We need to determine the Lagrange multipliers. On substituting Eq. (7.21) into Eq. (7.17), we get

$$\left(\frac{\lambda_1 + 1}{\lambda_1}\right) = \frac{\xi_m}{\frac{\partial \xi_m}{\partial \boldsymbol{D}_G} \cdot \boldsymbol{D}_G}, \tag{7.22}$$

and so Eq. (7.21) with Eq. (7.12) becomes

$$\boldsymbol{T} = 2\varrho\left[\left(\frac{\partial\hat{\psi}}{\partial \mathrm{I}_{B_G}} + \mathrm{I}_{B_G}\frac{\partial\hat{\psi}}{\partial \mathrm{II}_{B_G}}\right)\boldsymbol{B}_G - \frac{\partial\hat{\psi}}{\partial \mathrm{II}_{B_G}}\boldsymbol{B}_G^2\right] + \left(\frac{\xi_m}{\frac{\partial \xi_m}{\partial \boldsymbol{D}_G} \cdot \boldsymbol{D}_G}\right)\frac{\partial \xi_m}{\partial \boldsymbol{D}_G} + \hat{\lambda}\boldsymbol{I}. \tag{7.23}$$

where $\hat{\lambda} := \frac{\lambda_2}{\lambda_1}$ is the Lagrange multiplier due to the constraint of incompressibility.

Finally, the constitutive relations are given by

$$\boldsymbol{T} = p\boldsymbol{I} + 2\varrho\left[\left(\frac{\partial\hat{\psi}}{\partial \mathrm{I}_{B_{p(t)}}} + \mathrm{I}_{B_{p(t)}}\frac{\partial\hat{\psi}}{\partial \mathrm{II}_{B_{p(t)}}}\right)\boldsymbol{B}_{p(t)} - \frac{\partial\hat{\psi}}{\partial \mathrm{II}_{B_{p(t)}}}\boldsymbol{B}_{p(t)}^2\right], \tag{7.24a}$$

$$\boldsymbol{T} = \hat{\lambda}\boldsymbol{I} + 2\varrho\left[\left(\frac{\partial\hat{\psi}}{\partial \mathrm{I}_{B_G}} + \mathrm{I}_{B_G}\frac{\partial\hat{\psi}}{\partial \mathrm{II}_{B_G}}\right)\boldsymbol{B}_G - \frac{\partial\hat{\psi}}{\partial \mathrm{II}_{B_G}}\boldsymbol{B}_G^2\right] + \left(\frac{\xi_m}{\frac{\partial \xi_m}{\partial \boldsymbol{D}_G} \cdot \boldsymbol{D}_G}\right)\frac{\partial \xi_m}{\partial \boldsymbol{D}_G}, \tag{7.24b}$$

$$\boldsymbol{q}_h = -k(\theta)\mathrm{grad}(\theta), \quad s = -\frac{\partial\hat{\psi}}{\partial\theta}, \tag{7.24c}$$

$$\varrho\frac{\partial\psi}{\partial\alpha} = -\frac{\xi_d}{\dot{\alpha}}. \tag{7.24d}$$

The two equations Eqs. (7.24a), (7.24b) are to be equated and simplified to get the evolution equation for $\boldsymbol{B}_{\kappa_{p(t)}}$. This will be shown in the next sub-section when we choose specific forms for ψ and ξ.

2. Specific case

We choose the specific Helmholtz potential as

$$\hat{\psi} = A^s + (B^s + c_2^s)(\theta - \theta_s) - \frac{c_1^s}{2}(\theta - \theta_s)^2 - c_2^s\theta \ln\left(\frac{\theta}{\theta_s}\right) + \frac{\mu_G(1+\beta(\theta)\alpha)}{2\varrho}(\mathrm{I}_{B_G} - 3) + \frac{\mu_p(1+\gamma(\theta)\alpha)}{2\varrho}(\mathrm{I}_{B_{p(t)}} - 3) + F(\alpha,\theta), \tag{7.25}$$

where μ_G, μ_p are elastic parameters, θ_s is a reference temperature for the viscoelastic solid and the rates of mechanical dissipation, and the dissipation due to degradation as

$$\xi_m = \eta(1+\delta(\theta)\alpha)\left(\boldsymbol{D}_G \cdot \boldsymbol{B}_{p(t)}\boldsymbol{D}_G\right), \tag{7.26a}$$

$$\xi_d = \frac{D\left(\|\dot{\alpha}\|\right)^{\frac{n+1}{n}}}{(1-\alpha)^{\frac{1}{n}}}. \tag{7.26b}$$

where η is the viscosity, $\|.\|$ stands for absolute value. Here, β, γ and δ are material parameters that depend on temperature. Also, note from Eq. (7.26) that ξ_m, ξ_d are non-negative provided η, δ, D are also non-negative.

Now,

$$\begin{aligned} s &= -\frac{\partial\hat{\psi}}{\partial\theta} \\ &= -(B^s + c_2^s) + c_1^s(\theta - \theta_s) + c_2^s \ln\left(\frac{\theta}{\theta_s}\right) + c_2^s - \frac{\mu_G\alpha}{2\varrho}\frac{\partial\beta}{\partial\theta}(\mathrm{I}_{B_G} - 3) \\ &\quad - \frac{\mu_p\alpha}{2\varrho}\frac{\partial\gamma}{\partial\theta}(\mathrm{I}_{B_{p(t)}} - 3) - \frac{\partial F}{\partial\theta}. \end{aligned} \tag{7.27}$$

The internal energy ϵ is given by

$$\begin{aligned}\epsilon &= \psi + \theta s \\ &= A^s - B^s\theta_s + c_2^s\left(\theta - \theta_s\right) + \frac{c_1^s}{2}\left(\theta^2 - \theta_s^2\right) + \frac{\mu_G}{2\varrho}(\mathrm{I}_{B_G} - 3)\left[1 + \alpha\left(\beta - \theta\frac{\partial\beta}{\partial\theta}\right)\right] \qquad (7.28)\\ &\quad + \frac{\mu_p}{2\varrho}(\mathrm{I}_{B_{p(t)}} - 3)\left[1 + \alpha\left(\gamma - \theta\frac{\partial\gamma}{\partial\theta}\right)\right] + F - \theta\frac{\partial F}{\partial\theta}. \qquad (7.29)\end{aligned}$$

and the specific heat capacity C_v is

$$C_v = \frac{\partial\epsilon}{\partial\theta} = c_1^s\theta + c_2^s - \frac{\mu_G\alpha\theta}{2\varrho}(\mathrm{I}_{B_G} - 3)\frac{\partial^2\beta}{\partial\theta^2} - \frac{\mu_p\alpha\theta}{2\varrho}(\mathrm{I}_{B_{p(t)}} - 3)\frac{\partial^2\gamma}{\partial\theta^2} - \theta\frac{\partial^2 F}{\partial\theta^2}. \qquad (7.30)$$

Also, Eqs. (7.24a), (7.24b) reduce to

$$\boldsymbol{T} = p\boldsymbol{I} + \bar{\mu}_p\boldsymbol{B}_{p(t)}, \qquad (7.31a)$$

$$\boldsymbol{T} = \lambda\boldsymbol{I} + \bar{\mu}_G\boldsymbol{B}_G + \frac{\bar{\eta}}{2}\left(\boldsymbol{B}_{p(t)}\boldsymbol{D}_G + \boldsymbol{D}_G\boldsymbol{B}_{p(t)}\right), \qquad (7.31b)$$

where $\bar{\mu}_p = \mu_p\left(1 + \beta(\theta)\alpha\right)$, $\bar{\mu}_G = \mu_G\left(1 + \gamma(\theta)\alpha\right)$, $\bar{\eta} = \eta\left(1 + \delta(\theta)\alpha\right)$. We also note that we chose the functions for the material moduli ($\bar{\mu}_p$, $\bar{\mu}_G$, $\bar{\eta}$) such that they increase as α goes from 0 to 1. This is consistent with the experiments (see figure 5 in [146]) where it seen that the *elastic modulus* increases with aging. We further note that such a choice of functions for the material moduli is different from what Rajagopal et al. [145] have chosen in their work.

From Eq. (7.31)

$$(p - \lambda)\boldsymbol{I} + \bar{\mu}_p\boldsymbol{B}_{p(t)} = \bar{\mu}_G\boldsymbol{B}_G + \frac{\bar{\eta}}{2}\left(\boldsymbol{B}_{p(t)}\boldsymbol{D}_G + \boldsymbol{D}_G\boldsymbol{B}_{p(t)}\right), \qquad (7.32)$$

and so by pre-multiplying the above equation by $\boldsymbol{B}_{p(t)}^{-1}$ and taking the trace, we get

$$(p - \lambda) = \frac{\bar{\mu}_G\mathrm{tr}(\boldsymbol{B}_{p(t)}^{-1}\boldsymbol{B}_G) - 3\bar{\mu}_p}{\mathrm{tr}(\boldsymbol{B}_{p(t)}^{-1})}. \qquad (7.33)$$

Using Eq. (7.33) in Eq. (7.32), we arrive at the following equation:

$$\left[\frac{\bar{\mu}_G \mathrm{tr}(\boldsymbol{B}_{p(t)}^{-1}\boldsymbol{B}_G) - 3\bar{\mu}_p}{\mathrm{tr}(\boldsymbol{B}_{p(t)}^{-1})}\right]\boldsymbol{I} + \bar{\mu}_p \boldsymbol{B}_{p(t)} = \bar{\mu}_G \boldsymbol{B}_G + \frac{\bar{\eta}}{2}\left(\boldsymbol{B}_{p(t)}\boldsymbol{D}_G + \boldsymbol{D}_G\boldsymbol{B}_{p(t)}\right), \quad (7.34)$$

which can be re-written as

$$\left[\frac{\bar{\mu}_G \mathrm{tr}(\boldsymbol{B}_{p(t)}^{-1}\boldsymbol{B}_G) - 3\bar{\mu}_p}{\mathrm{tr}(\boldsymbol{B}_{p(t)}^{-1})}\right]\boldsymbol{I} + \bar{\mu}_p \boldsymbol{B}_{p(t)} = \bar{\mu}_G \boldsymbol{B}_G - \frac{\bar{\eta}}{4}\left(\boldsymbol{V}_{p(t)}\overset{\nabla}{\boldsymbol{B}}_{p(t)}\boldsymbol{V}^{-1}_{\kappa_{p(t)}} + \boldsymbol{V}^{-1}_{\kappa_{p(t)}}\overset{\nabla}{\boldsymbol{B}}_{p(t)}\boldsymbol{V}_{p(t)}\right), \quad (7.35)$$

where we have used Eqs. (5.13) and (7.34). Now, Eq. (7.24d) reduces to

$$\frac{\mu_G \beta(\theta)}{2}(\mathrm{I}_{B_G} - 3) + \frac{\mu_p \gamma(\theta)}{2}(\mathrm{I}_{B_{p(t)}} - 3) + \varrho\frac{\partial F}{\partial \alpha} = -\frac{D\|\dot{\alpha}\|^{\frac{n+1}{n}}}{\dot{\alpha}\,(1-\alpha)^{\frac{1}{n}}}. \quad (7.36)$$

We shall assume that

$$F(\alpha) = -\frac{k(\theta)}{\varrho}\alpha, \quad (7.37)$$

where k is a non-negative constant, then Eq. (7.36), for $n = 1$ reduces to

$$\frac{\mu_G \beta(\theta)}{2}(\mathrm{I}_{B_G} - 3) + \frac{\mu_p \gamma(\theta)}{2}(\mathrm{I}_{B_{p(t)}} - 3) - k = -\frac{D\|\dot{\alpha}\|^2}{\dot{\alpha}\,(1-\alpha)}. \quad (7.38)$$

Notice that the first two terms on the left hand side of Eq. (7.38) represent the dependence of the extent of oxidation on the deformation of the material.

Thus, with the current choice of the specific Helmholtz potential and the rate of dissipation, we arrive at the following constitutive equations:

$$\boldsymbol{T} = p\boldsymbol{I} + \mu_p\left(1 + \beta(\theta)\alpha\right)\boldsymbol{B}_{p(t)}, \quad (7.39)$$

where the evolution of the natural configuration is given by

$$\left[\frac{\mu_G\left(1+\gamma(\theta)\alpha\right)\mathrm{tr}(\boldsymbol{B}_{p(t)}^{-1}\boldsymbol{B}_G)-3\mu_p\left(1+\beta(\theta)\alpha\right)}{\mathrm{tr}(\boldsymbol{B}_{p(t)}^{-1})}\right]\boldsymbol{I}+\mu_p\left(1+\beta(\theta)\alpha\right)\boldsymbol{B}_{p(t)}$$
$$=\mu_G\left(1+\gamma(\theta)\alpha\right)\boldsymbol{B}_G-\frac{\eta}{4}\left(\boldsymbol{V}_{p(t)}\overset{\nabla}{\boldsymbol{B}}_{p(t)}\boldsymbol{V}_{\kappa_{p(t)}}^{-1}+\boldsymbol{V}_{\kappa_{p(t)}}^{-1}\overset{\nabla}{\boldsymbol{B}}_{p(t)}\boldsymbol{V}_{p(t)}\right), \tag{7.40}$$

and the evolution of α is given by Eq. (7.38). These constitutive relations reduce to the non-linear viscoelastic solid model derived in Chapter V when there is no degradation. In a general initial-boundary value problem, one has to solve the coupled equations Eqs. (7.1b), (7.38) along with Eqs. (7.39), (7.40), subject to appropriate initial and boundary conditions. In problems where temperature gradients are important one needs to also consider the balance of energy Eq. (7.1d).

3. Comparison with experimental data

In order to compare the predictions of our model with experimental data, we shall consider the problem of uniaxial extension, given by

$$x=\lambda(t)X,\quad y=\frac{1}{\sqrt{\lambda(t)}}Y,\quad z=\frac{1}{\sqrt{\lambda(t)}}Z, \tag{7.41}$$

within the context of this model. The velocity gradient is given by

$$\boldsymbol{L}=\mathrm{diag}\left\{\frac{\dot\lambda}{\lambda},-\frac{\dot\lambda}{2\lambda},-\frac{\dot\lambda}{2\lambda}\right\}. \tag{7.42}$$

We shall assume that the stretch $\boldsymbol{B}_{p(t)}$ is given by

$$\boldsymbol{B}_{p(t)}=\mathrm{diag}\left\{B,\frac{1}{\sqrt{B}},\frac{1}{\sqrt{B}}\right\}. \tag{7.43}$$

Straight forward calculations using Eq. (7.34) give

$$\frac{\dot B}{2}=\frac{B\dot\lambda}{\lambda}+\frac{\bar\mu_G}{\bar\eta}\frac{\lambda^2}{B}-\frac{\bar\mu_p}{\bar\eta}B-\left\{\frac{\frac{\bar\mu_G}{\bar\eta}\left(\lambda^3+2B^3\right)-3\frac{\bar\mu_p}{\bar\eta}\lambda B^2}{\lambda B\left(1+2B^{3/2}\right)}\right\}, \tag{7.44}$$

which can be re-written in the following form:

$$\dot{\lambda} = \lambda \left\{ \frac{\dot{B}}{2B} - \left[\frac{1}{\bar{\eta} B} \left(\bar{\mu}_G \frac{\lambda^2}{B} - \bar{\mu}_p B - \left(\frac{\bar{\mu}_G \left(\lambda^3 + 2B^3 \right) - 3\bar{\mu}_p B^2 \lambda}{B\lambda(1 + 2B^{3/2})} \right) \right) \right] \right\}. \tag{7.45}$$

Using Eq. (7.43) in Eq. (7.39), and also the fact that lateral surfaces are traction free, it is easy to see that

$$T_{11} = \bar{\mu}_p \left(B - \frac{1}{\sqrt{B}} \right), \tag{7.46}$$

and so

$$\dot{T}_{11} = \bar{\mu}_p \left(1 - \frac{1}{2\sqrt{B}} \right) \dot{B}. \tag{7.47}$$

In addition, Eq. (7.38) becomes

$$-\frac{\mu_G \beta(\theta)}{2} \left(\frac{\lambda^2}{B} - \frac{2\sqrt{B}}{\lambda} - 3 \right) - \frac{\mu_p \gamma(\theta)}{2} \left(B + \frac{2}{\sqrt{B}} - 3 \right) + k = \frac{D \| \dot{\alpha} \|^2}{\dot{\alpha} \left(1 - \alpha \right)}. \tag{7.48}$$

We shall also use logarithmic strain (or true strain) $\varepsilon = \ln\lambda$ as our strain measure in what follows.

We shall compare our model with the experimental data for PMR-15 from [146]. With the given $\dot{T}_{11}$ and material parameters, Eqs. (7.47), (7.45) were first solved using the initial condition that $B(0) = \lambda(0) = 1$ for a time of $\dfrac{T_{11}}{\dot{T}_{11}}$. Then, Eqs. (7.45), (7.46) were solved till the end of loading. Since in the experiments the aging in air was done without any load being applied, Eq. (7.38) was also solved without the first two terms on the left hand side using $\alpha(0) = 0$ as the initial condition. The ODEs were solved in MATLAB using the `ode45` solver. The following parameters were used for comparing the results predicted by our model to the experimental creep data for PMR-15 (under 10 MPa loading) that has been aged in air for various amounts of time (also see Fig. (35)): $\mu_p = 2 \times 10^9$ MPa, $\mu_G = 3.8 \times 10^8$ MPa, $\eta = 45 \times 10^{12}$ MPa.s, $\frac{k}{D} = 1.2 \times 10^{-6}$ s^{-1}, $\beta = 10$, $\gamma = 0.3$, $\delta = 0.5$. Also, since the experiments were done

under isothermal conditions, the balance of energy Eq. (7.1d) was not considered.

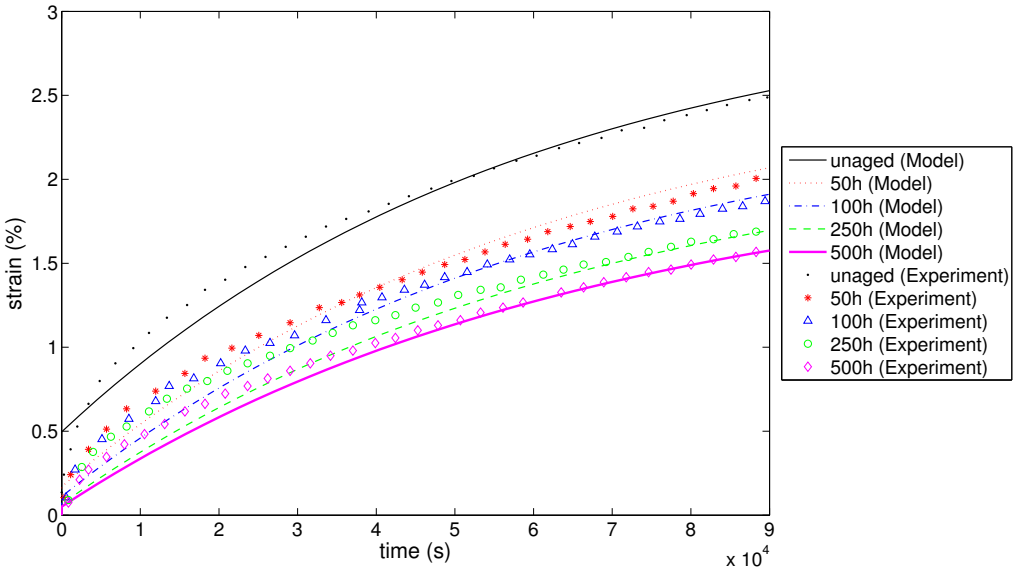

Fig. 35.: Comparison of the model predictions with experimental creep data by Ruggles-Wrenn and Broeckert [146] for PMR-15 at a loading of 10 MPa with $\dot{T}_{11} = 1$ MPa/s as the rate of loading. The amount of time that the sample is aged in air is also shown. The material parameters used are as follows: $\mu_p = 2 \times 10^9$ MPa, $\mu_G = 3.8 \times 10^8$ MPa, $\eta = 45 \times 10^{12}$ MPa.s, $\frac{k}{D} = 1.2 \times 10^{-6}$ s^{-1} , $\beta = 10$, $\gamma = 0.3$, $\delta = 0.5$.

D. Concluding remarks

A model for the degradation of polyimides due to oxidation has been developed in this chapter. Our model also accounts for the effect of deformation on the aging due to oxidation. However, there is no experimental data to corroborate this part of our model.

The limitations of our model are as follows:

1. Our model cannot predict the diffusion of oxygen and hence one cannot estimate the thickness of the oxidized layer on the surface of the resin.

2. The weight lost due to oxidation cannot be estimated using our model. For this one needs to understand the chemical kinetics. Once the chemical kinetics are established, an approach similar to ours can be used to couple these reaction kinetics to the deformation of the polymer. Our work in this chapter can be viewed as a first step towards this end.

CHAPTER VIII

SUMMARY AND FUTURE WORK

In summary, we first showed that different forms for the specific Helmholtz potential and the rate of dissipation can give rise to different three-dimensional models, upon maximizing the rate of dissipation, along with appropriate constraints. These three-dimensional models reduce to the same one-dimensional model. Next, we developed a thermodynamic framework for deriving rate-type models for viscoelastic fluids that do not possess instantaneous elasticity under creep. We then showed that bodies that are initially elastic in nature (and hence cannot creep or stress relax) can creep and stress relax due to degradation caused by diffusion of a fluid. We also showed that this creep and stress relaxation phenomena is different from that shown by viscoelastic bodies in that these phenomena depend on the geometry of the body. Next as a first step to model the various degradation processes on high temperature polyimides, we develop a framework to model the non-linear viscoelastic behavior of these polyimides. We also showed that the model developed using such a framework is a three-dimensional generalization of the standard linear solid. Then, such a framework is extended to include diffusion of a fluid as well as degradation due to oxidation. We showed that the numerical data obtained by solving different boundary valued problems using these models compare well with the experimental data for polyimides.

Directions for future work are as follows:

1. Develop better and more sophisticated experimental techniques for identifying the correct three-dimensional model.

2. Use the rate-type fluid models developed by using our framework in Chapter II to corroborate with experimental data for asphalt and other materials. Also,

extend such a framework to develop visco-elasto-plastic models.

3. Develop a finite element framework for coupling diffusion of a fluid and finite deformation of an elastic solid by incorporating techniques, that have been introduced recently [148], [149], to ensure non-negativity in concentration.

4. To model the anisotropic response of polyimide composites, our framework in Chapter V can be extended by modifying the Helmholtz potential.

5. Further experiments need to be carried out to get the creep and stress relaxation of different polyimides under different loading conditions and for various amounts of aging in oxygen. Also, one needs to perform experiments where simultaneous deformation and aging takes place to see how they are coupled.

6. One can easily extend our work in Chapter VII to include anisotropy in oxidation by introducing a tensor ($\boldsymbol{\alpha}$). In addition, for modeling oxidative degradation in polyimide composites, one can also use different variables α_m, α_f that represent the degradation due to oxidation in the polymer matrix and fiber, respectively. This approach is similar to Baek and Pence [150] who have used different variables to represent the degradation due to swelling in the composite matrix and fiber.

7. Our framework in Chapters VII and VIII can also be used to model degradation due to diffusion of moisture (or other fluids) and oxidation (or other chemical reactions) in materials like asphalt/asphalt derivatives, biomaterials. For this, one has to accordingly modify the terms in the Helmholtz potential and the rate of dissipation due to deformation.

8. Develop a finite element framework for all the viscoelastic models developed in

this dissertation. Such a framework can be used to solve more realistic finite dimensional problems.

REFERENCES

[1] R. Lakes, *Viscoelastic Solids*, Cambridge, UK: Cambridge University Press, 2009.

[2] J. C. Maxwell, "On the dynamic theory of gases," *Philosophical Transactions of the Royal Society of London*, vol. 157, pp. 49–88, 1867.

[3] L. Kelvin, "On the elasticity and viscosity of metals," *Proceedings of the Royal Society*, vol. 14, pp. 289–297, 1865.

[4] W. Voigt, "Ueber innere Reibung fester Körper, insbesondere der Metalle," *Annalen der Physik*, vol. 283, no. 12, pp. 671–693, 1892.

[5] D. R. Bland, *The Theory of Linear Viscoelasticity*, New York: Pergamon Press, 1960.

[6] K. R. Rajagopal and A. R. Srinivasa, "A thermodynamic framework for rate type fluid models," *Journal of Non-Newtonian Fluid Mechanics*, vol. 88, no. 3, pp. 207–227, 2000.

[7] W. N. Findley, J. S. Lai, and K. Onaran, *Creep and Relaxation of Nonlinear Viscoelastic Materials: With an Introduction to Linear Viscoelasticity*, Amsterdam: North-Holland Publishing Company, 1989.

[8] J. D. Ferry, *Viscoelastic Properties of Polymers*, New York: John Wiley & Sons Inc,, 1980.

[9] R. M. Christensen, *Theory of Viscoelasticity*, New York: Academic Press, 1971.

[10] J. H. Aklonis and W. J. MacKnight, *Introduction to Polymer Viscoelasticity*, New York: John Wiley & Sons, Inc., 1983.

[11] A. S. Wineman and K. R. Rajagopal, *Mechanical Response of Polymers: An Introduction*, Cambridge, UK: Cambridge University Press, 2000.

[12] A. C. Pipkin, *Lectures on Viscoelasticity Theory*, New York: Springer-Verlag, 1972.

[13] W. Flügge, *Viscoelasticity*, Waltham, MA: Blaisdell Publishing Company, 1967.

[14] A. C. Pipkin and T. G. Rogers, "A non-linear integral representation for viscoelastic behaviour," *Journal of the Mechanics and Physics of Solids*, vol. 16, no. 1, pp. 59–72, 1968.

[15] Y. C. Fung, *Biomechanics: Mechanical Properties of Living Tissues*, New York: Springer-Verlag, 1993.

[16] C. S. Drapaca, S. Sivaloganathan, and G. Tenti, "Nonlinear constitutive laws in viscoelasticity," *Mathematics and Mechanics of Solids*, vol. 12, no. 5, pp. 475–501, 2007.

[17] A. S. Wineman, "Nonlinear viscoelastic solids–a review," *Mathematics and Mechanics of Solids*, vol. 14, no. 3, pp. 300–366, 2009.

[18] A. Kaye, "Non-newtonian flow in incompressible fluids," Tech. Rep. 134, College of Aeronautics, Cranfield, UK, 1962.

[19] B. Bernstein, E. A. Kearsley, and L. J. Zapas, "A study of stress relaxation with finite strain," *Journal of Rheology*, vol. 7, pp. 391–410, 1963.

[20] K. R. Rajagopal and A. R. Srinivasa, "On the thermomechanics of materials that have multiple natural configurations. Part I: Viscoelasticity and classical plasticity," *Zeitschrift für Angewandte Mathematik und Physik (ZAMP)*, vol. 55, no. 5, pp. 861–893, 2004.

[21] K. R. Rajagopal and A. R. Srinivasa, "On the thermomechanics of materials that have multiple natural configurations. Part II: Twinning and solid to solid phase transformation," *Zeitschrift für Angewandte Mathematik und Physik (ZAMP)*, vol. 55, no. 6, pp. 1074–1093, 2004.

[22] K. E. Secor and C. L. Monismith, "Viscoelastic response of asphalt paving slabs under creep loading," *Highway Research Record*, vol. 67, pp. 84–97, 1965.

[23] M. C. Wang and K. Y. Lee, "Creep Behavior of cement stabilized soils," *Highway Research Record*, vol. 442, pp. 58–69, 1973.

[24] C. Y. Cheung and D. Cebon, "Experimental study of pure bitumens in tension, compression, and shear," *Journal of Rheology*, vol. 41, no. 1, pp. 45–74, 1997.

[25] M. K. Ghosh and K. L. Mittal (Editors), *Polyimides: Fundamentals and Applications*, New York: Marcel Deckker, Inc., 1996.

[26] D. Wilson, H. D. Stenzenberger, and P. M. Hergenrother (Editors), *Polyimides*, New York: Chapman and Hall, 1990.

[27] Y. I. Dimitrienko, *Thermomechanics of Composites under High Temperatures*, Dordrecht: Kluwer Academic Publishers, 1999.

[28] A. E. Green and P. M. Naghdi, "On thermodynamics and the nature of the second law," *Proceedings of the Royal Society of London. Series A, Mathematical and Physical Sciences*, vol. 357, no. 1690, pp. 253–270, 1977.

[29] K. R. Rajagopal and A. R. Srinivasa, "Mechanics of the inelastic behavior of materials: Part II - Inelastic response," *International Journal of Plasticity*, vol. 14, no. 10-11, pp. 969–995, 1998.

[30] H. Ziegler, "Some extremum principles in irreversible thermodynamics with application to continuum mechanics," in *Progress In Solid Mechanics*, I. N. Sneddon and R. Hill, Eds. 1963, vol. 4, pp. 91–113, Amsterdam: North-Holland Publishing Company.

[31] I. J. Rao and K. R. Rajagopal, "On a new interpretation of the classical Maxwell model," *Mechanics Research Communications*, vol. 34, no. 7-8, pp. 509–514, 2007.

[32] J. M. Burgers, "Mechanical considerations-model systems-phenomenological theories of relaxation and viscosity," in *First Report on Viscosity and Plasticity*. 1939, pp. 5–72, New York: Nordemann Publishing Company.

[33] J. M. Krishnan and K. R. Rajagopal, "Thermodynamic framework for the constitutive modeling of asphalt concrete: Theory and applications," *Journal of Materials in Civil Engineering*, vol. 16, no. 2, pp. 155–166, 2004.

[34] K. R. Rajagopal, "Multiple configurations in continuum mechanics," Reports of the Institute for Computational and Applied Mechanics 6, University of Pittsburgh, Pittsburgh, PA, 1995.

[35] J. Málek and K. R. Rajagopal, "A thermodynamic framework for a mixture of two liquids," *Nonlinear Analysis: Real World Applications*, vol. 9, no. 4, pp. 1649–1660, 2008.

[36] J. G. Oldroyd, "On the formulation of rheological equations of state," *Proceedings of the Royal Society of London. Series A, Mathematical and Physical Sciences*, vol. 200, no. 1063, pp. 523–541, 1950.

[37] K. R. Rajagopal and A. R. Srinivasa, "On the thermodynamics of fluids defined by implicit constitutive relations," *Zeitschrift für Angewandte Mathematik und Physik (ZAMP)*, vol. 59, no. 4, pp. 715–729, 2008.

[38] K. R. Rajagopal and A. R. Srinivasa, "On thermomechanical restrictions of continua," *Proceedings of the Royal Society of London. Series A: Mathematical, Physical and Engineering Sciences*, vol. 460, no. 2042, pp. 631–651, 2004.

[39] K. R. Rajagopal, "On implicit constitutive theories," *Applications of Mathematics*, vol. 48, no. 4, pp. 279–319, 2003.

[40] K. R. Rajagopal and A. R. Srinivasa, "Mechanics of the inelastic behavior of materials: Part I - Theoretical underpinnings," *International Journal of Plasticity*, vol. 14, no. 10-11, pp. 945–967, 1998.

[41] C. Eckart, "The thermodynamics of irreversible processes. IV. The theory of elasticity and anelasticity," *Physical Review*, vol. 73, no. 4, pp. 373–382, 1948.

[42] K. R. Rajagopal and A. R. Srinivasa, "Inelastic behavior of materials. Part II. Energetics associated with discontinuous deformation twinning," *International Journal of Plasticity*, vol. 13, no. 1-2, pp. 1–35, 1997.

[43] K. R. Rajagopal and A. R. Srinivasa, "On the thermomechanics of shape memory wires," *Zeitschrift für Angewandte Mathematik und Physik (ZAMP)*, vol. 50, no. 3, pp. 459–496, 1999.

[44] A. R. Srinivasa, "Large deformation plasticity and the Poynting effect," *International Journal of Plasticity*, vol. 17, no. 9, pp. 1189–1214, 2001.

[45] I. J. Rao and K. R. Rajagopal, "A thermodynamic framework for the study of crystallization in polymers," *Zeitschrift für Angewandte Mathematik und Physik (ZAMP)*, vol. 53, no. 3, pp. 365–406, 2002.

[46] K. Kannan, I. J. Rao, and K. R. Rajagopal, "A thermomechanical framework for the glass transition phenomenon in certain polymers and its application to fiber spinning," *Journal of Rheology*, vol. 46, pp. 977–999, 2002.

[47] S. C. Prasad, I. J. Rao, and K. R. Rajagopal, "A continuum model for the creep of single crystal nickel-base superalloys," *Acta Materialia*, vol. 53, no. 3, pp. 669–679, 2005.

[48] S. C. Prasad, K. R. Rajagopal, and I. J. Rao, "A continuum model for the anisotropic creep of single crystal nickel-based superalloys," *Acta Materialia*, vol. 54, no. 6, pp. 1487–1500, 2006.

[49] K. R. Rajagopal and A. S. Wineman, "A constitutive equation for nonlinear solids which undergo deformation induced microstructural changes," *International Journal of Plasticity*, vol. 8, no. 4, pp. 385–395, 1992.

[50] K. R. Rajagopal and A. R. Srinivasa, "Modeling anisotropic fluids within the framework of bodies with multiple natural configurations," *Journal of Non-Newtonian Fluid Mechanics*, vol. 99, no. 2-3, pp. 109–124, 2001.

[51] K. Kannan, "A note on aging of a viscoelastic cylinder," *Computers & Mathematics with Applications*, vol. 53, no. 2, pp. 324–328, 2007.

[52] K. Kannan and K. R. Rajagopal, "A thermomechanical framework for the transition of a viscoelastic liquid to a viscoelastic solid," *Mathematics and Mechanics of Solids*, vol. 9, no. 1, pp. 37–59, 2004.

[53] S. Karra and K. R. Rajagopal, "Development of three dimensional constitutive theories based on lower dimensional experimental data," *Applications of Mathematics*, vol. 54, no. 2, pp. 147–176, 2009.

[54] H. Ziegler, *An Introduction to Thermomechanics*, Amsterdam: North-Holland Publishing Company, 1983.

[55] H. Ziegler and C. Wehrli, "The derivation of constitutive relations from the free energy and the dissipation function," in *Advances in Applied Mechanics*, T. Y. Wu and J. W. Hutchinson, Eds. 1987, vol. 25, pp. 183–238, New York: Academic Press.

[56] L. Onsager, "Reciprocal relations in irreversible processes. I.," *Physical Review*, vol. 37, no. 4, pp. 405–426, 1931.

[57] P. Glansdorff and I. Prigogine, *Thermodynamic Theory of Structure, Stability and Fluctuations*, New York: Wiley-Interscience, 1971.

[58] I. Prigogine, *Introduction to Thermodynamics of Irreversible Processes*, New York: John Wiley & Sons, 1967.

[59] R. M. Christensen, *Theory of Viscoelasticity*, New York: Dover Publications, 2003.

[60] R. Chen and D. R. Tyler, "Origin of tensile stress-induced rate increases in the photochemical degradation of polymers," *Macromolecules*, vol. 37, no. 14, pp. 5430–5436, 2004.

[61] H. Bouadi and C. T. Sun, "Hygrothermal effects on the stress field of laminated composites," *Journal of Reinforced Plastics and Composites*, vol. 8, pp. 40–54, 1989.

[62] L. W. Cai and Y. Weitsman, "Non-Fickian moisture diffusion in polymeric composites," *Journal of Composite Materials*, vol. 28, pp. 130–154, 1994.

[63] Y. Weitsman, "Coupled damage and moisture-transport in fiber-reinforced, polymeric composites," *International Journal of Solids and Structures*, vol. 23, no. 7, pp. 1003–1025, 1987.

[64] J. M. Snead and A. N. Palazotto, "Moisture and temperature effects on the instability of cylindrical composite panels," *Journal of Aircraft*, vol. 20, pp. 777–783, 1983.

[65] S. Y. Lee and W. J. Yen, "Hygrothermal effects on the stability of a cylindrical composite shell panel," *Computers & Structures*, vol. 33, no. 2, pp. 551–559, 1989.

[66] H. Bouadi and C. T. Sun, "Hygrothermal effects on structural stiffness and structural damping of laminated composites," *Journal of Materials Science*, vol. 25, no. 1, pp. 499–505, 1990.

[67] G. A. Kardomateas and C. B. Chung, "Boundary layer transient hygroscopic stresses in orthotropic thick shells under external pressure," *Journal of Applied Mechanics*, vol. 61, pp. 161–168, 1994.

[68] Y. Weitsman, "Stress assisted diffusion in elastic and viscoelastic materials," *Journal of the Mechanics and Physics of Solids*, vol. 35, no. 1, pp. 73–94, 1987.

[69] S. Roy, K. Vengadassalam, Y. Wang, S. Park, and K. M. Liechti, "Characterization and modeling of strain assisted diffusion in an epoxy adhesive layer," *International Journal of Solids and Structures*, vol. 43, no. 1, pp. 27–52, 2006.

[70] A. V. Tobolsky and R. D. Andrews, "Systems manifesting superposed elastic and viscous behavior," *The Journal of Chemical Physics*, vol. 13, pp. 3–27, 1945.

[71] A. V. Tobolsky, I. B. Prettyman, and J. H. Dillon, "Stress relaxation of natural and synthetic rubber stocks," *Journal of Applied Physics*, vol. 15, pp. 380–395, 1944.

[72] A. S. Wineman and K. R. Rajagopal, "On a constitutive theory for materials undergoing microstructural changes," *Archives of Mechanics*, vol. 42, no. 1, pp. 53–75, 1990.

[73] H. E. Huntley, A. S. Wineman, and K. R. Rajagopal, "Load maximum behavior in the inflation of hollow spheres of incompressible material with strain-dependent damage," *Quarterly of Applied Mathematics*, vol. 59, no. 2, pp. 193–223, 2001.

[74] H. E. Huntley, A. S. Wineman, and K. R. Rajagopal, "Stress softening, strain localization and permanent set in the circumferential shear of an incompressible elastomeric cylinder," *IMA Journal of Applied Mathematics*, vol. 59, no. 3, pp. 309–338, 1997.

[75] H. E. Huntley, A. S. Wineman, and K. R. Rajagopal, "Chemorheological relaxation, residual stress, and permanent set arising in radial deformation of elastomeric hollow spheres," *Mathematics and Mechanics of Solids*, vol. 1, no. 3, pp. 267–299, 1996.

[76] A. S. Wineman and J. Shaw, "Scission and healing in a spinning elastomeric cylinder at elevated temperature," *Journal of Applied Mechanics*, vol. 69, no. 5, pp. 602–609, 2002.

[77] J. A. Shaw, A. S. Jones, and A. S. Wineman, "Chemorheological response of elastomers at elevated temperatures: experiments and simulations," *Journal of the Mechanics and Physics of Solids*, vol. 53, no. 12, pp. 2758–2793, 2005.

[78] K. R. Rajagopal and A. S. Wineman, "A note on viscoelastic materials that can age," *International Journal of Non-Linear Mechanics*, vol. 39, no. 10, pp. 1547–1554, 2004.

[79] J. K. Knowles, "The finite anti-plane shear field near the tip of a crack for a class of incompressible elastic solids," *International Journal of Fracture*, vol. 13, no. 5, pp. 611–639, 1977.

[80] H. S. Hou and Y. Zhang, "The effect of axial stretch on cavitation in an elastic cylinder," *International Journal of Non-Linear Mechanics*, vol. 25, no. 6, pp. 715–722, 1990.

[81] G. Saccomandi, "Some generalized pseudo-plane deformations for the neo-Hookean material," *IMA Journal of Applied Mathematics*, vol. 70, no. 4, pp. 550–563, 2005.

[82] K. R. Rajagopal and L. Tao, "On an inhomogeneous deformation of a generalized neo-Hookean material," *Journal of Elasticity*, vol. 28, no. 2, pp. 165–184, 1992.

[83] J. B. McLeod and K. R. Rajagopal, "Inhomogeneous non-unidirectional deformations of a wedge of a non-linearly elastic material," *Archive for Rational*

Mechanics and Analysis, vol. 147, no. 3, pp. 179–196, 1999.

[84] L. Tao, K. R. Rajagopal, and A. S. Wineman, "Circular shearing and torsion of generalized neo-Hookean materials," *IMA Journal of Applied Mathematics*, vol. 48, no. 1, pp. 23, 1992.

[85] J. P. Zhang and K. R. Rajagopal, "Some inhomogeneous motions and deformations within the context of a non-linear elastic solid," *International Journal of Engineering Science*, vol. 30, no. 7, pp. 919–938, 1992.

[86] K. R. Rajagopal, "Deformations of nonlinear elastic solids in unbounded domains," *Mathematics and Mechanics of Solids*, vol. 1, no. 4, pp. 463–472, 1996.

[87] A. Muliana, K. R. Rajagopal, and S. C. Subramanian, "Degradation of an Elastic Composite Cylinder due to the Diffusion of a Fluid," *Journal of Composite Materials*, vol. 43, pp. 1225–1249, 2009.

[88] S. Darbha and K. R. Rajagopal, "Unsteady motions of degrading or aging linearized elastic solids," *International Journal of Non-Linear Mechanics*, vol. 44, no. 5, pp. 478–485, 2009.

[89] K. R. Rajagopal, "Boundary layers in finite thermoelasticity," *Journal of Elasticity*, vol. 36, no. 3, pp. 271–301, 1994.

[90] C. Truesdell, W. Noll, and S. S. Antman, *The Non-linear Field Theories of Mechanics*, Berlin: Springer Verlag, 2004.

[91] P. Bhargava, "High temperature properties of HFPE-II-52 polyimide resin and composites," Ph.D. dissertation, Cornell University, Ithaca, NY, 2007.

[92] C. M. Falcone and M. B. Ruggles-Wrenn, "Rate dependence and short-term creep behavior of a thermoset polymer at elevated temperature," *Journal of Pressure Vessel Technology*, vol. 131, pp. 1–8, 2009.

[93] J. Málek and K. R. Rajagopal, "Mathematical issues concerning the Navier-Stokes equations and some of its generalizations," *Handbook of Differential Equations: Evolutionary Equations*, vol. 2, pp. 371–459, 2006.

[94] R. A. Schapery, "On the characterization of nonlinear viscoelastic materials," *Polymer Engineering and Science*, vol. 9, no. 4, pp. 295–310, 1969.

[95] A. H. Muliana and S. Sawant, "Responses of viscoelastic polymer composites with temperature and time dependent constituents," *Acta Mechanica*, vol. 204, no. 3, pp. 155–173, 2009.

[96] C. Marais and G. Villoutreix, "Analysis and modeling of the creep behavior of the thermostable PMR-15 polyimide," *Journal of Applied Polymer Science*, vol. 69, no. 10, pp. 1983–1991, 1998.

[97] E. Ahci and R. Talreja, "Characterization of viscoelasticity and damage in high temperature polymer matrix composites," *Composites Science and Technology*, vol. 66, no. 14, pp. 2506–2519, 2006.

[98] R. B. Hall, "Combined thermodynamics approach for anisotropic, finite deformation overstress models of viscoplasticity," *International Journal of Engineering Science*, vol. 46, no. 2, pp. 119–130, 2008.

[99] R. A. Schapery, "Application of thermodynamics to thermomechanical, fracture, and birefringent phenomena in viscoelastic media," *Journal of Applied Physics*, vol. 35, pp. 1451–1465, 1964.

[100] Y. R. Kim, D. N. Little, and R. L. Lytton, "Effect of moisture damage on material properties and fatigue resistance of asphalt mixtures," *Transportation Research Record: Journal of the Transportation Research Board*, vol. 1891, no. 1, pp. 48–54, 2004.

[101] K. R. Rajagopal, "On a hierarchy of approximate models for flows of incompressible fluids through porous solids," *Mathematical Models and Methods in the Applied Sciences*, vol. 17, no. 2, pp. 215–252, 2007.

[102] S. C. Cohen, "Postseismic deformation and stress diffusion due to viscoelasticity and comments on the modified Elsasser model," *Journal of Geophysical Research*, vol. 97, no. B11, pp. 15395–15,403, 1992.

[103] P. P. Singh, D. E. Maier, J. H. Cushman, and O. H. Campanella, "Effect of viscoelastic relaxation on moisture transport in foods. Part II: Sorption and drying of soybeans," *Journal of Mathematical Biology*, vol. 49, no. 1, pp. 20–34, 2004.

[104] H. Darcy, *Les Fontaines Publiques de la Ville de Dijon*, Paris: Victor Dalmont, 1856.

[105] A. Fick, "Uber diffusion," *Poggendorffs Annalen der Physik und Chemie*, vol. 94, no. 59-86, 1855.

[106] K. R. Rajagopal, "Diffusion through polymeric solids undergoing large deformations," *Materials Science and Technology*, vol. 19, no. 9, pp. 1175–1180, 2003.

[107] S. Baek and A. R. Srinivasa, "Diffusion of a fluid through an elastic solid undergoing large deformation," *International Journal of Non-Linear Mechanics*,

vol. 39, no. 2, pp. 201–218, 2004.

[108] M. A. Biot, "Theory of deformation of a porous viscoelastic anisotropic solid," *Journal of Applied Physics*, vol. 27, no. 5, pp. 459–467, 1956.

[109] D. S. Cohen and A. B. White Jr., "Sharp fronts due to diffusion and viscoelastic relaxation in polymers," *SIAM Journal on Applied Mathematics*, vol. 51, no. 2, pp. 472–483, 1991.

[110] D. A. Edwards and D. S. Cohen, "A mathematical model for a dissolving polymer," *AIChE Journal*, vol. 41, no. 11, pp. 2345–2355, 1995.

[111] S. J. Huang and C. J. Durning, "Nonlinear viscoelastic diffusion in concentrated polystyrene/ethylbenzene solutions," *Journal of Polymer Science Part B: Polymer Physics*, vol. 35, no. 13, pp. 2103–2119, 1997.

[112] R.A. Cairncross and C.J. Durning, "A model for drying of viscoelastic polymer coatings," *AIChE Journal*, vol. 42, no. 9, pp. 2415–2425, 1996.

[113] Q. Liu, X. Wang, and D. De Kee, "Mass transport through swelling membranes," *International Journal of Engineering Science*, vol. 43, no. 19-20, pp. 1464–1470, 2005.

[114] C. Truesdell, "Sulle basi della termomeccanica i," *Rendiconti Lincei*, vol. 8, no. 22, pp. 22–38, 1957.

[115] C. Truesdell, "Sulle basi della termomeccanica ii," *Rendiconti Lincei*, vol. 8, no. 22, pp. 158–166, 1957.

[116] R. J. Atkin and R. E. Craine, "Continuum theories of mixtures: Basic theory and historical development," *The Quarterly Journal of Mechanics and Applied Mathematics*, vol. 29, no. 2, pp. 209, 1976.

[117] A. Bedford and D. S. Drumheller, "Theories of immiscible and structured mixtures," *International Journal of Engineering Science*, vol. 21, no. 8, pp. 863–960, 1983.

[118] A. E. Green and P. M. Naghdi, "On basic equations for mixtures," *The Quarterly Journal of Mechanics and Applied Mathematics*, vol. 22, no. 4, pp. 427, 1969.

[119] I. Samohỳl, *Thermodynamics of Irreversible Processes in Fluid Mixtures*, Leipzig, Germany: Teubner, 1987.

[120] R. M. Bowen, "Compressible porous media models by use of the theory of mixtures," *International Journal of Engineering Science*, vol. 20, no. 6, pp. 697–735, 1982.

[121] K. R. Rajagopal and L. Tao, *Mechanics of Mixtures*, Farrer Road, Singapore: World Scientific, 1995.

[122] N. Mills, "Incompressible mixtures of Newtonian fluids," *International Journal of Engineering Science*, vol. 4, no. 2, pp. 97–112, 1966.

[123] J. Hron, J. D. Humphrey, and K. R. Rajagopal, "Material identification of nonlinear solids infused with a fluid," *Mathematics and Mechanics of Solids*, vol. 7, no. 6, pp. 629–646, 2002.

[124] S. C. Prasad and K. R. Rajagopal, "On the diffusion of fluids through solids undergoing large deformations," *Mathematics and Mechanics of Solids*, vol. 11, no. 3, pp. 291–305, 2006.

[125] C. Yang, G. He, Y. He, and P. Ma, "Densities and viscosities of N, N-Dimethylformamide + N-Methyl-2-pyrrolidinone and + Dimethyl Sulfoxide in

the temperature range (303.15 to 353.15) K," *Journal of Chemical & Engineering Data*, vol. 53, no. 7, pp. 1639–1642, 2008.

[126] R. Srinivasan, R. R. Hall, W. D. Wilson, W. D. Loehle, and D. C. Allbee, "Ultraviolet laser irradiation of the polyimide, PMDA-ODA (Kapton (TM)), to yield a patternable, porous, electrically conducting carbon network," *Synthetic Metals*, vol. 66, no. 3, pp. 301–307, 1994.

[127] E. Gattiglia and T. P. Russell, "Swelling behavior of an aromatic polyimide," *Journal of Polymer Science Part B: Polymer Physics*, vol. 27, no. 10, pp. 2131–2144, 1989.

[128] K. J. Bowles, D. S. Papadopoulos, L. L. Inghram, L. S. McCorkle, and O. V. Klan, "Longtime durability of pmr-15 matrix polymer at 204, 260, 288 and 316 ^{o}c," Tech. Rep. 210602, NASA, Hanover, MD, 2001.

[129] K. J. Bowles, L. Tsuji, J. Kamvouris, and G. D. Roberts, "Long-Term Isothermal Aging Effects on Weight Loss, Compression Properties, and Dimensions of T650-35 Fabric-Reinforced PMR-15 CompositesData," Tech. Rep. 211870, NASA, Hanover, MD, 2003.

[130] K. Pochiraju and G. P. Tandon, "Interaction of oxidation and damage in high temperature polymeric matrix composites," *Composites Part A: Applied Science and Manufacturing*, vol. 40, no. 12, pp. 1931–1940, 2009.

[131] G. P. Tandon, K. V. Pochiraju, and G. A. Schoeppner, "Modeling of oxidative development in PMR-15 resin," *Polymer Degradation and Stability*, vol. 91, no. 8, pp. 1861–1869, 2006.

[132] S. Roy, S. Singh, and G. A. Schoeppner, "Modeling of evolving damage in

high temperature polymer matrix composites subjected to thermal oxidation," *Journal of Material Science*, vol. 43, no. 20, pp. 6651–6660, 2008.

[133] T. de Donder and P. Van Rysselberghe, *Thermodynamic Theory of Affinity*, Palo Alto: Stanford University Press, 1936.

[134] P. Van Rysselberghe, "Reaction rates and affinities," *The Journal of Chemical Physics*, vol. 29, pp. 640–642, 1958.

[135] R. M. Bowen, "On the stoichiometry of chemically reacting materials," *Archive for Rational Mechanics and Analysis*, vol. 29, no. 2, pp. 114–124, 1968.

[136] R. M. Bowen, "Thermochemistry of reacting materials," *The Journal of Chemical Physics*, vol. 49, pp. 1625, 1968.

[137] I. Samohỳl, "Thermodynamics of reacting mixtures of any symmetry with heat conduction, diffusion and viscosity," *Archive for Rational Mechanics and Analysis*, vol. 147, no. 1, pp. 1–45, 1999.

[138] J. W. Nunziato and E. K. Walsh, "On ideal multiphase mixtures with chemical reactions and diffusion," *Archive for Rational Mechanics and Analysis*, vol. 73, no. 4, pp. 285–311, 1980.

[139] P. H. Björnbom, "The independent reactions in calculations of complex chemical equilibria," *Industrial & Engineering Chemistry Fundamentals*, vol. 14, no. 2, pp. 102–106, 1975.

[140] I. Fishtik and R. Datta, "De Donder relations in mechanistic and kinetic analysis of heterogeneous catalytic reactions," *Industrial & Engineering Chemistry Research*, vol. 40, no. 11, pp. 2416–2427, 2001.

[141] P. Germain, P. Suquet, and Q. S. Nguyen, "Continuum thermodynamics," *Journal of Applied Mechanics*, vol. 50, no. 4, pp. 1010–1020, 1983.

[142] M. Pekar, "Thermodynamics and foundations of mass-action kinetics," *Progress in Reaction Kinetics and Mechanism, 30*, vol. 1, no. 2, pp. 3–113, 2005.

[143] F. J. Zeleznik and S. Gordon, "Calculation of complex chemical equilibria," *Industrial & Engineering Chemistry*, vol. 60, no. 6, pp. 27–57, 1968.

[144] K. Kannan and K. R. Rajagopal, "A thermodynamical framework for chemically reacting systems," *Zeitschrift für Angewandte Mathematik und Physik (ZAMP)*, 2010, In Press.

[145] K. R. Rajagopal, A. R. Srinivasa, and A. S. Wineman, "On the shear and bending of a degrading polymer beam," *International Journal of Plasticity*, vol. 23, no. 9, pp. 1618–1636, 2007.

[146] M. B. Ruggles-Wrenn and J. L. Broeckert, "Effects of prior aging at 288^{o}C in air and in argon environments on creep response of PMR-15 neat resin," *Journal of Applied Polymer Science*, vol. 111, no. 1, pp. 228–236, 2009.

[147] K. R. Rajagopal and A. R. Srinivasa, "On the nature of constraints for continua undergoing dissipative processes," *Proceedings of the Royal Society A: Mathematical, Physical and Engineering Science*, vol. 461, no. 2061, pp. 2785–2795, 2005.

[148] K. B. Nakshatrala and A. J. Valocchi, "Non-negative mixed finite element formulations for a tensorial diffusion equation," *Journal of Computational Physics*, vol. 228, no. 18, pp. 6726–6752, 2009.

[149] K. Lipnikov, D. Svyatskiy, and Y. Vassilevski, "A monotone finite volume method for advection-diffusion equations on unstructured polygonal meshes," *Journal of Computational Physics*, vol. 229, no. 11, pp. 4017–4032, 2010.

[150] S. Baek and T. J. Pence, "On swelling induced degradation of fiber reinforced polymers," *International Journal of Engineering Science*, vol. 47, no. 11-12, pp. 1100–1109, 2009.

[151] M. Itskov, "On the theory of fourth-order tensors and their applications in computational mechanics," *Computer Methods in Applied Mechanics and Engineering*, vol. 189, no. 2, pp. 419–438, 2000.

APPENDIX A

APPENDIX FOR CHAPTER II

From Eq. (3.21) and Eq. (3.32) in [151]

$$\frac{\partial f(\mathbf{L}_1)}{\partial \mathbf{D}_1} = \frac{1}{2}\left(\frac{\partial f}{\partial \mathbf{L}_1} + \left(\frac{\partial f}{\partial \mathbf{L}_1}\right)^T\right). \tag{A.1}$$

Hence, using Eq. (A.1)

$$\begin{aligned}\frac{\partial}{\partial \mathbf{D}_1}\mathbf{B}_3.\left(\mathbf{F}_2\mathbf{L}_1\mathbf{F}_2^{-1} + \mathbf{F}_2^{-T}\mathbf{L}_1^T\mathbf{F}_2^T\right) &= \frac{\partial}{\partial \mathbf{D}_1}2\mathbf{B}_3.\mathbf{F}_2\mathbf{L}_1\mathbf{F}_2^{-1} \\ &= \frac{\partial}{\partial \mathbf{D}_1}2\mathbf{F}_2^T\mathbf{B}_3\mathbf{F}_2^{-T}.\mathbf{L}_1 \\ &= \mathbf{F}_2^T\mathbf{B}_3\mathbf{F}_2^{-T} + \mathbf{F}_2^{-1}\mathbf{B}_3\mathbf{F}_2.\end{aligned} \tag{A.2}$$

APPENDIX B

APPENDIX FOR CHAPTER III

In this section, we shall derive the constitutive relations when the rate of dissipation is of the form

$$\xi_m(\mathbf{D}_{p(t)}, \mathbf{D}_G) = \eta_p \mathbf{D}_{p(t)}.\mathbf{D}_{p(t)} + \eta_G \mathbf{D}_G.\mathbf{D}_G. \tag{B.1}$$

with the stored energy given by Eq. (3.34). Now, Eq. (3.33) reduces to

$$\mathbf{T} = p\mathbf{I} + \mu \mathbf{B}_{p(t)} + \eta_p \mathbf{D}_{p(t)}, \tag{B.2}$$

and

$$\mathbf{T} = \hat{\lambda}\mathbf{I} + \eta_G \mathbf{V}^{-1}_{\kappa_{p(t)}} \mathbf{D}_G \mathbf{V}_{\kappa_{p(t)}}. \tag{B.3}$$

Also, from Eqs. (B.2) and (B.3),

$$(p - \hat{\lambda}) = -\frac{\mu}{3} tr(\mathbf{B}_{p(t)}). \tag{B.4}$$

Equating Eqs. (B.2) and (B.3), pre-multiplying and post-multiplying by $\mathbf{V}_{\kappa_{p(t)}}$, and using Eqs. (3.15), (3.23), we get

$$(p - \hat{\lambda})\mathbf{B}_{p(t)} + \mu \mathbf{B}^2_{p(t)} + \frac{\eta_p}{2}\dot{\mathbf{B}}_{p(t)} = -\frac{\eta_G}{2}\mathbf{V}^{-1}_{\kappa_{p(t)}} \overset{\nabla}{\mathbf{B}}_{p(t)} \mathbf{V}_{\kappa_{p(t)}}. \tag{B.5}$$

It follows that, the constitutive relations for the choices of Eq. (3.34) and Eq. (B.1) for the specific Helmholtz potential and the rate of dissipation, are

$$\mathbf{T} = p\mathbf{I} + \mu \mathbf{B}_{p(t)} + \frac{\eta_p}{2}\mathbf{V}^{-1}_{\kappa_{p(t)}} \dot{\mathbf{B}}_{p(t)} \mathbf{V}^{-1}_{\kappa_{p(t)}}, \tag{B.6}$$

and

$$-\frac{\eta_G}{2}\mathbf{V}^{-1}_{\kappa_{p(t)}} \overset{\nabla}{\mathbf{B}}_{p(t)} \mathbf{V}_{\kappa_{p(t)}} = -\frac{\mu}{3} tr(\mathbf{B}_{p(t)})\mathbf{B}_{p(t)} + \mu \mathbf{B}^2_{p(t)} + \frac{\eta_p}{2}\dot{\mathbf{B}}_{p(t)}. \tag{B.7}$$

Eq. (B.7) is the evolution equation of the natural configuration.

APPENDIX C

APPENDIX FOR CHAPTER VI

A. Convergence of numerical results

Since the analytical solution for the problem is unknown, we perform an *engineering* convergence study of the solution using the described algorithm (see figure (36)). In this study, the error is calculated by taking the difference between solution of various grid sizes (5, 15, 25, ..., upto 351 points) and the solution found using a very fine grid of 401 points at the point $Z^\star = 0$ and at a time of $t^\star = 0.5$. Note that the error is propotional to logarithm of the spatial increment and hence the convergence rate is slow. The aim of our current work is not to present an optimal algorithm but to solve the coupled partial differential equations.

B. Derivation of the constitutive equation for the viscoelastic solid in the absence of diffusion

Here we show that in the absence of diffusion the derived constitutive equations reduces to a variant of the three-dimensional standard linear solid model given in Chapter V. Now, in the absence of diffusion of the fluid, we will have to drop the last term in (6.66) to get

$$\hat{\psi} = A^s + \left(B^s + c_2^s\right)(\theta - \theta_s) - \frac{c_1^s}{2}(\theta - \theta_s)^2 - c_2^s\theta \ln\left(\frac{\theta}{\theta_s}\right) + \frac{\mu_{G0} - \mu_{G1}\theta}{\rho^s\theta_s}(\mathrm{I}_{B^s_G} - 3) + \frac{\mu_{p0} - \mu_{p1}\theta}{\rho^s\theta_s}(\mathrm{I}_{B^s_{p(t)}} - 3). \tag{C.1}$$

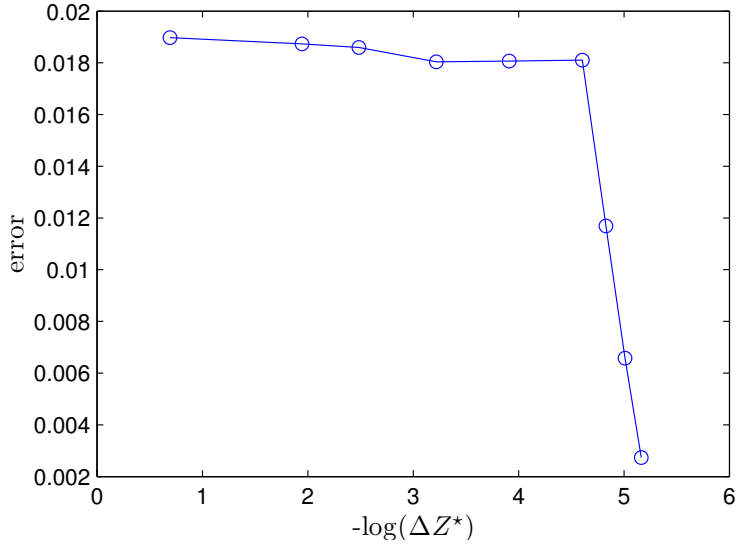

Fig. 36.: Engineering spatial convergence of the solution for p at $Z^\star = 0$ and at $t^\star = 0.5$. The time-step was chosen to be $\Delta t^\star = 0.025$.

We shall assume that the solid is incompressible in the absence of fluid. The constraint of incompressibility is given by

$$\mathrm{tr}\,(\boldsymbol{D}^s) = \mathrm{tr}\,(\boldsymbol{D}^s_G) = 0. \tag{C.2}$$

The reduced energy dissipation equation of the solid reduces to

$$\boldsymbol{T}^s \cdot \boldsymbol{D}^s - \left(\rho \frac{d\psi}{dt}\right)_{\theta\,\text{fixed}} = \xi_m. \tag{C.3}$$

In the absence of diffusion, there will be only be dissipation due to mechanical working of the solid, and so the rate of dissipation in this case would be

$$\xi_m = \gamma(\theta)\boldsymbol{D}^s_G \cdot \boldsymbol{D}^s_G. \tag{C.4}$$

Upon maximizing the rate of dissipation using (C.4), (C.2) as constraints (see Chapter V for details) we arrive at

$$\boldsymbol{T}^s = p\boldsymbol{I} + 2\bar{\mu}_p \boldsymbol{B}^s_{p(t)}, \tag{C.5a}$$

$$\boldsymbol{T}^s = \lambda\boldsymbol{I} + 2\bar{\mu}_G \boldsymbol{B}^s_G + \eta \boldsymbol{D}^s_G. \tag{C.5b}$$

From (C.5a), (C.5b) we have

$$(p-\lambda)\,\boldsymbol{I} + 2\bar{\mu}_p \boldsymbol{B}^s_{p(t)} - 2\bar{\mu}_G \boldsymbol{B}^s_G = \eta \boldsymbol{D}^s_G. \tag{C.6}$$

Taking the trace of (C.6), we get

$$3\,(p-\lambda) = -2\bar{\mu}_p \mathrm{tr}\left(\boldsymbol{B}^s_{p(t)}\right) + 2\bar{\mu}_G \mathrm{tr}\left(\boldsymbol{B}^s_G\right). \tag{C.7}$$

Hence, (C.7) in (C.6) gives

$$2\bar{\mu}_p \boldsymbol{B}^s_{p(t)} - 2\bar{\mu}_G \boldsymbol{B}^s_G = \frac{2}{3}\left[\bar{\mu}_p \mathrm{tr}\left(\boldsymbol{B}^s_{p(t)}\right) - \bar{\mu}_G \mathrm{tr}\left(\boldsymbol{B}^s_G\right)\right] + \eta \boldsymbol{D}^s. \tag{C.8}$$

The final constitutive equations for the viscoelastic solid are

$$\boldsymbol{T}^s = p\boldsymbol{I} + 2\bar{\mu}_p \boldsymbol{B}^s_{p(t)}, \tag{C.9}$$

with (C.8) being the evolution equation for the natural configuration of the viscoelastic solid. This is a variant of the model derived in Chapter V.

VITA

Satish Karra received his Bachelor of Technology degree in mechanical engineering from the Indian Institute of Technology (IIT) Madras, India, in 2005. He joined Texas A&M University in College Station in Fall 2005 and received his Master of Science and Doctor of Philosophy degrees in May 2007 and May 2011, respectively, also in the field of mechanical engineering. His research lies in the area of theoretical & computational modeling of the mechanical (specifically viscoelastic) behavior of geomaterials and aerospace materials. He is also interested in modeling the response of such materials under various degradation mechanisms such as temperature, diffusion of a fluid, and chemical reactions. He has also worked on topics in the field of non-Newtonian fluid mechanics that include modeling the response of synovial fluid, and on Maxwell fluid with pressure dependent viscosity and relaxation time.

He can be reached at satkarra@tamu.edu or via his Ph.D. advisor Prof. K. R. Rajagopal at the Department of Mechanical Engineering, 3123 TAMU, College Station, TX 77843-3123.

The typist for this thesis was Satish Karra.